

Wang, Yu (2025) Role of ER stress in vascular dysfunction and damage during hypertension. PhD thesis.

https://theses.gla.ac.uk/85582/

Copyright and moral rights for this work are retained by the author

A copy can be downloaded for personal non-commercial research or study, without prior permission or charge

This work cannot be reproduced or quoted extensively from without first obtaining permission from the author

The content must not be changed in any way or sold commercially in any format or medium without the formal permission of the author

When referring to this work, full bibliographic details including the author, title, awarding institution and date of the thesis must be given

Enlighten: Theses
<a href="https://theses.gla.ac.uk/">https://theses.gla.ac.uk/</a>
research-enlighten@glasgow.ac.uk



# Role of ER Stress in Vascular Dysfunction and Damage during Hypertension

Yu Wang BSc (Hons), MRes

Submitted in fulfilment of the requirements of the degree of Doctor of Philosophy

British Heart Foundation Glasgow Cardiovascular Research Centre
School of Cardiovascular & Metabolic Health
College of Medical, Veterinary and Life Sciences
University of Glasgow

## **Abstract**

Hypertension is a major risk factor for cardiovascular diseases and involves complex molecular mechanisms that are not fully understood. Recent evidence indicates that endoplasmic reticulum (ER) stress plays a crucial role in hypertension, particularly by affecting vascular function. This thesis explores the hypothesis that ER stress contributes to hypertension through mechanisms involving oxidative stress, calcium signalling dysfunction, and changes in microRNA (miRNA) expression. These processes can lead to increased vascular contractility, which may ultimately contribute to elevated blood pressure.

This study utilised both human vascular smooth muscle cells (VSMCs) and animal models to investigate the molecular mechanisms linking ER stress to hypertension. Using miRNA microarray analysis, 242 differentially expressed (DE) miRNAs were identified when comparing VSMCs from hypertensive (HT) individuals to those from normotensive (NT) individuals, each represented by one sample derived from three different individuals. These (DE) miRNAs were associated with key genes and proteins related to oxidative stress and calcium signalling, including Noxs, SOD2, catalase, and ER calcium channels, as determined through Ingenuity Pathway Analysis (IPA). Notably, ER stress induced by tunicamycin significantly altered the expression of oxidative stress markers (Noxs, SOD2, catalase) and calcium channels in HT VSMCs compared to NT VSMCs, indicating that ER stress regulates oxidative stress and potentially contributes to calcium signalling dysfunction.

Further insights were gained from studying a chronic Ang II-induced hypertensive mice model (LinA3). ER stress was found to specifically activate the PERK pathway, indicating selective ER stress activation in VSMCs under hypertensive conditions. In this model, oxidative stress was characterized by increased O<sub>2</sub>. generation, lipid peroxidation, irreversible protein oxidation, and altered antioxidants system of VSMCs compared to wild-type mice. The role of Nox4 in modulating the interaction between oxidative stress and ER stress was highlighted, as Nox4 deficiency led to changes in the expression of ER stress markers, including increased BIP and Chop in the kidneys of wild-type mice and increased PDI in the kidneys of LinA3 mice. These findings suggest a potential role for Nox4 in modulating ER stress in hypertension.

This study found that the pre-hypertensive factor endothelin-1 (ET-1) induces ER stress and that ER stress contributes to vascular hypercontractility, using spontaneously hypertensive rats (SHRSP) compared to normotensive Wistar Kyoto (WKY) rats. Our findings demonstrated elevated levels of ER stress in the hearts and VSMCs of SHRSP compared to normotensive controls, indicating a link between ER stress and hypertension. ET-1 was found to induce ER stress through both ETA and ETB receptors, leading to increased expression of ER stress markers such as ATF4, XBP1s, and BIP. Inhibition of ER stress resulted in reduced activation of the contractile machinery, establishing a connection between ER stress, calcium signalling dysfunction, and the enhanced contractile response observed in hypertension.

Lastly, in vivo treatment with the ER stress inhibitor 4-phenylbutyric acid (4PBA) in spontaneously hypertensive rats (SHR) demonstrated reduced blood pressure, improved endothelial function, and a tendency toward improved vascular structure. These findings suggest that ER stress is a critical mediator of vascular dysfunction and structural changes in hypertension and present ER stress inhibition as a potential therapeutic strategy for managing hypertension.

In conclusion, this thesis highlights the role of ER stress in mediating vascular dysfunction in hypertension, emphasizing its interactions with oxidative stress, calcium dysfunction, and the potential involvement of miRNA regulation. These findings lay the groundwork for the development of novel therapeutic strategies targeting ER stress to treat hypertension.

# **Table of Contents**

Abstract .			2
List of Tal	bles		8
List of Fig	gures		9
Acknowle	edgement		11
Author's	Declaration		13
Abbrevia	tions		14
Chapter 1	L Introd	uction	17
1.1	Hyper	tension	17
	1.1.1	Epidemiology	17
	1.1.2	Pathophysiology	.17
	1.1.3	Diagnosis and management	19
1.2	Vascul	lar dysfunction in hypertension	.20
	1.2.1	Vascular Structure	.21
	1.2.2	Endothelial dysfunction	21
	1.2.3	Vascular remodelling	23
	1.2.4	Vascular smooth muscle cells phenotypic switching	.24
	1.2.5	Vascular smooth muscle contraction	.25
1.3	Oxidat	tive stress	.27
	1.3.1	NADPH oxidases	.29
	1.3.2	Antioxidants	30
	1.3.3	Oxidative stress in hypertension	31
1.4	Endop	plasmic reticulum stress	31
	1.4.1	Unfolded protein response	31
	1.4.2	The function of ER stress	34
	1.4.3	ER stress and Oxidative stress	35
	1.4.4	ER stress and calcium dysfunction	.37
	1.4.5	ER stress in hypertension	.37
1.5	Interp	lay between ROS, ER stress, calcium dysfunction and implications	ir
hype	ertension		38
1.6	Micro	RNAs	40
	1.6.1	Biogenesis and function of microRNAs	.40
	1.6.2	MicroRNAs in ER stress	41
	1.6.3	MicroRNAs in hypertension	42
1.7	Hypot	hesis and aims	42
Chapter 2	2 Mater	ials and Methods	44
2.1	Gener	al lab practice	44
2.2	Mater	ials	44
	2.2.1	Reagents and suppliers	44
	2.2.2	Solutions and medium	46
	2.2.3	Antibodies	48
	2.2.4	Primers	49
	2.2.5	Software	.51
2.3	Anima	als and tissue collection	51
	2.3.1	Hypertensive mice model	51
	2.3.2	Hypertensive rat model	52
	2.3.3	Housing and husbandry	52
	2.3.4	Tissue harvest	52

	2.4	in vivo	) study	53
		2.4.1	4-PBA treatment	53
		2.4.2	Blood pressure measurement	53
	2.5	Gener	al cell culture procedure	54
		2.5.1	Primary culture of human vascular smooth muscle cells	54
		2.5.2	Primary culture of mouse vascular smooth muscle cells	55
		2.5.3	Primary culture of rat vascular smooth muscle cells	55
		2.5.4	General protocol for VSMCs culture	56
	2.6	RNA a	nalysis by real-time polymerase chain reaction	57
		2.6.1	RNA extraction	57
		2.6.2	Nucleic acid qualification	58
		2.6.3	DNase I treatment	58
		2.6.4	Reverse transcription	58
		2.6.5	SYBR green real-time PCR	59
		2.6.6	qPCR data analysis	59
	2.7	Protei	n analysis by western blotting	59
		2.7.1	Protein extraction	59
		2.7.2	Protein quantification	60
		2.7.3	Sample preparation	60
		2.7.4	Sodium dodecyl sulphate-polyacrylamide gel electrophoresis (	SDS-
		PAGE)	60	
		2.7.5	Immunoblotting for proteins	60
	2.8	Assess	sing redox status and oxidative stress	61
		2.8.1	Lucigenin-enhanced chemiluminescence	61
		2.8.2	Amplex™ Red assay	61
		2.8.3	Measurement of nitrotyrosine levels	62
		2.8.4	Lipid peroxidation by thiobarbituric acid-reacting substances a	ssay
	2.0	Calai	62	<b>6</b> 2
	2.9		m influx assay	
	2.10		raphy	
		2.10.1	Wire myography	
	2 4 4	2.10.2	Pressure myography	
	2.11		4s	
		2.11.1	miRNA extraction	
		2.11.2	Microarray of miRNAs	
		2.11.3	miRNA data analysis	
	2 4 2	2.11.4	Ingenuity Pathway Analysis	
Cl	2.12		ical analysis	
-	oter 3 erten	s Vascui sion 70	lar ER Stress, Oxidative Stress and Calcium Dysfunction in Hu	man
71-	3.1		iew	70
	3.2		hesis and aims	
	3.3		S	
		3.3.1	miRNA expression profile in hypertension	
		3.3.2	Differentially expressed miRNAs in hypertensive subjects	
			o target Noxs	
		3.3.3	Differentially expressed miRNAs in hypertensive subjects	
			o target antioxidants	
		3.3.4	Differentially expressed miRNAs in hypertensive subjects	
			o target Calcium channels	
		•		-

	3.3.5	MiR-200b-3p predicted targeting ER stress pathway81
	3.3.6	ER stress increases NADPH-dependent O <sup>2-</sup> production in
	hyper	tensive human VSMCs83
	3.3.7	Tunica induced ER stress influences Noxs expression in human
	VSMC	Cs 84
	3.3.8	Tunica induced ER stress influences antioxidants expression in
	huma	n VSMCs86
	3.3.9	Tunica induced ER stress influences calcium channel expression in
	huma	n VSMCs88
3.4	[	Discussion
	3.4.1	The role of miRNAs in VSMCs of HT and NT89
	3.4.2	DE genes/proteins and related DE miRNAs in VSMCs of HT91
	3.4.3	Effect of ER stress inducer in VSMCs93
Chapter 4	1 E	ER Stress and Oxidative Stress in an Ang II-dependent Model of
Hyperten	sion (l	.inA3 mice)
4.1	(	Overview97
4.2	ŀ	Hypothesis and aims100
4.3	F	Results
	4.3.1	Oxidative stress is increased in VSMCs from LinA3 mice 100
	4.3.2	NADPH oxidases expression is not increased in VSMCs from LinA3
	mice.	103
	4.3.3	Antioxidants expression are altered in VSMCs from LinA3 mice105
	4.3.4	Expression of ER stress makers is altered in VSMCs from LinA3 mice.
		107
	4.3.5	Noxs and antioxidants levels in kidney of LinA3 and Nox4 knock-out
	mice	109
	4.3.6	Role of ER stress in kidney of LinA3 and Nox4 knock-out mice111
4.4		Discussion
	4.4.1	Oxidative stress and ER stress in VSMCs of LinA3 mice114
	4.4.2	Nox4 deficiency altered oxidative stress and ER stress in kidney of
		nd LinA3 mice117
Chapter 5		Role of ET-1 Induced ER stress in vascular hypercontractility of WKY and
SHRSP ra		120
5.1		Overview
5.2		Hypothesis and aims123
5.3		Results
	5.3.1	ER stress response activation in VSMCs and Heart from SHRSP rats 124
	5.3.2	Effects of ET <sub>A</sub> R and ET <sub>B</sub> R on ER stress induced by ET-1 in VSMCs 131
	5.3.3	Altered ET-1 induced p-MLC <sub>20</sub> and Ca <sup>2+</sup> influx by ER stress inhibitors
	from	SHRSP rats139
	5.3.4	Altered vascular contraction by ER stress inhibitors from SHRSP rats
		142
5.4	[	Discussion
	5.4.1	ER stress in SHRSP144
	5.4.2	ET-1 induces ER stress in VSMC145
	5.4.3	ER stress involves in ET-1 induced contraction in hypertensive rats 147
Chapter 6	5 F	ER Stress Inhibitor 4-PBA Treatment in WKY and SHR Rats149
6.1		Overview
J. <u> </u>	`	179

6.2	Hypothesis and aims		150
6.3	R	esults	151
	6.3.1	ER stress inhibitor, 4PBA, attenuates systolic blood pressure 151	es in SHR
	6.3.2	Effect of 4PBA treatment on blood vessel function	154
	6.3.3	Effect of 4PBA treatment on blood vessel structure	156
6.4	D	Discussion	159
Chapter :	7 F	inal discussion	163
7.1	Е	R stress in different tissues and different hypertension models	163
	7.1.1	ER stress in hypertensive tissues	163
	7.1.2	ER stress in VSMCs of hypertension	164
7.2	R	legulators of ER Stress in Hypertension	165
	7.2.1	Oxidative stress regulating ER stress	165
	7.2.2	Induction of ER stress by vasoactive peptides	167
	7.2.3	MiRNAs and ER stress	168
7.3	Е	ffects of ER Stress in Hypertension	168
	7.3.1	ER stress in blood pressure regulation	168
	7.3.2	ER stress regulating oxidative stress	169
	7.3.3	ER stress inducing vascular hypercontractility	170
7.4	L	imitations of the study	173
Referenc		,	

# **List of Tables**

Table 2.1 Reagents used in the thesis	44
Table 2.2 Antibodies used for Western blotting	48
Table 2.3 Primers used in the RT-qPCR gene expression analysis	49
Table 3.1 Top10 miRNAs in each group	75
Table 3.2 The predicted targets of miRNA downregulated in HT	76
Table 3.3 The predicted targets of miRNA upregulated in HT	77

# **List of Figures**

Figure 1.1 Vascular smooth muscle contraction.	27
Figure 1.2 Sources of ROS in hypertension.	29
Figure 1.3 ER stress response.	34
Figure 1.4 Sources of ROS in the ER.	36
Figure 1.5 ER stress in hypertension.	38
Figure 1.6 miRNA biogenesis.	41
Figure 2.1 Illustration of the wire myography mounting heads with the mounted v	vessel64
Figure 2.2 Schematic of pressure myography chamber. A small vessel segment is	mounted
between two glass cannulas in the chamber. (Modified from ref (Shahid and Buys	s, 2013)).
	66
Figure 3.1 miRNA expression performance in miRNA array.	74
Figure 3.2 Differentially expressed miRNAs are predicted to target Noxs	76
Figure 3.3 Differentially expressed miRNAs are predicted to target antioxidants e	expression
in VSMC of hypertensive subjects.	78
Figure 3.4 Differentially expressed miRNAs are predicted to target Calcium chan	nel
expression in VSMC of hypertensive subjects.	80
Figure 3.5 ER stress markers in HT and miR-200c-3p in ER stress pathway	82
Figure 3.6 Effects of ER stress inducer on ROS generation in human VSMCs from	m
normotensive subjects and hypertensive subjects.	83
Figure 3.7 ER stress influence Noxs expression in human VSMCs.	85
Figure 3.8 ER stress influence antioxidants expression in human VSMCs	87
Figure 3.9 ER stress influences calcium channel expression in human VSMCs	88
Figure 4.1 ROS generation, lipid peroxidation and irreversible protein oxidation a	are
increased in VSMCs from LinA3 mice.	102
Figure 4.2 Expression of Noxs in VSMCs from WT and LinA3 mice	104
Figure 4.3 Expression of antioxidants in VSMCs from WT and LinA3 mice	106
Figure 4.4 ER stress markers expression and activation in VSMCs from WT and	LinA3
mice	108
Figure 4.5 Noxs and antioxidants expression in kidney from male of LinA3 and N	Vox4
knock-out mice.	110
Figure 4.6 ER stress markers expression in kidney from LinA3 and Nox4 knock-o	out mice.
	112
Figure 5.1 ER stress markers expression is increased in VSMCs from SHRSP cor	npared to
WVV rate	126

Figure 5.2 ER stress markers expression is not changed in mesenteric arteries from SHRSP
compared to WKY rats. 127
Figure 5.3 ER stress markers expression is not increased in aorta from SHRSP compared to
WKY rats. 128
Figure 5.4 ER stress markers expression is increased in heart from SHRSP compared to
WKY rats. 129
Figure 5.5 ER stress markers expression is not changed in kidney from SHRSP compared
to WKY rats
Figure 5.6 Effects of ETAR and ETBR on PERK pathway activation induced by ET-1 in
VSMCs
Figure 5.7 Effects of ETAR and ETBR on IRE1 pathway activation induced by ET-1 in
VSMCs
Figure 5.8 Effects of ETAR and ETBR on ER stress markers expression induced by ET-1
in VSMCs
Figure 5.9 Effect of ER stress inhibition on ET-1 induced signalling in VSMCs from WKY
and SHRSP rats
Figure 5.10 Effect of ER stress inhibition on ET-1 and U46619 induced vascular
contraction from WKY and SHRSP rats
Figure 6.1 Effect of ER stress inhibition on general parameters and blood pressure of
WKY and SHRSP rats
Figure 6.2 Effect of ER stress inhibition on vascular function of WKY and SHRSP rats.155
Figure 6.3 Effect of ER stress inhibition on vascular structure of WKY and SHRSP rats.

# **Acknowledgement**

First and foremost, I would like to express my sincere appreciation to my supervisors, Prof. Rhian Touyz and Dr. Augusto Montezano, for the opportunity to pursue my PhD in Touyz's lab. Their support, guidance, encouragement, and patience have been invaluable throughout this journey. I deeply admire their exceptional professionalism, expertise, and passion for research, which have inspired me in countless ways. Working in their lab has been a remarkable experience, and I feel truly fortunate to have learned from them.

I am also grateful to my supervisor Dr. Martin McBride for his assistance and support with my miRNA study, especially during the final year of my thesis.

A special thanks to Dr. Livia De Lucca Camargo for her dedication and thoughtful guidance. Her patience and meticulous teaching have greatly improved my lab skills, critical thinking, writing, and presentations. Her valuable ideas and direction for my experiments have been instrumental in my development.

I would also like to thank the senior lab members, Dr. Rashida Lathan, Dr. Karla Neves, Dr. Rheure Lopes, and Dr. Francisco Rios, for their generous assistance with research ideas and experimental guidance.

My appreciation extends to the lab technicians, particularly Mrs. Wendy Beattie, for her essential help with animal experiments and PCR techniques. Without her support, completing the in vivo experiments would have been much more challenging. I also value Mrs. Jackie Thomson's help with cell samples and lab safety, and Mr. John McAbney for his guidance in myography experiments. I am grateful to all members of Touyz's lab; it has been a pleasure working with you all.

I also wish to thank my friends and family. To my friend and roommate Jiayue, thank you for your daily care and support in both life and work. Thanks to my friends Xing, Zhiguo, Angie, Eva, Blessy, Rashida, Jithin, and Hannah for making my time in Glasgow full of warmth, happiness, and memorable moments. My deepest gratitude goes to my husband, Jiteng, for his unwavering support and encouragement, which brightens my life every day. To my parents, thank you for your constant support. And to my precious daughter, Annie, thank you for bringing warmth and joy into my life.

Finally, I want to thank the China Scholarship Council for supporting me with the scholarship, which covered my research and living costs during my PhD study. I also appreciate the University's support in covering additional living expenses due to the delays caused by COVID-19.

# **Author's Declaration**

I declare that the work presented in this thesis was carried out and written entirely by myself, except where explicitly referenced and acknowledged. This thesis has not been previously submitted, either in whole or in part, for a higher degree at this or any other institution. The research described in this thesis was conducted at the College of Medical, Veterinary, and Life Sciences, University of Glasgow, under the supervision of Professor Rhian M. Touyz, Dr. Augusto Montezano, Dr. Martin McBride, and Dr. Livia De Lucca Camargo.

## **Abbreviations**

**4-PBA** 4-phenylbutyric acid

Ach Acetylcholine
Ang II Angiotensin II

**ANOVA** One-way analysis of variance

**AP-1** Activator protein-1

ARE Antioxidant-related element

**BP** Blood pressure

Bip Binding immunoglobulin protein

**CAT** Catalase

[Ca<sup>2+</sup>]i Intracellular calcium concentration

**CCRCs** Cumulative concentration response curves

cDNA Complementary DNACKD Chronic kidney disease

**COSHH** Control of substances hazardous to health

**CSA** Cross-sectional area

**CVD** Cardiovascular disease

**DAG** 1,2-diacylglycerol

**DE** Differentially expressed

**DMEM** Dulbecco's Modified Eagle Medium

**DMSO** Dimethyl Sulfoxide

**DNA** Deoxyribonucleic acid

**DOCA** Deoxycorticosterone acetate

**DPBS** Dulbecco's Phosphate Buffered Saline without CaCl<sub>2</sub> and MgCl<sub>2</sub>

**ER** Endoplasmic reticulum

**ET-1** Endothelin-1

ETA Endothelin type A
ETB Endothelin type B

**FBS** Fetal Bovine Serum Heat Inactivated

**GPx** Glutathione peroxidase

H<sub>2</sub>O<sub>2</sub> Hydrogen peroxide

**HEPES** N'-2-Hydroxyethylpiperazine-N'-2 ethanesulphonic acid

**HIF-1** Hypoxia-inducible factor-1

**HO-1** Heme oxygenase-1

**HT** Hypertensive subjects

**hVSMC** Human VSMC

**ICAMS** Institute of Cardiovascular and Medical Sciences

IP<sub>3</sub> Inositol 1,4,5-trisphosphate

**IPA** Ingenuity<sup>®</sup> Systems Pathway Analysis

LinA3 TTRhRen

MAMs Mitochondria-associated ER membranes

MDA Malonaldehyde

miRNA MicroRNA

MLC20 Myosin light chain 20

MLCK Mmyosin light chain kinase

MLCP Myosin light chain phosphatase

mRNA Messenger RNA

**NADPH** Nicotinamide adenine dinucleotide phosphate

Nox NADPH oxidase

**Nrf2** Nuclear erythroid-related factor 2

NT Normotensive subjects

O<sub>2</sub> - Superoxide

**ONOO** Peroxynitrite

P/S Penicillin Streptomycin Dulbecco

**PBS** Phosphate-buffered saline

**PCR** Polymerase chain reaction

PLC Phospholipase C

Prdx Peroxiredoxins

Prx Peroxiredoxins

**PSS** Physiological salt solution

**PTP** Protein tyrosine phosphatases

**QIAGEN** QIAzol® Lysis Reagent

**qPCR** Quantitative polymerase chain reaction

**RAAS** Renin-angiotensin-aldosterone system

**RNA** Ribonucleic acid

**ROS** Reactive oxygen species

**RT** Reverse transcription

**RT-PCR** Real-time polymerase chain reaction

**SDS** Sodium dodecyl sulphate

**PAGE** Sodium dodecyl sulphate-polyacrylamide gel electrophoresis

**SHR** Spontaneously hypertensive rat

**SHRSP** Stroke-prone spontaneously hypertensive

SMGS Smooth muscle growth supplement
SMGS Smooth Muscle Growth Supplement

**SNP** Sodium nitroprusside

-SO<sub>3</sub>H Sulfonic acid

**SOD** Superoxide dismutase

**TBA** Thiobarbituric acid

**TBARS** Thiobarbituric acid reactive substances

**TBARS** Thiobarbituric acid-reacting substances

TCA Trichloroacetic acid

Trx Thioredoxin

TUDCA Tauroursodeoxycholic acid

Tunica Tunicamycin

**UPR** Unfolded protein response

Veh Vehicle

VSM Vascular smooth muscle

VSMCs Vascular smooth muscle cells

WKY Wistar Kyoto

WT Wild type

# Chapter 1 Introduction

# 1.1 Hypertension

Hypertension is a major risk factor for cardiovascular disease (CVD), chronic kidney disease (CKD), and cognitive impairment, and it significantly contributes to all-cause morbidity and mortality worldwide (MillsStefanescu and He, 2020, Oparil et al., 2018a). It is a chronic condition characterized by elevated blood pressure (BP), defined as a systolic blood pressure ≥140 mmHg and/or a diastolic pressure ≥ 90 mmHg in accordance with most major guidelines (Unger et al., 2020, Oparil et al., 2018a). The majority (90-95%) of patients with hypertension are diagnosed with essential (primary) hypertension. The precise etiology of essential hypertension remains poorly understood, necessitating a more detailed exploration of its molecular pathogenesis (Coffman, 2011, Tackling and Borhade, 2020).

## 1.1.1 Epidemiology

Globally, over one billion adults are afflicted with hypertension, representing about a quarter of the adult population(2017). From 1975 to 2015, high-income western and Asia Pacific regions experienced significant reductions in average systolic and diastolic blood pressure(2017). Conversely, average blood pressure has risen in regions such as East and Southeast Asia, South Asia, Oceania, and Sub-Saharan Africa(2017). During this 40-year period, the global count of adults with hypertension nearly doubled from 594 million to 1.13 billion, primarily in low- and middle-income countries. According to predictions, the number of people with hypertension could approach 1.5 billion by 2025 (Kearney et al., 2005). The Global Burden of Disease study indicates that non-optimal blood pressure is a major health concern, leading to approximately 9.4 million deaths and 212 million lost healthy life years annually, accounting for 8.5% of the global total (Oparil et al., 2018b, 2016).

# 1.1.2 Pathophysiology

The persistent blood pressure elevation is attributed to perturbations of the central nervous system, the kidney, and the vasculature (McMaster et al., 2015, Harrison, 2014). Pathophysiology mechanisms responsible for hypertension are multifactorial and complex, involving many regulatory systems, including the activation of the sympathetic nervous system (SNS), the renin-angiotensin-aldosterone system (RAAS), and the immune system

with consequential endothelial dysfunction, cardiovascular remodelling and renal dysfunction (Oparil et al., 2018a, Duvnjak, 2007). In addition, the pathophysiological mechanisms of hypertension also include other factors such as genetic predisposition, environmental influences (such as high sodium intake, excessive alcohol consumption, and significant mental stress), and the ageing process.

The RAAS plays a critical role in the pathogenesis of hypertension with a widespread effect on BP regulation, including increasing sodium reabsorption, water reabsorption, vasoconstriction, endothelial dysfunction, and vascular injury (Oparil et al., 2018b). The RAAS primarily functions to control pressure-volume homeostasis in the kidneys. Renin, synthesised and stored in juxtaglomerular cells of the kidneys, is released in response to stimuli such as reduced blood pressure, decreased sodium chloride concentration in the distal tubule, increased vasodilation, and SNS activation (Oparil et al., 2018b). Angiotensinogen, predominantly produced and secreted by the liver, undergoes cleavage by renin at its N-terminal, resulting in angiotensin I formation. Subsequently, Angiotensin-Converting Enzyme (ACE) removes two C-terminal amino acids from angiotensin I, forming angiotensin II (Ang II), the central effector of the RAAS. Ang II plays a crucial role in regulating BP by mediated vasoconstriction, aldosterone secretion, enhancing sodium reabsorption and increasing sympathetic outflow (Guo et al., 2001). Ang II exerts its physiological and pathophysiological effects through two G-protein coupled receptors: Ang II type 1 receptor (AT1-R) and Ang II Type 2 Receptor (AT2-R). AT1-R mediates the physiological effects of Ang II, such as vasoconstriction and sodium and water reabsorption. Pathologically, AT1-R activation results in oxidative stress, fibrosis, tissue remodelling, inflammation, and elevated blood pressure (Guo et al., 2001, Karnik et al., 2015). Conversely, AT2-R mediates protective actions by promoting anti-inflammatory responses, inhibiting fibrosis, reducing sympathetic outflow, and inducing vasodilation (Karnik et al., 2015). In addition, the ACE2/angiotensin-(1-7)/Mas receptor (MasR) axis also plays a pivotal role in vasodilation (Povlsen et al., 2020). Aldosterone, a hormone primarily regulated by Ang II, is crucial in maintaining salt-water balance, blood pressure control, and cardiovascular remodelling. Together, RAAS is essential in the development of hypertension (Williams, 2005).

The endothelium critically regulates vascular tone via the production of nitric oxide (NO) and other vasoregulatorys that contribute to the pathophysiology of hypertension (Panza et al., 1993). The factors released from endothelial cells include vasodilators such as prostacyclin and endothelium-derived hyperpolarising factors and vasoconstrictors such as

endothelin 1 (ET-1), Ang II, and thromboxane A2 (Oparil et al., 2018b). ET-1 is a potent 21-amino-acid vasoconstrictor peptide produced in multiple tissues and operates in a paracrine or autocrine fashion. It acts on two cell surface G-protein coupled receptors: the endothelin type A receptor (ET<sub>A</sub>R) and endothelin type B receptor (ET<sub>B</sub>R) on neighbouring endothelial or smooth muscle cells (Sandoval et al., 2014). ET<sub>A</sub>R and ET<sub>B</sub>R on smooth muscle lead to contraction and promote cellular proliferation and hypertrophy (Sandoval et al., 2014). In contrast, ET<sub>B</sub>R located on endothelial cells stimulates the production of nitric oxide and prostacyclin, inducing vasorelaxation (Oparil et al., 2018b). High levels of ET-1 have been observed in animal and human models of hypertension, which are implicated in causing end-organ damage, including vascular hypertrophy and remodelling (Trensz et al., 2019, Schiffrin, 1998, Kostov, 2021) In individuals with hypertension, while the circulating levels of ET-1 are not consistently elevated, there is a trend towards an enhanced sensitivity to its vasoconstrictor and hypertensive effects (Lazich and Bakris, 2011). Notably, the ET<sub>A</sub>R blocker has been suggested to attenuate the high BP in different animal models and human (Lazich and Bakris, 2011, Weber et al., 2009, Kohan and Barton, 2014). Besides, dual ET-1 receptor antagonists have been found to lower BP in patients with essential hypertension on phase 2 trial (McCoy and Lisenby, 2021, Angeli Verdecchia and Reboldi, 2021).

## 1.1.3 Diagnosis and management

Essential hypertension typically does not exhibit any noticeable, highlighting the importance of regular BP monitoring during medical consultations for adults. Blood pressure readings can vary due to time, environment, and measurement technique (BueltRichards and Jones, 2021). In healthcare settings, including physician's offices, hypertension is diagnosed when BP readings consistently exceed 140/90 mm Hg (BueltRichards and Jones, 2021). To ensure accuracy, these readings should ideally be obtained using an electronic device and by adhering to standard measurement protocols, which include repeated measurements (BueltRichards and Jones, 2021). Besides, the evaluation of a patient with hypertension should also include an assessment of their CVD risk, target organ damage, and associated clinical conditions that could impact BP or cause related organ damage, as well as the identification of features indicative of secondary hypertension (Oparil et al., 2018b).

The non-pharmacological management of patients with hypertension includes reduced salt intake, increased potassium intake, less alcohol intake, more physical activity, and avoiding obesity (Oparil et al., 2018b).

Antihypertensive pharmacotherapy has developed over several decades, with various classes of medications demonstrating substantial improvements in the morbidity and mortality rates associated with CVD (Ettehad et al., 2016). First-line medications include for hypertension treatment include ACE inhibitors (ACEI), Ang II receptor blockers (ARBs), calcium channel blockers (CCB), diuretics, and beta-adrenoreceptor blockers (Oparil et al., 2018b, CameronLang and Touyz, 2016, Frishman, 2016). The initial use of beta-blockers is controversial without any cardiovascular comorbidities in hypertension treatment(Whelton et al., 2018). The ACEI and ARBs reduce BP by acting in RAAS via inhibition of the production and action of Ang II, respectively (van Thiel et al., 2015). CCBs control BP by inhibiting calcium influx through L-type calcium channels, which leads to the relaxation of arteriolar smooth muscle and a consequent reduction in vascular peripheral resistance (Whelton et al., 2018). Diuretics decrease BP by enhancing urinary output and sodium excretion, effectively reducing body fluid volume (Silvade Figueiredo and Rios, 2019). Beta-blockers reduce BP by engaging with receptors in various tissues and modifying the sympathetic nervous system's activity that supplies these tissues, thus influencing cardiovascular responses (Silvade Figueiredo and Rios, 2019). In cases of severe hypertension, combination therapy tends to be more effective, though it is essential to consider the cumulative effects and potential adverse reactions of these drugs.

# 1.2 Vascular dysfunction in hypertension

Essential hypertension is characterised by increased cardiac output and peripheral resistance (Mayet and Hughes, 2003). While most patients with essential hypertension present with normal cardiac output, they exhibit elevated peripheral resistance (BeeversLip and O'Brien, 2001). Resistance vessels, particularly arteries with diameters smaller than 300 μm, are crucial in regulating vascular tone and blood flow (HeagertyHeerkens and Izzard, 2010, Naiel et al., 2019). According to Poiseuille's Law, vessel resistance is inversely proportional to the fourth power of the radius. Thus, small changes in arterial diameter have a major impact on vascular resistance and subsequently affect blood pressure (Welsh et al., 2018). In the early stages, changes in the vasculature are adaptive, but chronic conditions can cause maladaptive processes. This progression results in vascular remodelling and the development of rigid, stiff, and poorly compliant vessels, a

hallmark of chronic hypertension (Touyz et al., 2018, Intengan et al., 1999a). Resistance arteries undergo increased contractility, endothelial dysfunction, inflammation and structural remodelling, which are involved in both the cause and consequence of high blood pressure (Touyz et al., 2018). These vascular changes further impact other organs, such as the heart, kidneys, and brain, leading to target organ damage (Touyz et al., 2018).

#### 1.2.1 Vascular Structure

The vascular system is crucial as it contributes to and is a target of high blood pressure. Arteries are blood vessels that carry oxygenated blood away from the heart to organs and tissues throughout the body. The arterial system consists of large elastic arteries, resistance arteries, arterioles, and capillaries. The arterial wall is composed of three different anatomical regions: tunica intima, tunica media, and tunica adventitia (Touyz et al., 2018, Martinez-Quinones et al., 2018). The tunica intima, the innermost layer of the artery, consists of a single layer of vascular endothelial cells, underlain by a connective tissue basement membrane interspersed with elastic fibres (Cahill and Redmond, 2016). The tunica media, the thickest layer of the artery, comprises multiple layers of vascular smooth muscle cells (VSMCs). This layer provides structural support to the vessel and plays a crucial role in regulating constriction and dilatation of the blood vessels. Lastly, the tunica adventitia, the outermost layer, anchors the vessel to the surrounding tissues. It contains fibroblasts, adipocytes, connective tissue, and components of the extracellular matrix (Touyz et al., 2018).

# 1.2.2 Endothelial dysfunction

The endothelium, the body's largest endocrine organ, is critical in vascular health. It maintains the vascular tone and structure by balancing various processes, such as vasodilation and vasoconstriction, antithrombosis and prothrombosis, growth promotion and inhibition, anti-inflammatory and pro-inflammatory actions, and pro-oxidation and antioxidative effects, which are essential to ensure optimal vascular function (VaneAnggård and Botting, 1990, Higashi et al., 2003, Vanhoutte, 1989). Any imbalance of these processes could lead to endothelial dysfunction, which is easily identifiable by diminished vascular relaxation in response to endothelium-dependent vasodilators such as acetylcholine (Ach) (Münzel et al., 2008). It has been reported that individuals diagnosed with hypertension present with impaired endothelium-dependent relaxation in different resistance arteries (Higashi et al., 1999).

Endothelial dysfunction is characterised as a functional and reversible alteration in endothelial cells, primarily due to impaired availability of nitric oxide (NO) (Taddei et al., 2002). Endothelial cells play a crucial role in regulating vascular relaxation by releasing endothelium-derived nitric oxide, which stimulates soluble guanylate cyclase (sGC) in VSMCs, leading to an increase in intracellular cyclic guanosine monophosphate (cGMP), an essential process in the modulation of vascular tone (Benjamin and Vane, 1996, Huang et al., 1995). The mechanisms disrupting the bioavailability of endothelium-derived NO in hypertension include: i) reduced expression of endothelial nitric oxide synthase (eNOS), the primary enzyme for NO production; ii) decreased activation of eNOS; and iii) enhanced quenching of NO due to high levels of ROS (Touyz, 2002). In eNOS knockout mice, systolic blood pressure (SBP) elevation of nearly 30 mmHg compared to wild type highlights the essential role of nitric oxide in blood pressure regulation (Huang et al., 1995).

Endothelial dysfunction may lead to increased peripheral resistance through enhanced constriction and vascular remodelling of resistance arteries, which are associated with hypertension development and complications. Underlying mechanisms include impaired vascular shear stress, oxidative stress, inflammation, and RAAS activation (GalloVolpe and Savoia, 2021). Mechanical stimuli, such as changes in flow velocity and pressure within the vasculature, impact the tension of smooth muscle. Increased flow velocity (shear stress) elevates cytosolic calcium concentration by regulating ion channels, thus stimulating eNOS activity and NO synthesis in endothelial cells, while elevated pressure decreases NO bioavailability and ET-1 release (ZhouLi and Chien, 2014, Konukoglu and Uzun, 2017). Oxidative stress, marked by increased ROS levels, leads to endothelial dysfunction by reducing NO bioavailability through enhanced NO quenching (Touyz et al., 2020). Hypertensive patients have higher pro-inflammatory cytokine levels in plasma, which downregulate eNOS activity (Konukoglu and Uzun, 2017). Chronic inflammation also triggers oxidative stress, further impairing endothelial function (Touyz et al., 2020). RAAS, especially its key effector Ang II, affects endothelial function by regulating oxidative stress, vasoconstriction, and inflammation. Furthermore, the ACE-2/Ang(1-7)/Mas axis increases NO bioavailability and reduces ROS production during selective AT1R blockade, improving endothelial function and resistance artery remodelling (Povlsen et al., 2020).

Reducing BP does not directly restore endothelial function. However, some antihypertensive medications have been shown to improve endothelia function (Silvade Figueiredo and Rios, 2019). The ACEIs and ARBs are notably beneficial for endothelial

function, primarily through their mechanism of reducing oxidative and inflammatory effects triggered by Ang II, thereby ameliorating endothelial dysfunction (Taddei et al., 2002). CCBs exhibit pleiotropic effects that enhance endothelial function, including antioxidant effects and the promotion of eNOS activation (Taddei et al., 2002). Furthermore, some third-generation beta-blockers have been shown to have beneficial effects on the endothelium of hypertensive patients through antioxidant mechanisms (VirdisGhiadoni and Taddei, 2011).

#### 1.2.3 Vascular remodelling

The vascular wall, a dynamic autocrine-paracrine complex formed by the interaction of endothelial cells, smooth muscle cells, and fibroblasts, plays a pivotal role in vascularisation by detecting environmental changes, integrating intercellular communication signals, and influencing vascular structure and function through the local production of mediators (Rennade Las Heras and Miatello, 2013). Vascular remodelling indicates the structure changes of the vascular wall in response to pathological conditions that involve at least four cellular processes: cell proliferation, cell migration, cell death, and the synthesis or degradation of the extracellular matrix (Gibbons and Dzau, 1994).

In essential hypertension, the remodelling of resistance arteries is characterised by structure alterations in the vasculature, primarily attributed to increases in the media-to-lumen or wall-to-lumen ratios (Mulvany and Aalkjaer, 1990, Heagerty et al., 1993). Two types of remodelling are observed: inward eutrophic remodelling and inward hypertrophic remodelling (Schiffrin, 2012, Schiffrin, 2004). Inward eutrophic remodelling is characterised by decreasing outer lumen diameters and increased wall-to-lumen ratios, typically observed in the resistance arteries of essential hypertension. In contrast, inward hypertrophic remodelling involves VSMC hypertrophy or hyperplasia, commonly seen in secondary hypertension and other CVD (RizzoniAgabiti-Rosei and De Ciuceis, 2023). Patients with mild-to-moderate hypertension may exhibit eutrophic remodelling, as evidenced by a decreased media/lumen ratio, without alterations in media thickness or cross-sectional area in the resistance arteries of gluteal subcutaneous tissue (SchiffrinDeng and Larochelle, 1993). Increases in blood pressure associated with the RAAS are often linked to eutrophic remodelling, and AT1 antagonists have been shown to correct these changes in vessel structure over time (Schiffrin et al., 2000).

Remodelling of the extracellular matrix plays a crucial role in vascular remodelling, involving the deposition of proteins such as collagen, cell migration, secretion of components, and the reorganisation of the extracellular matrix and cell interactions (Schiffrin, 2004). The deposition of proteins within the matrix contributes to the reorganisation of vessel wall components and embeds a chronically vasoconstrictive state in small arteries of hypertensive animals and patients (Intengan et al., 1999b, Intengan et al., 1999a). The increase in protein deposition may also result from diminished activity of matrix metalloproteinases (MMPs), enzymes that degrade extracellular matrix proteins, as observed in the mesenteric arteries of SHR (Intengan and Schiffrin, 2000).

The inward remodelling of small vessels both results from and contributes to increased vasoconstriction. The underlying mechanisms involve changes in post-receptor signalling and oxidative stress during hypertension (Schiffrin, 2004). For example, Ang II binds to the AT1R, it triggers the activation of heterotrimeric G proteins, leading to a cascade of second messenger signalling that includes inositol trisphosphate (IP3), diacylglycerol (DAG), arachidonic acid, and reactive oxygen species (ROS) (Zeng and Yang, 2024). Consequently, downstream effectors such as phospholipases C, A, and D are activated, further influencing vasoconstriction and remodelling. Besides, Ang II induces oxidative stress by stimulating NADPH oxidases (Nox) to produce ROS, which could promote the proliferation of VSMCs and damage endothelial cells (Zeng and Yang, 2024). Furthermore, the abnormal function of ion channels, such as calcium, potassium, and sodium channels, can disrupt vascular tone regulation and contribute to vascular remodelling (Zeng and Yang, 2024).

# 1.2.4 Vascular smooth muscle cells phenotypic switching

In the vasculature, VSMCs play a pivotal role in regulating blood flow and distribution. In adult vessels, VSMCs express ion channels, signalling molecules and contractile proteins that are essential for regulating vessel contraction (Elmarasi et al., 2024). Differentiated VSMCs exhibit a high degree of plasticity, enabling them to adapt their phenotypes in response to local environmental changes (Brozovich et al., 2016). Physiologically, these cells exhibit low synthetic activity and proliferation rate, maintaining a primarily contractile phenotype, which is crucial for maintaining vascular tone and function (Zhang et al., 2021).

Contractile VSMCs have a spindle-shaped morphology and typically express specific contractile and cytoskeletal proteins, such as smooth muscle myosin heavy chain (SM-MHC), α-smooth muscle actin (α-SMA), calponin, and caldesmon (Chamley-CampbellCampbell and Ross, 1979). In contrast, synthetic or secretory VSMCs display a more elongated morphology, express proteins such as vimentin, collagen, and fibronectin, and participate in vascular repair and remodelling (Elmarasi et al., 2024). The population of dedifferentiated VSMCs can vary significantly within injured or diseased vasculature, such as in the context of hypertension (Elmarasi et al., 2024).

In hypertensive patients, VSMCs have the capacity to change into phenotypes that can withstand high blood pressure (Elmarasi et al., 2024). In large arteries, VSMCs express contractile genes that result in a tonic phenotype, whereas arterioles produce a phasic phenotype (OwensKumar and Wamhoff, 2004). Moreover, VSMCs can lose their contractile markers (SM-MHC, α-SMA, calponin, etc.) and change to a synthetic phenotype under biological stress signals. Synthetic VSMCs contribute to signalling molecules that promote cell proliferation, migration, fibrosis, and inflammation (Touyz et al., 2018). Studies have shown diminished expression of contractile markers in vessels exposed to high blood pressure, highlighting the connection between these proteins and impaired vascular function (Cao et al., 2022, Nemenoff et al., 2011).

#### 1.2.5 Vascular smooth muscle contraction

Vascular smooth muscle contraction is primarily regulated by the activation of contractile proteins in VSMCs (Touyz et al., 2018). This contraction involves the formation of actin-myosin cross-bridges, which is controlled by the phosphorylation state of myosin light chain 20 (MLC<sub>20</sub>) (Touyz et al., 2018). Myosin light chain kinase (MLCK) phosphorylates MLC<sub>20</sub>, promoting contraction, while myosin light chain phosphatase (MLCP) dephosphorylates MLC<sub>20</sub>, leading to relaxation (Yang and Hori, 2021, Touyz et al., 2018, Webb, 2003, Ito and Hartshorne, 1990).

A crucial event in vascular smooth muscle excitation-contraction coupling is the increase in intracellular calcium concentration ([Ca<sup>2+</sup>]i), which is regulated by mechanical, humoral, or neural stimuli<sup>39</sup>. The regulation of [Ca<sup>2+</sup>]i and calcium signalling is orchestrated by various plasma membrane channels, exchangers, and transporters, as well as intracellular stores like the sarcoplasmic reticulum, mitochondria, and calcium-binding proteins (Little et al., 1992). In hypertension, pro-hypertensive factors such as vasoactive peptides (Ang II

and ET-1) and neurohumoral stimuli (norepinephrine and acetylcholine) trigger the activation of G protein-coupled receptors (GPCRs) (Touyz et al., 2018). This activation stimulates phospholipase C (PLC), which subsequently generates the second messenger inositol trisphosphate (IP3) and diacylglycerol (DAG) (Matsumura et al., 1995). IP3 increases [Ca<sup>2+</sup>]i by stimulating its release from the sarcoplasmic reticulum, while DAG activates protein kinase C (PKC) (WynneChiao and Webb, 2009). Additionally, different calcium entry channels such as voltage-operated channels (VOC), receptor-operated channels (ROC), store-operated channels (SOC), transient receptor potential (TRP) channels, and Ca<sup>2+</sup>-permeable nonselective cation channels (NSCC) promote calcium influx, thus increasing [Ca<sup>2+</sup>]i (WynneChiao and Webb, 2009). Increased [Ca<sup>2+</sup>]i triggers MLCK activation and phosphorylates the MLC<sub>20</sub>, initiating the interaction between actin and myosin filaments, which leads to muscle contraction (Touyz et al., 2018).

In hypertensive vascular smooth muscle, the regulation of several mechanisms related to intracellular calcium homeostasis is disrupted, leading to abnormal calcium handling and elevated [Ca<sup>2+</sup>]i. Elevated [Ca<sup>2+</sup>]i has been observed in both experimental and human hypertension, which is attributed to increased calcium influx through calcium channels, enhanced release of calcium from the sarcoplasmic reticulum, reduced reuptake of calcium into the sarcoplasmic reticulum, and activation of the PLC-DAG-IP3 pathway (MatsudaLozinskaya and Cox, 1997, Misárková et al., 2016, BazanCampbell and Rapoport, 1992, TouyzDeng and Schiffrin, 1995).

Calcium-independent mechanisms, such as the DAG-PLC-PKC pathway and the RhoA-Rho kinase (ROCK) pathway, also regulate vascular smooth muscle contraction through calcium sensitisation, which maintains muscle force after the initial calcium signal dissipates (Touyz et al., 2018). Activation of PKC induces the phosphorylation of downstream signalling proteins, including CPI-17, which phosphorylated inhibits MLCP phosphatase activity by binding to its catalytic domain. Activation of GPCRs by vasoactive agents leads to the release of RhoA, which then activates ROCK (Touyz et al., 2018). Activated ROCK phosphorylates myosin phosphatase target subunit 1 (MYPT1) and CPI-17, inhibiting myosin light chain phosphatase (MLCP). This inhibition maintains MLC<sub>20</sub> phosphorylation and sustains muscle contraction (Lebeau et al., 2021).

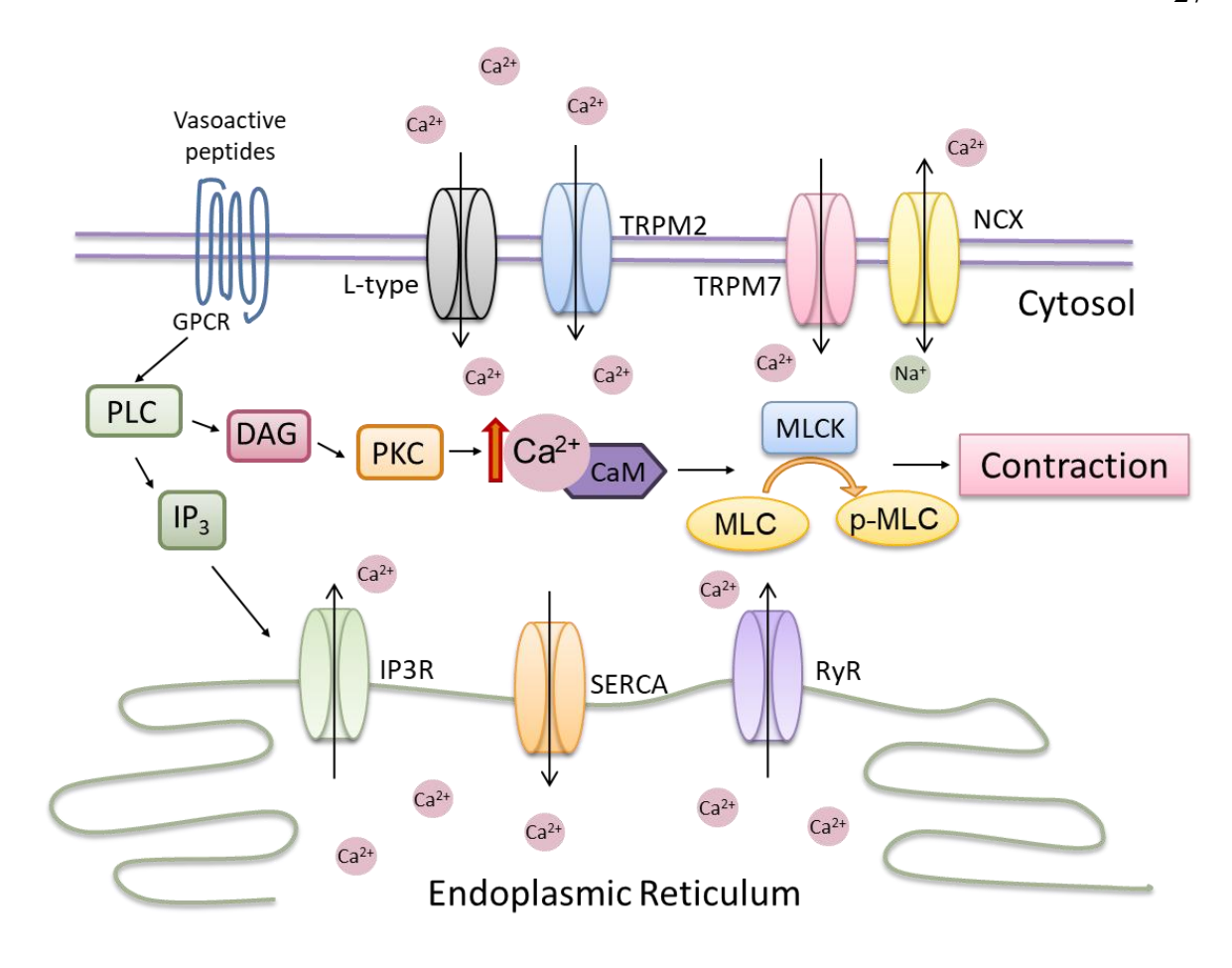


Figure 1.1 Vascular smooth muscle contraction.

Intracellular calcium concentration is increased by different signalling pathways and calcium channels, including plasma membrane channels, exchangers, and intracellular stores like the endoplasmic reticulum.

#### 1.3 Oxidative stress

Oxidative stress is characterised by increased bioavailability of reactive oxygen species (ROS), reduced nitric oxide (NO) levels and decreased antioxidant production in the vasculature observed in both experimental and human hypertension (RodrigoGonzalez and Paoletto, 2011, Montezano and Touyz, 2012, Brito et al., 2015). Physiologically, ROS are signalling molecules that regulate vascular structure and function. ROS are constantly generated by homeostatic cells and are essential in physiologically regulating all cellular functions (de Champlain et al., 2004). NADPH oxidants (Noxs) are the primary source of ROS in the vascular wall, and their activation has been strongly associated with the pathogenesis of hypertension (Majzunova et al., 2013). Nox-dependent ROS production can be triggered by stimulation of neurohumoral vasoconstrictor agents such as angiotensin II (AngII), endothelin-1(ET-1), and aldosterone (Aldo) (Montezano et al., 2015). The major ROS resulting from oxidative stress include hydrogen peroxide (H<sub>2</sub>O<sub>2</sub>) and

superoxide (O<sub>2</sub>-), which are electron donors and can damage DNA, RNA, proteins, and lipids, contributing to vascular remodelling and dysfunction in hypertension. Superoxide anion is a free radical, which serves as the origin of the cascade formatting of many other biologically relevant ROS (Loperena and Harrison, 2017). It is usually short-lived because of the rapid reduction by superoxide dismutase (SOD) to H<sub>2</sub>O<sub>2</sub>. Hydrogen peroxide is relatively stable under physiologic conditions as it is a non-radical ROS. It can be further reduced to water and oxygen by catalase or glutathione peroxidase (GPx).

ROS are products of natural mediators or metabolites of most cellular mechanisms and derive from many sources in different cellular compartments. Several enzymes are capable of producing ROS in hypertension by transferring electrons from an electron donor to molecular oxygen, including nicotinamide adenine dinucleotide phosphate (NADPH) oxidases (NOX), xanthine oxidoreductase (XOR), mitochondrial enzymes and uncoupled NO synthase (NOS) (Giustarini et al., 2009, Sorescu et al., 2002).

The nicotinamide adenine dinucleotide phosphate oxidases (Nox) are a rich source of ROS, particularly of superoxide and H<sub>2</sub>O<sub>2</sub>, in kidney and vasculature, which plays an essential role in renal dysfunction and vascular damage (Touyz, 2004, Feairheller et al., 2009). Nox is a primary source of ROS in the vascular wall, and its activation is strongly associated with the pathogenesis of hypertension (Majzunova et al., 2013). Significantly, Nox-dependent ROS production can be triggered by stimulation of neurohumoral vasoconstrictor agents such as angiotensin II, endothelin-1, urotensin-II (UT-II) and norepinephrine (NE) (Montezano et al., 2015). Xanthine oxidase (XO) is another source of ROS that has been shown to contribute to experimental hypertension (Shirakura et al., 2016) and human hypertension (Kohagura et al., 2016). In addition, functional uncoupling of eNOS leads to the production of superoxidase rather than protective NO (Kohagura et al., 2016), which has also been suggested to be an important source of ROS for hypertension (Roe and Ren, 2012). Finally, dysfunction of the mitochondrial respiratory chain during ATP synthesis increases the mitochondrial ROS formation (Radi et al., 2002).

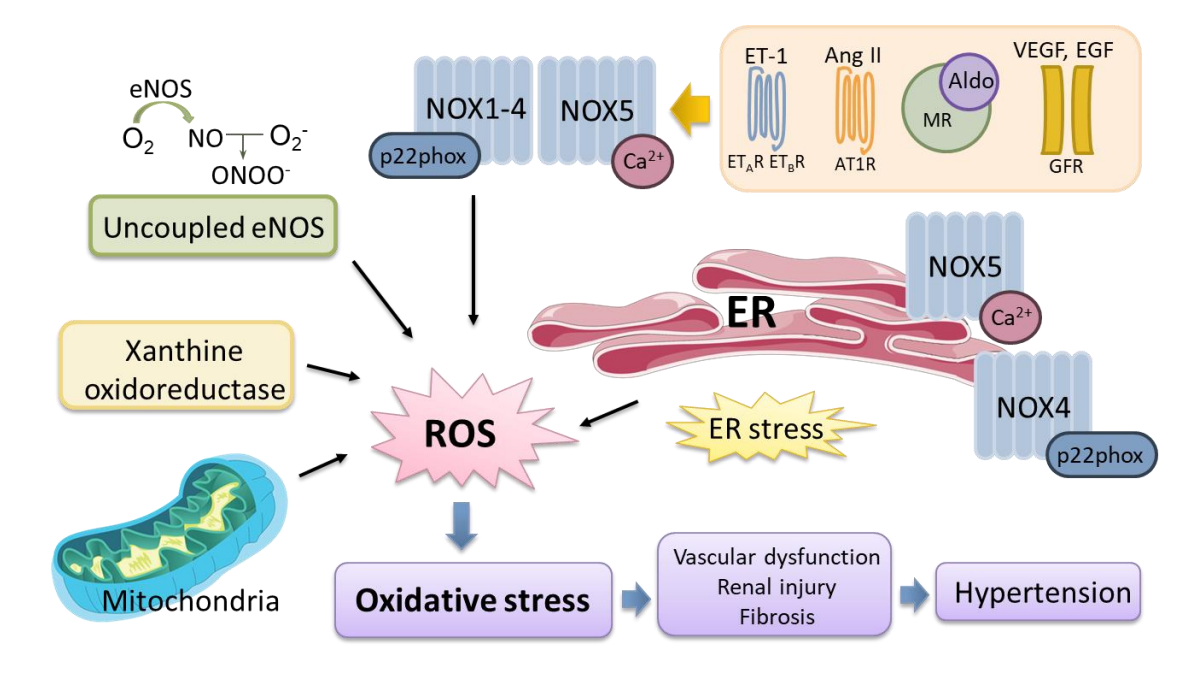


Figure 1.2 Sources of ROS in hypertension.

In hypertension, various enzymes contribute to the production of ROS by transferring electrons from electron donors to molecular oxygen. Key sources include NADPH oxidases, xanthine oxidoreductase (XOR), mitochondrial enzymes, and uncoupled nitric oxide synthase (NOS).

#### 1.3.1 NADPH oxidases

NADPH oxidases (NOX) are a family of enzymes that generate reactive oxygen species (ROS), playing critical roles in various cellular functions and disease processes. The NOX family consists of seven members: NOX1 to NOX5, and DUOX1 and DUOX2 (Montezano et al., 2015, Touyz et al., 2002). These enzymes transfer electrons from NADPH to oxygen, producing superoxide and hydrogen peroxide, which are essential for cellular signalling, host defence, and homeostasis (Touyz, 2004, Feairheller et al., 2009, Majzunova et al., 2013).

NOX enzymes have distinct tissue distributions and functions. The classical NADPH oxidase, Nox2, is a multi-subunit complex composed, including 2 membrane-associated components (Nox2 (gp91phox) and p22phox), three cytosolic subunits (p47-phox, p67-phox, p40-phox), and the small molecular weight GTPase Rac (Lambeth, 2004, Rastogi et al., 2016). During Nox2 activation, cytosolic proteins translocate to the membrane leading to transfer of one electron from NADPH to oxygen, producing superoxide anion. Nox1 is also associated with p22 phox and depends on translocation of cytosolic subunits NoxO1 (Nox organizer 1, p47phox homologue), NoxA1 (Nox activator 1, p67 phox homologue), p40

phox and Rac1 to activation and producing superoxide anion(Dutta and Rittinger, 2010). NOX3 is primarily expressed in the inner ear and is essential for the formation of otoconia, necessary for balance and hearing (Rousset et al., 2015). NOX4 is ubiquitously expressed and involved in processes such as cell differentiation, apoptosis, and fibrogenesis. Nox4 activation produces primarily rather than and does not need cytosolic subunits, and it is associated with p22phox in the membrane (Schurmann et al., 2015). NOX5 is a calcium-activated NADPH oxidase that localizes primarily in the perinuclear and endoplasmic reticulum regions, translocating to the plasma membrane upon activation (Touyz et al., 2019). It is tightly regulated by post-translational modifications and is activated by stimuli such as vasoactive agents, growth factors, and pro-inflammatory cytokines (Touyz et al., 2019). Duox1 and Duox2 are calcium-activated oxidases predominantly found in epithelial cells lining mucosal surfaces, with particularly high expression levels in the thyroid gland (van der VlietDanyal and Heppner, 2018).

Dysregulation of NOX enzymes is associated with numerous diseases. Overactivation of NOX2 is linked to cardiovascular diseases such as atherosclerosis and hypertension (Lassègue and Griendling, 2010). NOX4 has been implicated in diabetic nephropathy and pulmonary fibrosis, indicating its role in chronic kidney and lung diseases (Hecker et al., 2009, Jha et al., 2016). NOX-derived ROS also play a part in cancer progression, particularly in thyroid cancer where NOX4 contributes to hypoxia adaptation, enhancing cancer cell survival under low oxygen conditions(Tang et al., 2018). Inhibitors specific to NOX enzymes are being developed to treat conditions associated with excessive ROS production. For instance, NOX2 inhibitors are being explored for their potential to mitigate oxidative stress in cardiovascular diseases, while NOX4 inhibitors are considered for fibrotic diseases (Altenhöfer et al., 2015).

#### 1.3.2 Antioxidants

To maintain redox homeostasis, several antioxidant defence systems regulate ROS levels and defend cells from oxidative damage. O<sub>2</sub>-• serves as the origin of the cascade forming many other biologically relevant ROS (Loperena and Harrison, 2017), which is usually short-lived due to the rapid reduction by superoxide dismutase (SOD) to H<sub>2</sub>O<sub>2</sub> (Fridovich, 1997). On the contrary, H<sub>2</sub>O<sub>2</sub> is relatively stable under physiologic conditions as it is a non-radical ROS. It can be further reduced to water and oxygen by catalase, glutathione peroxidase (GPx), peroxiredoxins (Prx), and/or thioredoxin (Trx) reductase (Simic et al., 2006, Sui et al., 2005).

### 1.3.3 Oxidative stress in hypertension

Over production of ROS results in oxidative stress and drives target organ damage in hypertension (Coats and Jain, 2017), such as in the CNS (Lob et al., 2013, Zimmerman et al., 2002), in the kidney (Trott et al., 2014), and in the vasculature (Lee and Griendling, 2008). These damage in experimental hypertension in cardiac, vascular and renal injury and inflammation are redox-sensitive processes since the treatment with NADPH oxidase inhibitors, ROS scavengers, and anti-oxidant vitamins can normalise blood pressure and show cardiovascular and renal protection.

# 1.4 Endoplasmic reticulum stress

The ER is responsible for synthesising about one-third of all eukaryotic cell proteins. ER stress is a type of cellular stress that resolves the protein-folding defect and restores ER homeostasis by triggering an adaptive program known as the unfolded protein response (UPR). The UPR transmit the protein folding status information to nuclear and cytosol, therefore adjusting the capacity of protein folding in the cell. Prolonged activation of UPR can lead to apoptotic cell death, inflammation, fibrosis and VSMC phenotypic switch (Uchida et al., 2022a, Spitler and Webb, 2014).

# 1.4.1 Unfolded protein response

The canonical branches of the UPR signalling pathway are mediated by three ER transmembrane sensors: protein kinase RNA-like ER kinase (PERK), inositol requiring kinase 1(IRE1α), and activating transcription factor 6 (ATF6). Under normal, unstressed conditions, the luminal domains of these three sensors are capped by the ER resident chaperone binding immunoglobulin protein (Bip, also known as the 78 - kDa glucose-regulated protein (GRP78)) to keep inactive. When misfolded/unfolded proteins accumulate in the ER lumen, Bip is recruited to release the UPR sensors and prevents Ca<sup>2+</sup> release into the cytosol (Gutierrez and Simmen, 2018). Bip recognises and binds to unfolded or misfolded proteins and initialises the three parallel protein sensors of UPR (PERK, IRE1a and ATF6)(Young et al., 2012).

IRE1α is the oldest branch of UPR and is a Ser/Thr protein kinase conserved from yeast to humans. IRE1 consists of an N-terminal ER luminal domain, which senses the unfolded proteins, and a C-terminal cytosolic region initiates the UPR through serine/threonine protein kinase and endoribonuclease domains (Siwecka et al., 2021). IRE1α activation

involves dimerises and autophosphorylates, causing a conformational switch that elicits its endoribonuclease activity. The unfolded protein activated the IRE1 pathway via dimerisation and trans-autophosphorylation of the endoribonuclease domain, subsequently adapting cellular response by splicing the XBP1 mRNA. In this process, a 26-nucleotide intron from the mRNA encoding the transcription factor X box-binding protein 1 (XBP1) is trimmed by IRE1a, which changes the coding reading frame and results in the translation of a more active and stable protein XBP1s (spliced XBP1) (Hetz, 2012). XBP1s act as a transcription factor that upregulates the target genes involved in UPR and ERAD (ER-associated protein degradation) to promote cytoprotection and restore ER homeostasis (LeeIwakoshi and Glimcher, 2003). Activation of IRE1a also triggers a nonspecific endonuclease activity that selectively targets and rapidly degrades ER membraneassociated mRNA by a process known as regulated IRE1-dependent decay (RIDD) (Hollien and Weissman, 2006). Under prolonged or severe stress conditions, IRE1 activation could also activate the pro-apoptotic c-Jun N-terminal kinase (JNK), resulting in apoptosis (Siwecka et al., 2021). IRE1 is involved in inflammatory signals by recruitment of adaptor protein tumour necrosis factor (TNF) receptor-associated factor 2 (TRAF2) to activate apoptosis signal-regulating kinase 1 (ASK1) and downstream JUN N-terminal kinase (JNK) thus actives NF-κB pathway to promote apoptosis (Ron and Hubbard, 2008). Moreover, IRE1α can control the levels of the caspase family by cleaving microRNAs to regulate apoptosis (Upton et al., 2012).

PERK, similar to IRE1, is a type1 transmembrane Ser/Thr protein kinase that dimerises and autophosphorylates after Bip release. Activated PERK phosphorylate the serine 51 of translation initiation factor eIF2α (eukaryotic initiation factors), leading to global translational repression (Glembotski, 2007). EIF2α phosphorylation acts as a competitor of eIF2B, resulting in a lower level of the initiator Met-tRNAiMet delivery to the ribosomal machinery, thus broadly suppressing global protein synthesis and alleviating the demands of protein folding and processing in ER (TeskeBaird and Wek, 2011). Phosphorylated eIF2α allows the translation of selective mRNAs, such as activating transcription factor 4 (ATF4), containing a structural feature of open reading frames in their 5′ untranslated region (Harding et al., 2000). ATF4 transcriptional activity induces prosurvival transcriptional programs through the expression of genes involved in amino acid transport, ER resident chaperones and oxidative stress resistance (Harding et al., 2003). Besides eIF2α activation, PERK is also responsible for phosphorylating nuclear erythroid two p45-related factor 2 (NRF2), which dissociates from NRF2-Keap1 complex in the cytoplasm, allowing NRF2 to translocate to the nucleus and regulate the expression of oxidative genes

(Cullinan et al., 2003). Simultaneously, eIF2α phosphorylation facilitates the preferential translation of the transcription factor ATF4, which in turn activates the UPR genes transcription to help the cell cope with the stress. Notably, besides ER stress, viral infection and nutrient deficiency also lead to eIF2α phosphorylation - ATF4 pathway activation via GCN2 (general control non repressed 2) and dsRNA induced PKR respectively (OchoaWu and Terada, 2018, Pakos-Zebrucka et al., 2016). Overexpression of ATF4 proapoptotic transcriptional programs by upregulation of genes involved in programmed cell death, such as the transcription factor C/EBP homologous protein (CHOP) and growth arrest and DNA damage-inducible 34 (GADD34) (Celli and Tsolis, 2015, Toth et al., 2007). Thus, ATF4 serves as a vital point of the integrated stress response (Pakos-Zebrucka et al., 2016). ATF4, either alone or in conjunction with its downstream target CHOP, may also contribute to cell death when cellular homeostasis cannot be restored (Pakos-Zebrucka et al., 2016).

ATF6α is a type II ER membrane protein. Upon ER stress, 90kDa ATF6 α monomer translocates to the Golgi lumen and is cleaved resident site 1 proteases (S1P) followed site 2 proteases (S2P), thus releasing the N-terminal cytosolic 50kDa fragment p50 (OchoaWu and Terada, 2018). P50 is a functioning bZIP transcription factor and targets the ER stress response element in the genes, which promote ER maintenance and post-translational modification such as Bip, GRP94, and cysteine cross-linker PDI (protein disulfide-isomerase) (Ron and Walter, 2007b).

ERO1 is an ER-resident thiol oxidoreductase, which works as a protein disulfide oxidase and helps PDI with disulfide bond formation (Zito, 2015). ERO1 also contributes to correct protein folding and improves the stress cope ability in cells by upregulating through UPR (Zito, 2015). ERO1 is an ER-resident thiol oxidoreductase, which contributes to correct protein folding and improves the stress-coping ability in cells by upregulated through UPR (Zito, 2015). Ero1 also works as a protein disulfide oxidase and helps PDI with disulfide bond formation (Zito, 2015).

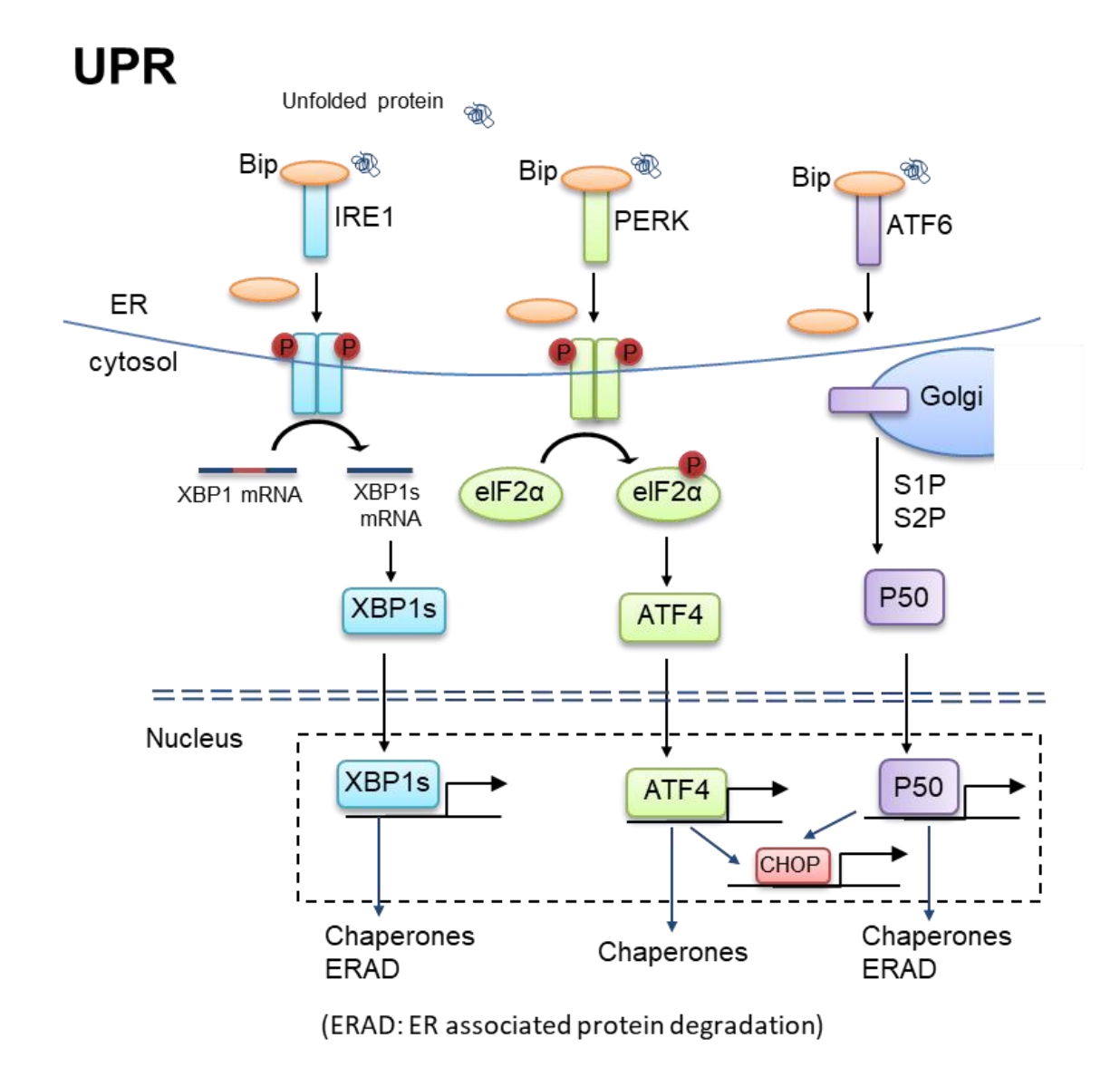


Figure 1.3 ER stress response.

The accumulation of unfolded proteins in the endoplasmic reticulum (ER) leads to their binding with Bip/GRP78, which in turn releases the ER stress sensors PERK, IRE1, and ATF6, thereby triggering ER stress activation. The dissociation from Bip allows PERK and IRE1 to oligomerise and ATF6 to translocate to the Golgi apparatus, collectively initiating the unfolded protein response (UPR). This response involves the transcriptional regulation of downstream effectors such as XBP1s, ATF4, P50, and CHOP, which enhance the production of UPR chaperones and activate ER-associated degradation (ERAD), ultimately exerting a protective effect by restoring protein homeostasis.

#### 1.4.2 The function of ER stress

ER stress plays a pivotal role in maintaining cellular homeostasis and function. The ER is crucial for protein folding, lipid metabolism, and calcium storage. When cells experience adverse conditions such as nutrient deprivation, hypoxia, or oxidative stress, the ER's capacity can be overwhelmed, leading to the accumulation of misfolded proteins. The

activation of UPR helps cells to cope stress by attenuating protein translation to avoid further misfolded/unfolded protein accumulation, activating transcription of ER stress-associated chaperones to facilitate the protein folding capacity, and rectifying the accumulation of protein by enhancing ER-associated degradation (ERAD) and autophagy (Groenendyk et al., 2010). While the primary function of the UPR is to promote cell survival and adaptation under stress conditions, chronic or unresolved ER stress can trigger apoptotic pathways. If the adaptive mechanisms fail, sustained activation of UPR sensors can lead to the induction of pro-apoptotic factors such as CHOP, thereby initiating programmed cell death to eliminate damaged cells. CHOP has been shown to induce cell death via upregulating pro-apoptotic BCL2 family (Galehdar et al., 2010) and death receptor DR5 under ER stress (Zou et al., 2008).

#### 1.4.3 ER stress and Oxidative stress

Redox signalling is involved in many different aspects of ER stress. Oxidative stress can lead to ER stress through thiol oxidation of ER molecular chaperones, disturbance in oxidative protein folding, and alterations in Ca<sup>2+</sup> levels in the ER(Eletto et al., 2014). On the contrary, ER stress can lead to oxidative stress by mitochondrial dysfunction, influencing Nox2 and Nox4 activation (LaurindoAraujo and Abrahao, 2014, Bhattarai et al., 2021). Moreover, Ang II is reported to increase ER stress markers in both in vivo and in vitro models. ER stress activation was involved in increased ROS generation and activation of proinflammatory, fibrotic and apoptotic pathways (Xu et al., 2009, Menikdiwela et al., 2019, Sepulveda-Fragoso et al., 2021). PERK can activate other signalling pathways, such as Nrf2/Keap1 and calcineurin/RyR2 (Liu et al., 2015).

Tunicamycin is known for its role in inducing ER stress by inhibiting N-linked glycan synthesis, which consequently leads to misfolded proteins and UPR activation. The increasing cellular ROS level by tunicamycin has been found in different cells, including PC12 cells (Yen et al., 2017a) and myoblasts (Anto et al., 2023). The activation of ER stress sensor PERK triggers the dissociation of Nrf2/Keap1 complexes, thus allowing Nrf2 to translocate into nuclear, which could contribute to increased antioxidants expression, such as GPx1, catalase and SOD (Cullinan et al., 2003).

Nox4 is the major Nox isoform that links ER stress to oxidative stress. Nox4 is involved in at least two of the three signalling branches of the UPR, and it is required for XBP1 splicing by IRE1 and in eIF2a phosphorylation by PERK (Sciarretta et al., 2013, Santos et

al., 2016, Chang et al., 2021, Kim et al., 2021, Janiszewski et al., 2005, Lee et al., 2020). Nox4 knockout mice do not affect eIF2a phosphorylation and ATF4 expression, suggesting there is no change in the PERK arm of the UPR. However, expression of Chop and Bip is increased in the kidneys of Nox4 knockout mice, suggesting a role for Nox4 in ER stress. The activation of ER stress response in the kidney from Nox4 knockout mice may differ from other tissues. Evidence in other studies showed that expression of Chop and ATF4 were decreased in Nox4 knockout aorta (Xie et al., 2017), expression of Chop and Bip was not changed by Nox4 silencing in human endothelial cells (Wu et al., 2010), and decreasing expression of ATF4 in cardiomyocytes of cardiac-specific Nox4 knockout mice (Sciarretta et al., 2013).

ER chaperone PDI upregulation has been found to be related to Nox4 activation. Nox4 is colocalised with PDI in cells such as rat kidney glomerular mesangial cells (BlockGorin and Abboud, 2009) and rabbit aortic smooth muscle cells (Miyano et al., 2020, Janiszewski et al., 2005). Evidence shows PDI overexpression increased Nox4 levels after Ang II stimulus, while PDI inhibition decreased Ang II-induced Nox4 activation in rabbit aortic smooth muscle cells (Fernandes et al., 2009) (Janiszewski et al., 2005).

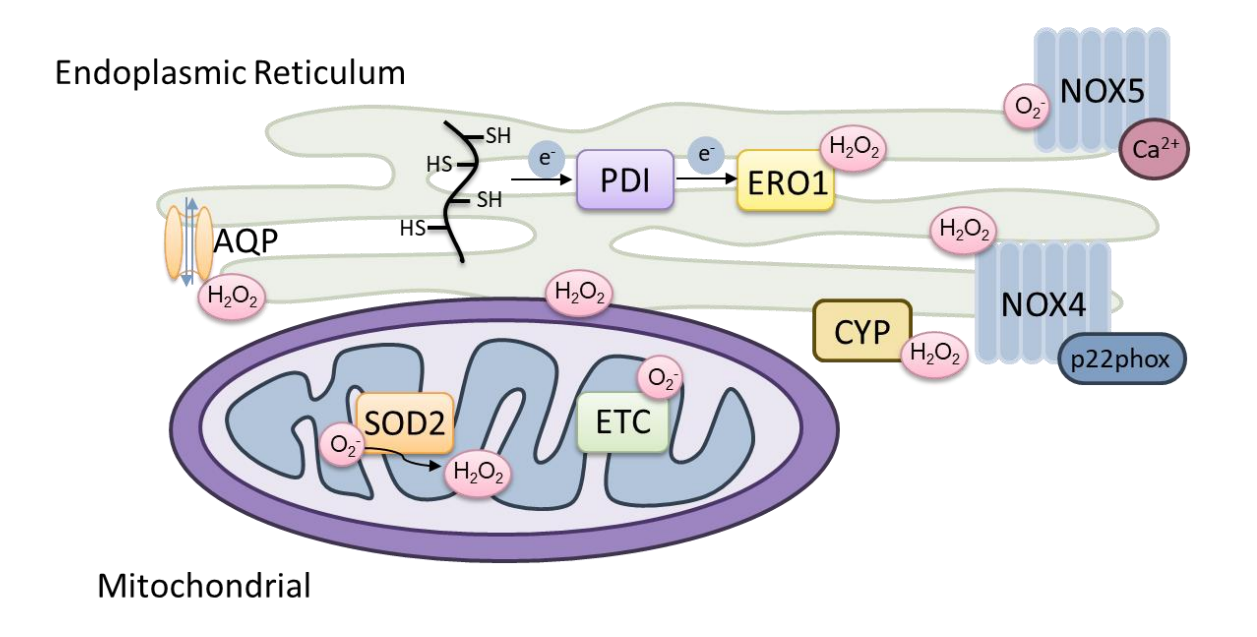


Figure 1.4 Sources of ROS in the ER.

During ER stress, several sources contribute to ROS generation. ER oxidoreductin 1 (ERO1), upregulated by CHOP, produces ROS during protein folding, leading to apoptosis. NADPH oxidases generate ROS, with NOX4 activating UPR sensors and NOX5 linked to ER stress-related apoptosis. Mitochondria-associated ER membranes (MAMs) increase mitochondrial ROS production via calcium transfer. Aquaporin 11 (AQP11) channels in the ER facilitate H2O2 transfer between the ER and mitochondria. Other key components include the electron transport chain (ETC), PDI, and SOD2.

# 1.4.4 ER stress and calcium dysfunction

ER plays a critical role in Ca<sup>2+</sup> homeostasis, and disruption of Ca<sup>2+</sup> homeostasis in the ER leads to activation of ER stress (GroenendykAgellon and Michalak, 2013). Intracellular Ca<sup>2+</sup> is mainly stored in the lumen of ER, which is essential for signalling and proper protein folding through the activity of Ca<sup>2+</sup>-binding chaperones (KuznetsovBrostrom and Brostrom, 1992). It has been found that ER stress inducer Tunicamycin increased cytosolic Ca<sup>2+</sup> in parallel with a reduction of ER Ca<sup>2+</sup> in VSMCs from mice (Liang et al., 2013). Also, it was demonstrated that 24h exposure of Tunicamycin can reduce ER Ca<sup>2+</sup> levels in HuH7 cells in a dose dependent manner (Lebeau et al., 2021). The activation of IP3R or inhibition of SERCA ultimately leads to Ca<sup>2+</sup>-store depletion, thus contributing to ER stress (Luciani et al., 2009, Kiviluoto et al., 2013). One possible reason for this effect is that some ER-resident chaperones require a high Ca<sup>2+</sup> concentration for their activity, such as calreticulin and Bip (Coe and Michalak, 2009, Corbett and Michalak, 2000). Furthermore, ER stress induced IP3R1 dysfunction through an impaired IP3R1-Bip interaction promotes cell death (Higo et al., 2010).

# 1.4.5 ER stress in hypertension

ER stress has been associated with many essential hypertensive models. Tunicamycin is an ER stress inducer that inhibits protein glycosylation. Tunicamycin infusion induces ER stress in mouse aortas in vivo and promotes elevation of systolic and diastolic blood pressure by increased vascular smooth muscle contractility. Ang II-induced hypertension in mice caused ER stress in the brain circumventricular subfornical organ (SFO) by increasing expression of Bip, p-PERK and CHOP. Injection of Ang II in mice induces Bip and CHOP expression in mesenteric arteries, myocardium, and aortas. Research has shown that long-term treatment with 4-PBA in SHRs leads to an increase in endothelial-dependent vascular dilation and a decrease in adrenergic-mediated vascular constriction in mesenteric arteries on both 5 week-old (Naiel et al., 2019) and 12 week-old (Carlisle et al., 2016) rats (treatment started age). Recent studies have highlighted the role of endoplasmic reticulum (ER) stress in essential hypertension and in blood pressure regulation (Young, 2017, Liang et al., 2013, Naiel et al., 2019, Choi et al., 2016b). ER stress has been associated with vascular dysfunction in many hypertensive models. ER stress activation has been demonstrated in cardiomyocytes (Qian et al., 2021, Wu et al., 2019, Zhou et al., 2020) and

in VSMCs from mesenteric arteries (Camargo et al., 2018) and aorta (Kim et al., 2018) from SHR. Previous studies have found that ER stress inhibitor 4PBA can attenuate the hypercontractility in mesenteric arteries of SHRSP (Camargo et al., 2018). Inhibition of ER stress leads to a decrease of hypercontractility in mesenteric arteries of both SHRSP (Camargo et al., 2018) and SHR (Naiel et al., 2019, Carlisle et al., 2016) and also in the aorta (SpitlerMatsumoto and Webb, 2013) of SHR. ER stress model induced by tunicamycin infusion in SD rats increased collagen production and vascular stiffening, where TUDCA or PBA treatment reduced ER stress in the aorta and showed improvement in attenuated vascular compliance.

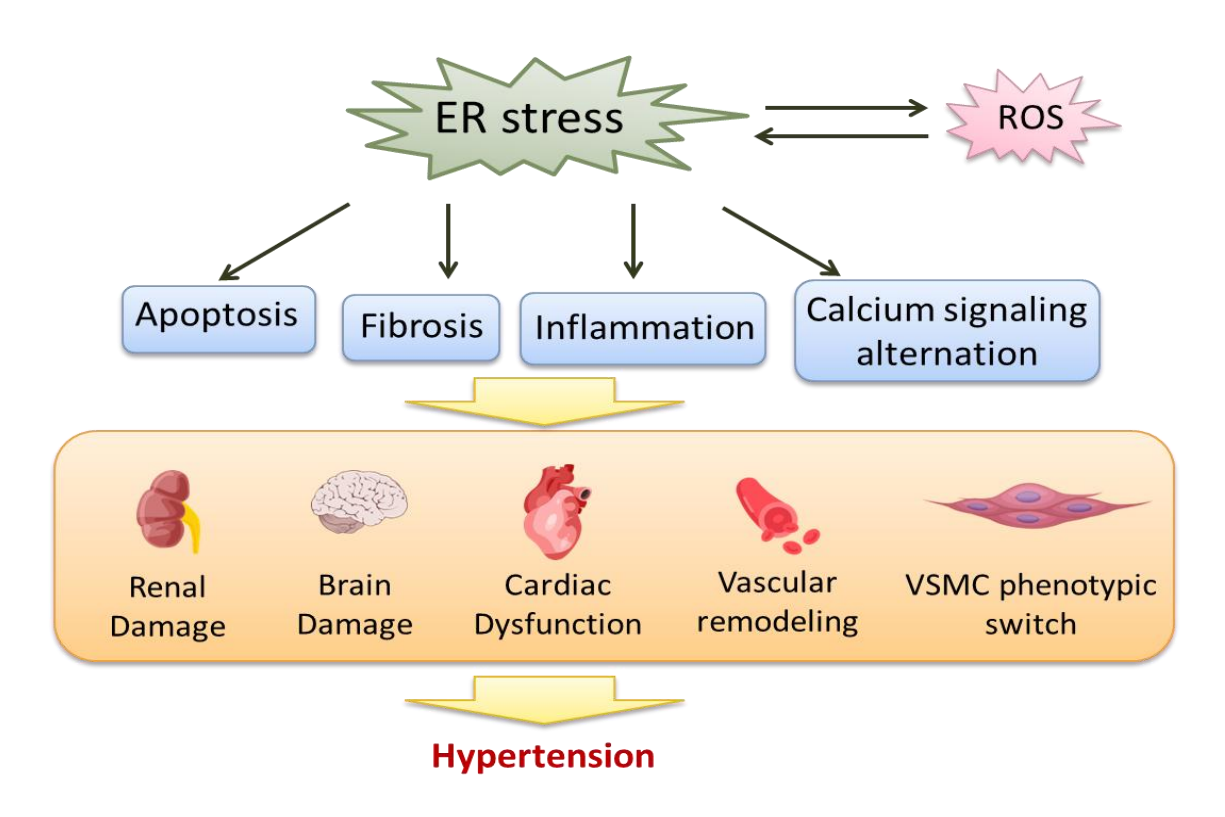


Figure 1.5 ER stress in hypertension.

ER stress and oxidative stress play a significant role in the progression of hypertension. These processes are associated with apoptosis, inflammation, fibrosis, and alterations in calcium signalling within the cardiovascular, renal, and central nervous systems.

# 1.5 Interplay between ROS, ER stress, calcium dysfunction and implications in hypertension

The intricate relationship between ROS and ER stress profoundly affects calcium homeostasis, a critical factor in vascular function and blood pressure regulation (Görlach et al., 2015). Under normal conditions, the ER acts as the major intracellular calcium reservoir, maintaining calcium balance within cells. Proper calcium handling is essential

for various cellular functions, including VSMC contractility (Berridge, 2002). ROS, however, can disrupt this balance by impairing the function of key calcium-handling proteins such as the SERCA, which sequesters calcium into the ER (Thompson et al., 2014).

Oxidative stress, driven by excessive ROS production, can cause oxidative modifications of SERCA, such as S-glutathionylation, which reduces its efficiency in pumping calcium into the ER (Adachi et al., 2004). This impairment leads to elevated cytosolic calcium levels and a corresponding depletion of ER calcium stores. The resulting increase in cytosolic calcium triggers calcium-dependent signaling pathways that promote VSMC contraction, contributing to increased vascular tone and the development of hypertension (Touyz et al., 2018).

ER stress activates the UPR as a compensatory mechanism to restore normal protein folding(Ron and Walter, 2007b). However, prolonged or unresolved ER stress promotes calcium release from the ER via inositol 1,4,5-triphosphate receptors (IP3Rs) and ryanodine receptors (RyRs). This release exacerbates calcium depletion in the ER and increases cytosolic calcium levels, perpetuating a vicious cycle of ER stress, oxidative stress, and calcium dysregulation.

The consequences of disrupted calcium homeostasis are not confined to VSMCs. Endothelial cells, which line the blood vessels, are similarly affected. Calcium signaling is crucial for the activation of endothelial nitric oxide synthase (eNOS), which generates nitric oxide (NO), a potent vasodilator (TranOhashi and Watanabe, 2000). Impaired calcium handling in endothelial cells, driven by both ROS and ER stress, reduces NO production, leading to endothelial dysfunction (Förstermann and Sessa, 2012). This reduction in NO availability increases vascular tone and contributes further to elevated blood pressure.

Overall, the interplay between ROS, ER stress, and calcium dysfunction plays a central role in the pathophysiology of hypertension. By disrupting calcium homeostasis in both VSMCs and endothelial cells, these processes lead to increased vascular contractility, impaired vasodilation, and the chronic elevation of blood pressure that characterizes hypertensive states.

# 1.6 MicroRNAs

# 1.6.1 Biogenesis and function of microRNAs

Growing evidence indicates the function of non-coding RNAs in vascular dysfunction, especially microRNAs (miRNA). MiRNAs are small 19 to 25 nucleotide non-coding RNAs that negatively regulate gene expression (Xie et al., 2005). One individual miRNA can target multiple genes, and a single mRNA may be regulated by several different miRNAs (Cai et al., 2009, Saito and Saetrom, 2010). Mature miRNA is generated through a series of cleavage steps (Figure 1.6). In the nucleus, miRNA is transcribed as a long primary transcript (pri-miRNA) with a hairpin structure by RNA polymerase II. Following association with the endonuclease Drosha, the pri-miRNA is cleaved into the ~70 nt hairpin sequence termed the precursor miRNA (pre-miRNA). Pre-miRNAs get exported to the cytoplasm through the interaction of exportin-5 and Ran-GTP. After cleaved by a cytoplasm RNase III endonuclease Dicer-1pre-miRNA releasing a ~22-nt long double stranded duplex which contains the mature miRNA guide strand and the passenger strand (miR\* strand) (Vishnoi and Rani, 2017, Bounds et al., 2017). The guide strand is selected by an Argonaute (Ago) family protein and loaded into the RNA-induced silencing (RISC) complex (Wang and Atanasov, 2019), while the passenger strand is degraded or, in the rare case, incorporated into the RISC (Bhaskaran and Mohan, 2014, Bounds et al., 2017). The mature miRNA with the RISC mediates further bind to 3' untranslated region (UTR) complementary sites of target mRNA, thus resulting in translational suppression (Davis-DusenberyWu and Hata, 2011). MiRNAs are named according to a standardised nomenclature system, such as dme-mir-100, where the prefix indicates the organism (e.g., "hsa-" for human), and the term "mir" is followed by a sequentially assigned number regardless of the organism. Some of the mature miRNA can be derived from either the 5' or 3' arm of the precursor duplex and is designated as dme-miR-100-5p or dme-miR-100-3p, respectively. Up until 2019, there are 1917 annotated hairpin precursors and 2654 mature miRNA sequences in the human genome (KozomaraBirgaoanu and Griffiths-Jones, 2019).

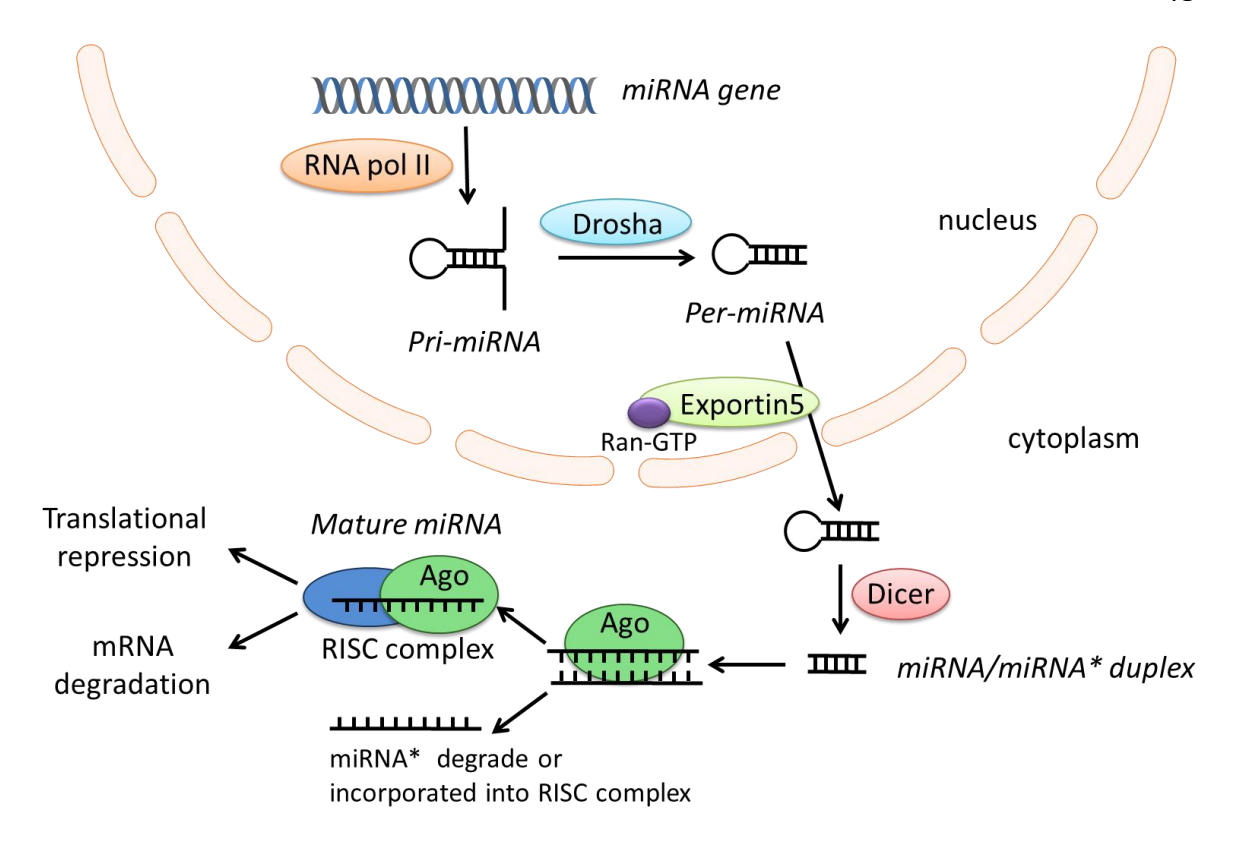


Figure 1.6 miRNA biogenesis.

miRNA transcribed as pri-miRNA by RNA pol II. Pir-miRNAs are processed into the ~70 nt hairpin sequence (pre-miRNA) by RNase III enzyme Drosha. Per-miRNA further get exported out of nucleus via the interaction of exportin-5 and Ran-GTP. In the cytoplasm, Dicer cleaves per-miRNA releasing a ~22 nt duplex containing the mature miRNA guide strand and the passenger strand. miRNA guide strand recognised by Ago family protein and incorporated into RISC complex, subsequently targets the 3'-UTR of mRNA, therefore giving rise to translational suppression.

#### 1.6.2 MicroRNAs in ER stress

miRNAs are essential in regulating vascular smooth muscle proliferation and contraction. Non-coding RNA also plays both regulators and effectors role in ER stress (McMahonSamali and Chevet, 2017). In vascular cells, both in vivo (mice) and in vitro experiments showed that miR-204 downregulate Sirt1 and promotes vascular ER stress and ER stress-induced endothelial dysfunction. Additionally, inhibition of miR-204 decreased ROS generation from ER stress (Kassan et al., 2017b). It was found that XBP1s directed miR-1274B transcription, thus targeting calponin h1 (CNN1) mRNA degradation and SMC proliferation (Zeng et al., 2015). This evidence suggests the potential role of miRNA and ER stress in the regulation of VSMC phenotypic switch.

# 1.6.3 MicroRNAs in hypertension

In hypertension, miRNAs are crucial regulators of vascular function and structure. They are involved in various cellular processes, including proliferation, differentiation, and apoptosis of VSMCs, which are key factors in the pathogenesis of hypertension.

Several miRNAs, such as miR-21, miR-126, and miR-204, have been identified as important players in hypertension. miR-21, one of the most extensively studied miRNAs, is known to promote VSMC proliferation and inhibit apoptosis, contributing to vascular remodelling and hypertension (LiWei and Wang, 2018). It has been shown to be upregulated in hypertensive patients and animal models, indicating its role in the disease's pathology (LiWei and Wang, 2018).

miR-126 is another miRNA that has been found to regulate endothelial function by maintaining vascular integrity and promoting angiogenesis (Bátkai and Thum, 2012). It targets multiple genes involved in these processes, and its dysregulation is associated with impaired vascular function and hypertension (Bátkai and Thum, 2012).

Additionally, miR-204 has been shown to downregulate Sirt1, leading to increased ER stress and endothelial dysfunction in hypertensive conditions (Kassan et al., 2017a). The inhibition of miR-204 has been demonstrated to reduce ROS generation from ER stress, suggesting its potential as a therapeutic target (MiaoChang and Zhang, 2018).

Overall, the evidence suggests that miRNAs play significant roles in regulating VSMC phenotype, endothelial function, and the overall pathophysiology of hypertension. Further research into miRNA-targeted therapies could provide new avenues for the treatment of hypertension and its associated complications.

# 1.7 Hypothesis and aims

In hypertension, prohypertensive factors influence the activation of ER stress, leading to vascular hypercontractility and dysfunction. This process involves changes in redox signalling, dysfunctional Ca<sup>2+</sup> homeostasis, and alterations in miRNAs in hypertension.

Aim 1: Assessing the relevant molecular changes of ER stress, miRNAs, and oxidative stress in human and/or experimental hypertension.

Aim 2: To study whether ER stress is modulated by prohypertensive factors such as AngII and ET-1, and whether it contributes to oxidative stress in the vasculature and kidneys, thereby promoting vascular hypercontractility in hypertension.

Aim 3: Investigating whether ER stress inhibition has protective effects on vascular hypercontractility and its potential in hypertension treatment.

# **Chapter 2** Materials and Methods

# 2.1 General lab practice

All experiments and procedures were carried out in laboratories located at the British Heart Foundation Glasgow Cardiovascular Research Centre, Institute of Cardiovascular and Medical Sciences (ICAMS). They were conducted under the guidance of the Control of Substances Hazardous to Health (COSHH) Risk Assessment Forms. All animal experiments were carried out under the regulations of the United Kingdom Home Office, the National Health and Medical Research Institute Animal Welfare Committee, and the Ethical Principles in Animal Experimentation from the West of Scotland Research Ethics Service (Licence No. 70/9021).

#### 2.2 Materials

# 2.2.1 Reagents and suppliers

Table 2.1 provides a list of all the reagents and their suppliers used in the thesis.

Table 2.1 Reagents used in the thesis

<b>Item Description</b>	Catalogue No.	<b>Supplier</b>
Cal-520, AM	ab171868	Abcam, Cambridge, UK
Nitrotyrosine ELISA Kit	ab113848	Abcam, Cambridge, UK
BQ-123	1188/500U	Bio-techne
Precision Plus Protein <sup>TM</sup> Dual Xtra	1610377	BioRad Laboratories,
Prestained Protein Standards	1010377	Hertfordshire, UK
TBARS (TCA Method) Assay Kit	700870	Cayman Chemical, Michigan,
		USA
Methanol	67-56-1	Fisher Scientific,
Wethanor		Loughborough, UK
Chloroform	67-66-3	Fisher Scientific,
Chlorotothi	07-00-3	Loughborough, UK
Glycine	56-40-6	Fisher Scientific,
Grychie	30-40-0	Loughborough, UK
Tris Base	77-86-1	Fisher Scientific,
THS Dasc	//-00-1	Loughborough, UK

D-Glucose anhydrous	50-99-7	Fisher Scientific,	
		Loughborough, UK	
Sodium chloride	7647-14-5	Fisher Scientific,	
South emorite		Loughborough, UK	
Sodium hydrogen carbonate	144-55-8	Fisher Scientific,	
Source in the second se		Loughborough, UK	
Dimethyl Sulfoxide (DMSO)	67-68-5	Fisher Scientific,	
		Loughborough, UK	
Dulbecco's Modified Eagle Medium	22320-022	Life Technologies/Invitrogen,	
(DMEM)	22320-022	Paisley, UK	
Smooth Muscle Growth Supplement	S 007 25	Life Technologies/Invitrogen,	
(SMGS)	S-007-25	Paisley, UK	
Dulbecco's Phosphate Buffered		T.C. T. 1 1	
Saline without CaCl <sub>2</sub> and MgCl <sub>2</sub>	14190-094	Life Technologies/Invitrogen,	
(DPBS)		Paisley, UK	
Penicillin Streptomycin Dulbecco	in Streptomycin Dulbecco		
(P/S)	15140-122	Paisley, UK	
etal Bovine Serum Heat Inactivated 10500-064		Life Technologies/Invitrogen,	
(FBS)	10500-064	Paisley, UK	
0.59/ Tayasia EDTA	10500-064	Life Technologies/Invitrogen,	
0.5% Trypsin-EDTA		Paisley, UK	
Phosphate-buffered saline (PBS)	003002	Life Technologies/Invitrogen,	
(tablets)	003002	Paisley, UK	
DNagal (Braga fras)	EN0521	Life Technologies/Invitrogen,	
DNase1 (Rnase free)	ENU321	Paisley, UK	
QIAzol Lysis Reagent	79306	Qiagen, Manchester, UK	
RNase-Free DNase Set (50)	79254	Qiagen, Manchester, UK	
miRNeasy Mini Kit (50)	217004	Qiagen, Manchester, UK	
4 Sodium Phenylbutyrate		Scandinavian Formulas	
Tween 20	9005-64-5	Sigma-Aldrich, Dorset, UK	
Soybean trypsin inhibitor	T-9003	Sigma-Aldrich, Dorset, UK	
Elastase	E-1250	Sigma-Aldrich, Dorset, UK	
Bovine Serum Albumin	9048-46-8	Sigma-Aldrich, Dorset, UK	
F12 Media	N6658	Sigma-Aldrich, Dorset, UK	

Potassium chloride	7447-40-7	Sigma-Aldrich, Dorset, UK	
Calcium chloride	0043-52-4	Sigma-Aldrich, Dorset, UK	
Aldosterone	A9477	Sigma-Aldrich, Dorset, UK	
Sodium nitroprusside (SNP)		Sigma-Aldrich, Dorset, UK	
BQ-788	B157-200UG	Sigma-Aldrich, Dorset, UK	
STF-083010	412510-10MG	Sigma-Aldrich, Dorset, UK	
PERK Inhibitor I, GSK2606414	516535	Sigma-Aldrich, Dorset, UK	
Pierce <sup>TM</sup> BCA Protein Assay Kit	23227	Thermo Fisher Scientific, Renfrew, UK	
High-Capacity cDNA Reverse	4368814	Thermo Fisher Scientific,	
Transcription Kit	4308814	Renfrew, UK	
Foot SVDDTM Cases Meter Miss	4205612	Thermo Fisher Scientific,	
Fast SYBRTM Green Mater Mix	4385612	Renfrew, UK	
Nitrocellulose Membrane	88018	Thermo Fisher Scientific,	
Null occurrence in the internal control of the interna		Renfrew, UK	
Ethanol absolute	64-17-5	VWR International,	
Ethanol absolute		Lutterworth, UK	
N'-2-Hydroxyethylpiperazine-N'-2	7365-45-9	VWR International,	
ethanesulphonic acid (HEPES)	7303-43-9	Lutterworth, UK	
Magnesium chloride hexahydrate	7791-18-6	VWR International,	
wagnesium emoriae nexanyarate		Lutterworth, UK	
Sodium dodecyl sulphate (SDS)	151-21-3	VWR International,	
Soutum dodecyr surphate (SDS)		Lutterworth, UK	
MgSO <sub>4</sub> ·7H <sub>2</sub> O	10034-99-8	VWR International,	
1115004 /1120		Lutterworth, UK	
Potassium dihydrogen phosphate	7778-77-0	VWR International,	
(KH <sub>2</sub> PO <sub>4</sub> )	,,,,,,,,,	Lutterworth, UK	
Collagenase type I; Elastase	LS004194 Worthington Biochemical Con		
Comagonato type i, Enabate	22001171	Lakewood, UK	

# 2.2.2 Solutions and medium

Protein lysis buffer (pH 7.4): HEPES (10 mM); Na<sub>3</sub>VO<sub>4</sub> (2 mM); Triton X-100 (0.5% v/v); Na<sub>4</sub>P<sub>2</sub>O<sub>7</sub> (50 mM); NaF (50 mM); NaCl (50 mM); Na<sub>2</sub>EDTA (5 mM); supplemented with PMSF (1 mM); aprotinin (1  $\mu$ g/ml); leupeptin (1  $\mu$ g/ml); pepstatin (1  $\mu$ g/ml)

**Lucigenin lysis buffer:** KH<sub>2</sub>PO<sub>4</sub>(20 mmol/L), EGTA (1 mmol/L), aprotinin (1 μg/mL), leupeptin (1 μg/mL), pepstatin (1 μg/mL), PMSF (1 mmol/L)

**6X Laemmli sample buffer:** SDS (10%, w/v); β-mercaptoethanol (6% v/v); bromophenol blue (0.012% w/v); glycerol (30% v/v); Tris-HCl (260 mM, pH 6.8)

Running buffer: Tris-Base (25 mM); glycine (193 mM); SDS (0.1% w/v); distilled water

**Transferring buffer:** Tris-Base (25 mM); glycine (193 mM); methanol (20% v/v); distilled water

**Tris-buffered saline-Tween 20 (TBST):** Tris-Base (20 mM, pH 7.6); NaCl (137 mM); Tween-20 (0.1% v/v); distilled water

**Blocking buffer:** Marvel Dried Skimmed Milk in TBS-T (5% w/v)

**Physiological Salt Solution (PSS) for myography:** NaCl (119 mM); KCl (4.7 mM); MgSO<sub>4</sub> (1.2 mM); NaHCO<sub>3</sub> (25 mM); KH<sub>2</sub>PO<sub>4</sub> (1.2 mM); CaCl<sub>2</sub> (2.5 mM); d-glucose (11 mM); distilled water; pH 7.4

High potassium physiological salt solution (KPSS) for myography: KCl (62.5 mM); MgSO<sub>4</sub> (1.2 mM); NaHCO<sub>3</sub> (25 mM); KH<sub>2</sub>PO<sub>4</sub> (1.2 mM); CaCl<sub>2</sub> (2.5 mM); d-glucose (11 mM); distilled water; pH 7.4

Calcium-free PSS for myography: NaCl (119 mM); KCl (4.7 mM); MgSO<sub>4</sub> (1.2 mM); NaHCO<sub>3</sub> (25 mM); KH<sub>2</sub>PO<sub>4</sub> (1.2 mM); d-glucose (11 mM); EDTA (23 μM); distilled water; pH 7.4

**HEPES physiological saline solution for calcium influx assay:** NaCl (130 mM); KCl (5 mM); MgCl<sub>2</sub>· 6H<sub>2</sub>O (1 mM); CaCl<sub>2</sub> (1 mM); d-glucose (10 mM); HEPES (20 mM); distilled water; pH 7.4

**Digestion solution for isolating cells:** BSA (0.2% w/v); collagenase (0.2% w/v); elastase (0.012% w/v); soybean trypsin inhibitor (0.036% w/v) in complete F-12 Ham medium

#### **VSMCs culture medium:**

Human VSMCs: DMEM (1 g/L D-Glucose, L-Glutamine, 25 mM HEPES, Pyruvate); 1X Smooth Muscle Growth Supplement; 1X Penicillin-Streptomycin (1000 U/ml)

Rat and mice VSMCs: DMEM (1 g/L D-Glucose, L-Glutamine, 25 mM HEPES, Pyruvate); 10% (v/v) FBS; 1X Penicillin-Streptomycin (1000 U/ml)

#### 2.2.3 Antibodies

Table 2.2 lists the antibodies used for Western blotting analysis.

Table 2.2 Antibodies used for Western blotting

Antibodies	Manufacturer	Catalogue No.	Host
	kindly provided by Prof.		
Nox5	David G. Harrison		Rabbit
	(Vanderbilt University)		
Nox1	Abcam	ab4200097	Rabbit
Nox4	Abcam	ab133303	Rabbit
Phospho-PERK (Thr980)	Cell signalling technology	3179s	Rabbit
(16F8) Rabbit mAb	Cen signaming technology	31775	Rubbit
PERK (C33E10) Rabbit mAb	Cell signalling technology	3192s	Rabbit
Phospho-eIF2α (Ser51) (D9G8)	Cell signalling technology	3398	Rabbit
XP® Rabbit mAb	Cen signaming technology	3370	Rabbit
eIF2α Antibody (D-3)	Santa cruz	133132	Mouse
ATF-4 (D4B8) Rabbit mAb	Cell signalling technology	11815s	Rabbit
CHOP (L63F7) Mouse mAb	Cell signalling technology	2895s	Mouse
ATF6	ThermoScientific	MA5-34918	Mouse
Ero1-Lα Antibody (YW-8)	Santa cruz	100805	Mouse
Phospho-IRE1 alpha (Ser724)	Invitrogen Antibodies	pa1-16927	Rabbit
Polyclonal Antibody	mvittogen Antibodies	pa1-10/27	Rabbit
IRE1α Antibody (B-12)	Santa cruz	390960	Mouse
XBP1 antibody [EPR22004]	Abcam	ab220783	Rabbit
bip	BD Biosciences	610978	Mouse
ATF6 Monoclonal Antibody	Invitrogen	MA5-34918	Mouse
(8D3)	mvinogen	1V1/AJ-JT/10	IVIOUSC
KLF4 Polyclonal Antibody	Invitrogen	PA5-27440	Rabbit
MYOCD Polyclonal Antibody	Invitrogen	PA5-100775	Rabbit

Anti-TAGLN/Transgelin antibody (ab14106)	Abcam	ab14106	Rabbit
phospho-ERK1/2 (T202/Y204)	Cell signalling	9101S	Rabbit
ERK1/2	Cell signalling	9102S	Rabbit
Phospho-Myosin Light Chain 2 (Ser19) Mouse mAb	Cell signalling technology	3675s	Mouse
Myosin Light Chain 2 (D18E2) Rabbit mAb	Cell signalling technology	8505s	Rabbit
Phospho-Myosin Light Chain 2 (Thr18/Ser19) Antibody	Cell signalling technology	3674s	Rabbit
PCNA	Santa Cruz Biotechnology	sc-56	Mouse
SOD2	Abcam	ab13533	Rabbit
GPx1			Rabbit
β-actin	Sigma-Aldrich	A2228	Mouse
α-tubulin	Abcam	ab4074	Rabbit
Anti-Mouse Alexa Fluor 680	Thermo Fisher	A21057	Goat
Anti-Rabbit Alexa Fluor 800	Thermo Fisher	A32735	Goat

# 2.2.4 Primers

Table 2.3 lists the primers to be used in RT-qPCR gene expression analysis.

Table 2.3 Primers used in the RT-qPCR gene expression analysis

Gene	Pair	Oligonucleotide Sequence
hGAPDH	Forward	5'-GAG TCA ACG GAT TTG GTC GT-3'
IIO/II DII	Reverse	5'-TTG ATT TTG GAG GGA TCT CG-3'
hCatalase _	Forward	5'-CGT GCT GAA TGA GGA ACA GA-3'
	Reverse	5'-AGT CAG GGT GGA CCT CAG TG-3'
hSOD1	Forward	5'ACA TTG CCC AAG TCT CCA AC-3'
	Reverse	5'-GAA GGT GTG GGG AAG CAT TA-3'
hSOD2	Forward	5'-GGA AGC CAT CAA ACG TGA CT-3'
	Reverse	5'-CTG ATT TGG ACA AGC AGC AA-3'
hNOX1	Forward	5'-GCA GGG AGA CAG GTC CCT TTT CC-3'
	Reverse	5'-TCA CGA TGT CAG TGG CCT TGT C-3'

hNOX2	Forward	5'-GTC ACA CCC TTC GCA TCC ATT CTC AAG TCA GT-3'
	Reverse	5'-CTG AGA CTC ATC CCA GAA AGT GAG GTA G-3'
hNOX4	Forward	5'-TGC AGC AAG ATA CCG AGA TG-3'
	Reverse	5'-GTG TCA ACG GAT TTG GTC GT-3'
hNOX5	Forward	5'-GCA GGA GAA GAT GGG GAG AT-3'
IINOAS	Reverse	5'-CGG AGT CAA ATA GGG CAA AG-3'
hCACNA1C	Forward	5'-GAA GCG GCA GCA ATA TGG GA-3'
IICACNATC	Reverse	5'-TTG GTG GCG TTG GAA TCA TCT-3'
hIP3R	Forward	5'-GCG GAG TCG ACA AAT GG-3'
IIIF3K	Reverse	5'-TGG GAC ATA GCT TAA AGA GGC A-3'
hSERCA	Forward	5'-AAA CCA CGG AGG AAT GTT TGG-3'
IISEKCA	Reverse	5'-AGC TCA TTG AGG CCG TAT TTC-3'
hNrf2	Forward	5'-TCC AGT CAG AAA CCA GTG GAT-3'
IIINI1Z	Reverse	5'-GAA TGT CTG CGC CAA AAG CTG-3'
hKeap1	Forward	5'-GTG TCC ATT GAG GGT ATC CAC C-3'
ПКсарт	Reverse	5'-GCT CAG CGA AGT TGG CGA T-3'
mGAPDH	Forward	5'-AAG TCG GTG TGA ACG GAT TTG -3'
	Reverse	5'-TGT AGA CCA TGT AGT TGA GGT CA -3'
mSOD1	Forward	5'ACA TTG CCC AAG TCT CCA AC-3'
msobi	Reverse	5'-GAA GGT GTG GGG AAG CAT TA-3'
mSOD2	Forward	5'-GGA AGC CAT CAA ACG TGA CT-3'
msobz	Reverse	5'- GCT TGA TAG CCT CCA GCA AC-3'
mNOX1	Forward	5'-TGT GCA GAC CAC AAC CTC AAA-3'
IIINOXI	Reverse	5'-GCC TAA TTC CTC CAT CTC CTG TT-3'
mNOX2	Forward	5'-ACT CCT TGG GTC AGC GAT TTG -3'
mivoxz	Reverse	5'-GTT CCT GTC CAG TTG TCT TCG -3'
mNOX4	Forward	5'-CCA GAA TGA GGA TCC CAG AA -3'
IMNUA4	Reverse	5'-AGC AGC AGC ATG TAG AA -3'
mHO-1	Forward	5'-CAG GTG ATG CTG ACA GAG GA-3'
	Reverse	5'-GCC AAC AGG AAG CTG AGA GT-3'
mDJ-1	Forward	5'-AGC CGG GAT CAA AGT CAC TG-3'
	Reverse	5'-GGT CCC TGC GTT TTT GCA TC-3'
mNrf2	Forward	5'-TGA GCC AAG CTA TAA GCC ATG A-3'

	Reverse	5'-AAT GGT TCT TGT GCC TGT GAA-3'
mKeap1	Forward	5'-TGC CCC TGT GGT CAA AGT G-3'
Reve	Reverse	5э-ППЕ ЕСП ПЕЕ ФСС ПЕС СЕП С-Зэ

#### 2.2.5 Software

The software used for data acquisition and analysis in this thesis is listed below:

- GraphPad Prism 5: GraphPad Software, San Diego, USA
- Image Studio Lite Ver 5.2: LI-COR Biotechnology; Cambridge, UK
- Ingenuity® Systems Pathway Analysis (IPA, http://www.ingenuity.com)
- Lab Chart Reader 8.1.13 Windows: AD Instruments Ltd, Oxford, UK
- NanoDrop 1000 v3.7.1 software: Thermo Fisher Scientific, Renfrew, UK
- QuantStudio<sup>TM</sup> Real-Time PCR Software: Applied BioSystems, California, USA
- ZEISS ZEN pro Imaging Software for Connected Microscopy: Carl Zeiss Ltd., Cambridge, UK

#### 2.3 Animals and tissue collection

# 2.3.1 Hypertensive mice model

TTRhRen mice (LinA3) are transgenic mice that express human active renin in the liver, thus releasing the human renin in the circulation. Generation of the LinA3 mice has been previously described (Prescott et al., 2000). Briefly, human prorenin cDNA was modified by adding a 3-kb region of the mouse transthyretin gene promoter upstream. The cDNA was then optimised by inserting a furin cleavage site between the prosegment and the active renin. Consequently, the prosegment is removed by ubiquitously expressed furin enzyme in the secretory pathway of expressing cells and generates active renin, resulting in chronic activation of the renin angiotensin aldosterone system. The LinA3 mice were originally derived on the FVB/N background but were transferred by back-crossing into

the C57BL/6J strain for this study. FVB background mice were used as wild type (WT) control. The generation of FVB/N and FVB mice was previously described (Prescott et al., 2000). VSMCs from the mesenteric arteries collected form these mice were used in Chapter 4.

WT and LinA3 hypertensive mice were crossed with Nox4 knock out mice. The Nox4 knock out mice were generated by crossing Nox4<sup>flox/flox</sup> with ERT2-Cre<sup>0/+</sup> transgenic mice as previously described (Schroder et al., 2012). Four genotypes of mice were generated: wild type (WT), LinA3, Nox4-deficient (Nox4-/-), and LinA3/Nox4-deficient (LinA3/Nox4-/-). The kidneys from both male and female mice were used in Chapter 4.

# 2.3.2 Hypertensive rat model

Male Stroke-prone spontaneously hypertensive (SHRSP) and Wistar Kyoto (WKY) rats used came from established colonies inbred in the Institute of Cardiovascular and Medical Sciences at the University of Glasgow since 1991 in Glasgow by brother-sister mating. Male spontaneously hypertensive (SHR) rats were from a company.

# 2.3.3 Housing and husbandry

Rats and mice were housed with 2-5 animals per cage in standard laboratory cages with sizzle nests, sawdust, and cardboard tubing. All animals were housed and bred under a humidity and temperature-controlled environment (21°C±3°C) and maintained on a 12-hour light/dark cycle, with access to tap water and standard diet (rat and mouse No.1 maintenance diet, Special Diet Services) ad libitum.

#### 2.3.4 Tissue harvest

The rats and mice for cell culture or myography were sacrificed by cervical dislocation, and the mesenteric beds were collected immediately and stored in a 50ml falcon tube with cold PBS on ice. The rats and mice were sacrificed by removing the blood to collect other tissues. Briefly, animals were anaesthetised using an induction box filled with 5% isoflurane in 1.5L/min medical oxygen. Once anaesthetised, the animals were placed in the supine position with their noses and mouths fully covered in an anaesthetic tube. All animals were checked to be fully under anaesthesia before opening the thoracic cavity and exsanguination. The blood was collected by cardiac puncture with a 21-gauge needle and drawn into a 5 mL syringe, then placed in the heparin tube and kept on ice. Plasma was

extracted by centrifuge of the heparin tube for 15 minutes at 3000 rpm at 4°C and stored at -80°C for further experiments. Urine was collected by aspiration from the bladder with a syringe and stored at -80°C for further experiments. Heart, kidney, aorta, and mesentery arteries were harvested, either snap-frozen in liquid nitrogen or fixed in a 10% formalin solution for histology. The frozen tissues were stored at -80°C and used for RNA or protein extraction. The fixed tissues were left in formalin solution overnight at room temperature and subsequently washed three times 5 minutes with PBS and stored in 70% ethanol at 4°C until further processing.

# 2.4 In vivo study

#### 2.4.1 4-PBA treatment

Male WKY and SHR rats were treated with 1 g/kg per day 4-PBA in drinking water or tap water for 5 weeks starting at 21 weeks old of age. 4-PBA dosage was adjusted in fresh drinking water twice a week. The body weight of each rat was measured twice a week to confirm that the loss of body weight was less than 20%.

#### 2.4.2 Blood pressure measurement

The systolic blood pressure (BP) of each rat was measured before and during the treatment once a week using tail cuff plethysmography ne (Evans et al., 1994). Before the experiment, rats were required to do 2 times pre-measurements in two different days to acclimatise them to the tail cuff procedure. The basal level of BP was measured before the treatment. Then the BP was measured once a week during the 5 weeks of treatment. Rats were pre-warmed in incubation boxes with heat lamps at 34°C for 10-20 minutes before measurements to ensure maximal vasodilation of the arteries in the tail. After warming, rats were gently restrained in a dry, warm towel and placed on a heating pad with only the tail exposed. The systolic BP was measured and recorded using equipment designed and built-in collaboration with the Electronics/Medical Devices Unit (NHS Greater Glasgow & Clyde). A blood pressure occlusion cuff was placed at the base of the tail and was connected to a cylinder of compressed air which permitted inflation (1mmHg to 250mmHg) and deflation of the cuff at a constant rate. The tail-cuff pressure was continuously recorded with a pressure transducer and pulse sensor placed distal to the tail. The pressure sensor measures blood pressure according to volume changes, which relies on volume pressure recording sensor technology. The signals from the pressure and pulse sensors were conveniently amplified and digitised in appropriate software on a laptop. The

inflation and deflation cycle were recorded and repeated until 12 consistent measurements were acquired. The maximum and minimum values were then excluded from 12 readings of each rat with the standard deviation below 20, and an average reading was taken for each animal to obtain mean systolic blood pressure.

# 2.5 General cell culture procedure

# 2.5.1 Primary culture of human vascular smooth muscle cells

Gluteal biopsies of subcutaneous fat were obtained under local anaesthetic from normotensive (NT; n = 10;  $120/74 \pm 3/3$  mmHg) and hypertensive (HT; n = 5,  $147/93 \pm 6/3$  mmHg) volunteers at the Ottawa Hospital Research Institute. The "n" number refers to different patients, and their details are described in the supplementary material of the previous study(Camargo et al., 2022). Ethics approval was obtained from the Ethics Board of the Ottawa Hospital Research Institute, Canada (no. 997392132). Written informed consent to participate in the study was obtained from each subject by the Declaration of Helsinki. Hypertension was defined as systolic blood pressure >140/90 mmHg or a history of hypertension on antihypertensive treatment.

Primary human VSMCs were isolated from small arteries of gluteal biopsies by enzymatic digestion, as we previously described (Touyz et al., 1999). Briefly, gluteal biopsies were cleaned by removing excess fat, connective tissue and adventitial. The cleaned arteries were incubated in F12 medium containing digestion mix (1% gentamicin, collagenase (type 1), elastase, soybean trypsin inhibitor, and BSA) in a falcon tube for 60 minutes at 37°C under constant agitation. The digested fragments were syringed through a 20-gauge needle for minimum 3 times to obtain a homogenised solution. Cells and debris were filtered through a 100 µm nylon filter, and the filtrate was collected in a sterile 50ml falcon tube. The filtrate was centrifuged for 4 minutes at 2000 rpm at room temperature. The cell pellet was resuspended in Ham's F-12 culture medium containing 10% FBS and cultured under normal cell culture conditions for the first 48 hours. After that, cells were grown in DMEM, supplemented with a smooth muscle growth supplement (SMGS) and 1% penicillin-streptomycin. The cells were passaged at 1:3 ratio at approximately 80-90% confluency until using passage (passage 3-7).

# 2.5.2 Primary culture of mouse vascular smooth muscle cells

The mesentery bed of 5 mice were collected and placed in a falcon tube containing F12 medium (F12 media with 25mM HEPES, 1% Pen/Strep and 10% FBS). Each mesentery bed was dissected by removing fat, veins and adventitial tissue in a petri dish containing F12 medium in cell culture hood. The cleaned mesenteric arteries were incubated in a 12.5 ml F12 medium containing digestion mix (25mg BSA, 25 mg Collagenase, 100mg Elastase and 4.5mg Soybean trypsin inhibitor) in a 50 ml falcon tube for 45-60 minutes (depending on the size of tissue) at 37°C under constant agitation. The digested fragments were syringed through a 21-gauge needle for a minimum of 3 times to obtain a homogenised solution. Cells and debris were filtered through a 100 µm nylon filter, and the filtrate was collected in a sterile 50ml falcon tube. The filtrate was centrifuged for 5 minutes at 2000 rpm at room temperature. The cell pellet was resuspended in 5 ml DMEM (DMEM containing 1% Pen/Strep and 10% FBS), distributed in a T25 flask (passage 0) and cultured under normal cell culture conditions. The medium of the flask was changed after 24 to 48 hours. The cells were passaged at 1:2 ratio at approximately 80-90% confluency until using passage (passage 3). The procedure for the isolation and setting up of primary mice VSMCs was performed with the help of Mrs Wendy Beattie.

Mice VSMCs were cultured in T75 or T150 culture flasks at 37°C in a humidified atmosphere of 5% CO<sub>2</sub> and 95% air. Cells were maintained in growth media containing DMEM supplemented with 10% FBS and 1% Pen/Strep. The cell culture media were replenished every 2-3 days. The cells were passaged at 1:4 ratio at approximately 80-90% confluency and using at passage 3-7.

# 2.5.3 Primary culture of rat vascular smooth muscle cells

Mesentery bed of 10 rats were collected and placed in a 50ml falcon tube containing F12 medium (F12 media with 25mM HEPES, 1% Pen/Strep and 10% FBS). Each mesentery bed was dissected by removing fat, veins and adventitial tissue in a petri dish containing F12 medium in cell culture hood. The cleaned mesenteric arteries were incubated in 25 ml F12 medium containing digestion mix (50mg BSA, 50 mg Collagenase, 100mg Elastase and 9mg Soybean trypsin inhibitor) in a 50 ml falcon tube for 60-90 minutes (depending on the size of tissue) at 37°C under constant agitation. The digested fragments were syringed in progression from 16-gauge, 18-gauge to 21-gauge needles to obtain a homogenised solution. Cells and debris were filtered through a 100 μm nylon filter and the

filtrate was collected in a sterile 50ml falcon tube. The filtrate was centrifuged for 5 minutes at 2000 rpm at room temperature. Cell pellet was resuspended in 15 ml DMEM (DMEM containing 1% Pen/Strep and 10% FBS), distributed in a T25 flask (passage 0) and cultured under normal cell culture conditions. Medium of flask was changed after 24 to 48 hours. The cells were passaged at 1:2 ratio at approximately 80-90% confluency until using passage (passage 3). The procedure of primary mice VSMCs isolation and setting up were kindly performed with the help from Mrs Wendy Beattie.

Rats VSMCs were cultured in T75 or T150 culture flasks at 37°C in a humidified atmosphere of 5% CO<sub>2</sub> and 95% air. Cells were maintained in growth media containing DMEM supplemented with 10% FBS and 1% Pen/Strep. The cell culture media were replenished every 2-3 days. The cells were passaged at 1:4 ratio at approximately 80-90% confluency and using at passage 3-7.

# 2.5.4 General protocol for VSMCs culture

#### 2.5.4.1 Cell passaging for experiment

VSMCs were passaged when reaching approximately 80%-90% confluency to avoid over confluence and improve cell growth. When passaging the cells, VSMCs were washed twice with sterile PBS and subsequently were trypsinised from the flask by adding 0.5% trypsin-EDTA solution (2ml for T75 and 4ml for T150) and incubated at 37°C until most of the cells were observed detached under the microscope. The trypsin was then inactivated by adding 2 times the volume of culture medium where the trypsinisation was stopped by FBS from the medium. The cell suspension was then transferred to a sterile 15 ml falcon tube and centrifuged at 1200 rpm for 3 minutes at room temperature. After removing the supernatant, the cell pellet was resuspended in 5ml of culture medium and then transferred into flasks for further growth or dishes for the experiment. The cells grew with 10ml medium in T75 flask or 15ml medium in T150 flask. The cells seeded in dishes were cultured with 3ml medium in 60mm dishes or 5ml medium in 100mm dishes. Before treatment, cells were quiescent by starved overnight in starving medium (DMEM content 1% Pen/Strep and 0.5% FBS).

#### 2.5.4.2 Cell freezing and thawing

Cells were frozen between P2 and P4 during the exponential growth phase. Cells were detached the same way as in Section 2.5.4.1. Then, the cell pellet was resuspended in 1 ml

freezing medium (DMEM with 30% FBS and 10% DMSO). The suspension was transferred into a cryovial (Alpha-laboratories, Hampshire, UK), which was then placed in a Mr. Frosty<sup>TM</sup> Freezing Container (ThermoFisher Scientific, Paisley, UK) filled with isopropanol in -80 °C. This ensures the cells freeze slowly and reduce the ice crystal formation. The cryovials were removed to liquid nitrogen for long-time storage after 24 hours.

When thawing the cells, the cryovials were collected from liquid nitrogen and placed into 37°C water bath to warm the cells rapidly. The cell suspension was transferred to a T75 flask with 10 ml culture medium. The cell culture medium was refreshed once the cell was attached to the flask.

# 2.6 RNA analysis by real-time polymerase chain reaction

Real-time polymerase chain reaction (RT-PCR) has been widely used to measure mRNA expression. This technique allows accurate quantification of starting amounts of complementary DNA (cDNA) generated from the mRNA template by reverse-transcriptase. The detection of RT-PCR is based on the changes of accumulated fluorescence during thermal cycling, which can be generated on an amplification plot and give a quantitative result of the amplified sequence (Kubista et al., 2006). Two common methods used to detect the PCR products are i) non-specific fluorescent dyes (such as SYBR) that bind to any double-stranded DNA and ii) fluorescently labelled sequence-specific DNA probes (such as TaqMan). The non-specific fluorescent dye SYBR Green is used in this thesis.

#### 2.6.1 RNA extraction

Total RNA was extracted from VSMCs using QIAzol® Lysis Reagent (QIAGEN), which is a phenol/guanidine-based reagent (Chomczynski and Sacchi, 1987) used to lysis total RNA from all classes of tissues. Cells were rinsed with ice-cold phosphate-buffered saline (PBS) and then homogenised directly by pipetting up and down with 700 µl Qiazol reagent. Frozen tissues were homogenised in 750 µl of QIAzol® using Precellys 24 tissue homogeniser. Cell or tissue lysates were collected into a 1.5 ml Eppendorf and stored at -80°C until needed. When needed, 200 µl chloroform was added to the lysates and mixed by turning the tube upside-down for 15 seconds. Lysates were incubated at room temperature for 2 minutes and then spun at 12,000g for 15 minutes at 4°C. The sample was separated into 3 distinct phases: the upper aqueous phase contains RNA, the middle

interphase contains DNA, and the lower organic phase contains proteins. The aqueous phase containing total RNA was carefully transferred into a new 1.5 ml Eppendorf and mixed with 500 µl isopropanol in an inverted tube 15-30 times. Samples were left for 15 minutes at room temperature, followed by centrifugation at 12,000g for 10 minutes at 4°C. The RNA precipitate was then washed with 500 µl 75% ethanol by centrifuged at 7,500g for 5 minutes at 4°C, followed by drying for 5 minutes at 37°C. RNA was re-suspended in 20 µl Ambion® nuclease-free water.

#### 2.6.2 Nucleic acid qualification

The quality and quantity of RNA were measured in a Nanodrop® ND-1000 spectrophotometer (Labtech International, Heathfield, UK) and NanoDrop 1000 v3.7.1 software. The absorbance of each sample was measured by spectrophotometer at 260 nm (RNA), 280n m (protein) and 230 nm (contaminations). 260 nm/280 nm absorbance ratios of approximately 2.0 is signified appropriate RNA purity.

#### 2.6.3 DNase I treatment

DNase I treatment was performed for all RNA samples after nanodrop to avoid the contamination of genomic DNA. Briefly, 10 µg of RNA from each sample were incubated with 0.1 U of DNase I and 1X DNase I buffer at 37°C for 1h and then incubated at 70°C for 10 minutes to terminate the enzyme reaction. The resulting RNA samples were left on ice and subsequently used for cDNA preparation.

# 2.6.4 Reverse transcription

Total RNA was reverse transcribed to complementary DNA (cDNA) using a High-Capacity cDNA Reverse Transcription Kit (#4368814/4374966). The reaction was performed in a u-shape bottom 96-well plate. Each reaction contained 2 µl 10x RT buffer, 2 µl 10x RT random primers, 0.8 µl 100 mM 25x dNTP mix, 1 µl MultiscribeTM reverse transcriptase, 1 µl RNase inhibitor and 13.2 µl sample with nuclease-free water contained 2 ug RNA. For negative controls, nuclease-free water was added in place of RNA. The plate was sealed tightly using adhesive transparent PCR film and incubated in a Thermal cycler (25°C for 10 minutes for primer annealing; 37°C for 120 minutes for reverse transcription, 85°C for 5 minutes for inactivation, 4°C for 10 minutes and 12°C forever).

# 2.6.5 SYBR green real-time PCR

Quantitative polymerase chain reaction (qPCR) was used to assess the expression of different genes. The GAPDH gene was used for internal control. cDNA of each sample was diluted with nuclease-free water into a concentration of 10 ng/µL. In a 384 well clear reaction plate, 3µl cDNA template (30 ng), was mixed with forward and reverse primers (300 nM), LightCycler<sup>TM</sup> 480 SYBR Green I Master Mix (5 µl), and nuclear-free water into 10µl volume in total applying to PCR amplification. The reaction of each sample was repeated twice to avoid loading errors. The mRNA expression was detected by QuantStudio TM 7 Flex System under the following four stages: one cycle at 50 °C for 2 min; one cycle at 95°C for 10 minutes for DNA polymerase activation; forty cycles at 95°C for 15s for DNA denaturation and 60°C for 1 minutes for annealing and extension; one cycle repeating last step. Negative controls without cDNA template were also included in all runs to test for the presence of extraneous nucleic acid contamination.

# 2.6.6 qPCR data analysis

The cycle threshold (Ct) value of each reaction was generated by QuantStudio<sup>TM</sup> Real-Time PCR v1.1 software. Relative changes in gene expression were performed using the comparative Ct method ( $\Delta\Delta$ Ct method)(Livak and Schmittgen, 2001). This method aims to compare the Ct value of the interested gene in all the groups to the control group after normalising to an endogenous reference gene (GAPDH). Briefly,  $\Delta$ Ct was calculated as a:  $\Delta$ Ct = Ct<sub>GOI</sub>- Ct<sub>Ref</sub>, where GOI indicates gene of interest, and Ref indicates endogenous reference gene. To obtain the different expression between groups,  $\Delta\Delta$ Ct values were generated by subtracting averaged  $\Delta$ Ct value of the control group from an averaged  $\Delta$ Ct value from experimental groups as:  $\Delta\Delta$ Ct =  $\Delta$ Ctsample -  $\Delta$ ctcontro. The relative expression of the interested gene was defined as fold change by calculated relative quantity (RQ) values as: RQ =  $2^{-\Delta\Delta$ Ct}.

# 2.7 Protein analysis by western blotting

#### 2.7.1 Protein extraction

Cells were washed twice with ice-cold phosphate-buffered saline (PBS) (Gibco, Cat no. 10010023) to remove residual media components. Cells were harvested by 100µl ice-cold protein lysis buffer. Lysates were collected in a 1.5 ml Eppendorf tube and sonicated for 5 seconds. Cell lysates were then centrifuged at 13,000 g for 10 minutes at 4 °C to separate

the protein. The supernatant containing protein was removed to a new 1.5 ml tube for the next step and kept on ice.

Frozen tissues were washed with PBS and then put into labelled 2ml micro tubes with around 10 bulk beads and 200µL lysis buffer. Each artery was homogenised twice in a tissue homogeniser (Precellys 24). Tissues were pelleted by centrifugation at 13,000 g for 10 minutes at 4 °C to separate the protein. The supernatant was removed for the next step and kept on ice.

#### 2.7.2 Protein quantification

The protein concentration from lysates was determined via BCA protein assay (Thermo Fischer). A protein standard curve was made by Bovine Serum Albumin (BSA) with a concentration range of 0-0.1M. The cell lysates 2 μl and standard 10 μl were added to a clear 96 well plate. Reagent A and B (A: B=50:1) were added with a volume of 50μL to each wall. The absorbance at 562nm values was read with a spectrophotometer (M2 Spectra Max) after 30 minutes incubate at 37°C. The protein concentrations of lysates were calculated using the standard curve.

# 2.7.3 Sample preparation

Samples were prepared with 20  $\mu$ g total protein in dH<sub>2</sub>O and 6x loading buffer and denatured at 95 °C for 5 minutes.

# 2.7.4 Sodium dodecyl sulphate-polyacrylamide gel electrophoresis (SDS-PAGE)

The Invitrogen NuPage Novex gel system (ThermoFisher) was used in western blotting. Protein was separated by molecular weight using SDS-PAGE. Protein samples and ladder were separated and loaded into Invitrogen Novex Tris-Glycine Mini Gels, 4-20% immersed in Tris-Glycine running buffer and run at 165V for about 60 minutes.

# 2.7.5 Immunoblotting for proteins

Following electrophoresis, the gels with proteins were transferred to a nitrocellulose membrane (ThermoFisher) by immersion in Tris-Glycine transfer buffer containing 20% methanol at 110V for 90 minutes on ice. The membranes were blocked in 3% BSA or 5% milk in TBST solution with constant agitation at room temperature for 1 hour. The

membranes were then probed with primary antibody in 3% BSA in TBST solution and incubated overnight at 4°C. Following 3 x 5 minutes washes with TBST, the membrane was incubated with the corresponding secondary antibodies diluted with 1% BSA in TBST solution for 1 hour at room temperature. The membrane was washed 3 times in 5 minutes with TBST, which was subsequently visualised by an infrared laser scanner (Odyssey CLx, LI-COR®). Images were quantified using the software Image Studio<sup>TM</sup> Lite.

# 2.8 Assessing redox status and oxidative stress

# 2.8.1 Lucigenin-enhanced chemiluminescence

Lucigenin-dependent chemiluminescence assay was performed to determine NADPH dependent ROS production (Minkenberg and Ferber, 1984). Cells were washed twice with ice-cold PBS and harvested in 160μl ice-cold lucigenin lysis buffer (20 mmol/L of KH<sub>2</sub>PO<sub>4</sub>, 1 mmol/L of EGTA, 1 μg/mL of aprotinin, 1 μg/mL of leupeptin, 1 μg/mL of pepstatin, and 1 mmol/L of PMSF).

 $50~\mu L$  of sample protein lysate was added into a white 96 well plate, and 175  $\mu L$  of assay buffer was added to each well. Luminescence was measured first for the basal conditions and then after adding substrate NADPH (100  $\mu$ mol/L) using the luminometer (AutoLumat LB 953, Berthold). The results were analysed by subtracting the basal readings from NADPH dependent luminescence signal and normalised to protein concentration.

# 2.8.2 Amplex™ Red assay

Hydrogen peroxide levels were evaluated in VSMCs using the Amplex Red Hydrogen Peroxide/Peroxidase assay kit (Invitrogen #A22188) according to the manufacturer's instructions. The Amplex Red assay is based on measuring the red fluorescent of oxidation product resorufin, which is generated by horseradish peroxidase (HRP) catalysed 10-acetyl-3,7- dihydroxypenoxazine oxidation in the presence of H<sub>2</sub>O<sub>2</sub> (Mohanty et al., 1997). The Amplex Red reagent, in combination with HRP, can react 1:1 with H<sub>2</sub>O<sub>2</sub> to produce the red fluorescent oxidation product with the maxima excitation of ~571 nm and emission of ~585 nm.

Briefly,  $50 \mu L$  of sample protein lysate was prepared as described in item 2.4 and  $50 \mu L$  of amplex red reagent was added into a clear 96 well plate (as advised in the kit manual). An  $H_2O_2$  standard curve was performed with samples as advised in the kit manual. The

absorbance at 560 nm values was read with spectrophotometer (M2 Spectra Max) after the plate incubated in the dark at room temperature for 30, 60, and 90 minutes, respectively. The results were analysed using the average of 3 time points with H<sub>2</sub>O<sub>2</sub> standard curve, then normalised by protein concentration in the cell lysate.

#### 2.8.3 Measurement of nitrotyrosine levels

3-nitrotyrosine modification of protein is a specific marker of oxidative damage mediated by peroxynitrite(Ahsan, 2013). To measure the peroxynitrite (ONOO-) formation, nitrotyrosine was assessed in cells using an ELISA kit (#ab113848, Abcam, Cambridge, UK) according to the manufacturer's instructions. The 96 well plate was read at an absorbance of 450 nm using a microplate reader after the reaction stopped by stop solution. Results were normalised to protein concentration.

# 2.8.4 Lipid peroxidation by thiobarbituric acid-reacting substances assay

Thiobarbituric acid-reacting substances (TBARS) assay (Item:700870, Cayman Chemical) was used as an indicator of oxidative stress in cells. Thiobarbituric acid-reacting substances are lipid peroxidation products that are measured as malonaldehyde (MDA) by a colourimetric method (RepettoSemprine and Boveris, 2012). MDA was assessed according to the manufacturer's instructions. Briefly, 20 µM cell lysates were mixed with 10% trichloroacetic acid (TCA) reagent and then boiled with thiobarbituric acid (TBA) colour reagent at 99°C for 1 hour to form MDA-TBA adduct. The boiled samples were immediately placed on ice for 10 minutes, followed by a 10-minute centrifuge at 1600g at 4°C. After 30 minutes incubate at room temperature, 200 µl supernatant of each sample was added to a 96 well plate, and the absorbance was read at 530-450 nm.

# 2.9 Calcium influx assay

VSMCs intracellular calcium transients were detected by Cal-520 acetoxymethyl ester (Cal-520AM, 5 × 10<sup>-6</sup> mol/L Abcam, ab171868) and imaged using live cell microscopy. Cells were grown in 12-well plates until 80-90% confluency. After the cells were ready for experiment or after inhibitor treatment, cells were incubated with 10<sup>-5</sup> mol/L Cal-520 AM in DMEM starving medium (containing 0.5% FBS and 1% Pen/Strep) at 37°C for 75 minutes followed by 30 minutes at room temperature avoid light. The dye in each well was replaced with 800 μl of HEPES buffer (pH 7.4) for 30 minutes before imaging. Fluorescent

image was performed using the inverted epifluorescence microscope (Axio Observer Z1 Live-Cell imaging system, Zeiss, Cambridge, UK) with excitation/emission wavelengths 490 nm and 525 nm, respectively. Images were acquired and analysed using Zen Pro (Zeiss, Cambridge, UK) software. Images were taken at 2-second intervals for 3 minutes, while 200  $\mu$ l stimuli (Ang II, 1 × 10–7 mol/L; or ET-1, 1 × 10–7 mol/L) were added 30 seconds after starting the experiment. The fluorescent signal was recorded, and the average of the first 30 seconds was regarded as basal measurement.

# 2.10 Myography

Wire and pressure myography have been extensively used as an ex vivo technique to study the function, structure, and mechanics of isolated intact vessel segments (Wenceslau et al., 2021).

# 2.10.1 Wire myography

Wire myography is a common in vitro technique to study the functional and mechanical responses of isolated small arteries developed by Mulvany and Halpern in 1977(Mulvany and Halpern, 1977).

#### 2.10.1.1 Vessel dissection and myography preparation

The WKY, SHRSP and SHR rats were sacrificed as described in section 2.3.2 (by cervical dislocation or exsanguination). The mesentery bed was gently removed from a 50 ml falcon tube containing cold DPBS and left on ice. The third order of mesenteric arteries was carefully dissected in physiological salt solution (PSS, pH 7.4) solution under a dissecting microscope. The arteries were cleaned by gently removing surrounding perivascular fat using dissection scissors and forceps and were cut into vessel rings approximately 2mm in length. The 2mm vessel segments were left on a glass tube with cold PSS on ice until mounting.

Before mounting, organ baths were washed 3 times with deionised water and then 3 times with 5 ml fresh cold PSS. The PSS from the final wash was left in the bath and bubbled with 95% O<sub>2</sub> and 5% CO<sub>2</sub>. The 2 mm mesenteric arteries were then mounted to the washed organ bath. Under a dissecting microscope, two 40 µm diameters of stainless wires were inserted into the vessel lumen, followed screwed to a force transducer and an adjusting micrometre in the organ bath, as shown in Figure 2.1.

Mounted vessels were allowed to equilibrate for a minimum of 30 minutes at resting tension in PSS while continuously gassed a mixture of 95%  $O_2$  and 5%  $CO_2$  and maintained at a constant temperature of 37 °C±0.5°C. Subsequently, all vessels were normalised using DMT normalisation procedure in LabChart software to reach their optimal pre-stretch tension. The normalisation standardised the baseline experimental conditions by allowing the comparable and optimal response of different sizes of vessels. The internal diameter of each vessel could be calculated by IC100/ $\pi$  after normalisation. Vessels with an internal diameter over 500  $\mu$ m (maximum size of resistance arteries) were excluded for the use of further experiments.

Following 10 min of equilibration, the viability of the vessels was assessed by exposure to KPSS (62.5 mM KCl). High concentrations of extracellular potassium (over 60 mM) depolarize VSMC membrane and lead to vasoconstriction by activating the voltage-gated calcium channels, thus maximising vasoconstriction. 5 ml of KPSS were added twice followed 3 times washing with warm PSS and 10 minutes equilibration to allow steady baseline generation. To assess endothelial function, vessels were pre-contracted with U46619 (10<sup>-7</sup> M) and then relaxed by acetylcholine (ACh, 10<sup>-6</sup> M). The vessels with functional endothelium (minimum attenuation of 80% relaxation of maximal contraction induced by U46619) were used in this thesis.

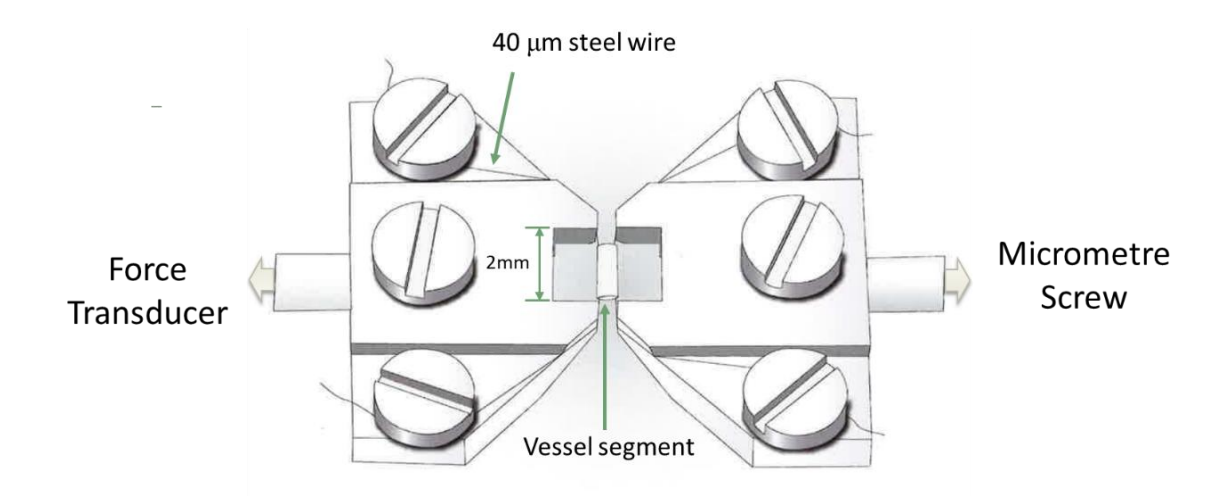


Figure 2.1 Illustration of the wire myography mounting heads with the mounted vessel.

The vessel segment was mounted to the organ bath by screwing two steel wires to 4 jaws. One wire was connected to a micrometre to adjust the vessel circumference, and the other wire was connected to a force transducer to records the tension on it.

#### 2.10.1.2 Cumulative concentration response curves (CCRCs)

investigate the vascular function from different conditions, cumulative concentration-response curves (CCRCs) to vasoconstrictors U46619 (the thromboxane A2 analogue) and ET-1, and to vasodilators Ach (endothelial-dependent relaxation) and sodium nitroprusside (SNP, nitric oxide (NO)-donor, endothelial-independent relaxation) were performed in this thesis. Specifically, for vasoconstrictors, vessels were exposed to half-log step cumulatively increasing concentrations of U46619 (from 1×10<sup>-10</sup> M, 3×10<sup>-10</sup> M to  $3\times10^{-6}$  M) or ET-1 (from  $1\times10^{-12}$  M,  $3\times10^{-12}$  M to  $1\times10^{-7}$  M). Additions of the next dose were made after 8 minutes or the maximal response of the preceding concentration. Similarly, for vasodilators, vessels were pre-contracted with U46619 (10<sup>-7</sup> M) until plateau and stable, then exposed to half-log step cumulatively increasing concentrations of Ach (from  $1 \times 10^{-10}$  M,  $3 \times 10^{-10}$  M to  $3 \times 10^{-5}$  M) or SNP (from  $1 \times 10^{-10}$  M,  $3 \times 10^{-10}$  M to  $3 \times 10^{-5}$  M). Additions of the next dose were made after 2 minutes or when the curves started going up. One vessel segment could run up to three curves with 3 times washing and 30 minutes equilibration in between. ET-1 or SNP CCRCs could not have any curve run afterwards. In some experiments, vessels were preincubated with pharmacological modulators before the curves.

The tension level of each vessel was recorded on LabChart software. Data was analysed using LabChart Reader (ADInstruments, Oxford, UK). The relaxation curves were presented as a percentage of relaxation relative to U46619 induced contraction. The contraction curves were presented as a percentage of contraction relative to KPSS induced contraction. Dose-response curves were plotted as the percentage of contraction or relaxation to the log concentration using log(agonist) vs. response (three parameters) model in the GraphPad Prism software, which were then analysed by comparing parameters of Bottom, Top or Log of EC50 of each curve extra using sum-of-squares F test.

# 2.10.2 Pressure myography

The vascular structure of mesenteric arteries from rats was assessed using pressure myography in the DMT pressure myograph system 110PXL (Danish Myo Technology, Aarhus, Denmark). A minimum 4-5 mm length vascular segment (from 3rd order or small 2nd order of rat mesenteric artery) with no branching or surrounding fat was dissected and mounted onto two small glass cannulas using nylon knots in a chamber (Figure 2.2) filled with ice-cold calcium-free PSS. The segment was tied off and secured to the two cannulas without any stretching by adjusting the micrometre. After mounting, the chamber was

placed under a microscope (Zeiss Axiovert 25 inverted microscope) equipped with a CCD Sony XC-75CE monochrome video camera (Zeiss) and connected to the computer with MyoView software (Danish Myo Technology, Aarhus, Denmark) that allows the image of arteries to be recorded and stored. The vessels were continually gassed with 95% O2/5% CO2 at 37°C in the calcium-free PSS during the experiment. All bubbles were removed from the system by gently perfusing the vessel and tubes with calcium-free PSS of approximately 20-30 mmHg pressure with the help of a 5 ml syringe through inlet to outlet valves. Before starting the protocol, the pressure was increased from 10mmHg to 70mmHg using the computer setting and leaving for 30 minutes for equilibration. After equilibration, the vessel was depressurised to 0 mmHg. It was then exposed to intraluminal pressure in a gradually increased range of physiological pressure (3 mmHg, 10 mmHg, 20 mmHg, 40 mmHg, 60 mmHg, 80 mmHg, 100 mmHg, and 120 mmHg) lasting 5 minutes periods each. After the experiment, the vessel was fixed by changing calcium-free PSS to 10% formalin at 120 mmHg for 30 minutes at room temperature and subsequently followed the histology steps in Section 2.3.

The internal and external diameter of the vessel were derived from MyoView software using LabChart Reader (ADInstruments, Oxford, UK). These measurements were used to calculate the wall thickness [(external diameter - internal diameter) / 2]. and the cross-sectional area  $[(\pi/4) \times (\text{external diameter}^2 - \text{internal diameter}^2)]$ .

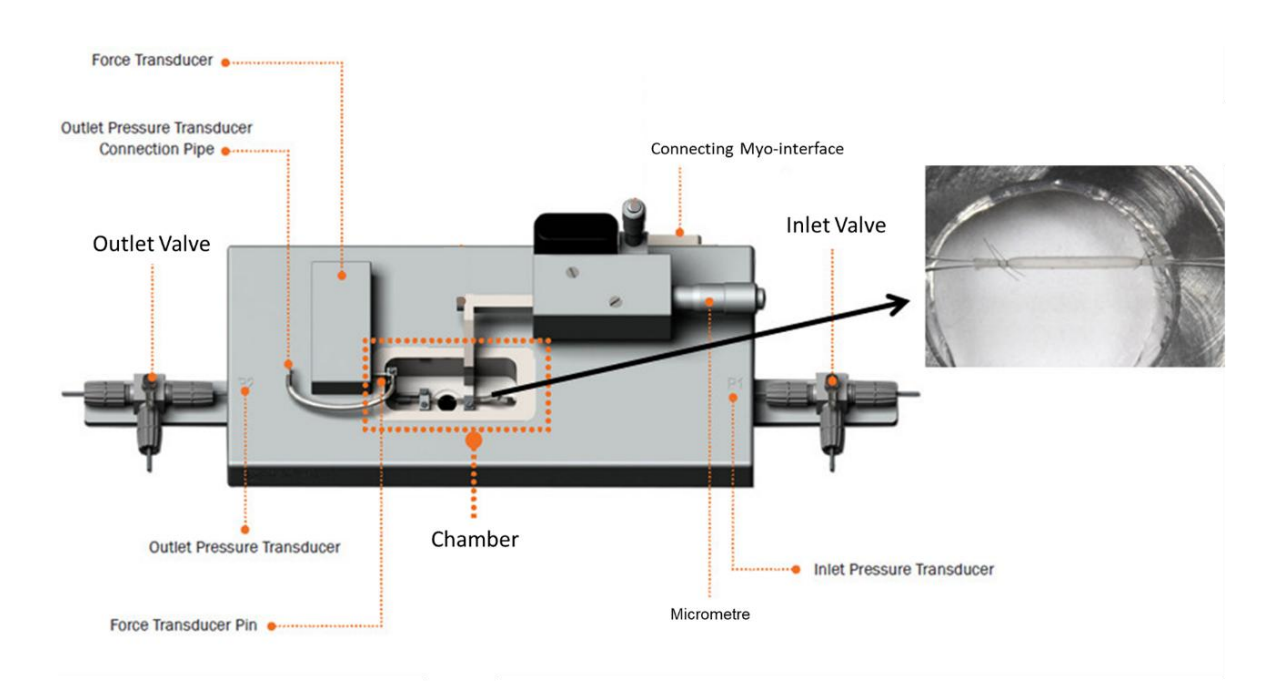


Figure 2.2 Schematic of pressure myography chamber. A small vessel segment is mounted between two glass cannulas in the chamber. (Modified from ref (Shahid and Buys, 2013)).

#### 2.11 miRNAs

#### 2.11.1 miRNA extraction

According to the manufacturer's instructions, the miRNeasy Mini Kit (QIAGEN, cat. no. 217004) was used to isolate total RNA, including the microRNA fraction from cells. Cells in each dish were disrupted with 700 µl Qiazol Lysis Reagent to release RNA and then incubated at room temperature for 5 minutes. The homogenates were mixed thoroughly with 140 µl chloroform and placed in room temperature for 2-3 minutes. After incubation, samples were centrifuged at 12000g at 4 °C for 15 minutes to separate RNA onto the aqueous phase. The aqueous phase contains RNA, which was then mixed with 525 µl 100% ethanol thoroughly by pipetting. Subsequently, the samples were transferred into an RNeasy Mini spin column and centrifuged at  $\geq 8000$ g at 4 °C for 15 s at room temperature to get the RNA crude extract. 350 µl Buffer RWT was pipetted on to samples and centrifuged at ≥ 8000g at 4 °C for 15 s at room temperature for washing. To remove the DNA from samples, 80 µl DNase mix buffer was pipetted directly on to the RNeasy mini spin column and left at in room temperature for 15 minutes. The samples were washed with 350 μl Buffer RWT and 500 μl Buffer RPE, respectively. After washing, 500 μl Buffer RPE was pipetted on to the samples and centrifuged for 2 minutes at  $\geq 8000g$  in room temperature to dry the column. RNA was finally eluted with 30 µl nuclease-free water for 1 minute and centrifuged at  $\geq$  8000g. The samples were stored at -80 °C until use.

The quality and quantity of RNA were measured in a Nano drop 100 (Thermo Scientific). The concentrations of RNA in each sample were adjusted with nuclease-free water to 5 ng/µl. 5 µl RNA samples from three different normotensive subjects were pooled into the normotensive sample (NT), and three different hypertensive subjects were pooled into the hypertensive sample (HT).

# 2.11.2 Microarray of miRNAs

MicroRNA expression was measured by TaqMan Advanced miRNA Assays, which include TaqMan Array Cards (Card A, cat. no. B3970; Card B, cat. no. B3963) and TaqMan Advanced miRNA cDNA Synthesis Kit according to the manufacturer's instructions. Card A and Card B included 754 different microRNAs with 8 exogenous controls and 4 repeated endogenous controls (has-miR-16-5p).

10ng of RNA from each group was used in this process. First, mature miRNAs were modified from total RNA by extending the 3' end of the mature transcript through poly (A) tailing reaction, then lengthening the 5' end by adaptor ligation reaction. The modified miRNAs performed a universal reverse transcription (RT) reaction and followed an amplification reaction to uniformly increase the amount of cDNA for all miRNAs. The samples were stored at -20°C until used the next day.

The cDNA templates were diluted 10 times by 0.1×Tris-EDTA buffer, pH 8.0. Then 440 μl diluted cDNA template was gently mixed with 880 μl TaqMan Fast Advanced Master Mix (2×) and 440 μl RNase-free water. These prepared PCR reaction mixes were loaded in array card A and B with 100 μl / reservoir. The filled cards were then centrifuged and sealed. The real-time PCR was run by QuantStudio TM 7 Flex System with the setup file SDS\_QS in TXT format to detect microRNA expression. PCR was run 3 stages with 1 μl reaction volume in each wall. The thermal cycle profile was as follows: an enzyme activation of 10 minutes at 92°C, 40 cycles denature (1 second at 95°C) and anneal/extend (20 seconds at 60°C). Primer sequences are listed in the attachment.

# 2.11.3 miRNA data analysis

The results were analysed by Data Assist software with 35 as the maximum allowable Ct value. Data was normalized by global mean normalization without undetermined miRNAs. Fold changes were determined by 2-(Ct (miRNA) - Ct (global mean)). miRNAs of interest were searched on miRBase, the main online public repository for assigning stable and consistent names to novel discovered miRNAs, and PubMed. The predicted gene target of miRNAs was searched on http://mirdb.org/ website, which provides an online database for miRNA target prediction and functional annotation developed by the computational model.

# 2.11.4 Ingenuity Pathway Analysis

Ingenuity® Systems Pathway Analysis (IPA, http://www.ingenuity.com) software was utilised to determine differentially expressed miRNAs and their putative targets differentially expressed mRNAs or proteins along with their miRNA Target Filter and molecular and cellular functions. miRNAs share the same seed sequence and are considered to have the same predicted targets. The sources of the miRNA Target Filter are miRecords, Tarbase and TargetScan. Only the mRNA/protein and miRNA with the inverse pair were chosen.

# 2.12 Statistical analysis

The results are presented as the mean ± standard error of the mean (SEM). A Student's t test was performed to compare the two groups. One-way analysis of variance (ANOVA) followed by Tukey test was used in multiple comparisons, as appropriate using GraphPad Prism 5.0 software. Outliers were identified and excluded based on the Grubbs' test or interquartile range (IQR) method, depending on the data distribution. Myography curves were analysed by calculating the maximal response (top or bottom effect) and the agonist concentration that produced 50% of the maximal effect (Log EC50) using nonlinear regression (curve fitting). To compare intracellular Ca² + levels, the area under the curve (AUC) was calculated and analysed using either the student's t-test or ANOVA, as appropriate. Statistical significance was determined as a p-value < 0.05, as indicated by symbols in each figure.

# Chapter 3 Vascular ER Stress, Oxidative Stress and Calcium Dysfunction in Human Hypertension

#### 3.1 Overview

Hypertension is a major risk factor for cardiovascular disease (CVD), chronic kidney disease (CKD), and cognitive impairment that is the contributor to all-cause morbidity and mortality worldwide (MillsStefanescu and He, 2020, Oparil et al., 2018a). Although therapeutic progress has been made over in the past few decades, the exact aetiology behind essential hypertension is still poorly understood and remains unknown in the majority of patients (90%) (Coffman, 2011, Tackling and Borhade, 2020, Bolivar, 2013). Therefore, a more precise understanding of the molecular pathogenesis is needed. The molecular mechanisms of hypertension are often associated with vascular dysfunction and prolonged chronic cell stress, such as endoplasmic reticulum (ER) stress and oxidative stress (Cicalese et al., 2021).

ER stress is a cellular process that repairs perturbations of ER function by activating a cytoprotective signalling pathway known as unfolded protein response (UPR). UPR is activated to maintain proteostasis when imbalances happen in protein synthesis, redox status, or Ca<sup>2+</sup> handling(Cicalese et al., 2021). Three ER transmembrane sensors detect the accumulation of unfolded proteins to initiate their mediated branches: PERK (protein kinase RNA-like ER kinase), IRE1 (inositol requiring kinase 1), and ATF6 (activating transcription factor 6). ER stress has been well known to play a role in hypertension. In animal models of hypertension, treatment with ER stress inhibitors 4-phenylbutyric acid (4-PBA) and/or tauroursodeoxycholic acid (TUDCA) has been shown to reduce ROS generation, calcium mishandling, vascular hypercontractility, apoptosis, fibrosis, inflammation, and high blood pressure (Bal et al., 2019a, Han et al., 2019b, Carlisle et al., 2016, Choi et al., 2016b, Naiel et al., 2019, Liang et al., 2013, Camargo et al., 2018, Kassan et al., 2012). Moreover, ER stress inducer tunicamycin increased vascular stiffening, apoptosis, fibrosis, and blood pressure in animal models (Spitler and Webb, 2014, Carlisle et al., 2016, Liang et al., 2013). However, how ER stress is involved in hypertensive human vasculature remains unclear.

Reactive oxygen species (ROS), intermediates of redox reactions, are constantly generated by homeostatic cells and are important in the physiologic regulation of all cellular functions, including in vascular cells (de Champlain et al., 2004). ROS levels can be modulated through enzymatic regulation, with Noxs upregulating ROS production and enzymatic antioxidants, including superoxide dismutase (SOD), catalase (CAT) and glutathione peroxidase (GPx), downregulating ROS levels(Sies and Jones, 2020). Increased ROS production (termed oxidative stress) has been implicated in pathologies of both experimental and human hypertension (RodrigoGonzalez and Paoletto, 2011, Montezano and Touyz, 2012, Brito et al., 2015). Studies have linked oxidative stress to ER stress signalling in hypertension-induced organ damage. ER stress inhibition reduced ROS production in brain circumventricular subfornical organ (SFO) Ang II-induced hypertensive mice(Young et al., 2012). On the other hand, Nox1 and Nox4 inhibition modulating IRE1 and PERK signalling in VSMCs from hypertensive rats (Camargo et al., 2018).

The ER serves as a major intracellular calcium storage, where it plays a crucial role in maintaining proper protein folding, facilitated by the action of Ca<sup>2+</sup>-binding chaperone proteins (KuznetsovBrostrom and Brostrom, 1992). ER calcium channels, such as the Ca<sup>2+</sup>-releasing channel inositol trisphosphate receptors (IP3Rs), and Ca<sup>2+</sup>-influx channel sarco/endoplasmic reticulum ATPase (SERCA), play a key role in regulating calcium homeostasis. ER stress has been implicated in the dysregulation of Ca<sup>2+</sup> handling in hypertension. ER stress disrupts calcium balance and contributes to the development of hypertension, as evidenced by inhibition of ER stress attenuated high SERCA expression in ventricular tissue of hypertensive rats (Bal et al., 2019a). Additionally, disturbances in Ca<sup>2+</sup> balance can lead to ER stress, as the inactivation of SERCA causes a decrease in ER Ca<sup>2+</sup> levels, triggering ER stress and increasing blood pressure (Liu et al., 2020).

Growing evidence indicates that non-coding RNAs, particularly microRNAs (miRNAs), play a crucial role in VSMCs dysfunction during hypertension (Zhang and Sun, 2021). MiRNAs are small non-coding RNAs consisting of 19 to 25 nucleotides that negatively regulate gene expression (Xie et al., 2005). Each miRNA can target multiple genes, while a single mRNA can be regulated by several different miRNAs (Cai et al., 2009, Saito and Saetrom, 2010). It has been widely found that non-coding RNA plays both regulators and effectors role in ER stress (McMahonSamali and Chevet, 2017). MiR1283 targets ATF4, thus reducing ER stress and cell apoptosis, which may be involved in hypertension(Chen et al., 2021). Differentially expressed miRNAs in SHR are related to ER stress-related gene Thbs4 (Palao et al., 2015a). In vascular cells, both in vivo (mice) and in vitro experiments showed that miR-204 downregulates Sirt1 and promotes vascular ER stress and ER stress-

induced endothelial dysfunction. Additionally, inhibition of miR-204 decreased ROS generation from ER stress (Kassan et al., 2017b). It was found that XBP1s directed miR-1274B transcription, thus targeting calponin h1 (CNN1) mRNA degradation and SMC proliferation (Zeng et al., 2015).

## 3.2 Hypothesis and aims

There is a gap in knowledge about the molecular mechanisms whereby ER stress regulates vascular dysfunction in human hypertension, especially regarding the role of miRNAs. While there is evidence that ER stress plays a role in hypertension-associated vascular damage and in the pathophysiology of high blood pressure, the underlying mechanisms involving oxidative stress, Ca<sup>2+</sup> signalling pathway, and miRNAs remain elusive. We hypothesise that in hypertension, the activation of ER stress influences redox signalling and leads to dysfunctional Ca<sup>2+</sup> homeostasis. These changes are associated with altered miRNA expression. This chapter aims to investigate the molecular mechanisms of ER stress in hypertensive human VSMCs, focusing on oxidative stress, calcium channels, and overall miRNA regulation. The specific aims are:

1. To investigate the miRNA expression profile in human VSMCs (hVSMCs) from hypertensive subjects (HT) compared with normotensive subjects (NT).

miRNA expression from VSMCs of human gluteal biopsies was assessed using the TaqMan Advanced miRNA Assays. Three samples from normotensive individuals were combined to create a pooled sample labelled as "NT." Similarly, three samples from hypertensive individuals were pooled together to create a pooled sample labelled as "HT." The differentially expressed (DE) miRNAs were analysed and identified based on their CT value and fold change.

2. To explore the potential targets of DE miRNAs, focus on the differentially expressed gene and protein associated with oxidative stress, calcium channels and ER stress in hVSMCs from HT and NT.

DE miRNAs were paired inversely with DE genes or proteins, and their putative relationship was analysed using the Ingenuity® Systems Pathway Analysis (IPA) software.

3. To study the potential of ER stress in regulating oxidative stress and Ca<sup>2+</sup> homeostasis.

Human VSMCs from NT and HT were stimulated with ER stress inducer tunicamycin (tunica) (5  $\mu$ g/ml) for 5h (short term) and 24h (long term). ROS generation, relevant genes and proteins expression were examined.

## 3.3 Results

### 3.3.1 miRNA expression profile in hypertension

miRNAs expression changed in VSMCs from hypertensive subjects (HT) as compared to normotensive subjects (NT) (Figure 3.1A). Among the 754 screened miRNAs, 287 were undetermined in both NT and HT, while 54 miRNAs were exclusively present in NT and another 54 in HT. Among the 359 miRNAs present in both NT and HT, 185 were highly expressed in HT, while 174 were highly expressed in NT.

We classified our findings into 4 groups (Figure 3.1B): 1. HT only: This group including miRNAs expressed only in HT. Results were ranked and presented from low to high based on the Ct value of the hypertensive sample, with Ct value less than 30 considered DE miRNAs and subject to further analysis (21 miRNAs); 2. NT only: This group including miRNAs expressed only in NT. Results were ranked and presented from low to high based on the Ct value of the normotensive sample, with Ct value less than 30 considered DE (differentially expressed) miRNAs and subject to further analysis (25 miRNAs); 3. HT>NT: miRNA upregulated in hypertensive subjects results were ranked and presented from high to low by hypertensive fold change (RQ) compared to normotensive, with a fold change over 1.5 considered DE miRNAs and subject to further analysis (60 miRNAs); 4. NT>HT: miRNA downregulated in hypertensive subjects results were ranked and presented from high to low based on normotensive fold change (RQ) compared to hypertensive, with a fold change over 1.5 considered DE miRNAs and subject to further analysis (136 miRNAs). The top 10 miRNAs in each group are listed in Table 3.1.

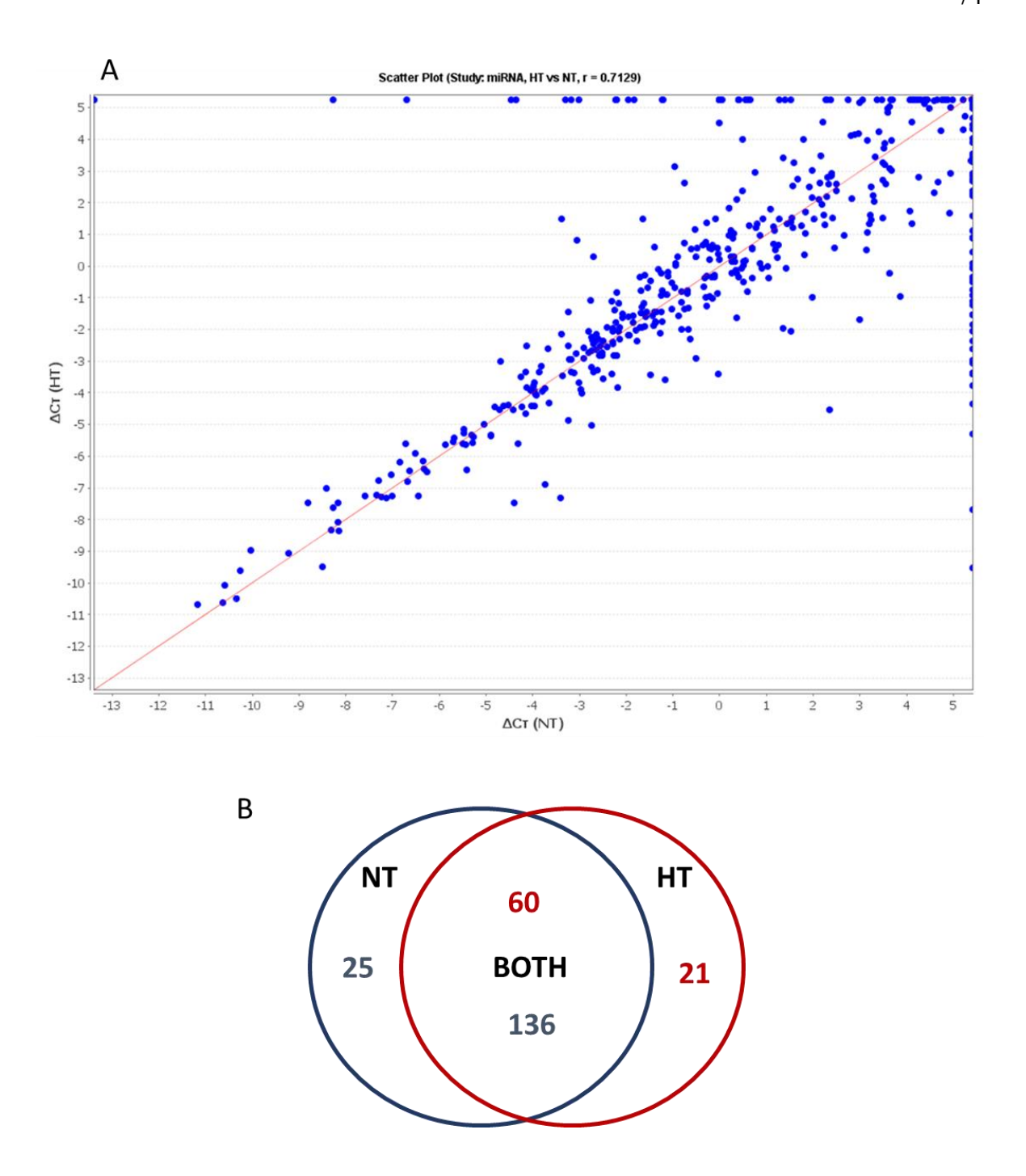


Figure 3.1 miRNA expression performance in miRNA array.

(A), The scattering figure shows the levels of individual miRNAs in HT and NT as analysed by microarray ( $\Delta$ Ct=Ct (miRNA) - Ct (global mean)). R²=0.7129. (B), The number of differentially expressed miRNA present in HT and/or NT. Red and blue circles represent the number of miRNAs highly expressed in HT and NT, respectively. The upper number (red) indicates the number of upregulated miRNAs in HT, and the lower number (blue) indicates the number of downregulated miRNAs in HT.

Table 3.1 Top10 miRNAs in each group

	HT only		NT only		HT>NT		NT>HT	
	miRNA	CT	miRNA	СТ	miRNA	Fold	miRNA	Fold
1	hsa-miR-647	20.23	hsa-miR-325	16.22	hsa-miR-181d-5p	95.678	hsa-miR-222-5p	-35.971
2	hsa-miR-99a-5p	22.07	hsa-miR-98-5p	21.32	hsa-miR-182-5p	23.057	hsa-miR-200c-3p	-28.571
3	hsa-miR-203a-3p	24.47	hsa-miR-548j-5p	22.89	hsa-miR-17-3p	20.751	hsa-miR-148a-3p	-21.277
4	hsa-miR-375	25.41	hsa-miR-1208	25.12	hsa-miR-1203	12.127	hsa-miR-889-3p	-18.051
5	hsa-miR-1294	25.99	hsa-let-7c-5p	25.23	hsa-miR-216a-5p	11.852	hsa-miR-454-5p	-14.045
6	hsa-miR-182-3p	26.34	hsa-miR-520g-3p	26.3	hsa-miR-671-3p	9.708	hsa-miR-579-3p	-12.87
7	hsa-miR-507	26.39	hsa-miR-617	26.41	hsa-miR-106b-5p	8.439	hsa-miR-146a-5p	-10.741
8	hsa-miR-412-3p	26.7	hsa-miR-9-5p	26.57	hsa-miR-381-3p	8.056	hsa-miR-143-5p	-9.852
9	hsa-miR-142-3p	26.79	hsa-miR-634	27.36	hsa-miR-378a-5p	7.717	hsa-miR-452-5p	-6.161
10	hsa-miR-542-5p	27.14	hsa-miR-636	27.39	hsa-miR-30b-3p	7.281	hsa-miR-129-5p	-5.711

# 3.3.2 Differentially expressed miRNAs in hypertensive subjects are predicted to target Noxs

Noxs are the major source of ROS in the vasculature that contribute to oxidative stress during hypertension (Majzunova et al., 2013). To examine whether Nox expression is altered in hypertensive VSMCs and whether any miRNA may be involved in the regulation of Noxs, we performed the Nox gene expression followed by miRNA analysis. Nox1 and Nox2 showed a significant increase, while Nox4 showed a substantial decrease in hypertensive human VSMCs (Figure 3.2 A, B, and C). Nox4 and Nox5 protein expression has been found to significantly increase in HT VSMCs from our previous research (Camargo et al., 2022). We subsequently analysed whether the DE (differentially expressed) Noxs were predicted targets of any DE miRNAs. Since miRNAs can either downregulated gene expression or protein translation, we inversely paired Nox4 to both upregulated and downregulated miRNAs.

From the analysis, it was found that no downregulated miRNAs were predicted to target Nox1 in HT. However, two of the DE miRNAs that were downregulated in HT were predicted to target Nox2 (CYBB): miR-205-5p, miR-376a-3p (Figure 3.2D, Table 3.2). In addition, four DE miRNAs were predicted to regulate Nox4 (Figure 3.2E), with two of them that were downregulated in HT: miR-550a-3p, miR-1226-5p (Table 3.2), and the other two were upregulated in HT: miR-1294, miR-330-5p (Table 3.3). Moreover, five DE miRNAs that were downregulated in HT were predicted to regulate Nox5: miR-149-3p, miR-505-5p, miR-324-5p, miR-186-5p, miR-491-5p (Figure 3.2F, Table 3.2).

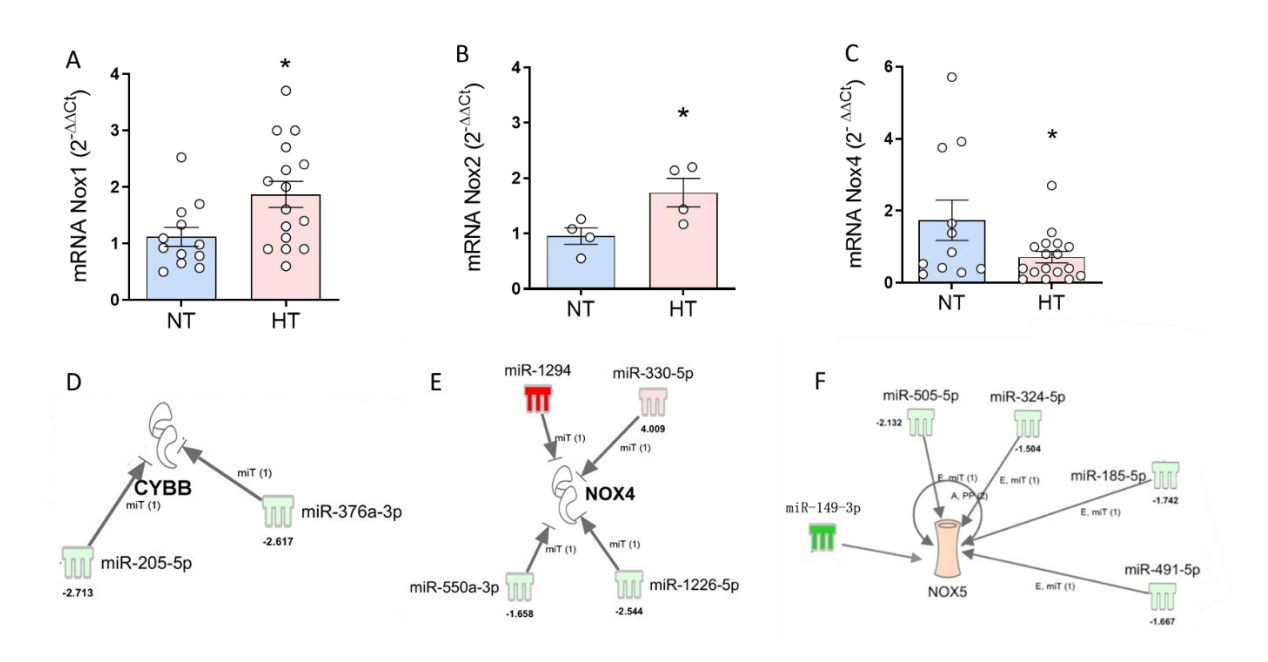


Figure 3.2 Differentially expressed miRNAs are predicted to target Noxs.

NADPH oxidases Nox1 (A), Nox2 (B), and Nox4 (C) gene expression of human VSMCs from NT (blue columns) and HT (red columns) were examined by real-time qPCR. The human GAPDH gene was used as an internal control. Data are presented as mean  $\pm$  S.E.M., n=11-16. The statistical significances were determined by student t-test, \*p<0.05 vs. NT. IPA was used to predict miRNA targets. MiRNAs (red: miRNAs upregulated in HT, green: miRNAs downregulated in HT) are inversely predicted to target genes Nox2 (D) Nox4 (E), protein Nox4 (E) and protein Nox5 (F).

Table 3.2 The predicted targets of miRNA downregulated in HT

Gene/Protein	Fold change	miRNA	Fold change
NOX2	1.66	miR-205-5p	-2.713
		miR-376a-3p	-2.617
NOX4	1.97(Camargo et al., 2022)	miR-1226-5p	-2.544
		miR-550a-3p	-1.658
NOX5	2.04(Camargo et al., 2022)	miR-149-3p	ND in HT
		miR-505-5p	-2.132
		miR-185-5p	-1.742
		miR-149-5p	-1.667
		miR-324-5p	-1.504
SOD2	4.43	miR-382-5p	-1.724

ND: Undetermined

Table 3.3 The predicted targets of miRNA upregulated in HT

Gene/Protein	Fold change	miRNA	Fold change
NOX4	2.42	miR-1294	ND in NT
		miR-330-5p	4.009
IP3R	1.64	miR-585-3p	3.29

ND: Undetermined

# 3.3.3 Differentially expressed miRNAs in hypertensive subjects are predicted to target antioxidants

Antioxidants are also an important part of regulating oxidative stress in hypertension. To assess whether DE miRNAs may contribute to antioxidant expression in HT, we examined the expression of some antioxidant genes followed by miRNA analysis. SOD is an enzyme that catalyses the dismutation of the superoxide (O2<sup>-</sup>) into molecular oxygen (O2) and hydrogen peroxide (H<sub>2</sub>O<sub>2</sub>). Two intracellular subtypes of SOD were determined in human VSMCs. SOD1, expressed in cytoplasm, was not changed in HT (Figure 3.3A). SOD2, expressed in mitochondria, was significantly increased in HT (Figure 3.3B). CAT and GPx catalyse the reduction of hydrogen peroxide. CAT was increased considerably in HT (Figure 2C). However, no downregulated miRNAs predicted to target CAT were found. Nuclear factor erythroid 2-related factor 2 (Nrf2) is a key transcription factor that regulates the expression of antioxidant proteins, including SOD (TonelliChio and Tuveson, 2018). Kelch-like ECH-associated protein 1 (Keap1) is an endogenous inhibitor of Nrf2 that under oxidative stress, it is oxidising and releases Nrf2 to translocate to the nucleus, promoting activation of antioxidant genes. In human VSMCs, there was no significant difference in gene expression between HT and NT for either Nrf2 (Figure 3.3D) or Keap1 (Figure 3.3E). Moreover, one of the DE miRNAs downregulated in HT was predicted to target SOD2: miR-328-5p (Figure 3.3F, Table 3.2).

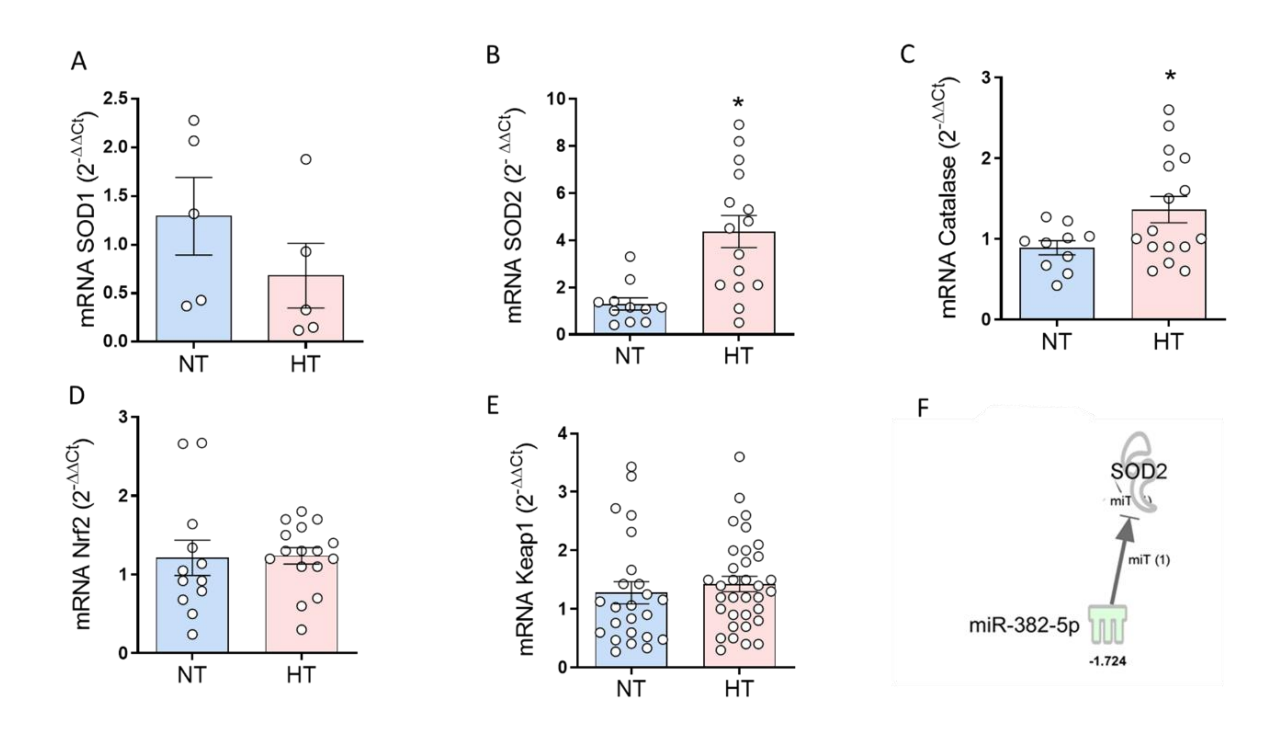


Figure 3.3 Differentially expressed miRNAs are predicted to target antioxidants expression in VSMC of hypertensive subjects.

Antioxidants SOD1 (A), SOD2 (B), Catalase (C) Nrf2 (D) and Keap1 (E) gene expression of human VSMCs from NT (blue columns) and HT (red columns) were determined by RT-qPCR. The human GAPDH gene was used as an internal control. Data are presented as mean ± S.E.M., n=11-16. The statistical significances were determined by student t-test, \*p<0.05 vs. NT. IPA was used to predict miRNA targets. MiRNAs (green: miRNA downregulated in HT) are inversely predicted to target genes SOD2 (F).

# 3.3.4 Differentially expressed miRNAs in hypertensive subjects are predicted to target Calcium channels

To determine whether calcium channels were altered and predicted to be targeted by DE miRNAs, we examined the expression of some calcium channel genes followed by miRNA analysis. CACNA1C encodes the subunits of the CaV1.2 L-type voltage-gated calcium channel, an important mediator of calcium influx and downstream signalling cascades. The expression of CACNA1C has no significant difference between NT and HT in human VSMCs (Figure 3.4A). IP3R (inositol 1,4,5-trisphosphate receptor) and SERCA (sarco/endoplasmic reticulum Ca<sup>2+</sup>-ATPase) are endoplasmic reticulum calcium channels responsible for Ca<sup>2+</sup> release from ER and influx into ER respectively. IP3R was significantly decreased in HT (Figure 3.4B). One of the differentially expressed miRNA up regulated in HT is predicted to target IP3R (ITPR3): miR-585-3p (Figure 3.4D, Table 3.2). SERCA was significantly increased in HT (Figure 3.3C), and no DE miRNAs were found to predict inversely target SERCA.

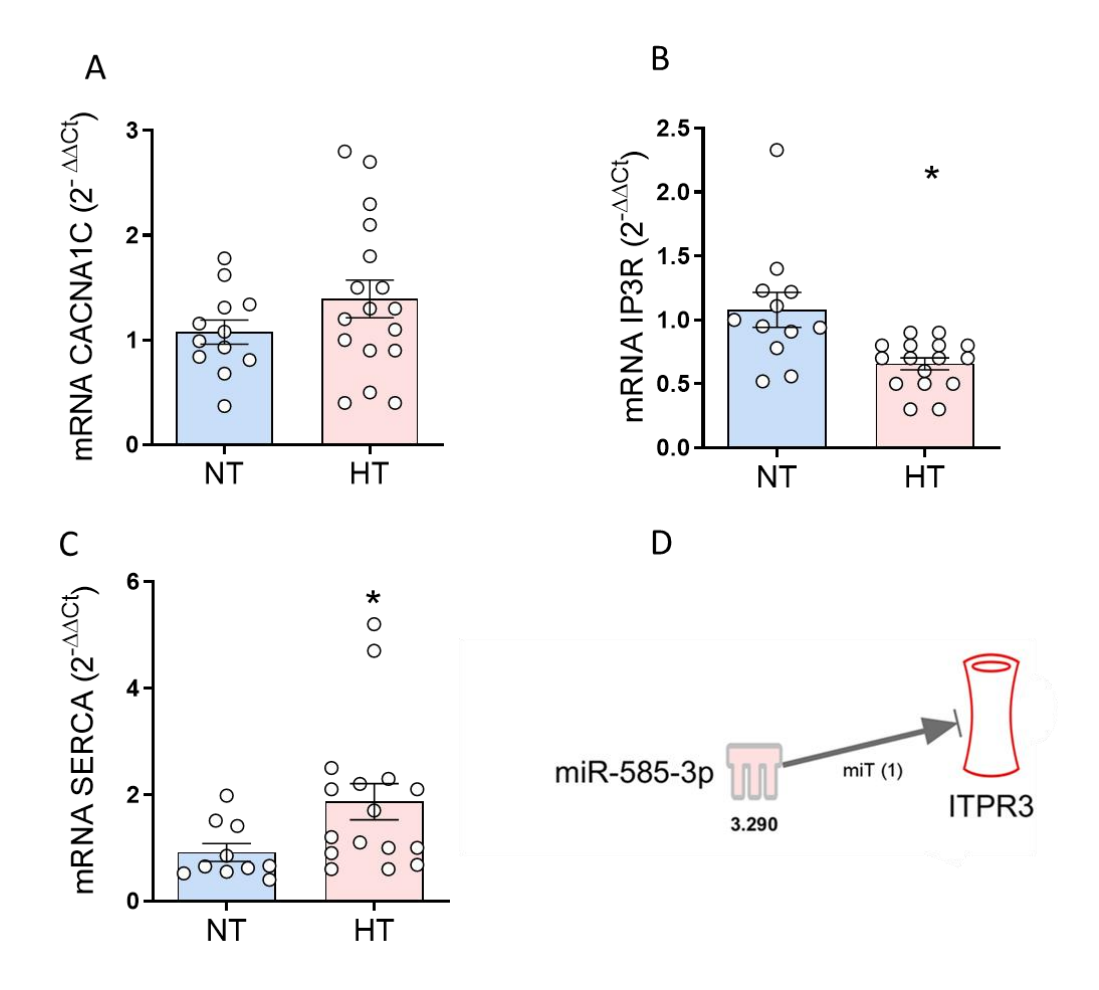


Figure 3.4 Differentially expressed miRNAs are predicted to target Calcium channel expression in VSMC of hypertensive subjects.

Calcium channel CACNA1C (A), IP3R (B) and SERCA (C) gene expression of human VSMCs from NT (blue columns) and HT (red columns) were determined by RT-qPCR. Human GAPDH gene was used as an internal control. Data are presented as mean  $\pm$  S.E.M., n=11-16. Statistical significances were determined by student t-test, \*p<0.05 vs. NT. IPA was used to predicted miRNA targets. MiRNA (red: miRNAs upregulated in HT) is inversely predicted to target IP3R (D).

## 3.3.5 MiR-200b-3p predicted targeting ER stress pathway

ER stress is essential in blood pressure regulation. To investigate if ER stress is activated in HT, we examined the expression of some ER stress markers. ER stress marker ATF4 gene expression increased, while CHOP and ATF6 gene expression did not change in HT. This suggests the potential of PERK pathway activation. Moreover, to investigate whether ER stress is involved in miRNA regulating in HT. IPA software canonical pathway section was used to identify predicted targets of DE miRNAs in the ER stress pathway. After analysis, miR-200c-3p, downregulated in HT with a 28.58-fold change, was found to be of particular interest. Results showed that miR-200b-3p has four different predicted targets related to ER stress pathway, including ASK1, JIK (IRE1-induced apoptosis signal), eIf2α, and P58IPK (DNAJ homolog subfamily C member 3) (Figure 3.5D). EIf2α is upstream of ATF4 (upregulated in our results), which suggested a potential link to the regulation of decreased miR-200c-3p.

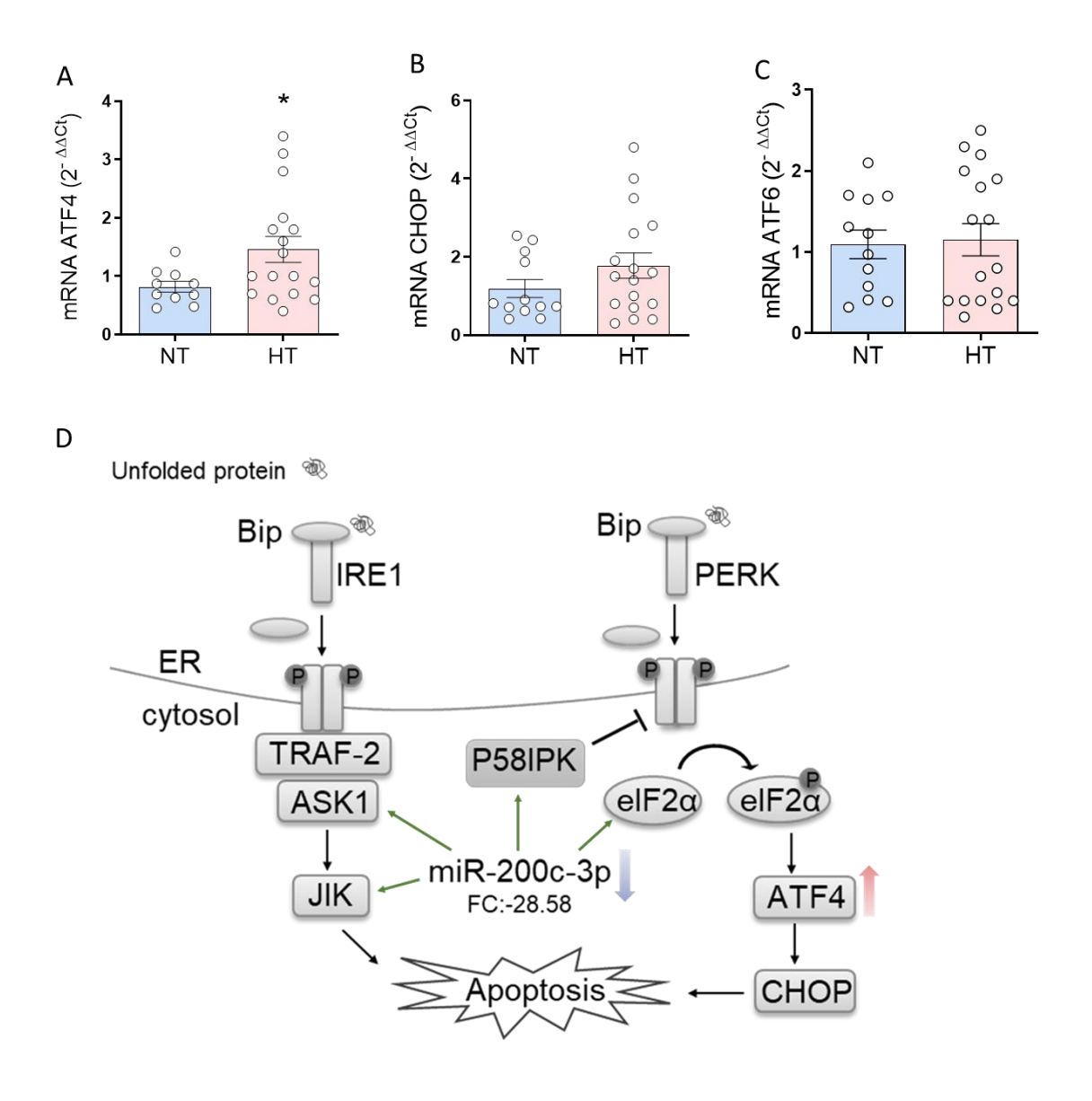


Figure 3.5 ER stress markers in HT and miR-200c-3p in ER stress pathway.

ATF4(A), CHOP(B), ATF6(C) gene expression of human VSMCs from NT (blue columns) and HT (red columns) were determined by RT-qPCR. The human GAPDH gene was used as an internal control. Data are presented as mean ± S.E.M., n=10-16. The statistical significances were determined by student t-test, \*p<0.05 vs. NT. The predicted targets of miR-200c-3p were analysed by IPA (D). ATF4 with the red colour arrow was upregulated in HT. miR-200c-3p with a blue colour arrow was downregulated in HT. The green line with arrow means the miRNA is predicted to target those molecules.

# 3.3.6 ER stress increases NADPH-dependent O<sup>2-</sup> production in hypertensive human VSMCs

The major ROS resulting from oxidative stress include hydrogen peroxide (H<sub>2</sub>O<sub>2</sub>) and superoxide (O<sub>2</sub><sup>-</sup>), which are electron donors and can damage DNA, RNA, proteins, and lipids, thus contributing to vascular remodelling and dysfunction in hypertension. To evaluate whether ER stress contributes to oxidative stress in hypertension, we assessed ROS generation in VSMCs from NT and HT. We also stimulated VSMCs with the ER stress inducer tunica. We found that NADPH-dependent O<sub>2</sub><sup>-</sup> generation (Figure 3.6A) was increased in HT compared to NT. Treatment with tunica did not affect O<sub>2</sub><sup>-</sup> generation in NT (Figure 3.6B), but it led to a significant increase in HT after 24h of treatment (Figure 3.6C). Moreover, we observed that H<sub>2</sub>O<sub>2</sub> generation (Figure 3.6D) was also increased in HT, but it was not affected by tunica stimulation (Figure 3.6E and F). These results suggest that ER stress may play a role in hypertension-related oxidative stress by inducing NADPH-dependent O2– generation but not H<sub>2</sub>O<sub>2</sub> generation.

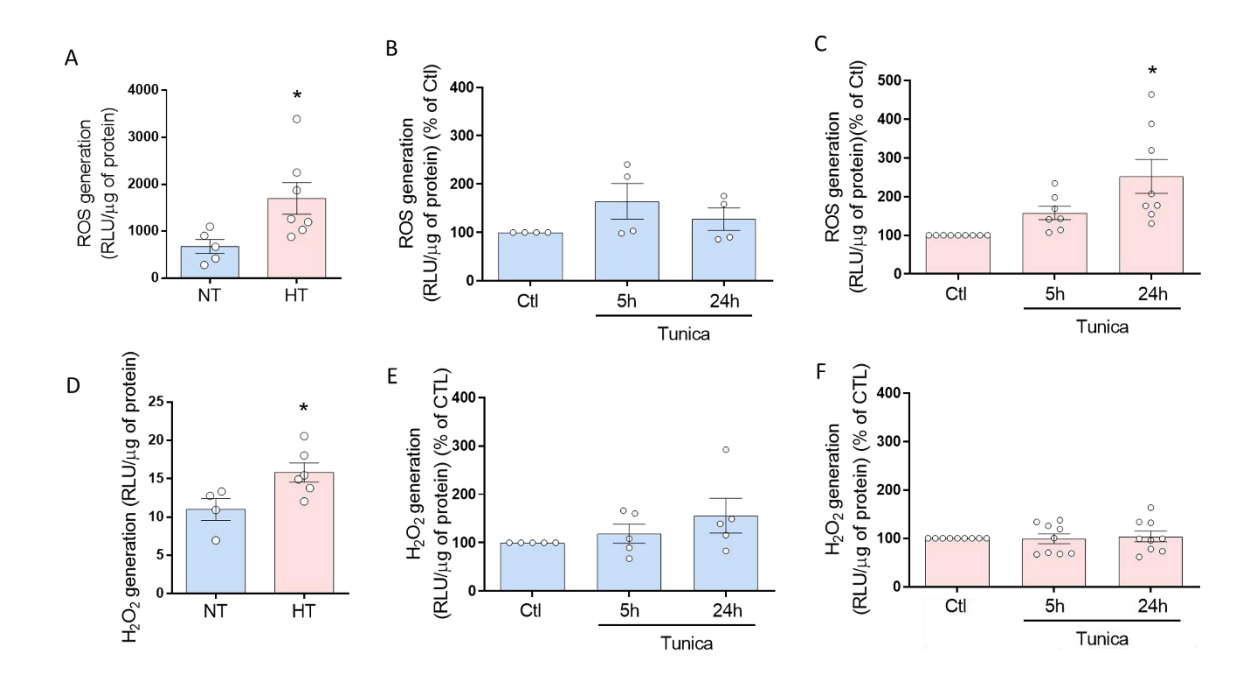


Figure 3.6 Effects of ER stress inducer on ROS generation in human VSMCs from normotensive subjects and hypertensive subjects.

The human VSMCs from NT (blue columns) and HT (red columns) were treated with Tunica (5  $\mu$ g/ml) (5h and 24h). NADPH-dependent ROS (A,B,C) was determined by lucigenin-derived chemiluminescence and NADPH-dependent H<sub>2</sub>O<sub>2</sub> was generation (D,E,F) was determined by Amplex red in NT and HT subjects. Data are presented as mean  $\pm$  S.E.M., n=4-11. Data were analysed using one-way ANOVA followed by a Tukey test or student t-test for two groups comparing. \*p<0.05 vs. control.

## 3.3.7 Tunica induced ER stress influences Noxs expression in human VSMCs

To investigate the mechanism of ER stress influencing ROS level in human VSMCs, we assessed Noxs expression after tunica treatment. Tunica 24h treatment significantly increased Nox1 gene expression in NT but not in HT (Figure 3.7A). However, tunica did not alter Nox1 expression at the protein level (Figure 3.7B and C). Different from Nox1, Nox4 gene expression decreased after 24h of tunica treatment in NT but not in HT (Figure 3.7D), while Nox4 protein level was not changed by tunica (Figure 3.7E and F). Tunica increased Nox2 gene expression in both 5h and 24h of treatment in NT but not in HT (Figure 3.7G), the protein expression was not determined due to the unavailability of an appropriate antibody. Nox5 protein expression increased after 24 h tunica treatment in both NT and HT (Figure 3.7H and I). The gene expression data for Nox5 was not shown due to the low or undetermined CT value. These findings suggest that ER stress may play a role in Noxs expression, and the increasing ROS generation in HT may be related to Nox5.

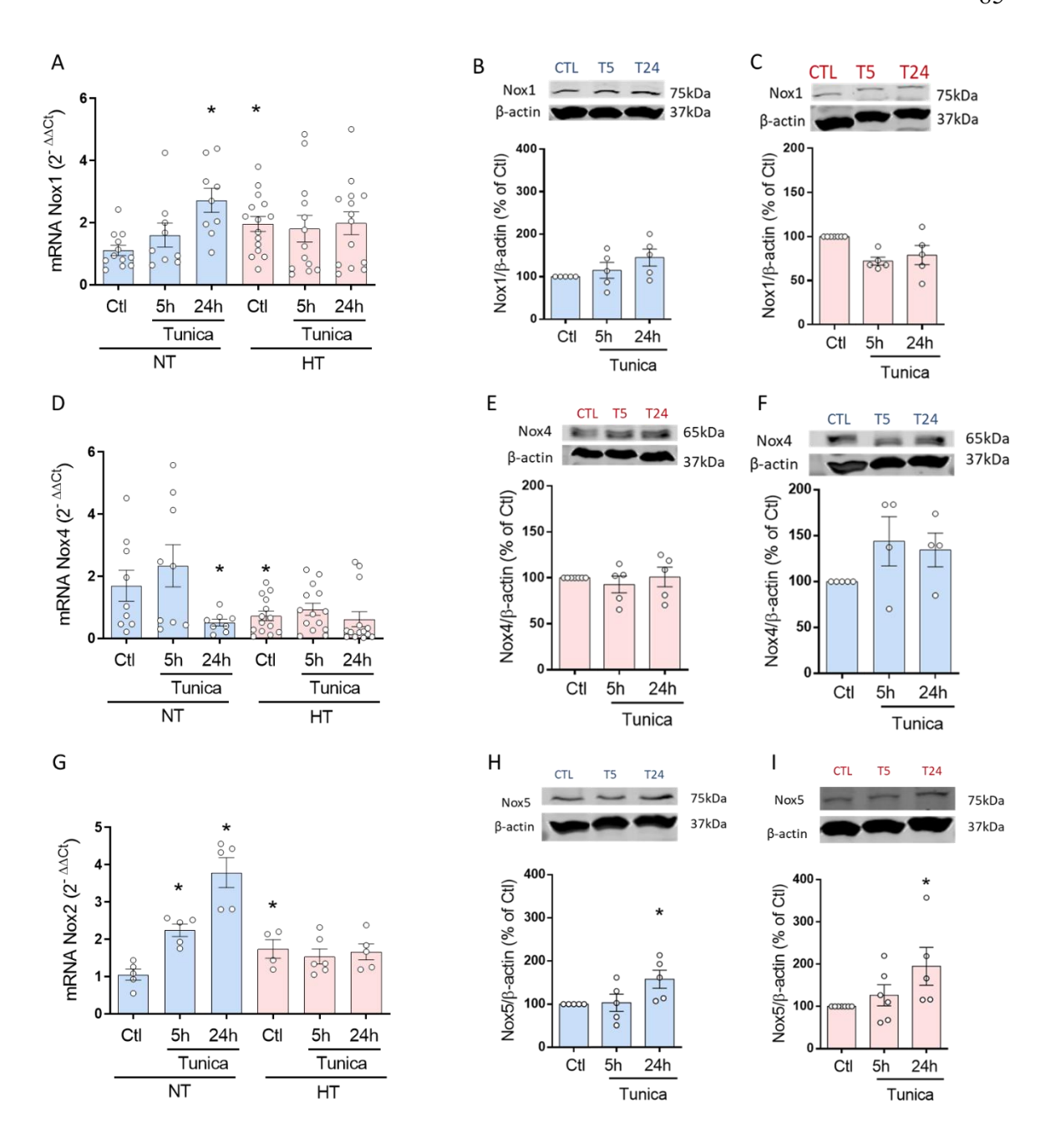


Figure 3.7 ER stress influence Noxs expression in human VSMCs.

The human VSMCs from NT (blue columns) and HT (red columns) were treated with Tunica (5  $\mu$ g/ml) (5h and 24h). Nox1 (A), Nox2 (G) and Nox4 (D) gene expression were determined by RT-qPCR. The human GAPDH gene was used as an internal control. Nox1 (B, C), Nox4 (E, F), and Nox5 (H, I) protein expression were determined by Western blotting with  $\beta$ -actin as loading control. Data are presented as mean  $\pm$  S.E.M., n=5-16. Statistical significances were determined by one-way ANOVA followed by a Tukey test or student t-test for two groups comparing. \*p<0.05 vs. control.

# 3.3.8 Tunica induced ER stress influences antioxidants expression in human VSMCs

To explore whether ER stress regulates ROS generation through antioxidants in human VSMCs, we assessed the antioxidants expression with the ER stress inducer tunica. Treatment with tunica significantly reduced SOD2 gene expression (Figure 3.8A) in both NT and HT. CAT, which is involved in the decomposition of H<sub>2</sub>O<sub>2</sub>, was increased after tunica 24h treatment in NT (Figure 3.8B) but not in HT. Nrf2 expression was increased after tunica 24h stimulation in NT and 5h and 24h in HT (Figure 3.7C). Keap1 as a negative regulator of Nrf2 was increased only after 24h tunica treatment in both NT and HT (Figure 3.7 D). These findings suggest ER stress could affect antioxidants expression, and decreased SOD2 expression may contribute to ROS generation in HT.

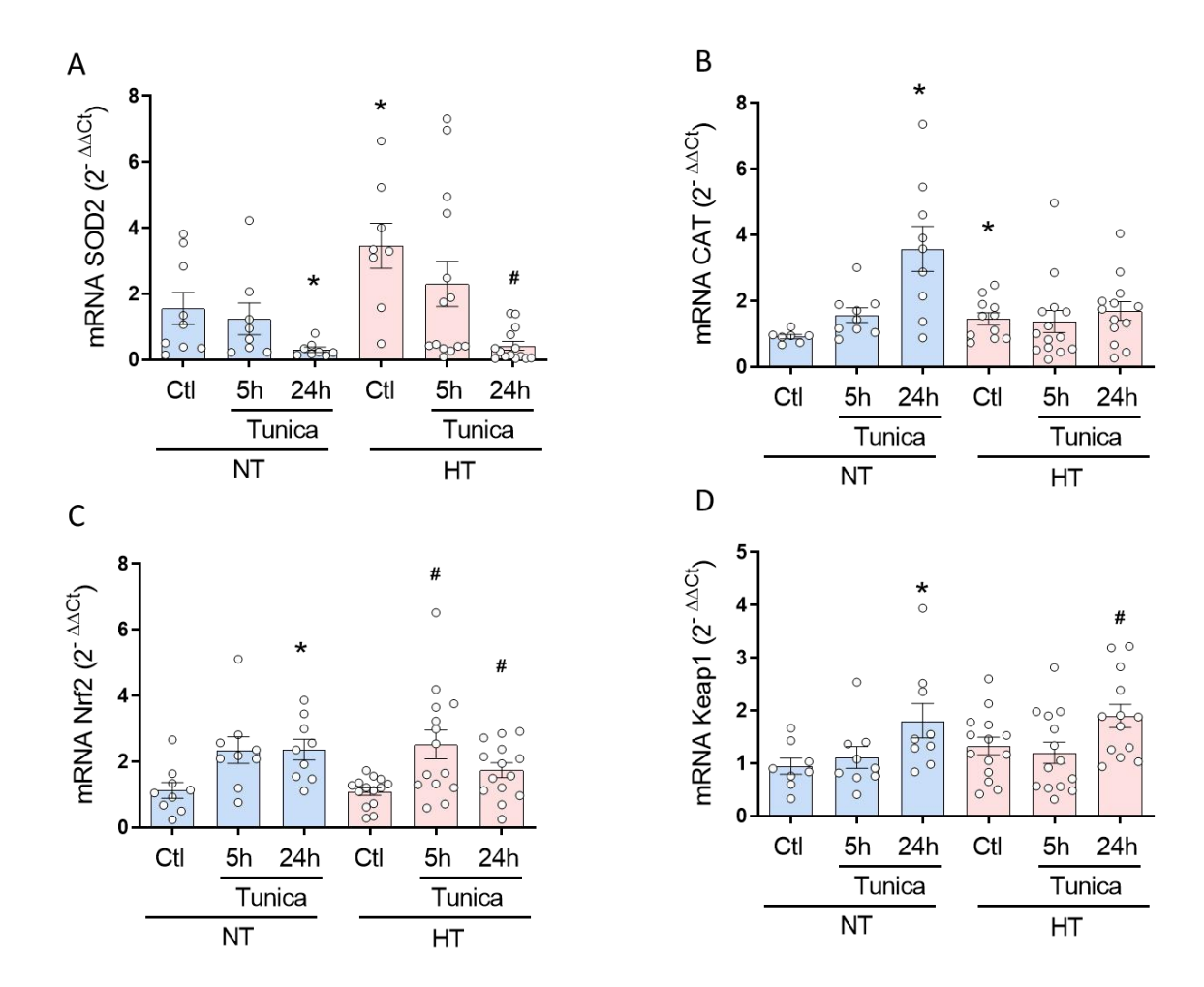


Figure 3.8 ER stress influence antioxidants expression in human VSMCs.

The human VSMCs from NT (blue columns) and HT (red columns) were treated with Tunica (5  $\mu$ g/ml) (5h and 24h). SOD2 (A), catalase (B), Nrf2 (C) and Keap1 (D) gene expression were determined by RT-qPCR. The human GAPDH gene was used as an internal control. Data are presented as mean  $\pm$  S.E.M., n=5-16. Statistical significances were determined by one-way ANOVA followed by a Tukey test or student t-test for two groups comparing. \*p<0.05 vs. NT control, #p<0.05 vs. HT control.

## 3.3.9 Tunica induced ER stress influences calcium channel expression in human VSMCs

Intracellular free calcium concentration is important in vascular smooth muscle contraction during hypertension, which is controlled by calcium channels(Touyz et al., 2018). ER stress has been linked to disruption in calcium homeostasis, which may contribute to the development of hypertension. Therefore, we investigated the effects of ER stress on calcium channel gene expression in VSMCs. Treatment of human VSMCs with 24h tunica induced downregulation of L-type calcium channel (Figure 3.9 A) and upregulation of IP3R (Figure 3.9 B) in both NT and HT. No significant effect of tunica was observed on SERCA mRNA levels (Figure 3.9C).

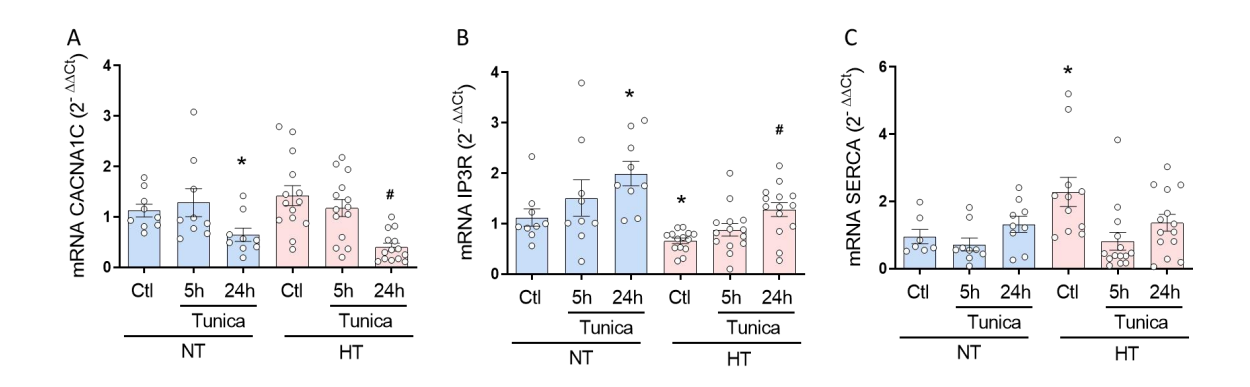


Figure 3.9 ER stress influences calcium channel expression in human VSMCs.

The human VSMCs from NT (blue columns) and HT (red columns) were treated with Tunica (5  $\mu$ g/ml) (5h and 24h). CACNA1C (A), IP3R (B) and SERCA (C) gene expression were determined by RT-qPCR. The human GAPDH gene was used as an internal control. Data are presented as mean  $\pm$  S.E.M., n=5-16. Statistical significances were determined by one-way ANOVA followed by a Tukey test or student t-test for two groups comparing. \*p<0.05 vs. NT control, #p<0.05 vs. HT control.

#### 3.4 Discussion

This chapter focuses on the molecular regulation in VSMCs related to the crosstalk between ER stress, oxidative stress, calcium channels, and miRNA, comparing HT and NT. Firstly, we identified 242 differentially expressed (DE) miRNAs in VSMCs of HT compared to NT and linked them to target genes of interest, including Noxs, antioxidants, calcium channels, and ER stress markers. Regarding gene expression, we observed increased expression of Nox1, Nox2, SOD2, catalase, and the calcium channel SERCA, alongside decreased expression of Nox4 and the calcium channel IP3R in VSMCs from HT. To further investigate whether ER stress affects oxidative stress and calcium channel expression in VSMCs, we used the ER stress inducer tunicamycin. We found that tunicamycin reduced the expression of SOD2 and the L-type calcium channel while increasing the expression of Nox5, nrf2, keap1, and IP3R in both NT and HT. Additionally, tunicamycin increased the gene expression of Nox1, Nox2, and catalase while decreasing Nox4 expression in VSMCs from NT, but not in HT. These findings suggest crosstalk between oxidative stress/calcium channels and ER stress, highlighting the different mechanisms by which ER stress affects oxidative stress in hypertension.

#### 3.4.1 The role of miRNAs in VSMCs of HT and NT

The remodelling and injury of resistance arteries are key characteristics in the development and progression of hypertension, to which the phenotype switching and dysfunction of VSMCs significantly contributes (Guzik and Touyz, 2017). The VSMCs used in this chapter were obtained from small arteries from adult human gluteal biopsies, as previously described (Camargo et al., 2022). MiRNAs play a crucial role in regulating the dysfunction of VSMCs caused by hypertension (Zhang and Sun, 2021). To investigate whether miRNA expression changes in VSMCs of hypertensive patients, we compared miRNA profiles of VSMCs from resistance arteries of hypertensive and normotensive humans. The analysis revealed that 242 miRNAs exhibited differential expression between HT and NT. Unexpectedly, the number of DE miRNAs in our results was higher than in similar research. Some studies have shown changes in miRNA expression in human blood samples. For example, 30 DE miRNAs were found in whole blood of HT and NT subjects in South African individuals (Matshazi et al., 2021), and 27 DE miRNAs were identified in human plasma samples of HT and NT individuals (Li et al., 2011). In comparison to WKY and

SHR rats, there are 6 DE miRNAs identified in arterial blood samples and 10 DE miRNAs identified in venous blood samples (Jin et al., 2021), 27 DE miRNAs identified in exosomes (Liu et al., 2019b), 1 DE miRNA identified in adult mesenteric arteries (Palao et al., 2015b). Furthermore, in Ang II-induced hypertensive mice, 35 DE miRNAs have been found after 14 days of treatment (Huo et al., 2019). These findings, together with ours, suggest the role of miRNAs in hypertension. There are two main reasons that might explain why our study identified more DE miRNAs than similar studies. Firstly, we used human cell cultures, and the absence of a complete circulatory system in these cultures, including factors such as blood flow and neighbouring endothelial cells, likely influenced the miRNA regulation. Secondly, and perhaps more crucially, our use of pooled samples (one sample from groups of three hypertensive and three normotensive individuals, respectively) without repeated analyses could have impacted the accuracy.

We focused on the top 10 miRNAs in four different groups, as shown in Table 4, with the potential to regulate vascular dysfunction. Notably, miR-181d-5p, the most overexpressed miRNA in HT patients compared to NT controls, is a positive regulator of cancer cell migration by regulating p38 MAPK pathway (SongPark and Ryu, 2013), and colorectal cancer cell proliferation and migration by regulating PI3K/AKT pathway (Liu et al., 2023). These findings suggest a potential role for miR-181d-5p in regulating VSMC proliferation and migration, requiring further experimentation. Additionally, miR-182-3p, only expressed in HT, has been implicated in vascular remodelling by targeting myeloidassociated differentiation marker gene via regulating KLF4 translocation into the cytoplasm in pulmonary arterial hypertension (Sun et al., 2020), suggesting a possible involvement of miR-182-3p in VSMC differentiation. In contrast, miR-222-5p, most highly expressed in NT compared to HT, is known to inhibit VSMC differentiation by targeting aSMA and ROCK2 (Gu et al., 2018). However, it has also been found to promote cell proliferation and migration in VSMC of atherosclerosis mice model (Liu et al., 2022) and in placenta cells (Dong et al., 2020), indicating a complex mechanism that requires further exploration in our model. In the NT-only group, miR-325, which has the highest expression, was found to be downregulated in preeclamptic patients (Lazar et al., 2012). miR-9-5p (NT only) has been implicated as a negative regulator of cell proliferation and migration in HeLa cell (Zhang et al., 2016), and could also target Nox4 to suppress fibroblasts(Fierro-Fernandez et al., 2015). miR-129-5p, downregulated in HT, was found to be a negative regulator of endothelial cell migration and proliferation (Soufi-Zomorrod et al., 2016), and inhibit ROS-induced autophagy and apoptosis in heart cells (ZhangZhang and Zhang, 2018). These are similar trends to our results and suggest the potential of miR-

325, miR-9-5p, and miR-129-5p in improving high blood pressure, oxidative stress and vascular change. Furthermore, miR-143-5p, although higher in NT than HT in our study, was observed at increased levels in pulmonary artery smooth muscle cells in patients with pulmonary arterial hypertension (Deng et al., 2015). These contrasts underscore the need for further research into the role of miR-143-5p in smooth muscle function.

## 3.4.2 DE genes/proteins and related DE miRNAs in VSMCs of HT

Increasing ROS bioavailability and altered redox signalling plays a key role in the onset and progression of hypertension (Montezano and Touyz, 2014, Camargo et al., 2022, Griendling et al., 2021). In human VSMCs, Noxs are the major enzymatic sources of ROS including Nox1, Nox2, Nox4, and Nox5, thus activating downstream redox sensitive molecules (Ismail et al., 2009, Konior et al., 2014, Santillo et al., 2015). From the results, the generation of ROS was increased in VSMCs from HT, processes could be associated with dysregulation of Noxs and antioxidants, which may be controlled by inversely expressed DE miRNAs. It has been well-studied that there is an increase in Noxs in hypertensive models and individuals (Landmesser et al., 2002, RodrigoGonzalez and Paoletto, 2011, TouyzTabet and Schiffrin, 2003, Nosalski et al., 2020, Camargo et al., 2018, Camargo et al., 2022). As expected, Nox1 and Nox2 gene expression was increased in our HT VSMCs, but the protein expression was not changed from the previous study (Camargo et al., 2022). Previous studies from our group showed Nox4 and Nox5 protein expression to be increased in HT VSMCs210. However, our study did not detect Nox5 mRNA, and Nox4 gene expression was decreased. The different trends in gene and protein expression may be caused by other regulators, such as miRNAs, during the translation of proteins. IPA analysis has highlighted some miRNAs, which may contribute to these DE Noxs and thus influence hypertension. miR-205-5p, which has lower expression in HT and was predicted to target Nox2, was found to be downregulated by oxidative stress and to regulate VEGFA-angiogenesis (Oltra et al., 2020). miR-330-5p, which showed lower expression in HT and was predicted to target Nox4, was demonstrated to inhibit the proliferation and migration of human VSMCs (Chen et al., 2022). miR-185-5p, which is downregulated in HT and predicted target Nox5, has been found to inhibit cell migration by targeting ROCK2 in hepatocellular carcinoma (Niu and Tang, 2019). Moreover, miR-149-5p, which is also downregulated in HT and predicted to target Nox5, has been found to decrease ER stress markers in endothelial cells of type two diabetes (Yuan et al., 2017).

As for antioxidants, SOD2 plays a vital role in protecting mitochondrial function by removing mitochondria-derived O<sub>2</sub>. (Palma et al., 2020). Studies have observed reduced SOD2 activity in aorta of Ang II-infused mice (Dikalova et al., 2017) and aortic VSMCs of SHR (Chen et al., 2020). Besides, some studies found no significant change of SOD2 in mesenteric arteries of Ang II-induced hypertensive mice or rats (KangSullivan and Pollock, 2018, Gongora et al., 2006). CAT is an enzyme that converts H<sub>2</sub>O<sub>2</sub> into water and oxygen. CAT levels have been found to increase in SHR kidney (Sundaram et al., 2013). In our results, SOD2 and CAT gene expression were increased in HT. It is possible that these antioxidants were upregulated to counteract oxidative stress. Further experimentation is required to confirm their activation. IPA analysis highlighted alterations in miRNAs targeting some of these antioxidant genes. miR-382-5p, which was downregulated in HT in our study and predicted to target SOD2, has been shown to target SOD2 in CD34+ cells from primary myelofibrosis and its dysregulation was associated with ROS accumulation and oxidative DNA damage (Rossi et al., 2018).

Intracellular calcium plays a crucial role in the development of hypertension and is also linked to oxidative stress and ER stress (Groenendyk Agellon and Michalak, 2021, Touyz et al., 2018). Thus, we examined the expression of ER calcium channels and L-type calcium channels. ROS in VSMCs is essential in modulating calcium homeostasis (Touyz et al., 2018). Exogenous addition of H<sub>2</sub>O<sub>2</sub> in VSMCs alters calcium transients, while O<sub>2</sub>. generation induces intracellular calcium mobilization (Touyz, 2005). Changes in the internal redox state could lead to an increase in the cytosol calcium level. Possible mechanisms include inhibition of SERCA, activation of IP3R, and activation of L-type calcium channels. Studies have identified that increasing ROS could irreversibly oxidise SERCA, leading to elevated blood pressure and induction of ER stress (Scherer and Deamer, 1986, Liu et al., 2020). In our study, increased ROS levels may cause irreversible SERCA oxidation, leading to its degradation. As a compensatory mechanism, the mRNA level of SERCA is upregulated, as observed in the present study. Additionally, we found a decrease in IP3R gene expression in HT, which may also serve as a compensatory response to lower intracellular calcium during hypertension. No significant difference was observed in L-type calcium channel between HT and NT. The expression of calcium channels does not directly indicate calcium movement within cells. It is necessary to evaluate their activation to further confirm the role of calcium channel. Matching our DE miRNAs, miR-585-3p, which is highly expressed in HT and predicted to target IP3R, has been shown to inhibit cell growth and proliferation in colon cancer (Liu et al., 2019a).

ER stress has been indicated in hypertensive VSMCs (Camargo et al., 2018). We observed an increase in ATF4 gene expression, which indicates the potential activation of the PERK pathway. IPA analysis showed that miR-200c-3p, downregulated in HT, has been found to have multiple targets in the ER stress pathway. miR-200c-3p was found to be upregulated in cases of pulmonary arterial hypertension-superior vena cava (Chouvarine et al., 2020) and in mice with Ang II injection (Huo et al., 2019). Moreover, miR-200b also triggers UPR in diabetic model (Gu et al., 2016). eIF2α as the predicted target of miR-200c-3p could be regulated by PERK, oxidative stress, and P58IPK (OchoaWu and Terada, 2018), which is another predicted target of miR-200b-3p. Besides, miR-200c-3p was shown to be highly expressed in the resistant vessels of Ang II-induced hypertensive mice (Huo et al., 2019). This suggests an important role of the miR-200c-3p in regulating hypertension. Together, these findings indicate the potential role of miR-200b-3p in regulating ER stress in hypertensive VSMCs.

These potential DE miRNAs may be involved in the molecular mechanisms of vascular dysfunction and are related to oxidative stress and ER stress, thereby making them interesting targets for future research.

#### 3.4.3 Effect of ER stress inducer in VSMCs

Tunicamycin, known for its role in inducing ER stress by inhibiting N-linked glycan synthesis and consequently leading to misfolded proteins and UPR activation(Zhang et al., 2020), was chosen as the ER stress inducer in our study. The increasing cellular ROS level by tunicamycin has been found in different cells, including PC12 cells (Yen et al., 2017a) and myoblasts (Anto et al., 2023). In this study, tunicamycin triggered ER stress activation and increased NADPH-dependent O<sub>2</sub>- production in HT cells without affecting H<sub>2</sub>O<sub>2</sub> generation. Conversely, ROS levels in NT cells remain unchanged under ER stress. This suggests that ER stress may specifically trigger oxidative stress in VSMC under hypertensive conditions, while the response in NT cells implies a different regulatory mechanism.

In HT, increasing O<sub>2</sub>- production could be attributed to altered expression of Noxs and antioxidants. Nox5 is a calcium-sensitive Nox isoform that produces O<sub>2</sub>- and H<sub>2</sub>O<sub>2</sub>(Fulton, 2009), which has been found associated with ER stress (Sui et al., 2023, Zhu et al., 2023). SOD2 in mitochondria transforms O<sub>2</sub>- into O<sub>2</sub> and H<sub>2</sub>O<sub>2</sub>, which can then be converted into water by other enzymes such as CAT and GPx1 (Palma et al., 2020). The increasing

expression of Nox5 and decreasing expression of SOD2 by tunicamycin in HT may contribute to the elevated production of O<sub>2</sub>. A study found decreased SOD activity by tunicamycin on rat skeletal muscle L6 cell lines (Anto et al., 2023), which is similar to our results. There has been no research to date explicitly examining tunicamycin's effects on Nox5. Alterations in Nox5 and SOD2 expression were observed in both NT and HT. However, as Nox1, Nox2, and Nox4 expression was not changed in HT subjects, the ROS may also contribute from other sources, such as mitochondria, and/or other enzymes like xanthine oxidase and cyclooxygenases, which warrants further investigation.

The absence of increased ROS generation in NT cells suggests a different redox regulation in HT. The activation of ER stress sensor PERK triggers dissociation of Nrf2/Keap1 complexes, thus allowing Nrf2 translocated into nuclear, which could contribute to increased antioxidants expression, such as GPx1, CAT and SOD (Cullinan et al., 2003). In our study, activation of ER stress resulted in increased gene expression of both Nrf2 and Keap1. However, the actual activation of Nrf2 requires further investigation. No increased expression in SOD2 and catalase in HT might indicate a lack of enhanced Nrf2 activity. This could be influenced by other mechanisms, such as less Nrf2 translation or blocked Nrf2 translocation by increased keap1. Notably, the increase in Nrf2 expression occurred after 5 hours of treatment in HT, whereas it was observed after 12 hours in NT, suggesting a distinct mechanism of Nrf2 regulation in HT. The underlying mechanisms warrant further investigation.

Similarly to HT, ER stress activation in NT led to an increase in Nox5, Nrf2, and Keap1 expression and a decrease in SOD2 expression. Besides, tunicamycin treated NT VSMCs also showed a decrease in Nox4 expression and an increase in Nox1, Nox2, and catalase. In vasculature, Nox1 and Nox2 require specific cytosolic subunits for activation and predominantly generate O2<sup>--</sup>, whereas Nox4 is constitutively activated and produces primarily H<sub>2</sub>O<sub>2</sub>. Nox2 and Nox4 have been shown to be upregulated in response to ER stress. Specifically, the expression of these genes increases when endothelial cells from coronary arteries are treated with tunicamycin (Galán et al., 2014). Additionally, Nox2 levels were found to be elevated in macrophages in mice experiencing ER stress (Li et al., 2010). The activation of the IRE1 pathway has also been linked to the increased expression of Nox4 (Pedruzzi et al., 2004). Our results show the protein expression of Nox4 has no significant change, although the gene level decreased, indicating other mechanisms may be involved, and the underlying reason needs further study. Notably, Nox2 seems sensitive to ER stress, as evidenced by the increased expression observed after 5 hours of treatment.

While an increase in the gene expression of Nox1 and Nox2 was observed, Nox1 protein expression was not changed, and their activation was not measured. Different protective mechanisms in healthy cells may contribute to maintaining normal ROS levels. For example, ER stress itself can inhibit mRNA translation, thereby reducing the protein folding load (Zeeshan et al., 2016). Increasing CAT levels, probably linked to enhanced Nrf2 expression, suggests that NT VSMCs may address oxidative stress through a different regulation of antioxidant pathways compared to HT VSMCs.

ER plays a critical role in Ca<sup>2+</sup> homeostasis, and disruption of Ca<sup>2+</sup> homeostasis in the ER leads to activation of ER stress (Groenendyk Agellon and Michalak, 2013). The activation of IP3R or inhibition of SERCA ultimately leads to Ca<sup>2+</sup>-store depletion, thus contributing to ER stress (Luciani et al., 2009, Kiviluoto et al., 2013). One possible reason for this effect is some of the ER-resident chaperones require a high Ca<sup>2+</sup> concentration for their activity, such as calreticulin and Bip (Coe and Michalak, 2009, Corbett and Michalak, 2000). Furthermore, ER stress induced IP3R1 dysfunction through an impaired IP3R1-Bip interaction promotes cell death (Higo et al., 2010). Our results showed that tunicamycin upregulated IP3R gene expression, which may decrease ER Ca<sup>2+</sup> load and subsequently induce further ER stress. However, other studies have shown that treatment with tunicamycin resulted in a decrease in IP3R expression and an increase in RYR1 mRNA expression in pancreatic beta cells (Zhang et al., 2023), which may be due to the different mechanisms in different cells. Additionally, we found that activated ER stress leads to decreased L-type calcium channel gene expression, similar to findings in another study (Liu et al., 2018). This decreasing L-type calcium channel expression may protect cells by reducing cytosolic Ca<sup>2+</sup> load. These changes were only detected after 24 hours of treatment, not after 5 hours, suggesting that tunicamycin may not directly target calcium channel expression. Instead, the effect could be a compensatory response to help resolve the altered cellular environment, as these changes were not specifically observed in HT VSMC. However, gene expression does not directly reflect Ca<sup>2+</sup> load in the cell. The activation of these Ca<sup>2+</sup> channels needs to be evaluated in future studies.

In conclusion, we identified DE miRNAs in human HT VSMCs and highlighted some DE miRNAs related to our interested DE genes. Moreover, we propose that ER stress may act as a master regulator of oxidative stress in the context of hypertension, as it leads to increased ROS generation, which may be contributed to by changes in Nox5 and the antioxidant SOD. Nox1, Nox2, and Nox4 may not be as relevant to the increased ROS generation in hypertension.

# Chapter 4 ER Stress and Oxidative Stress in an Ang II-dependent Model of Hypertension (LinA3 mice)

#### 4.1 Overview

Essential hypertension is characterised by increased cardiac output and peripheral resistance, attributed to perturbations of the central nervous system, the kidney, and the vasculature (McMaster et al., 2015) (Harrison, 2014). The renin-angiotensin-aldosterone system (RAAS) activation plays a major pathophysiological role underlying the development of hypertension and progressive renal injury. (Forrester et al., 2018, Manrique et al., 2009) Angiotensin II (Ang II), considered a potent active hormone of RAAS, has a complex influence on the subcellular mechanisms (Kim and Iwao, 2000). One crucial component of Ang II signalling effects is redox-dependent signalling mediated by reactive oxygen species (ROS) production (Touyz, 2000).

ROS are constantly generated as a regular product of cellular metabolism by homeostatic cells and are essential in the physiologic regulation of all cellular functions (de Champlain et al., 2004). ROS can be classified into two major groups: free radicals such as superoxide (O2-+), and nonradical derivatives of oxygen like hydrogen peroxide (H2O2) and peroxynitrite (ONOO-) (Paravicini and Touyz, 2008). ROS causes oxidative post-translational modification of cysteine residues in proteins. These modifications trigger structural and functional changes in proteins, modulating their function and affecting redox-sensitive pathways. Increased ROS bioavailability can lead to oxidative stress that alters the redox state in cells and tissues. ROS can further oxidise cysteine residues in proteins into irreversible oxidative modifications such as sulfonic acid (–SO3H), which promote protein degradation or change of function, altering cellular signalling. Because of its reactive nature, ROS can also damage DNA, RNA, and lipids (Schieber and Chandel, 2014), therefore contributing to vascular dysfunction and renal damage in experimental and human hypertension (RodrigoGonzalez and Paoletto, 2011, Montezano and Touyz, 2012, Brito et al., 2015).

To maintain redox homeostasis, several antioxidant defence systems regulate ROS levels and defend cells from oxidative damage. O<sub>2</sub>-• serves as the origin of the cascade forming many other biologically relevant ROS (Loperena and Harrison, 2017), which is usually short-lived due to the rapid reduction by superoxide dismutase (SOD) to H<sub>2</sub>O<sub>2</sub> (Fridovich,

1997). On the contrary, H<sub>2</sub>O<sub>2</sub> is relatively stable under physiologic conditions as it is a non-radical ROS. It can be further reduced to water and oxygen by catalase, glutathione peroxidase (GPx), peroxiredoxins (Prx), and/or thioredoxin (Trx) reductase (Simic et al., 2006, Sui et al., 2005). O<sub>2</sub>-\* reacts efficiently with nitric oxide, leading to ONOO-formation, which causes protein functional modification by nitration of tyrosine (Sies and Jones, 2020).

The major source of Ang II-stimulated ROS generation in the cardiovascular and renal system is NADPH oxidase, which has seven isoforms, including Nox1-5, Duox1, and Duox2 (Montezano et al., 2015, Touyz et al., 2002). NADPH oxidase activation has been strongly associated with the pathogenesis of hypertension and plays an essential role in vascular damage and renal dysfunction (Touyz, 2004, Feairheller et al., 2009, Majzunova et al., 2013). The classical NADPH oxidase, Nox2, is a multi-subunit complex composed, including 2 membrane-associated components (Nox2 (gp91phox) and p22phox), three cytosolic subunits (p47-phox, p67-phox, p40-phox), and the small molecular weight GTPase Rac (Lambeth, 2004, Rastogi et al., 2016). During Nox2 activation, cytosolic proteins translocate to the membrane leading to transfer of one electron from NADPH to oxygen, producing O<sub>2</sub>-. Nox1 is also associated with p22 phox and depends on translocation of cytosolic subunits NoxO1 (Nox organizer 1, p47phox homologue), NoxA1 (Nox activator 1, p67 phox homologue), p40 phox and Rac1 to activation and producing O<sub>2</sub>-• (Dutta and Rittinger, 2010). Nox4 activation produces primarily H<sub>2</sub>O<sub>2</sub> rather than O<sub>2</sub>-• and does not need cytosolic subunits, and it is associated with p22phox in the membrane (Schurmann et al., 2015). As a key regulator of Nox activation, Ang II induces p47-phox phosphorylation, subsequently promoting p47-phox interaction with p22-phox, therefore increasing superoxide production. Ang II-induced ROS production is involved in cell growth, contraction, and inflammation (Landmesser et al., 2002, Li and Shah, 2003, Brandes et al., 2002).

Nox4 is the most abundantly expressed Nox isoform in the renal system, and it is highly expressed in renal tubules, renal fibroblasts, glomerular mesangial cells, and podocytes (Gill and Wilcox, 2006). The function of Nox4 in the kidney is still unclear. On the one hand, Nox4 silencing could prevent Ang II-induced oxidative stress in kidney cells. Ang II has been found to upregulate Nox4 protein via the activation of Src and PDK-1, and Nox4 silencing prevents Ang II-induced increase in intracellular ROS generation in rat glomerular mesangial cells (Block et al., 2008). In human kidney cells, Nox4 silencing prevented Ang II-induced DNA damage mediated by AT1R, which could not be achieved

by silencing of Nox2 (Fazeli et al., 2012). On the other hand, Nox4 has been shown to have a protective effect in the kidney (Babelova et al., 2012). Nox4 expression decreased in tubular cells from all type of chronic kidney disease patients, and overexpression of Nox4 did not cause kidney injury (Rajaram et al., 2019). Our previous results showed that Nox4 deficiency is related to an increase of blood pressure and renal fibrosis (Lacchini et al., 2017). In addition, endothelial Nox4 overexpression promotes vasodilation and decreases Ang II-induced hypertension (Ray et al., 2011).

Recently, endoplasmic reticulum (ER) stress has been linked to oxidative stress in the pathophysiology of numerous diseases including hypertension (Carlisle et al., 2016). Accumulating evidence suggests increasing ROS production is an integral component of ER stress (Higa and Chevet, 2012). Nox4, as an ER transmembrane protein, is the major Nox isoform that may contribute to this effect. Evidence suggests Nox4 could activate eIF2α pathway of ER stress by increasing eIF2α phosphorylation and ATF4 translation, thus enhancing cell survival. Nox4 dependent ROS accumulation increases activation of autophagy through selectively activating the PERK/eIF2α/ATF4 ER stress pathway in cardiomyocytes (Sciarretta et al., 2013). Nox4-mediated ROS inhibited PP1 activity resulting in enhanced activation of the eIF2α/ATF4 pathway in the ER and is protective against acute cardiac or kidney injury (Santos et al., 2016). Nox4 is also associated with IRE1 phosphorylation and downstream xbp1s expression, which is another signalling pathway of ER stress. IRE1a pathway activation mediated by Nox4 derived ROS is involved in age-dependent vascular dysfunction (Lee et al., 2020). Other evidence suggests the link between Nox4 dependent ROS generation and IRE1 pathway activation in cancer cells (Chang et al., 2021, Kim et al., 2021). Moreover, Nox4 was shown to colocalization with ER chaperone PDI. Loss of PDI resulted in the decrease of Ang II-induced Nox4 activation in vascular smooth muscle cells (Janiszewski et al., 2005).

To study how oxidative stress and ER stress work in chronic Ang II-induced hypertension, we used the LinA3 (TTRhRen) mice, a hypertensive mouse model with chronic activation of the renin-angiotensin system. LinA3 mice are transgenic mice that express human active renin in the liver, thus releasing human renin in the circulation (Prescott et al., 2000, Burger et al., 2014). It has been previously demonstrated that LinA3 mice have about 86% active renin in the circulation, exhibit a significantly high systolic blood pressure, and develop vascular dysfunction in resistance arteries and cardiac hypertrophy in an AT1 receptor-dependent manner (Prescott et al., 2000, Touyz et al., 2005). To study the role of

Nox4 in oxidative stress and ER stress in hypertension, we also used Nox4-deficient WT mice and Nox4-deficient LinA3 mice.

## 4.2 Hypothesis and aims

Oxidative stress and ER stress are involved in experimental hypertension, and accumulating evidence suggests a crosstalk between these two processes. However, the molecular mechanisms underlying the interaction between oxidative stress and ER stress in hypertension await more investigation. We hypothesise that ER stress and oxidative stress play a chronic role in Ang II-dependent hypertension, and Nox4 plays a protective effect on ER stress. The aim of this project is to study the molecular mechanisms of ER stress and oxidative stress and their crosstalk through Nox4 in a chronic Ang II-dependent model of hypertension. For this, we investigated in 14–19-week-old LinA3 hypertensive mice, littermates wild-type (WT) control mice and their corresponding Nox4 deficient mice:

1. If oxidative stress and ER stress activation is involved in vascular dysfunction associated with chronic Ang II-dependent hypertension.

We performed in-vitro study in VSMC obtained from mesenteric arteries of LinA3 hypertensive mice and WT mice to assess the expression of oxidative stress and ER stress markers.

2. If Nox4 deficiency altered oxidative stress and/or ER stress in kidney of WT and LinA3 mice.

LinA3 transgenic mice were bred with Nox4-deficient mice to generate Nox4-deficient mice with a chronic Ang II-mediated cardiovascular injury. The expression of oxidative stress and ER stress markers were assessed in the kidney of wild-type mice (WT), LinA3, WT Nox4-deficient (Nox4-/-), and LinA3 Nox4-deficient (LinA3/Nox4-/-).

#### 4.3 Results

#### 4.3.1 Oxidative stress is increased in VSMCs from LinA3 mice.

First, we investigated whether oxidative stress happened in LinA3 mice VSMCs assessing ROS generation and oxidation of lipid and proteins. Figure 4.1A shows NADPH-dependent O<sub>2</sub> generation was increased in baseline conditions of LinA3 mice. No changes

were observed in basal levels of H<sub>2</sub>O<sub>2</sub> (Figure 4.1B) or ONOO (Figure 4.1C) in VSMCs from LinA3 mice compared to WT. Oxidative stress is characterised by increased intracellular ROS levels, resulting in damage to lipids and proteins. Lipid peroxidation was detected by TBARS (Thiobarbituric Acid Reactive Substances) assay. As shown in Figure 4.1D, TBARS levels were higher in VSMCs from LinA3 mice. Another marker of oxidative stress is irreversible protein oxidation. Protein tyrosine phosphatases (PTP), critically involved in the control of cell signalling related to vascular function(Stoker, 2005), and the antioxidants peroxiredoxins (Prdx) can undergo irreversible oxidative modifications of cysteine residues (–SO<sub>3</sub>H), resulting in protein inactivation (NiforouCheimonidou and Trougakos, 2014). Our results demonstrate that irreversible protein oxidation of peroxiredoxin (Figure 4.1E) was higher in VSMCs from LinA3 mice, while there were no differences in PTPs oxidation (Figure 4.1F) between the groups.

Altogether, these results suggest that VSMCs from LinA3 mice display oxidative stress characterized by increased O<sub>2</sub>-• generation, lipid oxidation and irreversible protein oxidation.

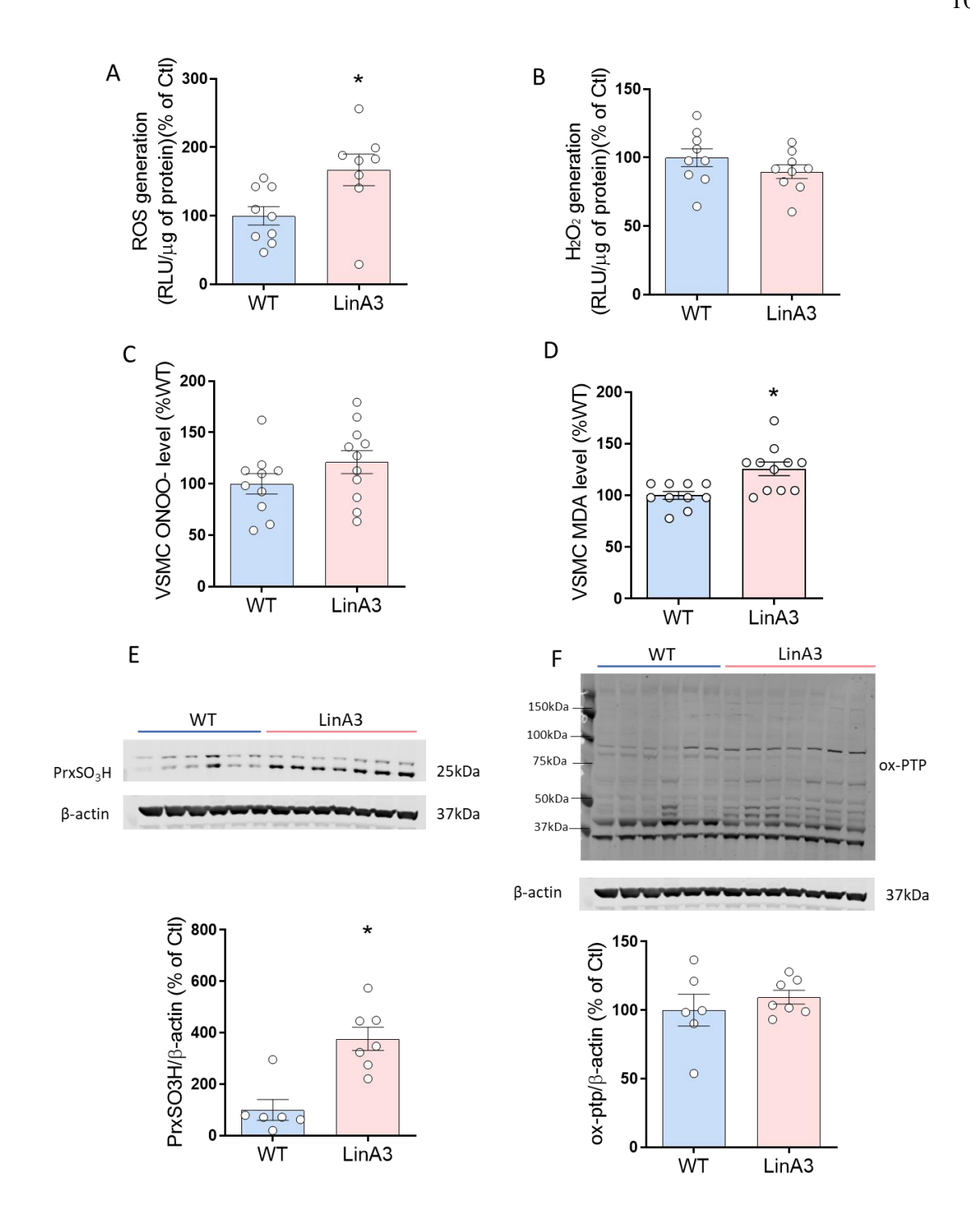


Figure 4.1 ROS generation, lipid peroxidation and irreversible protein oxidation are increased in VSMCs from LinA3 mice.

The generation of  $\cdot O_2^{-*}$  (A) was measured by lucigenin assay,  $H_2O_2$  (B) was measured by Amplex red, ONOO level was measured by nitrotyrosine ELISA (C). Peroxidation of lipids (TBARS) was measured by lipid peroxidation assay kit (D). Irreversible protein oxidation in VSMCs from WT (blue columns) LinA3 (pink columns) was assessed by immunoblotting of peroxiredoxin hyperoxidation (E) and oxidized PTPs (F).  $\beta$ -actin was used as loading control. Data are presented as mean  $\pm$  S.E.M., n=6-11. Statistical significances were determined by student t-test, \*p<0.05 compared to WT mice.

## 4.3.2 NADPH oxidases expression is not increased in VSMCs from LinA3 mice.

Oxidative stress refers to an imbalance between ROS generation and antioxidant defences. Noxs are the primary source of ROS in the vascular wall. To assess whether Noxs are contributing to oxidative stress in VSMCs from LinA3 mice, we examined Noxs gene and/or protein expression. Nox1 expression was not changed in LinA3 VSMCs on both gene (Figure 4.2A) and protein level (Figure 4.2B). Nox2 gene expression was decreased in LinA3 VSMCs (Figure 4.2C). Nox4 is constitutively activated and produces primarily H<sub>2</sub>O<sub>2</sub>. Nox4 expression was not changed in LinA3 VSMCs on both gene (Figure 4.2D) and protein level (Figure 4.2E). These findings indicate that Nox1, Nox2 and Nox4 expression are not upregulated in LinA3 VSMCs.

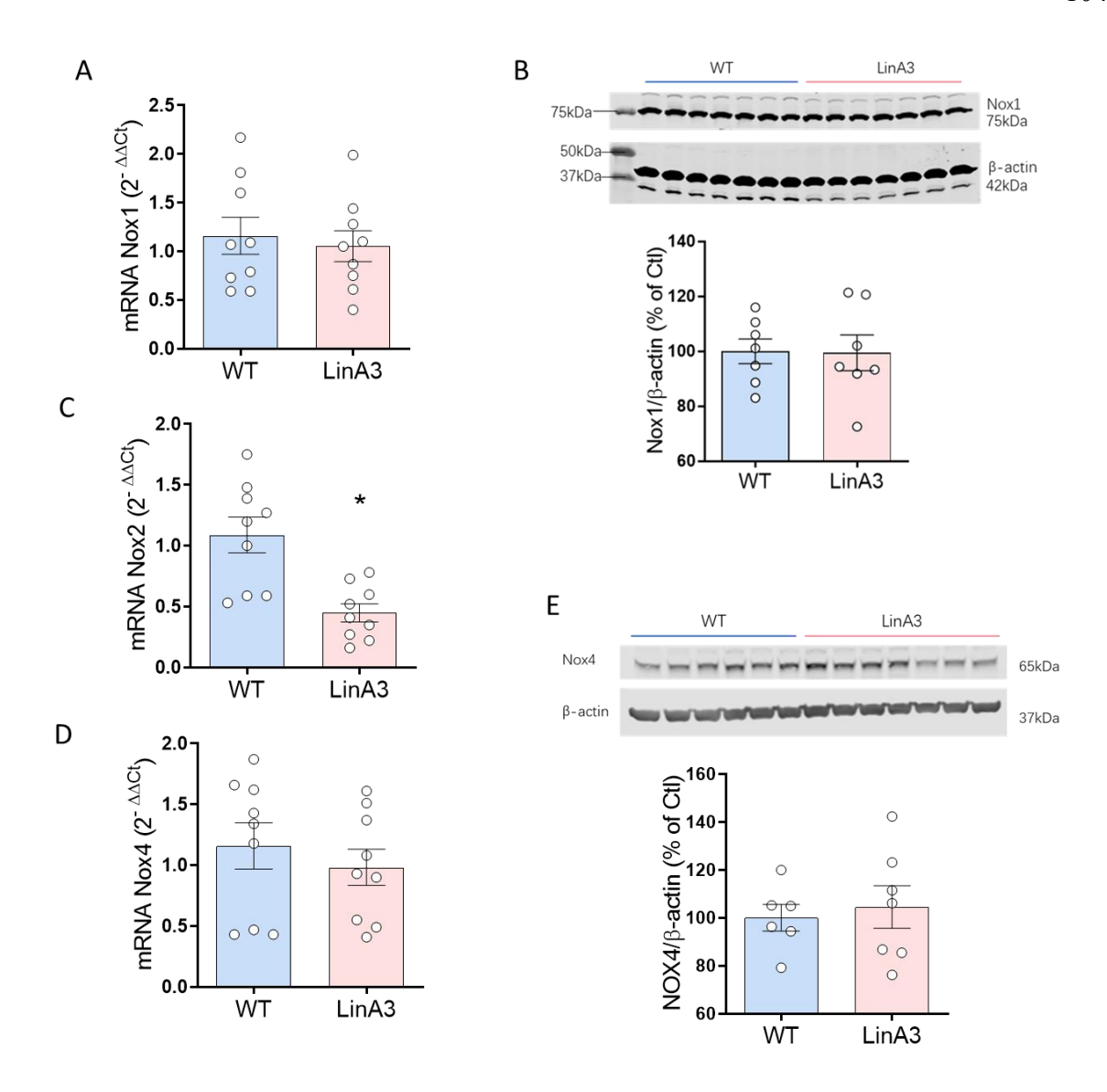


Figure 4.2 Expression of Noxs in VSMCs from WT and LinA3 mice.

Gene expression of Nox1 (A), Nox2 (C), and Nox4 (D) in VSMCs from WT (blue columns) and LinA3 mice (pink columns) was assessed by real-time qPCR. GAPDH gene was used as an internal control. Protein expression of Nox1 (B), and Nox4 (E) in VSMCs from WT (blue columns) and LinA3 mice (pink columns) was assessed by immunoblotting.  $\beta$ -actin was used as loading control. Data are presented as mean  $\pm$  S.E.M., n=6-9. Statistical significances were determined by student t-test, \*p<0.05 compared to WT mice.

## 4.3.3 Antioxidants expression are altered in VSMCs from LinA3 mice.

Other factors that affect oxidative stress involve antioxidant defences. To assess whether changes of antioxidants contribute to oxidative stress in VSMCs from LinA3 mice, we examined antioxidant enzymes gene and/or protein expression. VSMCs express two intracellular subtypes of SOD, including intracellular copper zinc SOD (CuZn-SOD; SOD1), and mitochondrial manganese SOD (Mn-SOD; SOD2). Expression of SOD1 was not changed in VSMCs from LinA3 mice (Figure 4.3A). SOD2 expression was significantly increased in VSMCs from LinA3 at protein level (Figure 4.3B), but not at gene level (Figure 4.3C). DJ-1 has antioxidant activity as it scavenges H<sub>2</sub>O<sub>2</sub> through oxidation of Cys106 (Wilson, 2011). DJ-1 gene expression (Figure 4.3D) was significantly decreased in VSMCs from LinA3 mice.

Nuclear erythroid-related factor 2 (Nrf2)/antioxidant-related element (ARE) shows a protective role in cellular adaptation to redox stress (Mozzini et al., 2017, Duckers et al., 2001). When cells are exposed to oxidative stress, Nrf2 accumulates in the nucleus and triggers the expression of antioxidant genes, including heme oxygenase-1 (HO-1) and GPx1. In VSMCs from LinA3 mice, Nrf2 gene expression (Figure 4.3E) and GPx1 protein expression (Figure 4.3F) were decreased, while expression of HO-1 gene was increased (Figure 4.3G). To further confirm the mechanism underlying Nrf2 pathway regulation, we assessed the gene expression of two inhibitors of Nrf2 activation, Keap1 and Bach1. Keap1 regulate Nrf2 by dissociation of the inhibitory complex (Smith et al., 2016). Bach1 is a transcriptional repressor that competes with Nrf2, leading to negative regulation of the antioxidants (ReichardMotz and Puga, 2007). There were no changes in Keap1 (Figure 4.3H) and Bach1 (Figure 4.3I) gene expression in LinA3 mice compared to WT mice. These findings suggest changes in the expression of antioxidant enzymes in LinA3 that may contribute to oxidative stress in LinA3 VSMCs.

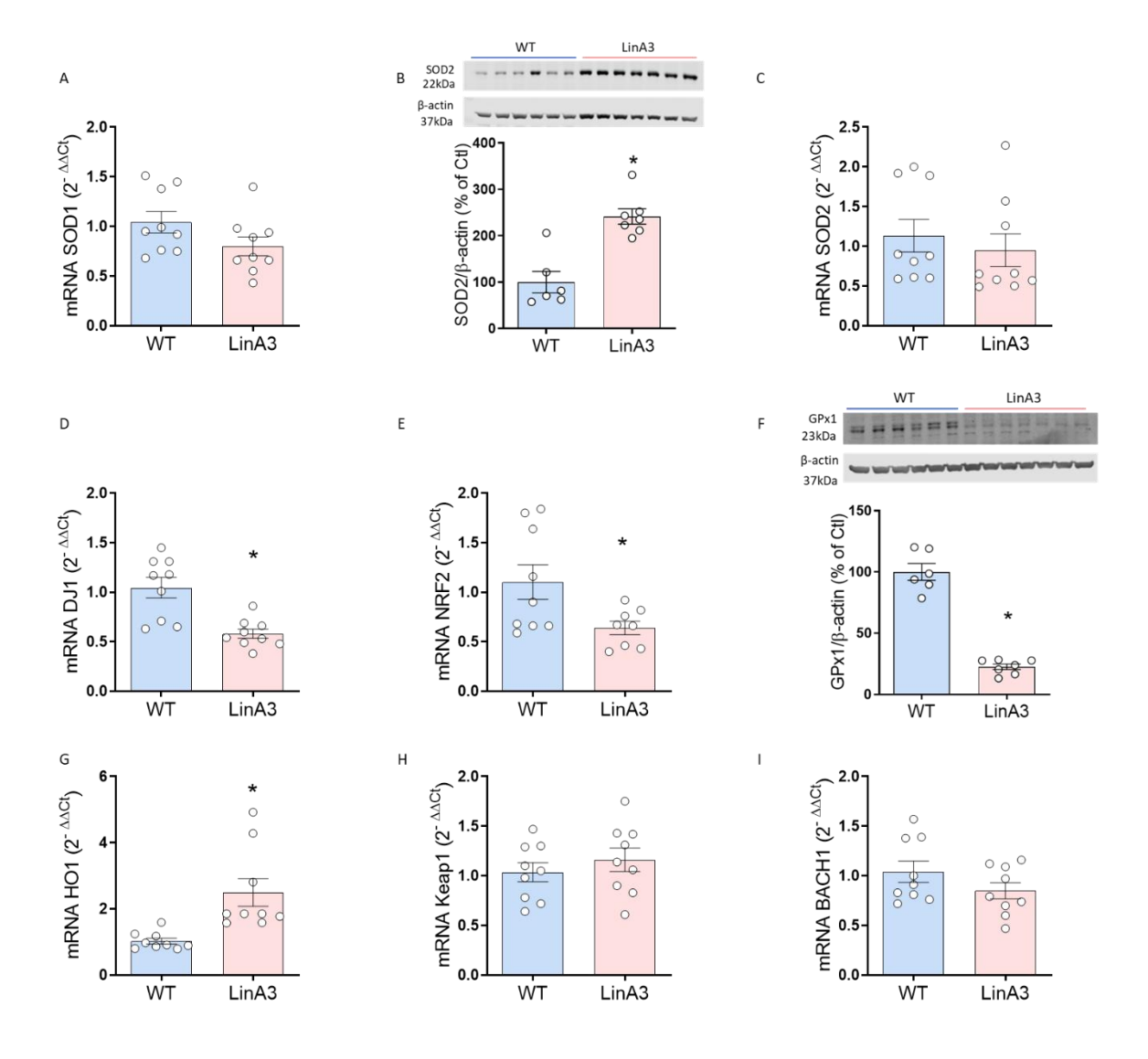


Figure 4.3 Expression of antioxidants in VSMCs from WT and LinA3 mice.

Gene expression of SOD1 (A), SOD2 (C), DJ1 (D), Nrf2 (E), HO1 (G), Keap1 (H) and Bach1(I) in VSMCs from WT (blue columns) and LinA3 mice (pink columns) was assessed by real-time qPCR of. The GAPDH gene was used as an internal control. Protein expression of SOD2 (B), and GPx1 (F) in VSMCs from WT (blue columns) and LinA3 mice (pink columns) was assessed by immunoblotting.  $\beta$ -actin was used as a loading control. Data are presented as mean  $\pm$  S.E.M., n=6-9. Statistical significances were determined by student t-test, \*p<0.05 compared to WT mice.

## 4.3.4 Expression of ER stress makers is altered in VSMCs from LinA3 mice.

To investigate whether ER stress is activated in LinA3 mice VSMCs, ER stress markers basal levels were determined by immunoblotting and qPCR. Total PERK protein expression (Figure 4.4A) was decreased, and PERK activation (Figure 4.4B) was increased in VSMCs from LinA3 mice. Total elf2a protein expression (Figure 4.4C) was decreased, while elf2a activation (Figure 4.4D), one of the downstream targets of PERK activation, was not changed in LinA3 VSMC. Total IRE1a (Figure 4.4E) was increased while IRE1a activation (Figure 4.4F) was decreased in VSMCs from LinA3 mice. Unspliced Xbp1 protein expression (Figure 4.4G) was reduced in LinA3 VSMCs, while the activated spliced form xbp1s protein expression (Figure 4.4H) was not changed. The downstream of xbp1s is ATF4, which was not changed at the gene level (Figure 4.4I) in LinA3 VSMCs. UPR sensor ATF6 gene expression (Figure 4.4J) was decreased in LinA3 VSMCs. These findings suggest that in LinA3 mice, the PERK pathway is activated, while the IRE1 and ATF6 pathways of the UPR are downregulated.

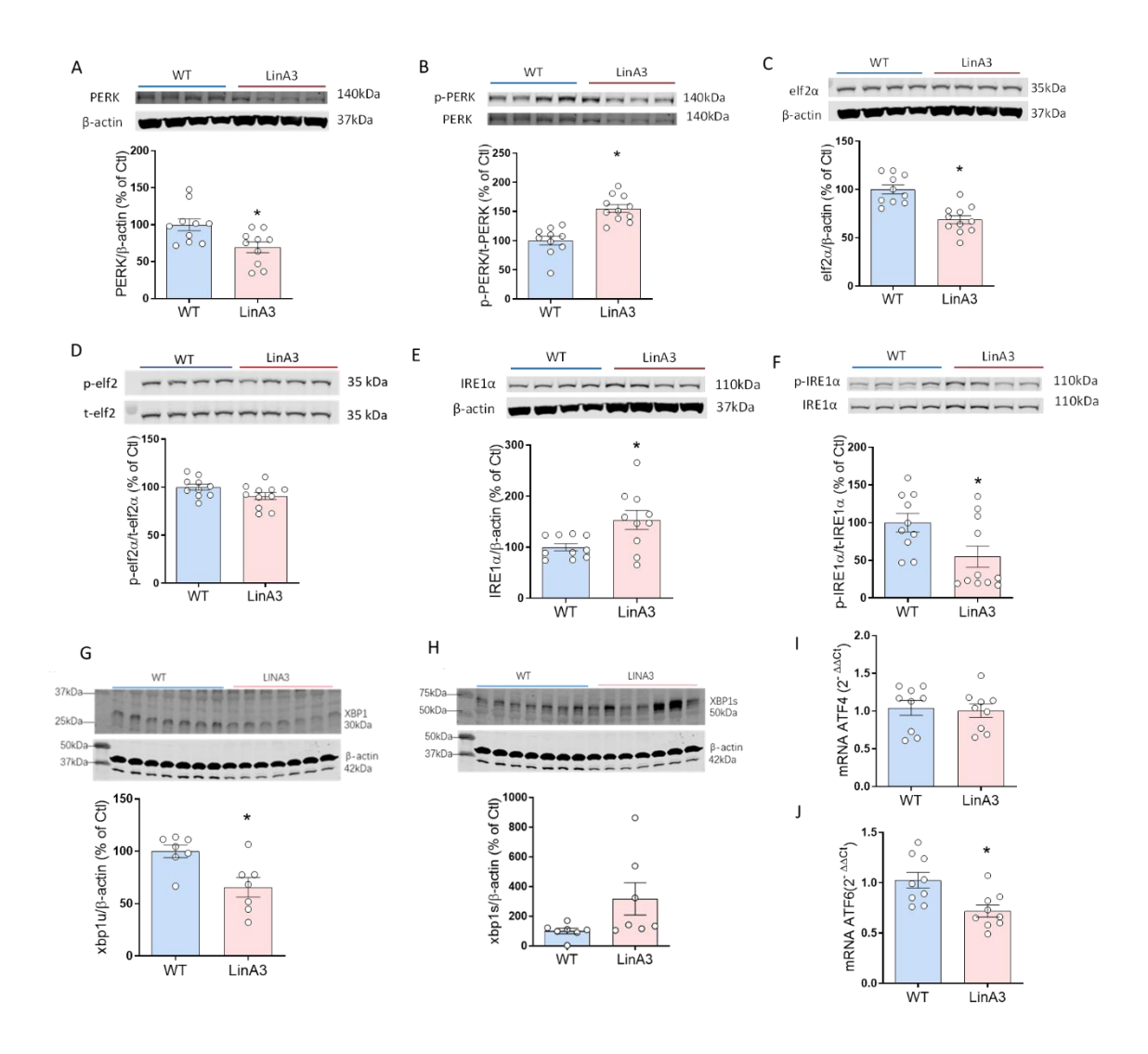


Figure 4.4 ER stress markers expression and activation in VSMCs from WT and LinA3 mice.

The protein expression of VSMCs from WT (blue columns) and LinA3 mice (pink columns) was assessed by immunoblotting of total PERK (A), PERK activation (B), total elf2a (C), elf2a activation (D), total IRE1a (E), IRE1a activation (F), XBP1s (G) and XBP1u (H).  $\beta$ -actin was used as a loading control, and protein activation was calculated by (phosphorylated protein/ $\beta$ -actin) / (total protein/ $\beta$ -actin), where phosphorylated and total protein were in the same membrane. Gene expression of VSMCs from WT (blue columns) and LinA3 mice (pink columns) was assessed by real-time qPCR of ATF4 (I) and ATF6 (J). The GAPDH gene was used as an internal control. Data are presented as mean  $\pm$  S.E.M., n=7-11. Statistical significances were determined by student t-test, \*p<0.05 compared to WT mice.

### 4.3.5 Noxs and antioxidants levels in kidney of LinA3 and Nox4 knock-out mice

Renal oxidative stress is an important process underlying Ang II-induced renal damage in hypertension. To investigate whether Nox4 deficiency affects oxidative stress in chronic Ang II-dependent hypertension in kidney, we assessed Noxs and antioxidants expression in kidney from wild type (WT), LinA3, Nox4-deficient (Nox4-/-), and LinA3/Nox4-deficient (LinA3/Nox4-/-). Nox4 gene expression (Figure 4.5A) was significantly decreased in Nox4-deficient mice, indicating the success of the Nox4-deficient model. Nox4 deletion did not affect Nox2 gene expression in both groups (Figure 4.5B). Antioxidant SOD2 gene (Figure 4.5C) and protein (Figure 4.5D) expression did not change between groups in male kidneys. Gpx1 gene (Figure 4.5E) and protein (Figure 4.5F) expression were significantly decreased in LinA3/Nox4-deficient compared to LinA3 kidney. These findings suggest a role for GPx1 in chronic Ang II hypertensive model in Nox4-deficient mice.

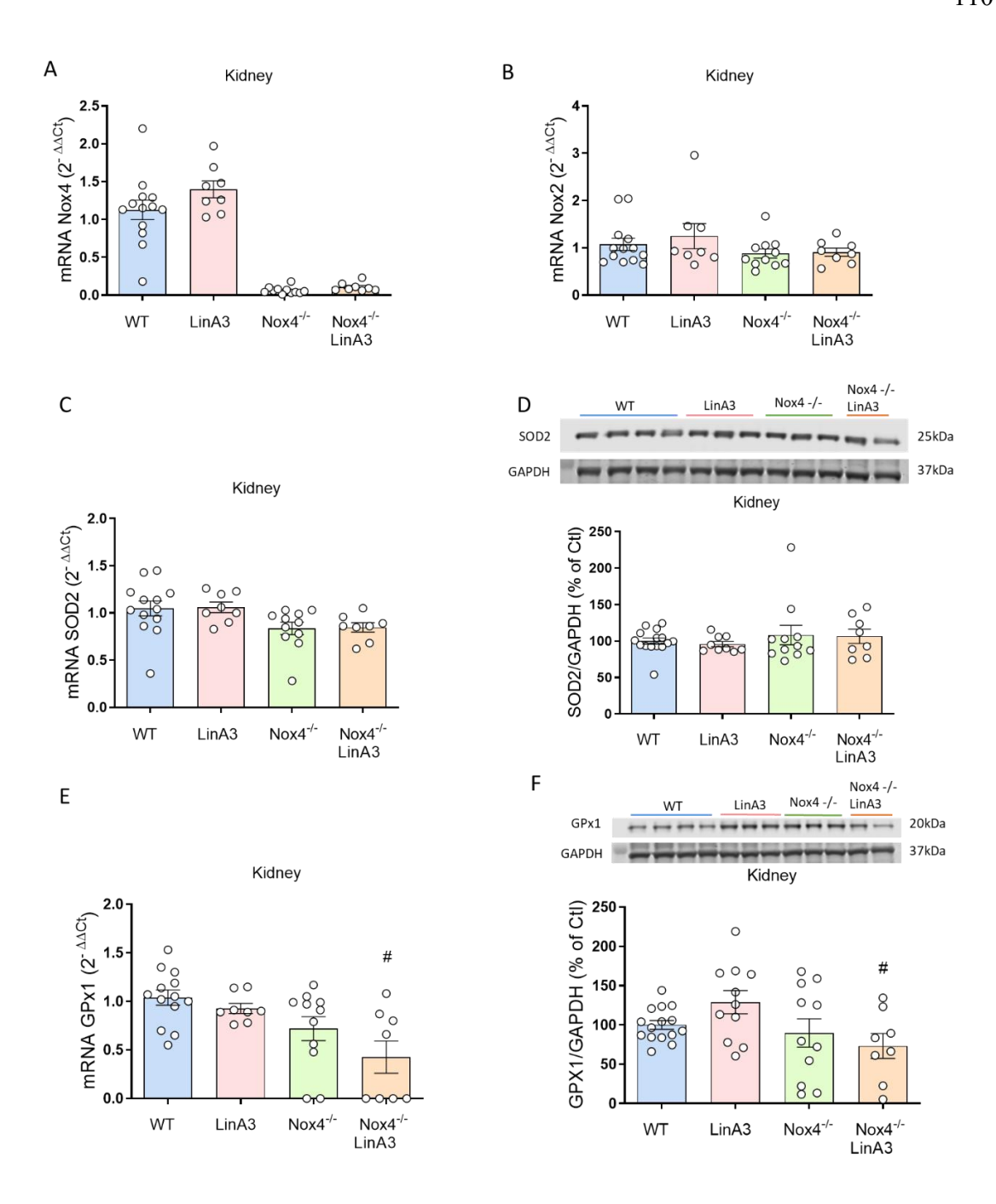


Figure 4.5 Noxs and antioxidants expression in kidney from male of LinA3 and Nox4 knock-out mice.

The gene expression of Nox4 (A), Nox2 (B), SOD2 (C) and GPx1 (E) in kidney from WT (blue columns), LinA3 (pink columns), Nox4 knock-out (green columns) and Nox4 knock-out/LinA3 (orange columns) mice of male was assessed by real-time qPCR. Mice GAPDH gene was used as an internal control. Protein expression of SOD2 (D) and GPx1 (F) in kidney from WT (blue columns), LinA3 (pink columns), Nox4 knock-out (green columns) and Nox4 knock-out/LinA3 (orange columns) mice of male was assessed by immunoblotting. GAPDH was used as loading control. Data are presented as mean ± S.E.M., n=8-13. Statistical significances were determined by one-way ANOVA followed by a Tukey test, \*p<0.05 vs. WT, \*p<0.05 vs. LinA3.

### 4.3.6 Role of ER stress in kidney of LinA3 and Nox4 knock-out mice

To investigate whether Nox4 deficiency (Nox4-/- mice) affects ER stress in the kidney from chronic Ang II-dependent hypertension mice model, we assessed ER stress makers expression in the kidney from wild type (WT), LinA3, Nox4-deficient (Nox4-/-), and LinA3/Nox4-deficient (LinA3/Nox4-/-).

Elf2a activation (Figure 4.6A) was not changed in the kidney from Nox4-deficient and LinA3 mice. Protein expression of the ER chaperone PDI was increased in kidney of LinA3 mice, and that effect was attenuated in Nox4-deficient LinA3 mice (Figure 4.6B). No differences were observed in gene expression of ATF4 (Figure 4.6C), ATF6 (Figure 4.6D) or unspliced xbp1 (Figure 4.6G) between groups. Gene expression of ER chaperones Bip (Figure 4.6E) and Chop (Figure 4.6F) was significantly increased in Nox4-deficient mice compared to WT. However, there were no significant changes between LinA3 and LinA3/Nox4-/- mice. These results suggest that Nox4 deficiency could influence ER stress in mice, through upregulation of BiP and CHOP, and this effect seems to be independent of Ang II-dependent hypertension. In hypertension, Nox4 seems to be involved in upregulation of PDI expression.

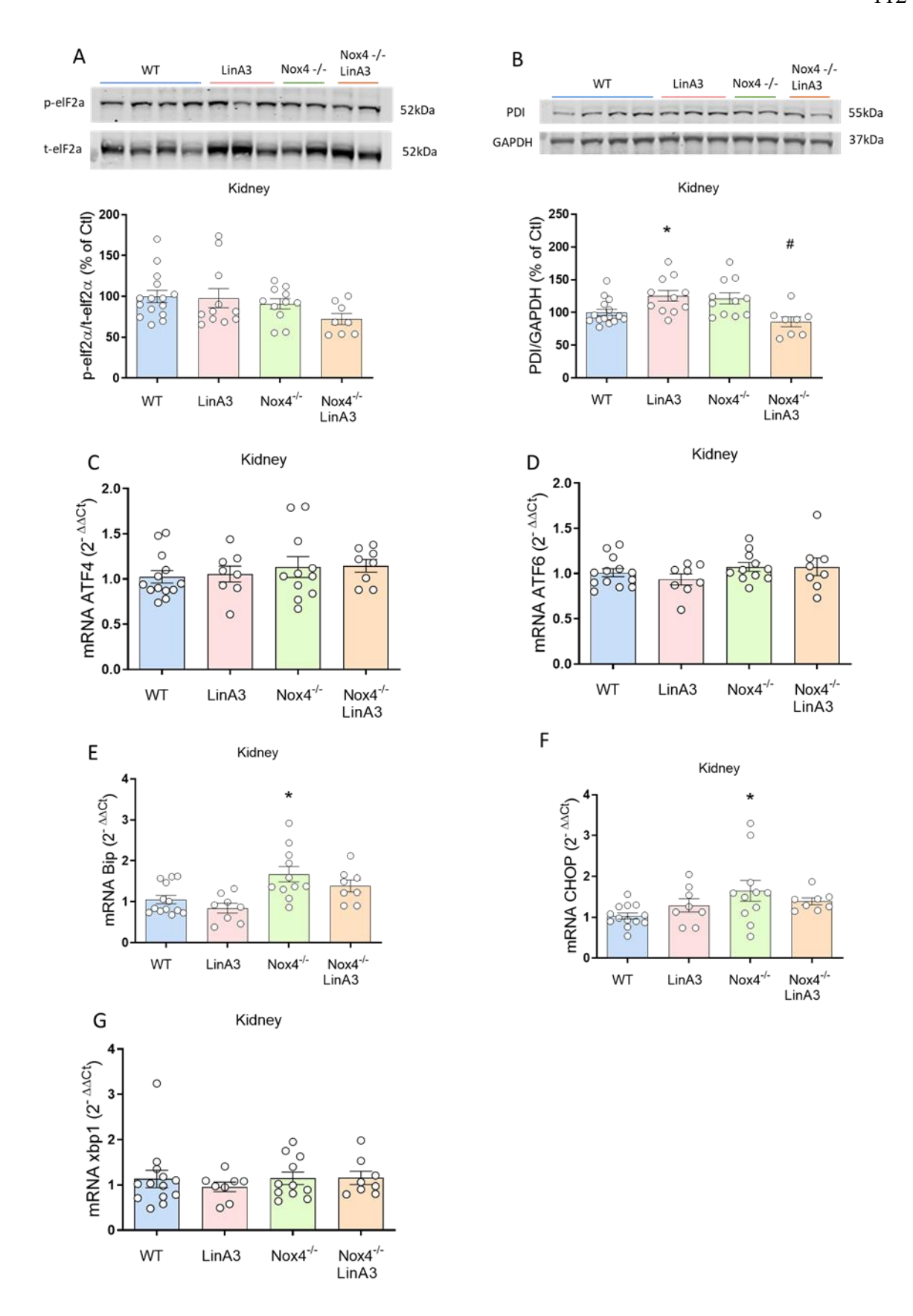


Figure 4.6 ER stress markers expression in kidney from LinA3 and Nox4 knock-out mice.

In Protein expression of elf2a activation (A) and PDI (B) in the kidneys from WT (blue columns), LinA3 (pink columns), Nox4 knock-out (green columns) and Nox4 knock-out/LinA3 (orange columns) mice of the male were assessed by immunoblotting. GAPDH was used as a loading control. Gene expression of ATF4 (C), ATF6 (D), Bip (E), Chop (F)

and xbp1 (G) in the kidney from WT (blue columns), LinA3 (pink columns), Nox4 knockout (green columns) and Nox4 knock-out/LinA3 (orange columns) mice of male was assessed by real-time qPCR. Mice GAPDH gene was used as an internal control. Data are presented as mean  $\pm$  S.E.M., n=8-13. Statistical significances were determined by one-way ANOVA followed by a Tukey test, \*p<0.05 vs. WT, \*p<0.05 vs. LinA3.

#### 4.4 Discussion

RAAS has been found to be related to both oxidative stress and ER stress. To investigate the interplay between oxidative stress and ER stress in Ang II-dependent hypertension, we used a mouse model of hypertension with chronic activation of the RAAS. Here we investigated the presence of oxidative stress and ER stress in LinA3 mice compared to WT mice. Major findings from the study show that: i) Oxidative stress is increased in LinA3 VSMCs characterised by increased O<sub>2</sub>. generation, lipid peroxidation, and irreversible protein oxidation. ii) expression of antioxidants Nrf2, DJ-1 and Gpx1 are decreased in LinA3 VSMCs. iii) ER stress makers expression is altered, with increased activation of only the PERK pathway in LinA3 VSMCs. iv) In kidney, oxidative stress markers were not changed, whereas ER stress marker PDI expression increased in LinA3 mice, an effect dependent on Nox4. v) Nox4 deficiency increased ER stress markers bip and chop gene expression in kidney, independent of hypertension.

#### 4.4.1 Oxidative stress and ER stress in VSMCs of LinA3 mice

LinA3 mice is a chronic Ang II-dependent hypertension model with elevated blood pressure and cardiac hypertrophy (Touyz et al., 2005). Previous studies from our lab have demonstrated vascular dysfunction of mesenteric arteries in LinA3 mice, which was characterised by increased U46619-induced vasoconstriction and reduced endothelium-dependent vasodilation (Alves-Lopes et al., 2021). Change of redox environment in VSMCs may contribute to vascular dysfunction in LinA3 mice via post-translational oxidative modification of proteins related to vascular contraction (Touyz et al., 2018). We demonstrated that NADPH-induced O2<sup>--</sup> generation and peroxidation of lipids were increased in LinA3 mice. Exposure to a high level of ROS can lead to irreversible protein oxidation of cysteine residues forming sulfonic acid (–SO<sub>3</sub>H). Prxs proteins contain a conserved cysteine residue and are particularly sensitive to oxidation (Poynton and Hampton, 2014). Our results showed increased expression of PrxSO<sub>3</sub>H, supporting the changing to a more oxidising environment in LinA3 mice.

NADPH oxidases are the major source of ROS in the vessel wall. Many studies have demonstrated an increase in NADPH oxidase activity in the vasculature and kidneys in Ang II-induced hypertension (Landmesser et al., 2002, RodrigoGonzalez and Paoletto,

2011, TouyzTabet and Schiffrin, 2003). Although oxidative stress was observed in LinA3 mice in our study, the expression of NADPH oxidase was not increased. Similar results have been demonstrated in a previous study that protein expression of Nox1, Nox2, and Nox4 were not changed in kidney of LinA3 mice (Touyz et al., 2005). One possible reason may be that LinA3 mice have chronic activation of RAAS, and the plasma Ang II level is lower than acute Ang II models (Prescott et al., 2000) (Gomolak and Didion, 2014). Another model that has chronic RAAS activation and increased NADPH oxidase expression is the spontaneously hypertensive rats (SHR) (Touyz et al., 2005). However, this model is multifactorial and not only dependent on Ang II like the LinA3 mice. Upregulation of NADPH oxidase can lead to increased activity. Whereas other factors can contribute to increased activity, such as the expression of different subunits and posttranslational modifications of Noxes and its subunits. Whether Noxs participate in oxidative stress in LinA3 mice needs further investigation to access Nox activation. In addition, there could be alternative superoxide sources that contribute to the increasing oxidising environment apart from NADPH oxidase, including mitochondria, xanthine oxidase, uncoupled endothelial nitric oxide synthase, and cytochrome P450 enzymes, which need further exploration.

Another important player in ROS regulation is antioxidant enzymes. SODs are important enzymes in the control of O2- levels. We observed no change in gene expression of intracellular SOD1 in VSMCs between WT and LinA3 mice. Other studies have shown contrasting results related to SOD1 expression in Ang II-induced hypertensive models, including decreased SOD1 in mesenteric arteries of Ang II-induced hypertensive rats (KangSullivan and Pollock, 2018), increased SOD1 in mesenteric arteries of Ang IIinduced hypertensive mice (Gongora et al., 2006), and no change of SOD1 expression in aorta of Ang II-induced hypertensive mice (Fukai et al., 1999). On the other hand, in this study we found increased SOD2 expression. SOD2 protects mitochondrial function by eliminating mitochondria-derived O<sub>2</sub>-• (Palma et al., 2020). Other studies found reduced SOD2 activity in aorta of Ang II-infused mice (Dikalova et al., 2017), or no change of SOD2 in mesenteric arteries of Ang II-induced hypertensive mice or rats (KangSullivan and Pollock, 2018, Gongora et al., 2006). The different results of our study may relate to the use of isolated cells instead of whole tissues and also to the use of a chronic Ang II model. The results suggest there could be an increase in mitochondrial ROS induced by chronic exposure to high Ang II levels. As intracellular O<sub>2</sub>- remains high in our model, the increase in SOD2 levels may not be enough to properly control oxidative stress in our experimental model. In addition, increased ROS generation can inactivate some antioxidant enzymes, such as SOD1, that can be inactivated by the reaction of  $H_2O_2$  with its copper centre (Kim and Kang, 1997).

HO-1 is a stress-response protein that induces cellular protection in oxidative stress, inflammation, and apoptosis associated with cardiovascular disease (Zhao et al., 2013, Abraham and Kappas, 2011, Abraham and Kappas, 2008). HO-1 has been shown to have vascular protective effects and prevent the development of hypertension (Abraham and Kappas, 2011, Hosick and Stec, 2012). In our study, HO-1 is upregulated in chronic Ang II mice VSMCs. Similar results have been observed in Ang II—infused rat aortas (Ishizaka et al., 1997) and Ang II-treated human aortic endothelial cell (Yang et al., 2019). As HO-1 is an oxidant-sensitive gene, increased oxidative stress can trigger the upregulated HO-1 in chronic Ang II mice. Moreover, the higher expression of HO-1 may explain the downregulated NOX2 expression in LinA3 mice since HO-1 induction has been shown to decrease heme-containing protein gp91phox by decreasing cellular heme content (Taille et al., 2004).

One of the regulators of SOD and HO-1 expression is the redox-sensitive transcription factor Nrf2. Prolonged ROS production activates the Nrf2 redox signalling pathway through Nrf2 phosphorylation and translocation to the nucleus, leading to transcription regulation of targeted antioxidant genes, such as HO-1, SOD and GPx1 (Ichikawa et al., 2009, TonelliChio and Tuveson, 2018). In our study, Nrf2 gene expression is decreased in LinA3 mice. Negative regulators of Nrf2, Keap1 and Bach1 showed no change in gene expression in our model. Similar results have been observed in other studies, such as reduced Nrf2 levels and no changes in keap1 expression in human umbilical vein endothelial cells after Ang II treatment (Chen et al., 2019) and decreased Nrf2 expression in Ang II-treated rats aortic VSMCs (He et al., 2020). Decreased Nrf2 expression could contribute to oxidative stress by reducing the expression of target antioxidant genes. In our study, expression of HO-1 and SOD were increased, while GPX1 levels, another downstream target of Nrf2, are downregulated in LinA3 mice. Nrf2 can regulate over 200 genes, and the regulation of its targets depends on the duration and intensity of oxidative stress (Chen et al., 2015). Moreover, HO-1 and SOD2 gene expression could also be regulated by other transcription factors such as AP-1 (activator protein-1), NF-κB and HIF-1 (hypoxia-inducible factor-1)(Medina et al., 2020, Kim et al., 2017, ZelkoMariani and Folz, 2002). Nevertheless, the downregulation of Nrf2 and GPx1 may contribute to oxidative stress and tissue damage in LinA3 mice. Evidence has shown that in Ang IIdependent hypertension mice, knocking out GPx1 mice could enhance oxidative stress,

thus accelerating cardiac hypertrophy and dysfunction (Ardanaz et al., 2010). In addition, the antioxidant DJ-1 also prevents Keap1/Nrf2 association, supporting its activation (Liu et al., 2014, Yan et al., 2015). The decreased gene expression of DJ1 may also contribute to oxidative stress in LinA3 mice by decreasing ROS scavenging and reducing Nrf2 activation.

Redox signalling is involved in many different aspects of ER stress. Oxidative stress can lead to ER stress through thiol oxidation of ER molecular chaperones, disturbance in oxidative protein folding, and alterations in Ca<sup>2+</sup> levels in the ER(Eletto et al., 2014). On the contrary, ER stress can lead to oxidative stress by mitochondrial dysfunction, influencing Nox2 and Nox4 activation (LaurindoAraujo and Abrahao, 2014, Bhattarai et al., 2021). Moreover, Ang II is reported to increase ER stress markers in both in vivo and in vitro models, and ER stress activation was involved in increased ROS generation and activation of proinflammatory, fibrotic and apoptotic pathways (Xu et al., 2009, Menikdiwela et al., 2019, Sepulveda-Fragoso et al., 2021). In our results, chronic Ang II release in LinA3 mice increased only activation of the PERK pathway. Although the ratio of PERK activation was increased, the amount of total PERK was decreased, which may explain why no changes were observed in downstream eIF2a activation and ATF4 expression. However, PERK can activate other signalling pathways, such as Nrf2/Keap1 and calcineurin/RyR2 (Liu et al., 2015), that remain to be investigated. Moreover, the activation of IRE1 pathway and total ATF6 expression decreased in LinA3 mice. The results indicate that the UPR arms of the ER stress response are differentially regulated in LinA3 mice, and the downstream effects require further investigation. The changes in redox environment may influence the expression and activation of ER stress markers in LinA3 mice, by oxidation of ER calcium channels (Chernorudskiy and Zito, 2017), oxidation of UPR proteins such as IRE1 (Lee et al., 2020), and changes in expression of microRNA (Sepulveda-Fragoso et al., 2021).

# 4.4.2 Nox4 deficiency altered oxidative stress and ER stress in kidney of WT and LinA3 mice.

Previous studies investigated the role of Nox1 and Nox2 in LinA3 mice. While both Nox1 and Nox2 (Touyz et al., 2005) deficiency reduced renal oxidative stress, none of them decreased blood pressure in LinA3 mice. Unlike Nox1 and Nox2, Nox4 has been found to be both cardiovascular protective and injurious (Schroder et al., 2012, Schurmann et al., 2015, Morawietz, 2018). Interestingly, a previous study from our group found Nox4

deficient mice and LinA3/Nox4 deficient mice are both hypertensive compared to WT (Lacchini et al., 2017), which confirmed the protective effect of Nox4 in hypertension. Moreover, renal remodelling demonstrated by increased fibrosis has been found in Nox4 deficient mice, LinA3 mice and LinA3/Nox4 deficient mice (Lacchini et al., 2017), suggesting Nox4 may be cardiovascular-renal protective. Some studies found that Nox4 deficiency had no effect on blood pressure (Schroder et al., 2012), (Bouabout et al., 2018) and demonstrated Nox4 deficiency enhanced the effect of Ang II with evidence of increased aortic inflammatory cytokines expression and aortic media hypertrophy (Schroder et al., 2012).

Nox4 is highly expressed in the kidney and mediates redox signalling by generating predominantly H<sub>2</sub>O<sub>2</sub>. Nox4 deletion mouse model has been well studied with no abnormal development, physiology, or known phenotype has been found, unless the mice are in a stressed condition (Gray et al., 2016, Schurmann et al., 2015, Schroder et al., 2012, Zhang et al., 2010). It is also has been demonstrated that Nox4 knockout mice have more kidney fibrosis than WT mice, suggesting a protective effect in the kidneys (Lacchini et al., 2017, Nlandu Khodo et al., 2012). A previous study indicated that Nox4 deletion did not change cardiac Nox2 and p22<sup>phox</sup> levels but decreased the H<sub>2</sub>O<sub>2</sub> generation in kidney (Zhang et al., 2010). Similarly, our results showed kidney levels of Nox2 were unaffected by Nox4 deletion. Additionally, no changes were observed in the levels of antioxidants SOD and GPx1, suggesting Nox4 protective effect is not related to changes in the expression of oxidative stress-related genes. However, in stressed condition, Nox4 deletion changes the redox environment. A study has shown that Nox4 silencing protects against Ang IIinduced increase in intracellular ROS generation in rat glomerular mesangial cells (Block et al., 2008). Another study demonstrated that Nox4 silencing lower activation of antioxidant system, as HO-1 levels were reduced in aorta of Ang II infusion Nox4 deficient mice (Schroder et al., 2012). In our results, LinA3/Nox4-/- mice shown decreased GPx1 expression compared to LinA3 mice. GPx1, as an antioxidant enzyme, mainly functions in catalysing the reduction of H<sub>2</sub>O<sub>2</sub> into water. Although there is not enough evidence of the mechanism underlying the downregulation of GPx1 in LinA3/Nox4-/- mice it is likely that Nox4 is important in maintaining the redox homeostasis in oxidative stress triggered by chronic renin-angiotensin system activation. Together, evidence indicates that Nox4 plays a protective role in Ang II-induced oxidative stress by maintaining the antioxidant defence system.

Nox4 is the major Nox isoform that links ER stress to oxidative stress. Nox4 is involved in at least two of the three signalling branches of the UPR. It is required for XBP1 splicing by IRE1 and in eIF2a phosphorylation by PERK (Sciarretta et al., 2013, Santos et al., 2016, Chang et al., 2021, Kim et al., 2021, Janiszewski et al., 2005, Lee et al., 2020). Nox4 knockout mice did not affect eIF2a phosphorylation and ATF4 expression, suggesting there were no changes in the PERK arm of the UPR. However, expression of Chop and Bip were increased in kidneys of Nox4 knockout mice, suggesting a role for Nox4 in ER stress. The activation of ER stress response in the kidneys of Nox4 knockout mice may be different from that of other tissues. Evidence in other studies showed that expression of Chop and ATF4 were decreased in Nox4 knockout aorta (Xie et al., 2017), expression of Chop and Bip was not changed by Nox4 silencing in human endothelial cells (Wu et al., 2010), and decreasing expression of ATF4 in cardiomyocytes of cardiac-specific Nox4 knockout mice (Sciarretta et al., 2013).

ER chaperone PDI upregulation has been found to be related to Nox4 activation. Nox4 is colocalised with PDI in cells such as rat kidney glomerular mesangial cells (BlockGorin and Abboud, 2009) and rabbit aortic smooth muscle cells (Miyano et al., 2020, Janiszewski et al., 2005). Evidences shown PDI overexpression increased Nox4 levels after Ang II stimulus, while PDI inhibition decreased Ang II-induced Nox4 activation in rabbit aortic smooth muscle cells (Fernandes et al., 2009) (Janiszewski et al., 2005). Our results shown in kidney of LinA3 mice, expression of PDI was increased compared to WT mice. This effect was blocked by Nox4 deletion. It is possible that Nox4 and PDI may have crosstalk that plays an important role in Ang II-induced signalling. However, the mechanisms involved need further examination.

To conclude, our study highlights the changes in oxidative and ER stress in chronic Ang II-dependent hypertension. From the analysis of NADPH oxidases, antioxidants, and the ER stress profile in VSMCs, we found that the expression of Noxs and ER stress markers was not strongly associated with increased oxidative stress in LinA3 male model. However, we found that Nox4 is involved in the maintenance of the antioxidant profile in VSMCs and in the ER stress response in kidneys from LinA3 male mice. Since LinA3 mice did not show a strong correlation with Noxs and ER stress, we selected a hypertensive rat model for the study on other chapters.

# Chapter 5 Role of ET-1 Induced ER stress in vascular hypercontractility of WKY and SHRSP rats

#### 5.1 Overview

Pathophysiological mechanisms contributing to the development of hypertension include vascular smooth muscle (VSM) contraction. Both calcium-dependent and calcium-independent signalling mechanisms are involved in VSM contraction by regulating the balance of the myosin light chain kinase (MLCK) and myosin light chain phosphatase (MLCP) to trigger myosin light chain 20 (MLC20) phosphorylation (Thr18/Ser19), which activates VSM contraction by promoting actin-myosin cross-bridge formation to control blood pressure (Yang and Hori, 2021, Touyz et al., 2018, Webb, 2003, Ito and Hartshorne, 1990).

Vascular smooth muscle cell (VSMC), which is the predominant constituents of the arterial vessel wall, is highly plastic and involved in VSM contraction. Physiologically, VSMCs are quiescent and exhibit low levels of growth. However, under pathological conditions such as hypertension, VSMCs switch from the contractile phenotype to the synthetic phenotype, characterised by a reduction of contractile filaments and related molecules and a rise in organelles formation and related protein synthesis (Touyz et al., 2018, Bacakova, 2018, Ashraf and Al Haj Zen, 2021). These perturbations and altered function in VSMCs influence vascular tone and reactivity, thus contributing to increased vascular resistance and high blood pressure.

In hypertension, molecular mechanisms of VSMCs phenotypic switch are complex, where vasoactive peptides such as endothelin-1 (ET-1) are important (WynneChiao and Webb, 2009). ET-1 is one of the most potent vasoconstrictor agents with long-lasting effects on vascular tone (Yanagisawa et al., 1988). It is a 21-amino-acid peptide produced primarily by vascular endothelial and smooth muscle cells (Sandoval et al., 2014). ET-1 acts in a paracrine or autocrine manner on two cell surface G-protein coupled receptors: endothelin type A (ET<sub>A</sub>) receptor and endothelin type B (ET<sub>B</sub>) receptor. ET<sub>A</sub> receptors are mainly located in VSMCs, and activation of ET<sub>A</sub> receptors mediates vasoconstriction (Sandoval et al., 2014). ET<sub>B</sub> receptors are mainly located in endothelial cells and cause vasodilatory effects on ET-1 activation by releasing vasodilators that act on VSMCs. In contrast, ET<sub>B</sub> receptors located in VSMCs result in vasoconstriction as ET<sub>A</sub> receptors. Activation of ET<sub>A</sub>

and/or ET<sub>B</sub> receptors in VSMCs triggers phospholipase C (PLC) activation, resulting in the generation of the second messenger inositol 1,4,5-trisphosphate (IP<sub>3</sub>) and 1,2-diacylglycerol (DAG) (Touyz et al., 2018, Araki et al., 1989). IP3 induces the release of intracellular Ca<sup>2+</sup> from sarcoplasmic reticulum, and DAG causes activation of protein kinase C, which in turn leads to an elevation in the intracellular Ca<sup>2+</sup>concentration (Little et al., 1992, XuanWang and Whorton, 1994). ET-1 mediated vasoconstriction by VSMCs is a more sustained contraction and stimulates Ca<sup>2+</sup> influx via plasma Ca<sup>2+</sup> channels and/or by releasing the Ca<sup>2+</sup> from internal Ca<sup>2+</sup> stores (WynneChiao and Webb, 2009, Miyauchi and Sakai, 2019). In pathological conditions such as hypertension, alteration in these signalling components can induce an over stimulated state resulting in maintained vasoconstriction and ultimately causing elevation of blood pressure (Kostov, 2021).

Abnormalities of the ET-1 signalling system have been linked to the regulation of vascular tone and elevation of blood pressure and contribute to the pathogenesis of hypertension. The plasma ET-1 level in essential hypertension is currently controversial; however, there is a local rise in vascular walls' ET-1 levels, which is likely to have physiological significance (Pinto-Sietsma and Paul, 1998, Kumagae et al., 2010, Kostov, 2021). The increased vascular ET-1 expression has been found in both animal and human models of hypertension, which causes end-organ damage, including vascular hypertrophy and remodelling (Trensz et al., 2019, Schiffrin, 1998, Kostov, 2021). Both ET<sub>A</sub> and ET<sub>B</sub> receptors have shown an important role in the development of hypertension. ET<sub>A</sub> receptor antagonists BQ123 markedly reduced blood pressure in SHRSP rats (Nishikibe et al., 1993) and deoxycorticosterone acetate (DOCA)-salt-induced hypertensive rats (WarnerAllcock and Vane, 1994). Pharmacological or genetic inhibition of ET<sub>B</sub> receptor activity results in salt-sensitive hypertension in mice and rats (Gariepy et al., 2000, Pollock and Pollock, 2001). In addition, approximation, as a dual ET-1 receptor antagonist, has recently demonstrated a significant reduction in blood pressure compared to placebo in patients with essential hypertension on phase 2 trial (McCoy and Lisenby, 2021, AngeliVerdecchia and Reboldi, 2021).

Recent studies have highlighted the role of endoplasmic reticulum (ER) stress in essential hypertension and in blood pressure regulation (Young, 2017, Liang et al., 2013, Naiel et al., 2019, Choi et al., 2016b). ER stress is a type of cellular stress that resolves the protein-folding defect and restores ER homeostasis by triggering an adaptive program known as the unfolded protein response (UPR). Prolonged activation of UPR can lead to apoptotic cell death, inflammation, fibrosis and VSMC phenotypic switch (Uchida et al., 2022a). The

ER chaperone protein Bip recognises and binds to unfolded or misfolded proteins and initialises the three parallel protein sensors of UPR (PERK, IRE1a and ATF6) (Young et al., 2012). PERK activation leads to phosphorylation of translation initiation factor eIF2α at serine-51. EIF2\alpha phosphorylation acts as a competitor of eIF2B, resulting in a lower level of the initiator Met-tRNAiMet delivery to the ribosomal machinery, thus broadly suppressing global protein synthesis and alleviating the demands of protein folding and processing in ER (TeskeBaird and Wek, 2011). Simultaneously, eIF2α phosphorylation facilitates the preferential translation of the transcription factor ATF4, which in turn activates the UPR genes transcription to help the cell cope with the stress. Notably, besides ER stress, viral infection and nutrient deficiency also lead to eIF2α phosphorylation -ATF4 pathway activation via GCN2 (general control non repressed 2) and dsRNA induced PKR respectively (OchoaWu and Terada, 2018, Pakos-Zebrucka et al., 2016). Thus, ATF4 serves as a vital point of the integrated stress response (Pakos-Zebrucka et al., 2016). ATF4 itself or, together with its downstream target CHOP, may also contribute to cell death when cellular homeostasis cannot be restored (Pakos-Zebrucka et al., 2016). IRE1 consists of an N-terminal ER luminal domain, which senses the unfolded proteins, and a Cterminal cytosolic region initiates the UPR through serine/threonine protein kinase and endoribonuclease domains (Siwecka et al., 2021). The unfolded protein activated the IRE1 pathway via dimerisation and trans-autophosphorylation of the endoribonuclease domain, subsequently adapting cellular response by splicing the XBP1 mRNA. Under prolonged or severe stress conditions, IRE1 activation also could activate the pro-apoptotic c-Jun Nterminal kinase (JNK) and result in apoptosis (Siwecka et al., 2021). ERO1 is an ERresident thiol oxidoreductase, which contributes to correct protein folding and improves the stress cope ability in cells by upregulated through UPR (Zito, 2015). Ero1 also works as a protein disulfide oxidase and helps PDI with disulfide bond formation (Zito, 2015).

ET-1 has been associated with ER stress in many diseases, including preeclampsia (Jain et al., 2012), pulmonary hypertension (Yeager et al., 2012) and kidney disease (Hsu et al., 2021, De Miguel et al., 2017). Induction of ER stress by ET-1 has been shown in rat pulmonary artery smooth muscle cells dependent on both ET<sub>A</sub> and ET<sub>B</sub> receptors (Yeager et al., 2012) and in human JEG-3 choriocarcinoma cells through PLC-IP3 pathway dependent on ET<sub>B</sub>R (Jain et al., 2012). Besides, ER stress activation has been shown to mediate the release of ET-1 in rat aortic rings (Padilla and Jenkins, 2013) and in human aortic endothelial cells treated with fatty acids (Zhang et al., 2018).

The underlying molecular mechanism of ET-1 involved in UPR is unknown. However, activation of ER calcium channels and contractile machinery may play a role. The ET-1 has the potential to disrupt ER Ca<sup>2+</sup> homeostasis by releasing calcium from the ER (VigneBreittmayer and Frelin, 1992, Jain et al., 2012). Many ER stress chaperones, such as Bip, and calreticulin, are calcium dependent and contribute to calcium homeostasis in the ER lumen (KrebsAgellon and Michalak, 2015). Disturbance of calcium homeostasis during hypertension impacts Ca<sup>2+</sup>-dependent chaperone function, leading to ER stress. For example, blocking the sarco/endoplasmic reticulum ATPase SERCA leads to a decrease in ER Ca<sup>2+</sup> concentration and subsequently induces PERK/ eIF2α and CHOP pathways (Luciani et al., 2009, Liu et al., 2020). Conversely, UPR activation alters the expression of ER chaperones and has a cross talk with the activation of ER calcium channels. During ER stress, disturbance of calcium homeostasis results in increasing intracellular Ca<sup>2+</sup> concentration, thus contributing to vascular smooth muscle hypercontractility and vascular remodelling observed in hypertension (Liang et al., 2013).

### 5.2 Hypothesis and aims

Vasoactive peptide ET-1 is involved in the activation of ER stress, and both ET-1 and ER stress are associated with calcium dysfunction in hypertension. However, whether ET-1 is related to ER stress in essential hypertension and the underlying molecular mechanisms remains elusive. We hypothesise that in hypertension, ET-1 induces ER stress response. ER stress-associated proteins regulate vascular signalling pathways, leading to dysfunctional Ca<sup>2+</sup> homeostasis and activation of pro-contractile machinery responses. To investigate this, we used the adult stroke-prone spontaneously hypertensive rat (SHRSP) as a hypertensive animal model, which is related to both ER stress and ET-1 (Camargo et al., 2018, Iglarz and Schiffrin, 2003, Nishikibe et al., 1993), and the same age Wistar Kyoto rat (WKY) as normotensive control.

#### Aims:

1 To investigate the protein expression profile of ER stress markers in tissue and VSMCs from hypertensive and normotensive rats.

ER stress markers expression was assessed in the heart, kidney, aorta, mesenteric arteries and VSMCs from mesenteric arteries obtained from male WKY and SHRSP by immunoblotting.

2 To explore whether ET-1 induces ER stress via ETA or/and ETB receptor in VSMCs.

VSMCs from WKY and SHRSP were stimulated with ET-1 (100nM) for 24h in the absence and presence of ET<sub>A</sub>R (BQ123, 10uM) and ET<sub>B</sub>R (BQ788, 10uM) antagonists. ER stress makers expression and activation were examined by immunoblotting.

3 To study the role of ER stress inhibition on the contraction signalling in VSMCs.

VSMCs from WKY and SHRSP were stimulated with ET-1 (100nM) for 24h in the absence and presence of chemical chaperones (4-PBA, 1mM), IRE1 endonuclease activity inhibition (STF083010, 60uM) or PERK inhibition (GSK2606414, 5uM). ER stress maker ATF4 expression and contraction signalling maker p-MLC<sub>20</sub> were examined by immunoblotting. Ca<sup>2+</sup> mobilization was examined by live cell microscope using specific fluorescent indicators.

4 To investigate the role of ER stress inhibition on vasoconstriction in experimental hypertension.

Mesenteric arteries from WKY and SHRSP were pre-incubated with IRE1 inhibition (STF083010, 60uM) or PERK inhibition (GSK2606414,5uM) for 30 minutes. Contraction dose–response curves were performed in response to U46619 and ET-1 via wire myography.

#### 5.3 Results

# 5.3.1 ER stress response activation in VSMCs and Heart from SHRSP rats

To determine whether ER stress activation could be observed in SHRSP rats, we assessed the protein expression of ER stress markers in VSMCs and tissues derived from SHRSP and WKY rats.

Firstly, we confirmed increased expression of ER stress makers in VSMCs from mesenteric arteries (Figure 5.1). UPR activation includes three signalling pathway branches: IRE1a, PERK and ATF6. The expression level of total IRE1a and its downstream active/spliced form of xbp1 were higher in SHRSP, while the inactive form xbp1u is not changed in SHRSP, suggesting the activation of IRE1 pathway (Figure 5.1 A-

D). Activation of the PERK pathway was observed by increased expression of total and phosphorylated eIF2a (Figure 5.1E and F) and ATF4 (Figure 5.1G) in SHRSP. Expression of ATF6 was increased in SHRSP (Figure 5.1H), suggesting activation of the ATF6 pathway. Additionally, expression levels of ER chaperones PDI (Figure 5.1I), CHOP (Figure 5.1J), BIP (Figure 5.1K), and ERO1a (Figure 5.1L) were also higher in SHRSP, thus suggesting the activation of ER stress response in VSMCs of SHRSP.

Then, we investigated whether UPR was activated in whole vessels and other target organs in hypertension. To test this, we evaluated ER stress-related protein expression levels in mesentery arteries, aorta, heart, and kidney in SHRSP and WKY rats. In mesentery arteries (Figure 5.2), no differences were observed in expression and phosphorylation levels of IRE1a (Figure 5.2A and B) and eIF2a (Figure 5.2C and D), suggesting the inactivation of IRE1 and PERK signalling pathway in mesentery arteries of SHRSP rats. There were also no differences in the expression of ER chaperones Bip (Figure 5.2E), Ero1a (Figure 5.2F), PDI (Figure 5.2G), and CHOP (Figure 5.2H), suggesting the UPR is activated in VSMCs of mesentery arteries but is not significantly changed in the whole mesentery arteries from SHRSP rats.

Aorta is another important vessel in cardiovascular disease and has functional and structural changes during hypertension(Laurent and Boutouyrie, 2015, Lindesay et al., 2018). To assess whether ER stress is involved in changes of aorta in SHRSP rats, we measured ER protein expression in aorta (Figure 5.3). There were no differences in expression and phosphorylation levels of IRE1a (Figure 5.3A and B) and eIF2a (Figure 5.3C and D), and no increasing expression of ER chaperones Ero1a (Figure 5.3E), PDI (Figure 5.3F), Bip (Figure 5.3G), and CHOP (Figure 5.3H) were observed, suggesting the UPR is not activated in aorta of SHRSP rats.

In the heart of SHRSP rats (Figure 5.4), results showed higher phosphorylation and expression levels of IRE1a (Figure 5.4A and B), and higher phosphorylation form of eIF2a (Figure 5.4D), suggesting the activation of both IRE1 and PERK pathway. The expression level of ER chaperone Ero1a (Figure 5.4E) was higher in SHRSP, although expression levels of PDI (Figure 5.4F), Bip (Figure 5.4G) and CHOP (Figure 5.4H) were not increased in heart from SHRSP compared to WKY. The results suggest activation of ER stress response in the heart from SHRSP rats.

In kidney of SHRSP rats (Figure 5.5), no changes were observed in the expression of ER stress-related proteins, including eIF2a (Figure 5.5A and B), Bip (Figure 5.5C), CHOP (Figure 5.5D), Ero1a (Figure 5.5E), and PDI (Figure 5.5F), suggesting ER stress may not be activated in kidney from SHRSP.

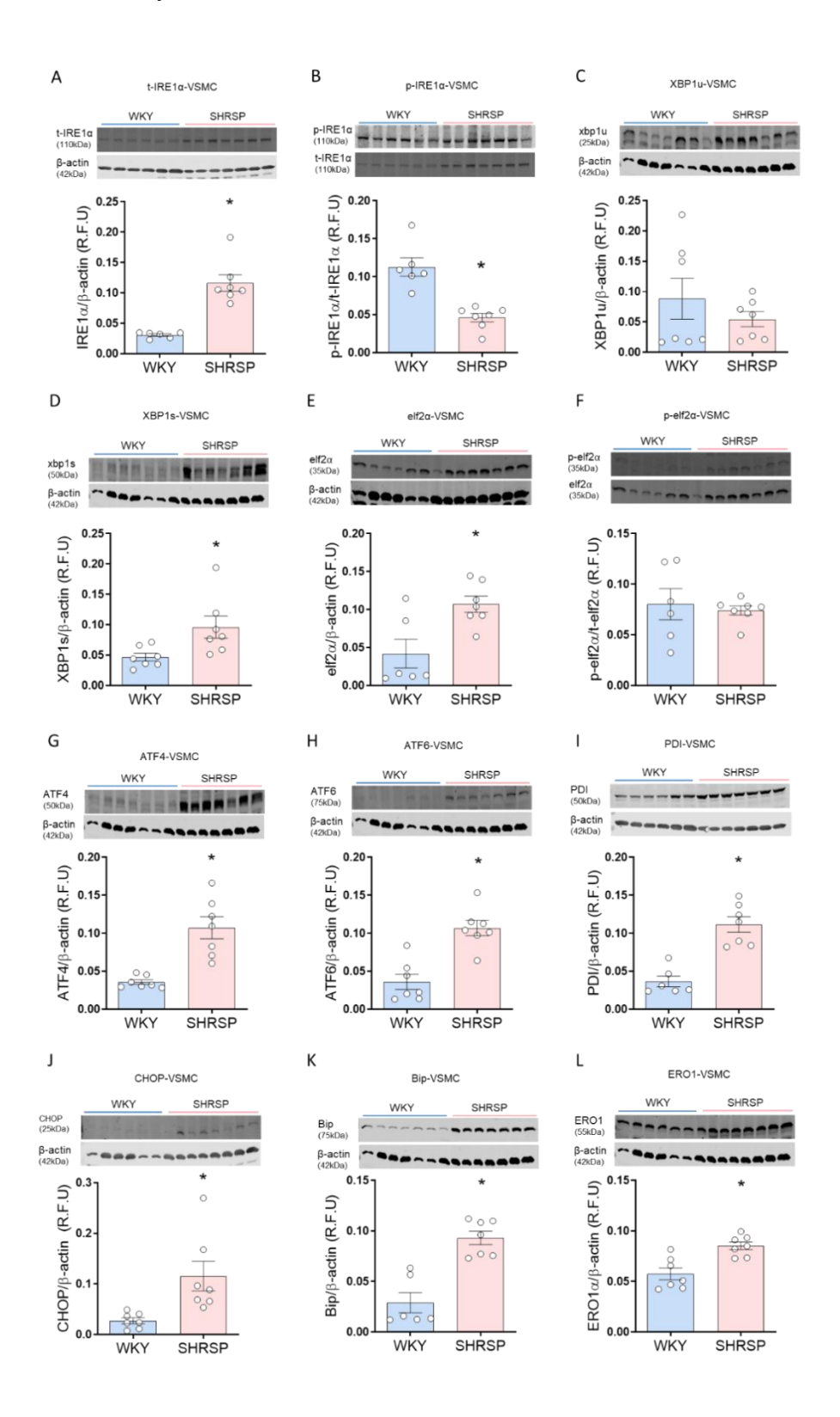


Figure 5.1 ER stress markers expression is increased in VSMCs from SHRSP compared to WKY rats.

The protein expression of IRE1a (A), p-IRE1a (B), XBP1u (C), XBP1s (D), eIF2a (E), p-eIF2a (F), ATF4 (G), ATF6 (H), PDI (I), CHOP (J), BIP (K), and ERO1a (I) in VSMCs from WKY (blue columns) and SHRSP (pink columns) rats was assessed by immunoblotting.  $\beta$ -actin was used as a loading control. Data are presented as mean  $\pm$  S.E.M., n=6-7. Statistical significances were determined by student t-test, \*p<0.05 compared to WKY rats.

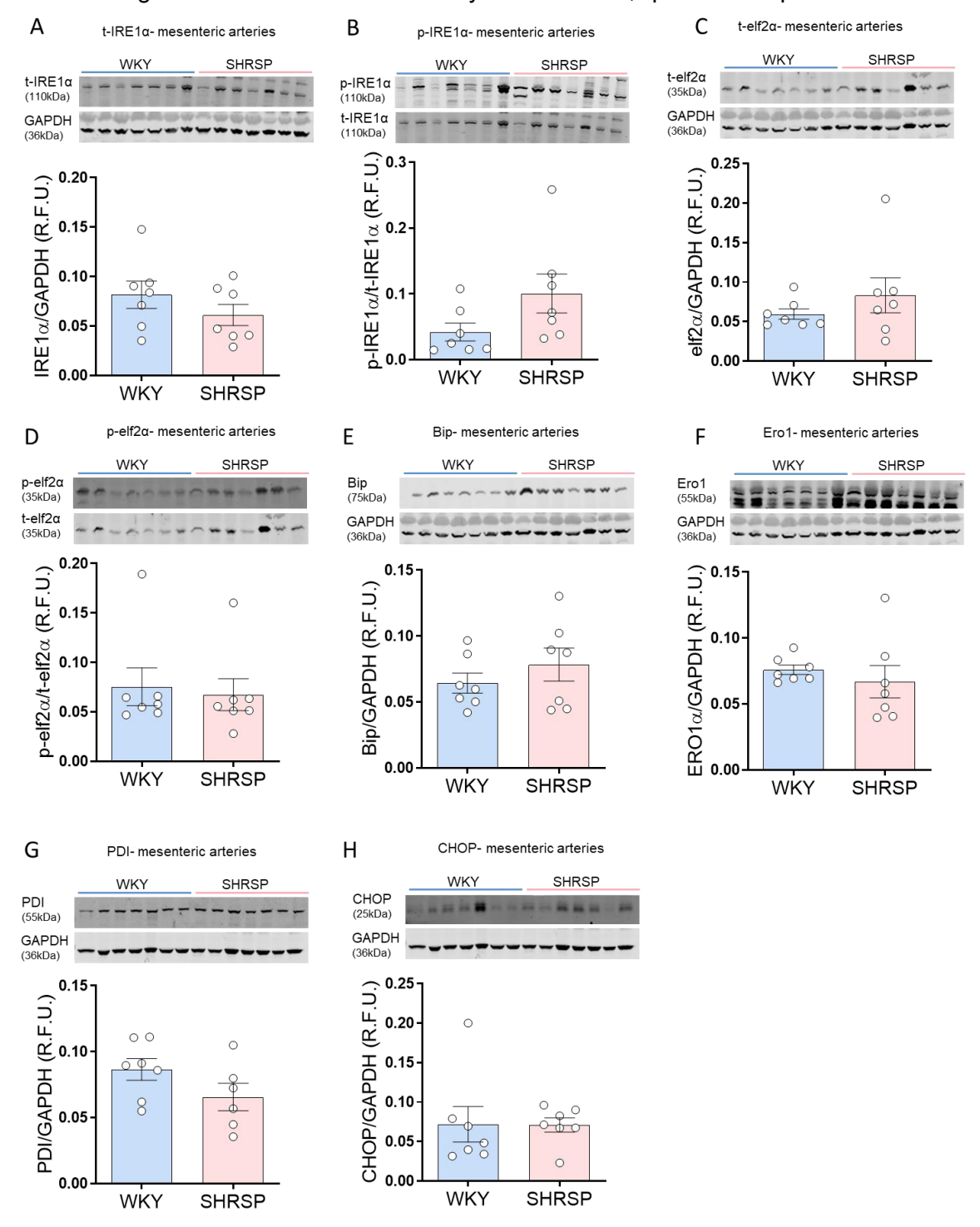


Figure 5.2 ER stress markers expression is not changed in mesenteric arteries from SHRSP compared to WKY rats.

The protein expression of IRE1a (A), p-IRE1a (B), eIF2a (C), p-eIF2a (D), BIP (E), ERO1a (F), PDI (G), and CHOP (H) in mesenteric arteries from WKY (blue columns) and SHRSP (pink columns) rats was assessed by immunoblotting. GAPDH was used as loading control. Data are presented as mean ± S.E.M., n=6-7. Statistical significances were determined by student t-test, \*p<0.05 compared to WKY rats.

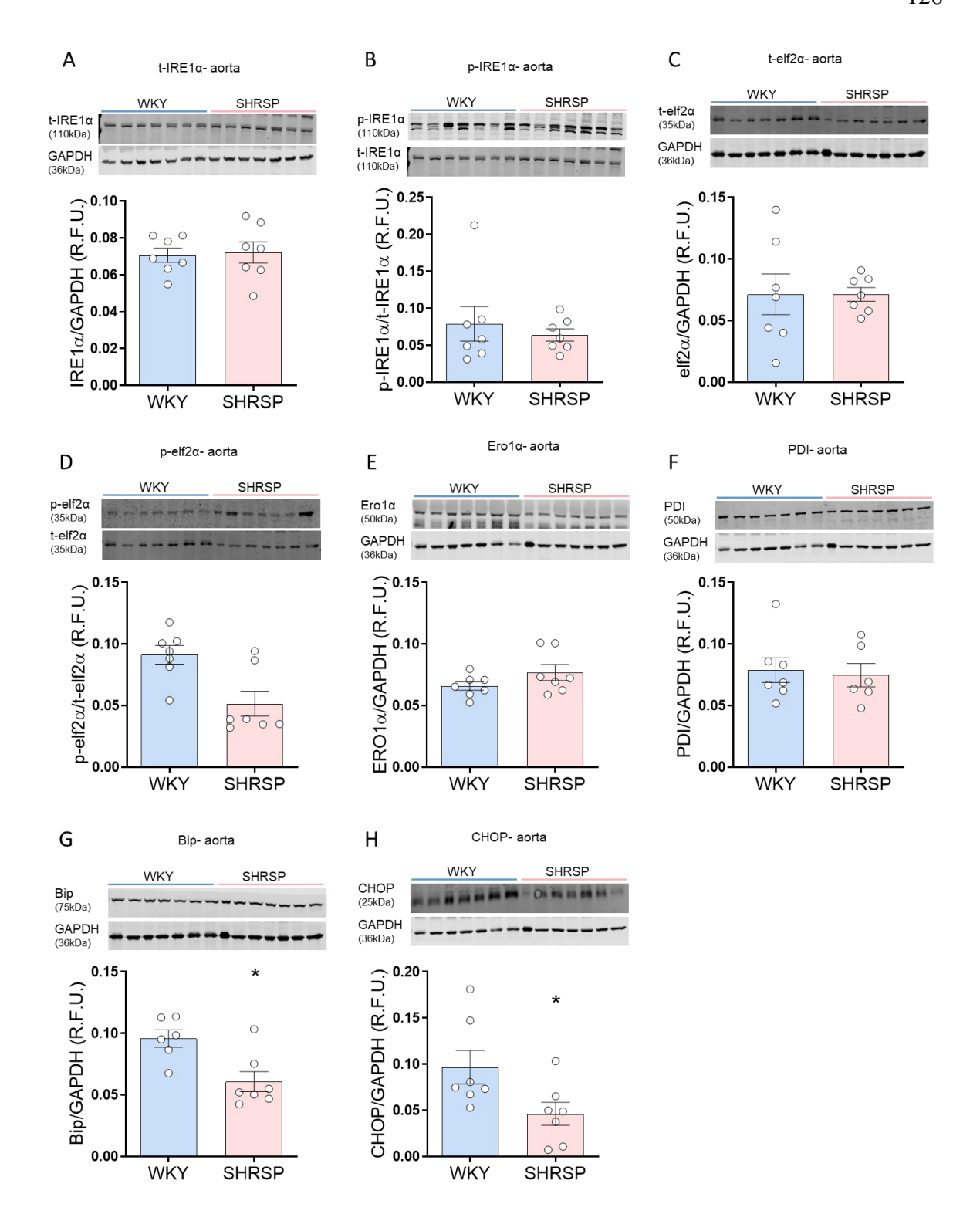


Figure 5.3 ER stress markers expression is not increased in aorta from SHRSP compared to WKY rats.

The protein expression of IRE1a (A), p-IRE1a (B), eIF2a (C), p-eIF2a (D), ERO1a (E), PDI (F), BIP (G), and CHOP (H) in aorta from WKY (blue columns) and SHRSP (pink columns) rats was assessed by immunoblotting. GAPDH was used as loading control. Data are presented as mean ± S.E.M., n=6-7. Statistical significances were determined by student t-test, \*p<0.05 compared to WKY rats.

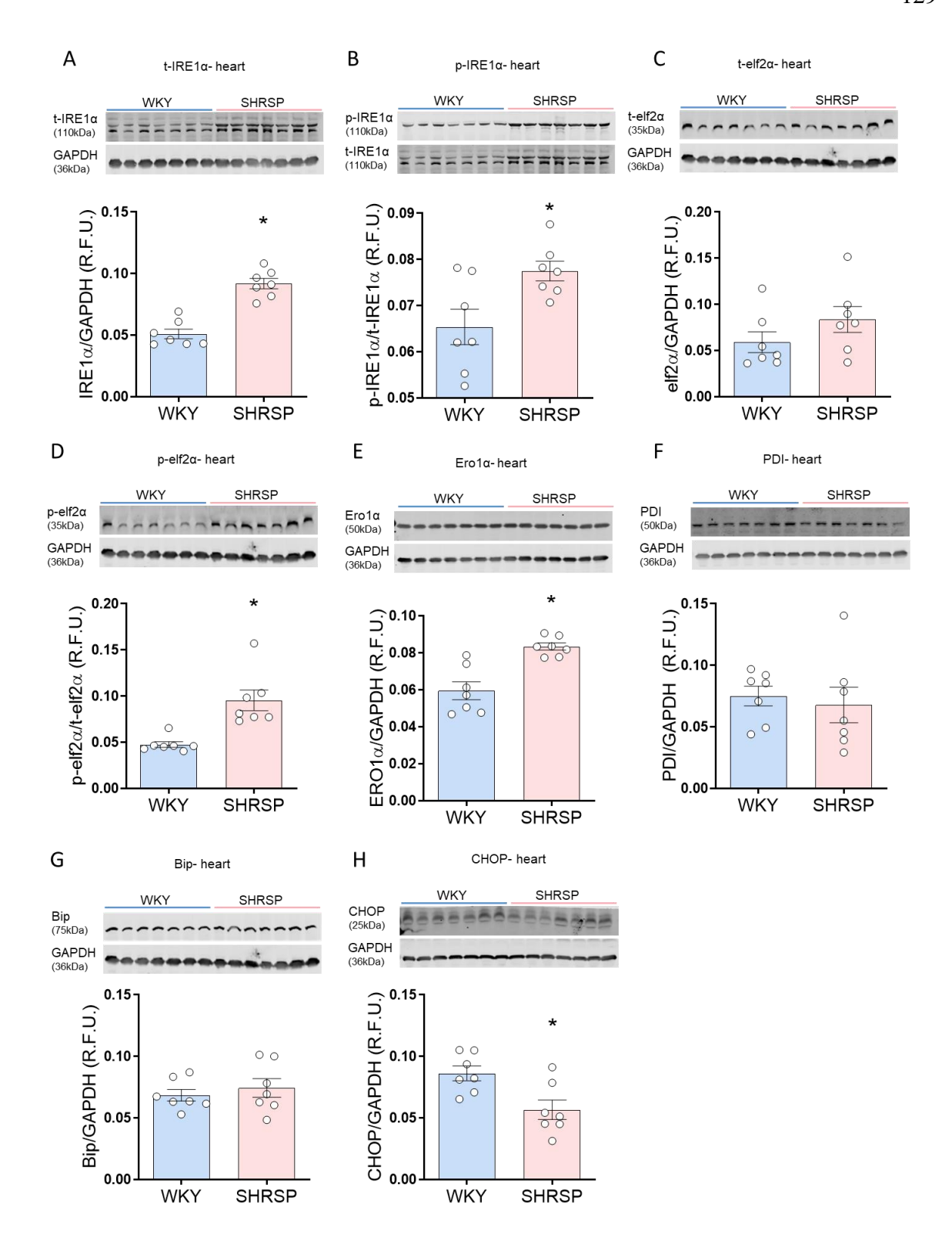


Figure 5.4 ER stress markers expression is increased in heart from SHRSP compared to WKY rats.

The protein expression of IRE1a (A), p-IRE1a (B), eIF2a (C), p-eIF2a (D), ERO1a (E), PDI (F), BIP (G), and CHOP (H) in the heart from WKY (blue columns) and SHRSP (pink columns) rats was assessed by immunoblotting. GAPDH was used as a loading control. Data are presented as mean ± S.E.M., n=6-7. Statistical significances were determined by student t-test, \*p<0.05 compared to WKY rats.

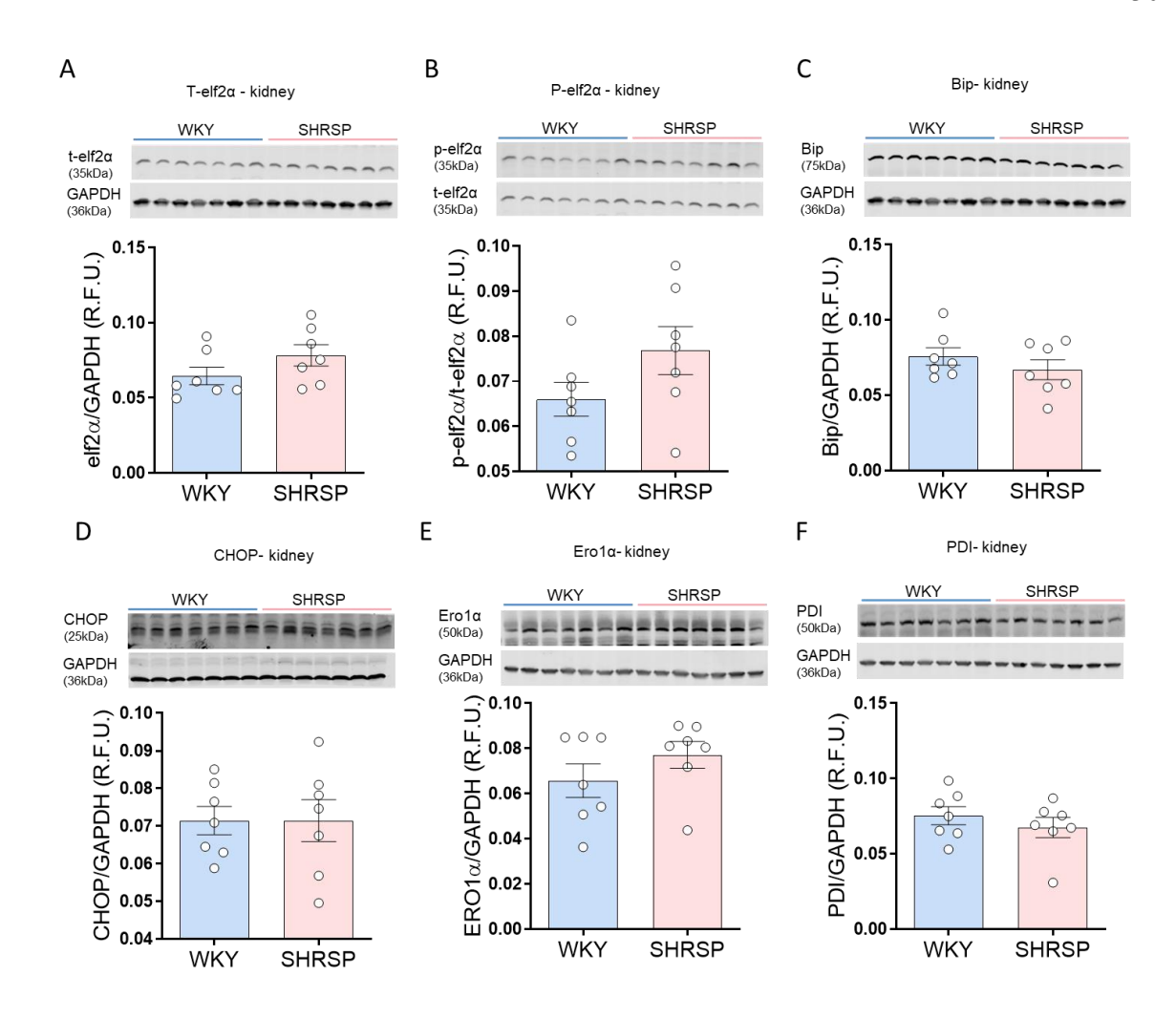


Figure 5.5 ER stress markers expression is not changed in kidney from SHRSP compared to WKY rats.

The protein expression of eIF2a (A) p-eIF2a (B), BIP (C), CHOP (D), ERO1a (E), and PDI (F) in kidney from WKY (blue columns) and SHRSP (pink columns) rats was assessed by immunoblotting. GAPDH was used as loading control. Data are presented as mean  $\pm$  S.E.M., n=7. Statistical significances were determined by student t-test, \*p<0.05 compared to WKY rats.

### 5.3.2 Effects of ET<sub>A</sub>R and ET<sub>B</sub>R on ER stress induced by ET-1 in VSMCs

To evaluate the possible molecular mechanisms underlying the activation of UPR in VSMCs from SHRSP, we treated the WKY and SHRSP cells with the vasoactive peptide ET-1. To study whether ET-1 induces ER stress response in an ETA or ETB receptor-dependent manner, we assessed the expression of ER stress markers in cells stimulated with ET-1 for 24 hours in the presence and absence of ET<sub>A</sub>R receptor antagonist (BQ123, 10uM), and ET<sub>B</sub>R receptor antagonist (BQ788, 10uM) in both WKY and SHRSP.

The results showed that regarding the PERK pathway, ET-1 induced eIF2a activation only in SHRSP but not in WKY (Figure 5.6A and B). Moreover, VSMCs treated with ET-1 showed increased ATF4 expression in both WKY and SHRSP (Figure 5.6C and D). In WKY, ET-1 failed to increase ATF4 expression in cells treated with both ET<sub>A</sub>R and ET<sub>B</sub>R antagonists (Figure 5.6C). In SHRSP, ET<sub>A</sub>R and ET<sub>B</sub>R antagonists significantly reduced baseline and ET-1-induced ATF4 expression (Figure 5.6D). Expression of CHOP, as one of the downstream chaperones of ATF4, is not changed by ET-1 treatment (Figure 5.6E and F), whereas baseline expression of CHOP in SHRSP was attenuated by ET<sub>A</sub>R antagonist (Figure 5.6F). These findings suggest ET-1 is involved in the activation of ATF4 in VSMCs from both WKY and SHRSP, and the mechanism is related to ET<sub>A</sub>R and ET<sub>B</sub>R receptor activation.

When looking at the IRE1 pathway, the activation of IRE1 did not change after ET-1 stimulation in WKY and SHRSP (Figure 5.7A). However, BQ123 and BQ788 treatment reduced IRE1a activation in SHRSP (Figure 5.7A and B), suggesting IRE1a activation may be dependent on ET<sub>A</sub>R and ET<sub>B</sub>R in SHRSP. The expression levels of xbp1 active form, xbp1s, were increased by ET-1 stimulation in WKY and attenuated by ETBR antagonist treatment (Figure 5.7C). However, these changes were not observed in SHRSP (Figure 5.7D), suggesting ET-1 is able to influence IRE1 pathway activation in WKY in an ETBR-dependent manner. Expression of xbp1unspliced (xbp1u) was not influenced by ET-1 in both strains. However, treatment with ET<sub>A</sub>R and ET<sub>B</sub>R antagonists reduced xbp1u baseline level in SHRSP (Figure 5.7E and F).

The expression of ER chaperone BIP was increased by ET-1 in both strains (Figure 5.8A and B), ET<sub>B</sub>R antagonist treatment significantly reduced BIP expression in WKY. Additionally, ET-1 failed to increase BIP expression in SHRSP in the presence of BQ788,

suggesting that ET-1 induced BIP expression is ETBR dependent. Expression of ERO1was increased by ET-1 via ET<sub>B</sub>R only in SHRSP (Figure 5.8C and D). The expression of ER chaperone PDI was not changed by ET-1 stimulation in both strains (Figure 5.8E and F). Together, the findings suggest ET-1 induced ER stress in VSMCs via upregulation of ATF4, XBP1s and BIP in an ETBR dependent manner. In hypertension, ET<sub>A</sub>R and ET<sub>B</sub>R play a role in regulation of ER stress.

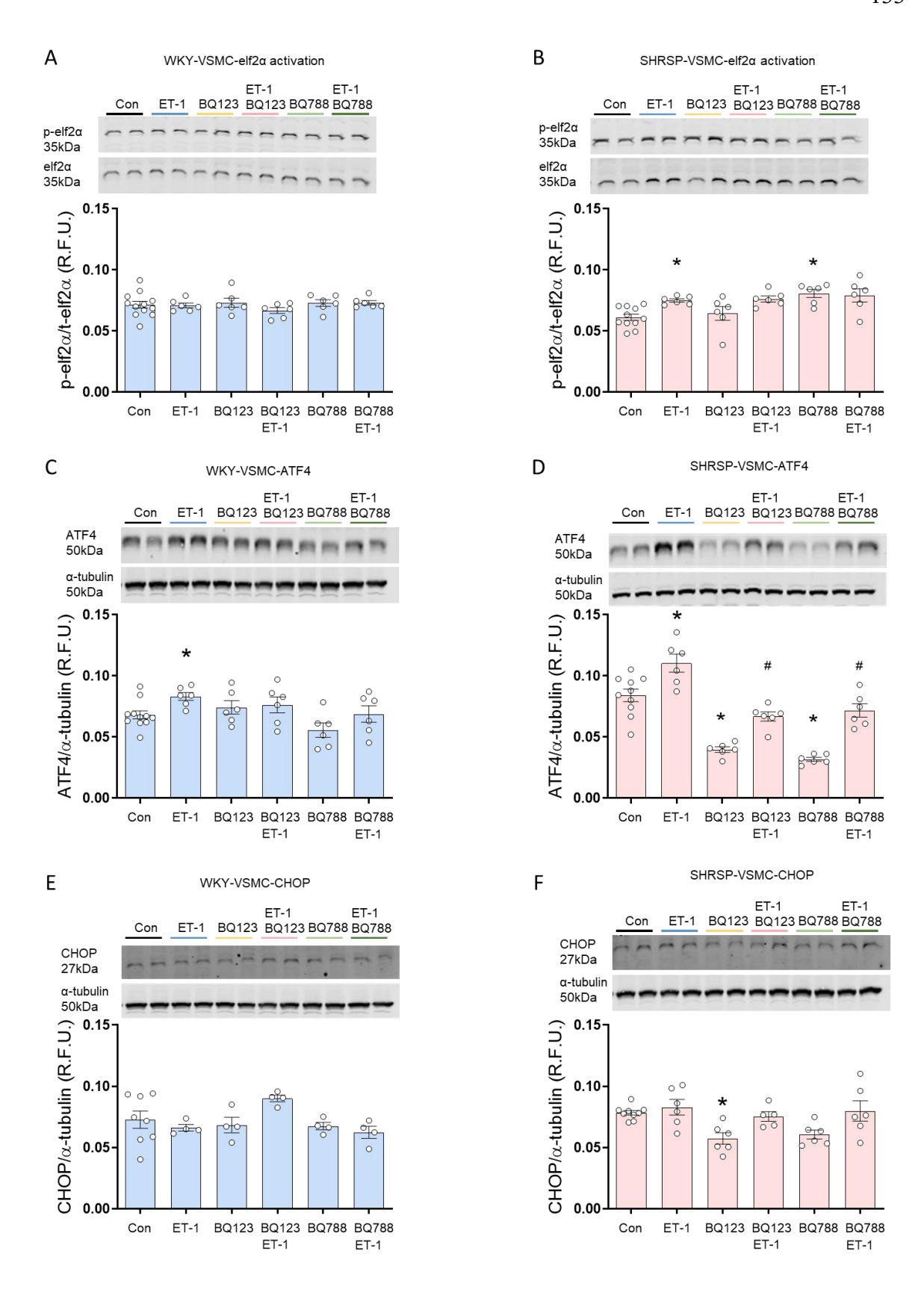


Figure 5.6 Effects of ETAR and ETBR on PERK pathway activation induced by ET-1 in VSMCs.

VSMCs from WKY (blue columns) and SHRSP (pink columns) were treated with ET-1 (100nM, 24h) and/or ET $_{\rm A}$ R antagonist BQ123 (10uM, 24h), ET $_{\rm B}$ R antagonist BQ788 (10uM, 24h). Protein expression of eIF2a activation (A), ATF4 (C), and CHOP (E) in VSMCs from WKY (blue columns) rats was assessed by immunoblotting. Protein expression of eIF2a activation (B), ATF4 (D), and CHOP (F) in VSMCs from SHRSP (pink

columns) rats was assessed by immunoblotting.  $\beta$ -actin was used as loading control. Data are presented as mean  $\pm$  S.E.M., n=4-6. Statistical significances were determined by one-way ANOVA followed by a Tukey test, \*p<0.05 compared to control group, #p<0.05 compared to ET-1 group.

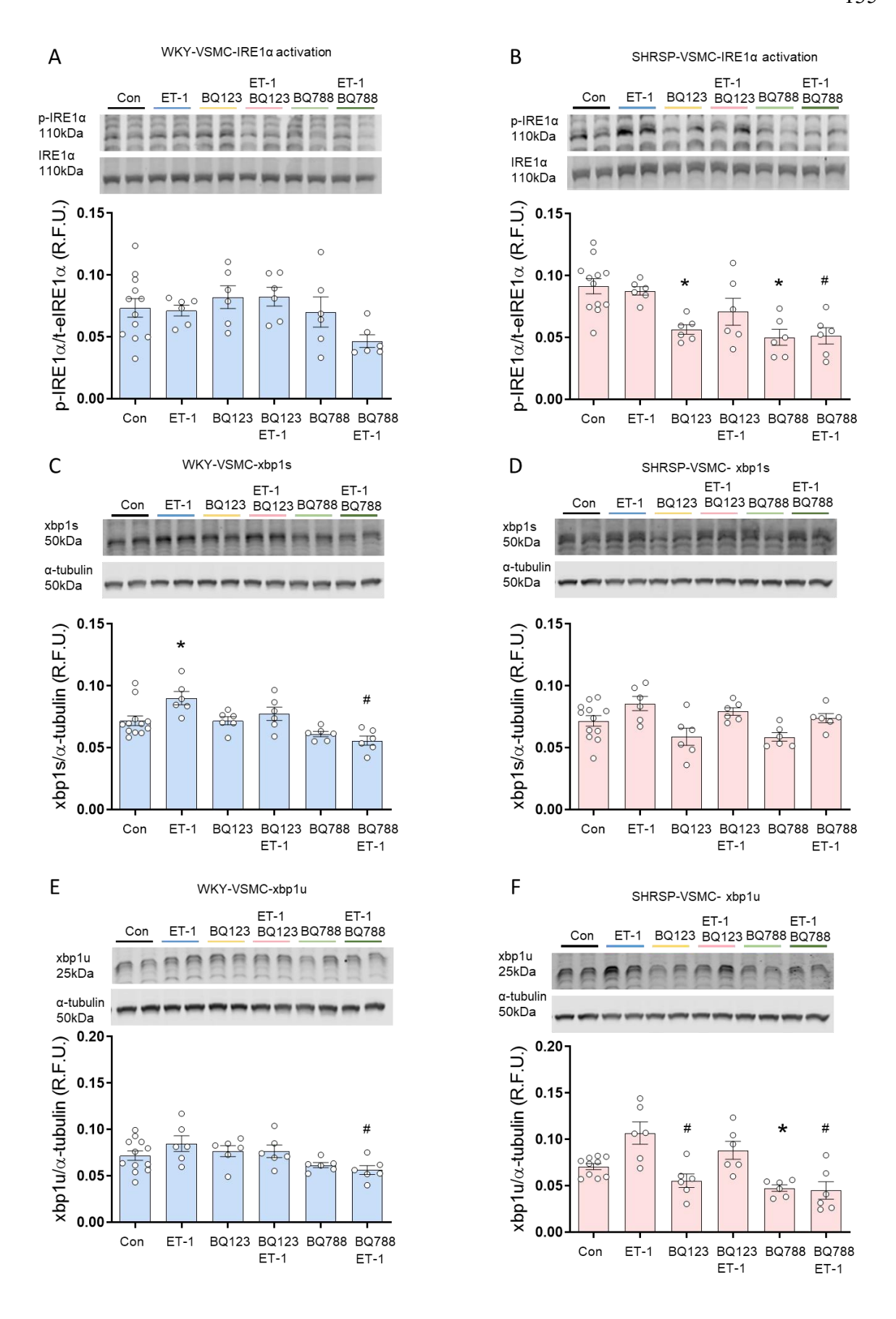


Figure 5.7 Effects of ETAR and ETBR on IRE1 pathway activation induced by ET-1 in VSMCs.

VSMCs from WKY (blue columns) and SHRSP (pink columns) were treated with ET-1 (100nM, 24h) and/or ET<sub>A</sub>R antagonist BQ123 (10uM, 24h), ET<sub>B</sub>R antagonist BQ788

(10uM, 24h). Protein expression of IRE1a activation (A), xbp1s (C), and xbp1u (E) in VSMCs from WKY (blue columns) rats was assessed by immunoblotting. Protein expression of IRE1a activation (B), xbp1s (D), and xbp1u (F) in VSMCs from SHRSP (pink columns) rats was assessed by immunoblotting.  $\beta$ -actin was used as loading control. Data are presented as mean  $\pm$  S.E.M., n=4-6. Statistical significances were determined by one-way ANOVA followed by a Tukey test, \*p<0.05 compared to control group, \*p<0.05 compared to ET-1 group.

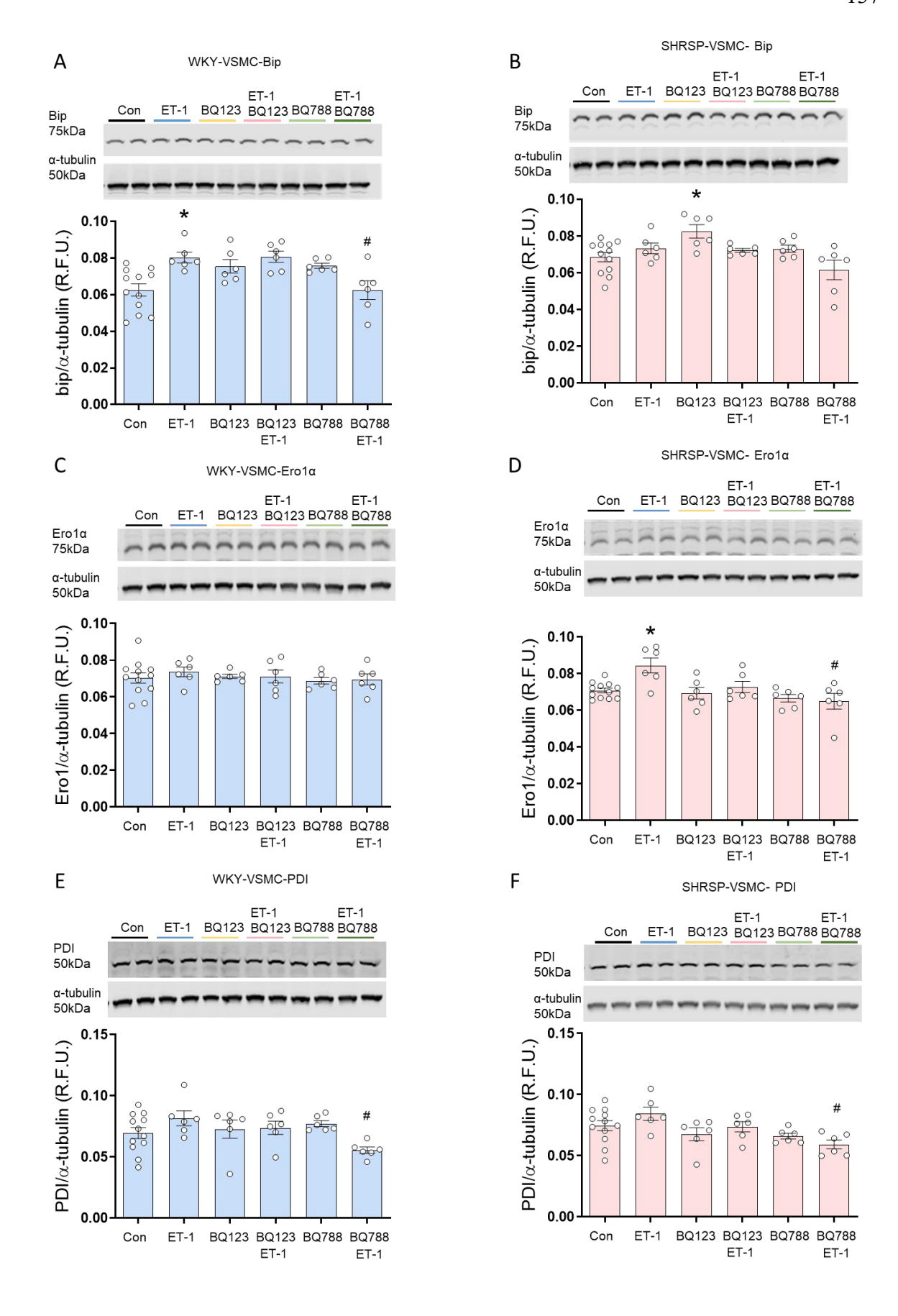


Figure 5.8 Effects of ETAR and ETBR on ER stress markers expression induced by ET-1 in VSMCs.

VSMCs from WKY (blue columns) and SHRSP (pink columns) were treated with ET-1 (100 nM, 24h) and/or ET<sub>A</sub>R antagonist BQ123 (10uM, 24h), ET<sub>B</sub>R antagonist BQ788

(10uM, 24h). Protein expression of BIP(A), ERO1a (C), and PDI (E) in VSMCs from WKY (blue columns) rats was assessed by immunoblotting. Protein expression of BIP(B), ERO1a (D), and PDI (F) in VSMCs from SHRSP (pink columns) rats was assessed by immunoblotting.  $\beta$  -actin was used as loading control. Data are presented as mean  $\pm$  S.E.M., n=4-6. Statistical significances were determined by one-way ANOVA followed by a Tukey test, \*p<0.05 compared to control group, \*p<0.05 compared to ET-1 group.

### 5.3.3 Altered ET-1 induced p-MLC<sub>20</sub> and Ca<sup>2+</sup> influx by ER stress inhibitors from SHRSP rats

One of the important pathophysiological mechanisms promoting the development of hypertension is VSMCs contraction. Critical to VSMC contraction is an increase in intracellular Ca<sup>2+</sup> concentration, which induces phosphorylation of myosin light chain 20 (p-MLC<sub>20</sub>), stimulates myosin–actin interaction and consequent vascular contraction (Touyz et al., 2018). To investigate whether ET-1-induced ER stress affects the contractile machinery in hypertensive VSMCs, we assessed the ET-1-induced phosphorylation of MLC<sub>20</sub> and intracellular calcium influx in the presence and absence of three ER stress inhibitors: 4PBA (chemical chaperone), GSK2606414 (PERK inhibitor), and STF083010 (IRE1 endonuclease activity inhibitor).

As the expression level of ATF4 from PERK pathway was higher with ET-1 treatment in VSMCs from both WKY and SHRSP, we assessed the effect of ER stress inhibitors on basal and ET-1-induced ATF4 expression. In WKY, as expected, PERK inhibitor GSK2606414 reduced ET-1-induced ATF4 expression, and IRE1 inhibitor STF083010 increased basal ATF4 expression (Figure 5.9 A). In SHRSP, ER stress inhibitors did not change basal ATF4 expression but attenuated ET-1-induced ATF4 levels (Figure 5.9B), suggesting a different mechanism of ER stress regulation by ET-1 in hypertension.

Phosphorylation of MLC<sub>20</sub> was not significantly changed with 24h ET-1 stimulation or with ER stress inhibitors treatment in WKY (Figure 5.9C). However, the expression of p-MLC<sub>20</sub> was increased by ET-1. It was attenuated by all three ER stress inhibitor treatments (Figure 5.9D), suggesting ER stress is involved in the activation of contractile machinery only in SHRSP.

To confirm whether ER stress contributes to ET-1-induced vascular contraction in SHRSP, we assessed the intracellular calcium levels using fluorescent calcium indicator Cal-520 acetoxymethyl ester. VSMCs were treated with ER stress inhibitors 4PBA, GSK2606414, and STF083010 24 hours before stimulation with ET-1. ET-1 rapidly increased Ca<sup>2+</sup> transients in WKY that were not altered by ER stress inhibition (Figure 5.9E and F). In SHRSP, ET-1-induced changes in intracellular Ca<sup>2+</sup> levels were decreased by GSK2606414 and STF083010 treatment (Figure 5.9G and H). These results suggest that ET-1-induced overactivation of contractile machinery is related to the activation of ER stress in VSMCs from SHRSP.

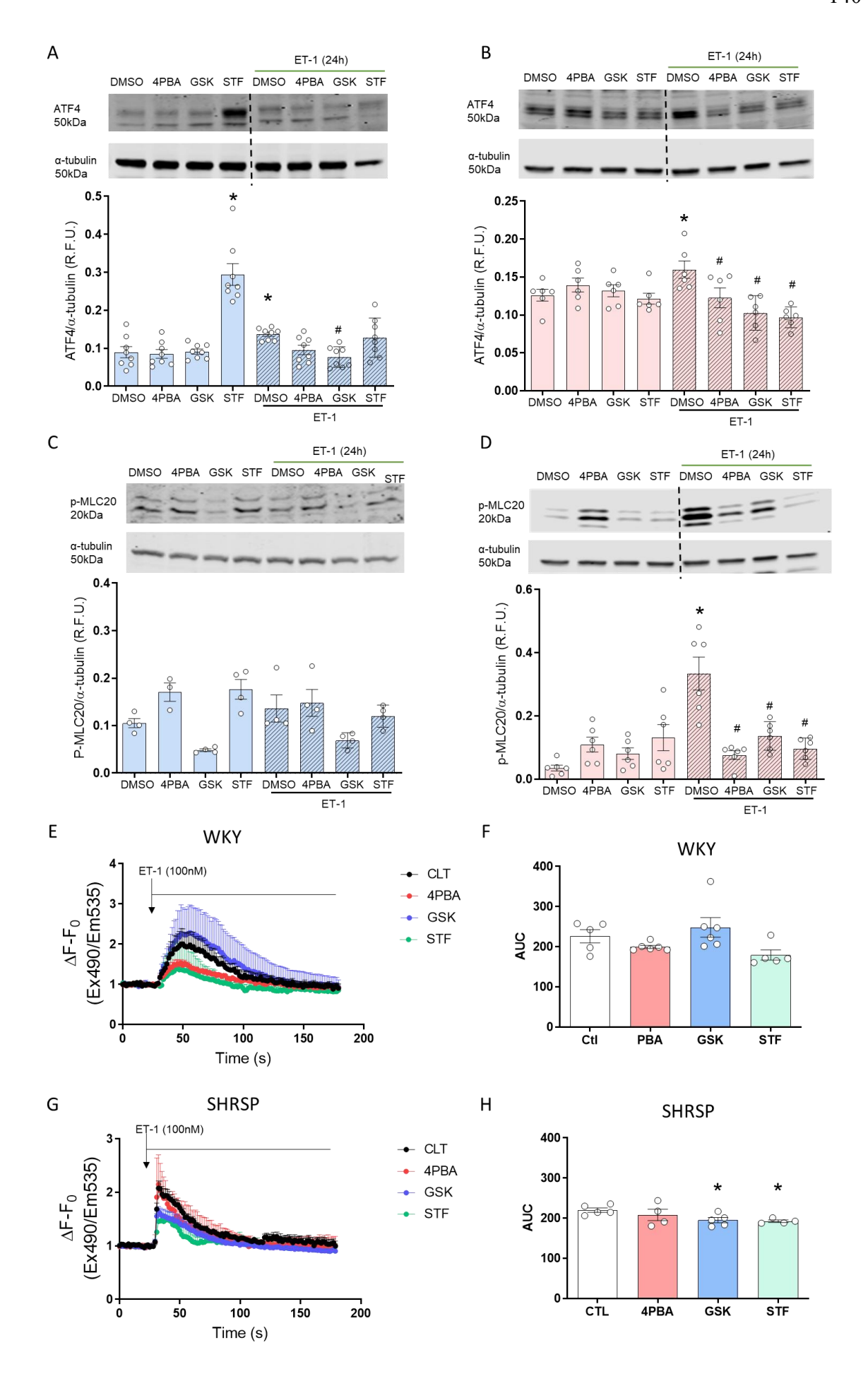


### Figure 5.9 Effect of ER stress inhibition on ET-1 induced signalling in VSMCs from WKY and SHRSP rats.

VSMCs from WKY (blue columns) and SHRSP (pink columns) were treated with ET-1 (100nM, 24h) and/or ER stress inhibitors 4-PBA (1mM, 24h), STF083010(60uM for protein, 30uM for calcium, 24h), GSK2606414 (0.5uM, 24h). Protein expression of ATF4 (A), and p-MLC20 (C) in VSMCs from WKY (blue columns) rats was assessed by immunoblotting. Protein expression of ATF4 (B), and p-MLC20 (D) in VSMCs from SHRSP (pink columns) rats was assessed by immunoblotting. β-actin was used as loading control. Calcium influx induced by ET-1(100nM) in VSMCs from WKY (E and F) and SHRSP (G and H) rats measured by live cell microscopy using the fluorescent probe, CAL520 - AM. AUC represent area under curve. Data are resented as mean ± S.E.M., n=4-7. Statistical significances were determined by one-way ANOVA followed by a Tukey test, \*p<0.05 compared to control/DMSO.

## 5.3.4 Altered vascular contraction by ER stress inhibitors from SHRSP rats

To investigate whether ER stress influences vascular contractility, vascular contraction was assessed by wire myography in mesenteric arteries from WKY and SHRSP. Contractile responses to U46619 (thromboxane-receptor agonist) and ET-1 were increased in SHRSP compared with vessels from WKY rats (Figure 5.10A and C).

The pre-incubation of vessels with GSK2606414 had no significant effect on the contractile response in WKY (Figure 5.10A and C). However, in SHRSP, pre-incubation with GSK2606414 resulted in partial reduction of the EC50 for both U46619 and ET-1 induced contractions, and also decreased Emax for both U46619 and ET-1 induced contractions to the level observed in WKY rats (Figure 5.10A and C). These results suggest inhibition of PERK signalling pathway may have the potential to improve vascular hypercontractility in hypertension.

Pre-incubation of vessels with STF083010 resulted in decreased ET-1 and U46619-induced contraction in both WKY and SHRSP rats (Figure 5.10 B and D). These findings suggest that the IRE1 signalling pathway is not only involved in vascular contraction but also raises concerns about potential toxicity to all vessels.

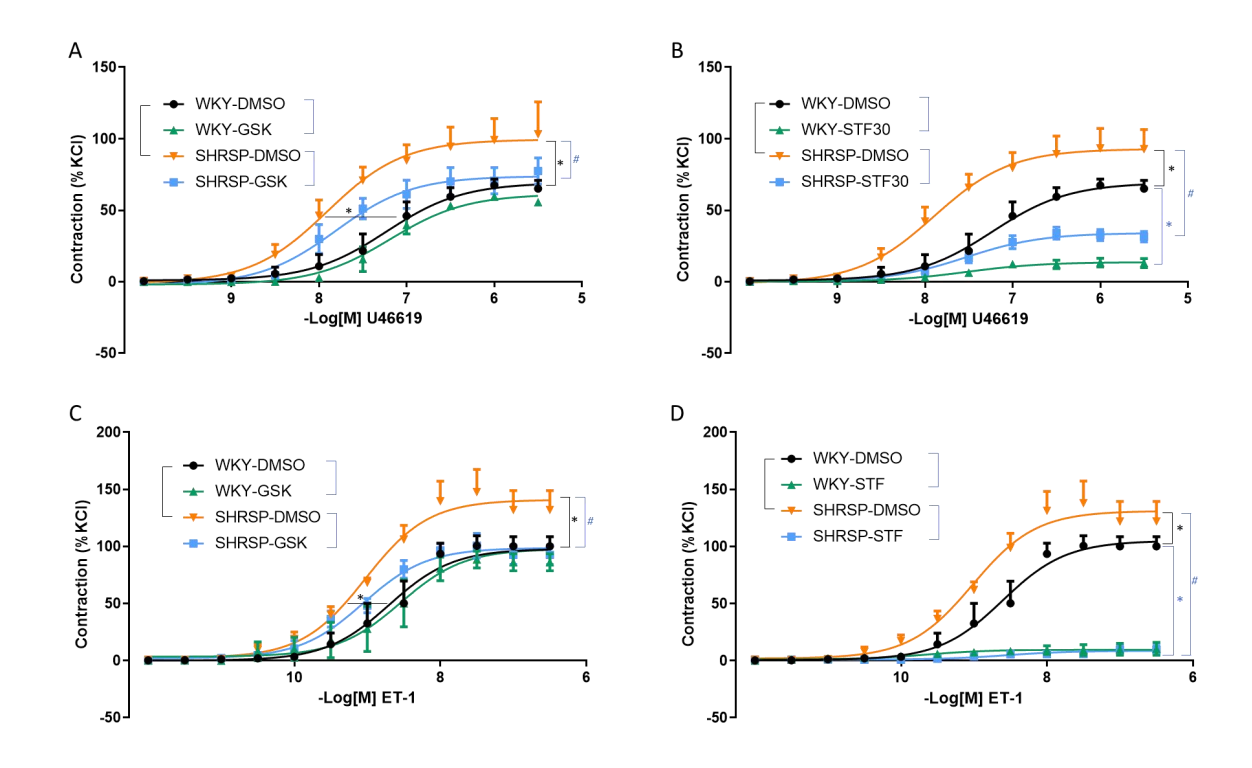


Figure 5.10 Effect of ER stress inhibition on ET-1 and U46619 induced vascular contraction from WKY and SHRSP rats.

Vascular contractility to U46619 and ET-1 assessed by wire myography in mesenteric arteries from WKY and SHRSP rats. Vessels were pre-incubated ER stress inhibitors GSK2606414 (0.5uM, 30min) (A and C) and STF083010 (30uM, 30min) (B and D). Contraction dose–response curves were performed in response to U46619 (A and B) and ET-1 (C and D). Results were expressed as a percentage of the maximal response to KCI. Differences in half maximal effective concentrations (EC50) and maximal contraction (Emax) across groups are shown by \*p<0.05 vs WKY or \*p<0.05 SHRSP. Data are resented as mean  $\pm$  S.E.M., n=6-8.

### 5.4 Discussion

Major findings of this study show: i) UPR pathway is activated in VSMCs and heart of SHRSP compared to WKY; ii) ET-1 induced upregulation of ER stress proteins ATF4, XBP1s and BIP in an ET<sub>B</sub>R dependent manner in cells from normotensive rats; iii) In hypertension, ER stress activation is depending on both ET<sub>A</sub>R and ET<sub>B</sub>R. iii) Inhibition of ER stress reduced activation of the contractile machinery and vasoconstriction in SHRSP.

#### 5.4.1 ER stress in SHRSP

ER stress has been associated with vascular dysfunction in many hypertensive models. ER stress activation has been demonstrated in cardiomyocytes (Qian et al., 2021, Wu et al., 2019, Zhou et al., 2020) and in VSMCs from mesenteric arteries (Camargo et al., 2018) and aorta (Kim et al., 2018) from SHR. Similarly, our results showed that the ER stress response is activated in VSMC from the SHR substrain, SHRSP. However, there was no increase in the expression of ER stress markers in whole tissue from mesenteric arteries and aorta. Apart from VSMCs, artery tissues also include endothelial cells and different types of adventitia cells, including fibroblasts, pericytes, nerves, progenitor cells, and immunomodulatory cells. One possible reason that we didn't detect ER stress activation in arteries may be that ER stress may play different roles in different cell types, which needs further investigation.

The heart and the kidneys have an important role in pathophysiology of hypertension. Therefore, we investigated expression of ER stress markers in the heart and tissue from SHRSP. We found increased activation of IRE1 and PERK arms of ER stress in the heart from SHRSP, suggesting a role for ER stress in cardiac dysfunction associated with hypertension. Similar results have been found in other studies, such as increased PERK, ATF4, ATF6, Bip and CHOP expression in cardiac tissue of SHR (Zhou et al., 2020, Qian et al., 2021). On the other hand, in the kidneys there were no differences in expression of ER stress markers between the groups.

Altogether, our results highlight the role of ER stress in VSMC and in VSMC and in the heart from the SHRSP experimental model. We and others previously demonstrated that ER stress inhibition decreased hypercontractility in arteries of both SHRSP (Camargo et al., 2018) and SHR (Naiel et al., 2019, Carlisle et al., 2016), (SpitlerMatsumoto and Webb,

2013), however the molecular mechanisms involved in activation of ER stress in VSMC remain incompletely understood.

#### 5.4.2 ET-1 induces ER stress in VSMC

ET-1 is a potent vasoconstrictor that has been implicated in VSMC dysfunction in hypertension. Plasma ET-1 levels in different hypertensive models are not the same (Suzuki et al., 1990, Pinto-Sietsma and Paul, 1998, Iglarz and Schiffrin, 2003), with higher or normal levels observed in human hypertension, higher in SHR plus DOCA-salt hypertensive rat and lower or not change in SHR and/or SHRSP. However, circulating levels of ET-1 cannot reflect a locally acting (Pinto-Sietsma and Paul, 1998, Iglarz and Schiffrin, 2003), levels of ET-1 in specific tissue are vital in functional research as they could directly modulate cellular functions. In SHRSP, the endothelin system is activated in vessels, as evidenced by preproendothelin-1 mRNA levels were increased in mesenteric arteries (Sharifi et al., 1998).

It has been found that ET-1 induces ER stress in pulmonary artery smooth muscle (Yeager et al., 2012), renal tissues (De Miguel et al., 2017), and placental tissues during pre-eclampsia(Jain et al., 2012), but not yet in hypertension. Inhibition of either ET-1 or ER stress reduced blood pressure in hypertensive rats (Li and Schiffrin, 1995, Naiel et al., 2019). It is possible that one of the molecular mechanisms of ET-1 induced increase in blood pressure is induction of vascular dysfunction by activation of ER stress via higher vascular ET-1 levels. To investigate the role of ET-1 in ER stress we measured the ER stress markers expression after ET-1 stimulation in the presence of ET-1 receptor antagonists. ER stress inducers, such as tunicamycin and thapsigargin, cause upregulation of ER stress target genes over 24h. Therefore, cells were stimulated with ET-1 for 24h.

In cells from WKY rats, we observed that ET-1 induced the expression of ATF4 but not phosphorylation of eIF2 $\alpha$ . Since phosphorylation is a rapid event, stimulation with ET-1 may cause phosphorylation of eIF2 $\alpha$  at an earlier time point. It has been found the level of phosphorylated eIF2 $\alpha$  peaked one hour after stimulation with ER stress inducer thapsigargin and significantly declined eight hours later (Novoa et al., 2003). The dephosphorylation of eIF2 $\alpha$  may be caused by ATF4 mediated upregulation of GADD34, a stress response phosphatase cofactor, that promotes dephosphorylation of eIF2 $\alpha$  and translational recovery to terminate integrated stress response (TeskeBaird and Wek, 2011). One possibility is that ET-1-induced transient ER stress response leads to the activation of

this negative feedback loop, which helps restore protein synthesis and normal cell functioning. Moreover, we observed that ET-1 induced the expression of Xbp1s and molecular chaperone BIP in an ET<sub>B</sub>R dependent manner in VSMC from WKY. Similarly, it has been found ET-1 increases Xbp1s expression dependent on both ET<sub>A</sub>R and ET<sub>B</sub>R in rat pulmonary artery smooth muscle cells (Yeager et al., 2012). Our results showed that in VSMC under normotensive conditions, ET-1 induces ER stress in VSMC via activation of ET<sub>B</sub>R.

In VSMCs from hypertensive rats, our results showed ER stress is activated at baseline, and inhibition of either ET<sub>A</sub>R or ET<sub>B</sub>R reduced the levels of ER stress markers (ATF4, CHOP, XBP1u and phosphorylation of IRE1). Evidence demonstrated that VSMC itself can produce ET-1 (Russo et al., 1999), and changes in ET-1 response can be caused by dysfunctional ET-1 receptor signalling (Tykocki and Watts, 2010). One hypothesis is that in hypertension VSMC may produce ET-1, which induces ER stress through activation of ET-1 receptors. Additionally, in hypertension it seems to be a cooperative effect of ET<sub>A</sub>R and ET<sub>B</sub>R in ET-1 induced ER stress, while only ET<sub>B</sub>R reduced ER stress signalling in normotensive rats. The underlying molecular mechanism of ET-1 receptors alterations in hypertension is incompletely understood. However, a synergistic effect of ET<sub>A</sub>R and ET<sub>B</sub>R has been previously demonstrated in the vasculature (Inscho et al., 2005) and in the kidneys (Boesen and Pollock, 2010). It has been shown that ET<sub>A</sub>R and ET<sub>B</sub>R can form heterodimers in rat mesenteric arteries (Kapsokalyvas et al., 2014). However, further investigation is required to evaluate if heterodimerisation plays a role in ET-1-induced ER stress.

In the present study we demonstrated that ET-1 induced ER stress in VSMC from normotensive and hypertensive rats. ET-1 further increased some of the UPR signalling pathways in SHRSP such as ATF4 and Ero1 expression, suggesting increased levels of ET-1 could potentiate the ER stress response in hypertension. Inhibition of ET<sub>A</sub>R and ET<sub>B</sub>R in ET-1 treated VSMCs reduced expression of ATF4, supporting the important role of ET-1 receptors in ET-1 mediated ER stress in hypertension. A possible mechanism involved in ET-1 induced ER stress is dysregulation of ER calcium, as most ET-1 responses are Ca<sup>2+</sup> dependent (Tykocki and Watts, 2010). ER Ca<sup>2+</sup> regulates the formation of chaperones (Stevens and Argon, 1999) and Ca<sup>2+</sup> dependent post-translational modifications (Ellgaard et al., 2016). ET-1 can induce Ca<sup>2+</sup> release from the ER (Tykocki and Watts, 2010), disrupting Ca<sup>2+</sup> homeostasis and therefore, affecting the folding and maturation of several proteins, leading to ER stress (KrebsGroenendyk and Michalak, 2011).

# 5.4.3 ER stress involves in ET-1 induced contraction in hypertensive rats

The rise in intracellular Ca<sup>2+</sup> is the principal process in VSMCs contraction. Both ET<sub>A</sub>R and ET<sub>B</sub>R mediate changes in intracellular Ca<sup>2+</sup> concentration triggered by ET-1 in VSMCs, and this is supported by evidence showing that the ET<sub>B</sub>R agonist S6c increases intracellular Ca<sup>2+</sup> to half of the ET-1 induced intracellular Ca<sup>2+</sup> response in VSMCs from rat mesenteric arteries (Schiffrin and Touyz, 1998). The increase in Ca<sup>2+</sup> mediated by ET<sub>A</sub>R or ET<sub>B</sub>R leads to formation of Ca<sup>2+</sup>-calmodulin complex, which induces MLC phosphorylation, actin-myosin interaction promoting vascular smooth muscle contraction (Hynynen and Khalil, 2006). Our study suggested ET-1 induced sustained activation of the contractile machinery in VSMC from SHRSP, an effect mediated by ER stress. Additionally, our findings indicate that this phenomenon contributes to vascular hypercontractility underlying hypertension. In our results, prolonged exposure to ET-1(24h) increased MLC<sub>20</sub> phosphorylation only in SHRSP. This effect was reversed by ER stress inhibitors, suggesting prolonged activation of MLC<sub>20</sub> by ET-1 is dependent on ER stress. A previous study has demonstrated that ER stress inducers Tunicamycin and MG132 increased phosphorylation of MLC with a peak at 12 hours and increased vascular contraction and blood pressure. These effects were reduced by ER stress inhibitor 4-PBA (Liang et al., 2013).

Intracellular Ca<sup>2+</sup> is mainly stored in the lumen of ER, which is essential for signalling and for proper protein folding through the activity of Ca<sup>2+</sup>-binding chaperones (KuznetsovBrostrom and Brostrom, 1992). Some studies showed that ER stress leads to the release of Ca<sup>2+</sup> from the ER lumen, resulting in an increase in intracellular Ca<sup>2+</sup>, which supports our hypothesis that ER stress can affect vascular contraction via Ca<sup>2+</sup>. It has been found that ER stress inducer Tunicamycin increased cytosolic Ca<sup>2+</sup> in parallel with a reduction of ER Ca<sup>2+</sup> in VSMCs from mice (Liang et al., 2013). Also, it was demonstrated that 24h exposure of Tunicamycin can reduce ER Ca<sup>2+</sup> levels in HuH7 cells in a dose dependent manner (Lebeau et al., 2021). Our results showed that ER stress plays a role in ET-1 induced Ca<sup>2+</sup> influx only in SHRSP.

Targeting specific pathways of ER stress signalling can be a more effective approach for the treatment of certain conditions. For example, selectively block PERK arm has shown to be more effective than non-specific inhibition with 4PBA or specific inhibition of IRE1 or ATF6 in ameliorating pulmonary vascular remodelling (Shimizu et al., 2021). Inhibition of

IRE1 could specifically enhance efferocytosis and cholesterol transport and reduce atherosclerosis progression in mice (Yildirim et al., 2022). From the result, specifically block IRE1 or PERK arm of ER stress showed a better effect than 4PBA in improving ET-1 induced Ca<sup>2+</sup> influx, and effectively reducing vessels hypercontractility in hypertension. The result suggests that specifically targeting the IRE1 or PERK arm of the ER stress response may be a promising strategy for treating hypertension, but more research is needed to fully understand the potential benefits and limitations of this approach.

In summary, this study evaluated ET-1 and its receptors, which are involved in ER stress and contribute to vascular hypercontractility during hypertension. Moreover, we identify changes in Ca<sup>2+</sup> influx induced by ET-1 in hypertension may involve the specific arms of ER stress response PERK and IRE1. These findings suggest a novel pathway between ET-1 and ER stress in vascular biology, which might expand the understanding of pathophysiology of hypertension.

# Chapter 6 ER Stress Inhibitor 4-PBA Treatment in WKY and SHR Rats

### 6.1 Overview

Hypertension, characterised by elevated blood pressure (BP), is a chronic disease defined as a systolic blood pressure  $\geq$  140 mmHg and/or a diastolic pressure  $\geq$  90 mmHg in accordance with most major guidelines (Unger et al., 2020, Oparil et al., 2018a). The majority (90-95%) of patients with hypertension are diagnosed with essential hypertension. Blood pressure is influenced by cardiac output and peripheral resistance (Mayet and Hughes, 2003). Most patients with essential hypertension exhibit a normal cardiac output but an elevated peripheral resistance (BeeversLip and O'Brien, 2001). Arteries with a diameter size under 300  $\mu$ m are considered resistance vessels, which play a vital role in regulating the regional distribution of vascular tone and blood flow (HeagertyHeerkens and Izzard, 2010, Naiel et al., 2019). According to Poiseuille's Law, vessel resistance is inversely proportional to the fourth power of the radius. Thus, slight changes in arterial lumen, either functional or structural, result in a major impact on vascular resistance and subsequently affect blood pressure (Welsh et al., 2018).

The spontaneously hypertensive rat (SHR) is a widely used animal model to study human essential hypertension and displays vascular damage. In comparison to its non-hypertensive control strain Wistar Kyoto (WKY) rat, the SHR exhibits elevated systolic blood pressure as early as 6 weeks after birth (Takeuchi et al., 2021). At this prehypertensive age, SHR resistance blood vessels start to show impaired endothelium-dependant relaxation (BennettHillier and Thurston, 1996) and increased contractile responses (Naiel et al., 2019, SpitlerMatsumoto and Webb, 2013), along with an increased media: lumen ratio and hypertrophy of the medial layer (Intengan et al., 1999a, LeeDickhout and Sandow, 2017, Dickhout and Lee, 1997). Around the age of 21 weeks, SHR rats typically have a blood pressure of about 180-200 mmHg, whereas most WKY rats maintain a blood pressure below 140 mmHg (Takeuchi et al., 2021, Rodriguez-Iturbe et al., 2005, Chen et al., 1998).

Hypertension is associated with endoplasmic reticulum (ER) stress. Accumulation of unfolded or misfolded protein in the ER leads to ER stress. Misfolded proteins bind to the ER resident chaperone BiP, which in turn is released from the ER stress sensor proteins IRE1, PERK, and ATF6, activating the unfolded protein response (UPR). Prolonged ER

stress results in cellular dysfunction, contributing to the development of diseases such as hypertension. ER stress has been linked to blood pressure regulation, as treatment with ER stress inducer tunicamycin increases blood pressure in mice, while the ER stress inhibitors 4PBA or TUDCA decrease blood pressure in animal models (Young, 2017, Liang et al., 2013, Naiel et al., 2019). ER stress could be associated with changes in blood pressure through vascular dysfunction (Camargo et al., 2018). Growing research has indicated the potential role of ER stress in blood vessels from SHR (Carlisle et al., 2016, SpitlerMatsumoto and Webb, 2013, Naiel et al., 2019, Liang et al., 2013).

# 6.2 Hypothesis and aims

Extensive evidence demonstrated that ER stress contributes to vascular injury associated with hypertension. In vitro study, we found ER stress markers expression is higher in VSMCs (obtained from mesenteric resistance arteries) from SHRSP rats compared with WKY rats. Moreover, pre-incubation with ER stress inhibitors improves vessel hypercontractility in hypertensive rats. To further evaluate the protective effects of inhibiting ER stress on resistance vessel function and structure in vivo, we hypothesised that inhibition of endoplasmic reticulum stress would ameliorate functional and structural changes in resistance vessels during hypertension, ultimately leading to a reduction in blood pressure. We used ER stress inhibitor 4PBA, a low-molecular-weight chemical chaperone that alleviates ER stress by assisting protein folding. The specific aims are:

1. To evaluate the effect of 4-PBA treatment on general parameters and blood pressure of WKY and SHR.

Twenty-one-week-old WKY and SHR male rats were randomised into either 4PBA treated (4PBA) or untreated (Veh) groups. 4PBA-treated rats received a dose of 1g/kg/day of 4PBA in the drinking water for 5 weeks, while non-treated rats received normal tap water. Systolic blood pressure (tail cuff method) and body weight were measured at week 0 (before treatment) and once a week during the 5 weeks of 4PBA treatment. Heart, kidney, and spleen weights were measured and normalised by tibia length on the collection day.

2. To evaluate whether vascular dysfunction observed in SHR rats is ameliorated upon 4PBA treatment.

Small mesenteric arteries from 4PBA treated and untreated WKY and SHR rats were isolated. Contraction dose-response curves were performed in response to U46619 and ET-1 via wire myography. Relaxation dose-response curves were performed in response to Ach (endothelial - dependent relaxation), and SNP (endothelial - independent relaxation) via wire myography.

3. To evaluate whether vascular remodelling and mechanical properties changed in WKY and SHR with 4-PBA treatment.

Small mesenteric arteries from 4PBA treated and untreated WKY and SHR rats were isolated. Pressure myography was performed, and media-to-lumen ratio, wall thickness, cross - sectional area, and vascular stiffness were measured.

### 6.3 Results

# 6.3.1 ER stress inhibitor, 4PBA, attenuates systolic blood pressures in SHR

To examine the effect of inhibiting ER stress on the development of hypertension, rats were randomized into either 4PBA treated (4PBA) or untreated (Veh) groups and received a dose of 1g/kg/day of 4PBA in the drinking water for 5 weeks, while systolic blood pressure measurements were taken each week.

At the beginning of the experiment (week 0), systolic BP was significantly higher in SHR rats (180.1  $\pm$  1.2 mmHg) compared to WKY rats (151.9  $\pm$  0.7 mmHg). Systolic BP was similar between WKY-Veh and WKY-4PBA groups before and during the 5-week treatment of 4PBA (Figure 6.1A and B). BP was similar between SHR-Veh (175.1  $\pm$  1.3 mmHg) and SHR-4PBA (186.5  $\pm$  2.6 mmHg) groups before 4PBA treatment (week 0). Differences between the two groups were observed after 4 weeks of treatment with 4PBA. Systolic BP was significantly lower in SHR rats with 4PBA treatment on week 4 (180.0  $\pm$  1.3 mmHg vs. 169.5  $\pm$  1.6 mmHg) and week 5 (176.5  $\pm$  1.7 mmHg vs. 162.3  $\pm$  2.0 mmHg) (Figure 6.1A and B).

4PBA treated rats showed a trend of less body weight gain during the 5-week treatment period (Figure 6.1C), but no significant reduction in body weight was observed compared to nontreated rats at the end of experiments in both WKY and SHR rats (Figure 6.1D).

Organ size was not significantly altered by 4-PBA treatment. At week 5, the results revealed a slight trend decrease in heart weight (Figure 6.1E), no effect on kidney weight (Figure 6.1F), and a slight trend decrease in spleen weight (Figure 6.1G) with 4PBA treatment. Overall, no significant changes were observed in body weight and organ size between any of the four groups.

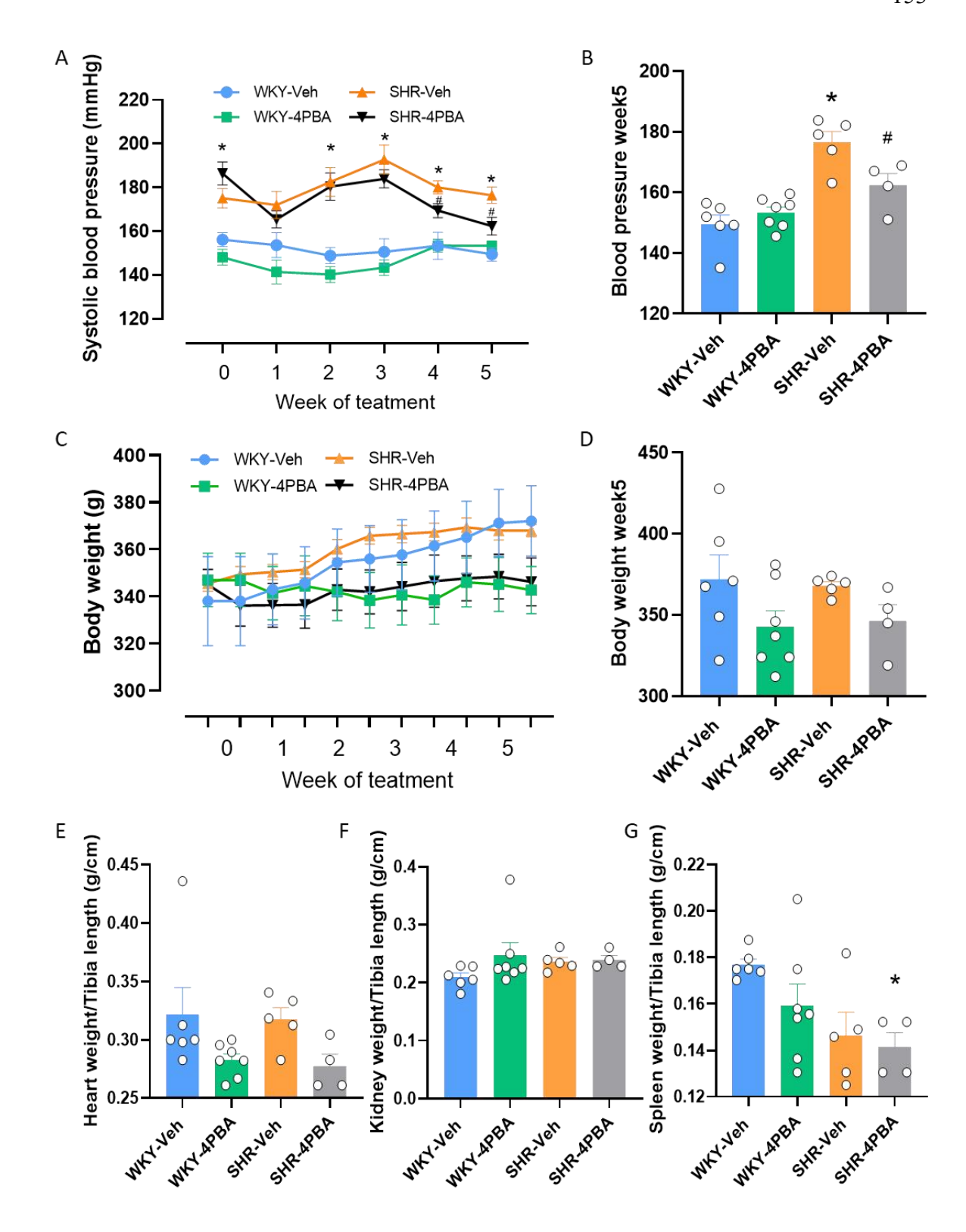


Figure 6.1 Effect of ER stress inhibition on general parameters and blood pressure of WKY and SHRSP rats.

21-week-old rats were randomly assigned to either the vehicle group (normal drinking water) or the 4PBA group (1 g/kg/day 4PBA in drinking water) for a duration of 5 weeks. Four groups are WKY-Veh (blue, n=6), WKY-4PBA (green, n=7), SHR-Veh (orange, n=5), and SHR-4PBA (grey, n=4). WKY Blood pressures were measured via tail cuff plethysmography before the treatment and at the end of each week (A and B). Body weight was assessed every half week (C). Body weight (D), heart weight (E), kidney weight (F)and spleen weight(G) were assessed at the end of treatment. Data are presented as mean ± S.E.M. Statistical significances were determined by one-way

ANOVA followed by a Tukey test or student t-test, \*p<0.05 compared to WKY-Veh, #p<0.05 compared to SHR-Veh.

#### 6.3.2 Effect of 4PBA treatment on blood vessel function

To investigate whether ER stress inhibition influences vascular reactivity, small mesenteric resistance arteries were isolated from WKY and SHR rats for wire myography. Cumulative concentration-response curves (CCRC) to the U46619 (contraction), ET-1 (contraction), acetylcholine (Ach) (endothelial - dependent relaxation), and sodium nitroprusside (SNP) (endothelial - independent relaxation) were performed in all groups to assess vascular function. Vascular contraction induced by U46619 and ET-1 was high in SHR rats compared to WKY rats. However, 4PBA treatment did not affect contractile responses in both WKY and SHR rats in the results (Figure 6.2 A and B). Ach-induced vasorelaxation was not changed in SHR-Veh rats compared to WKY-Veh rats (Figure 6.2 C). Compared with SHR-Veh rats, EC50 in 4PBA-treated SHR was significantly decreased (Figure 6.2C). Vessels from SHR rats were more sensitive to SNP-induced relaxation compared to WKY rats (Figure 6.2 D).

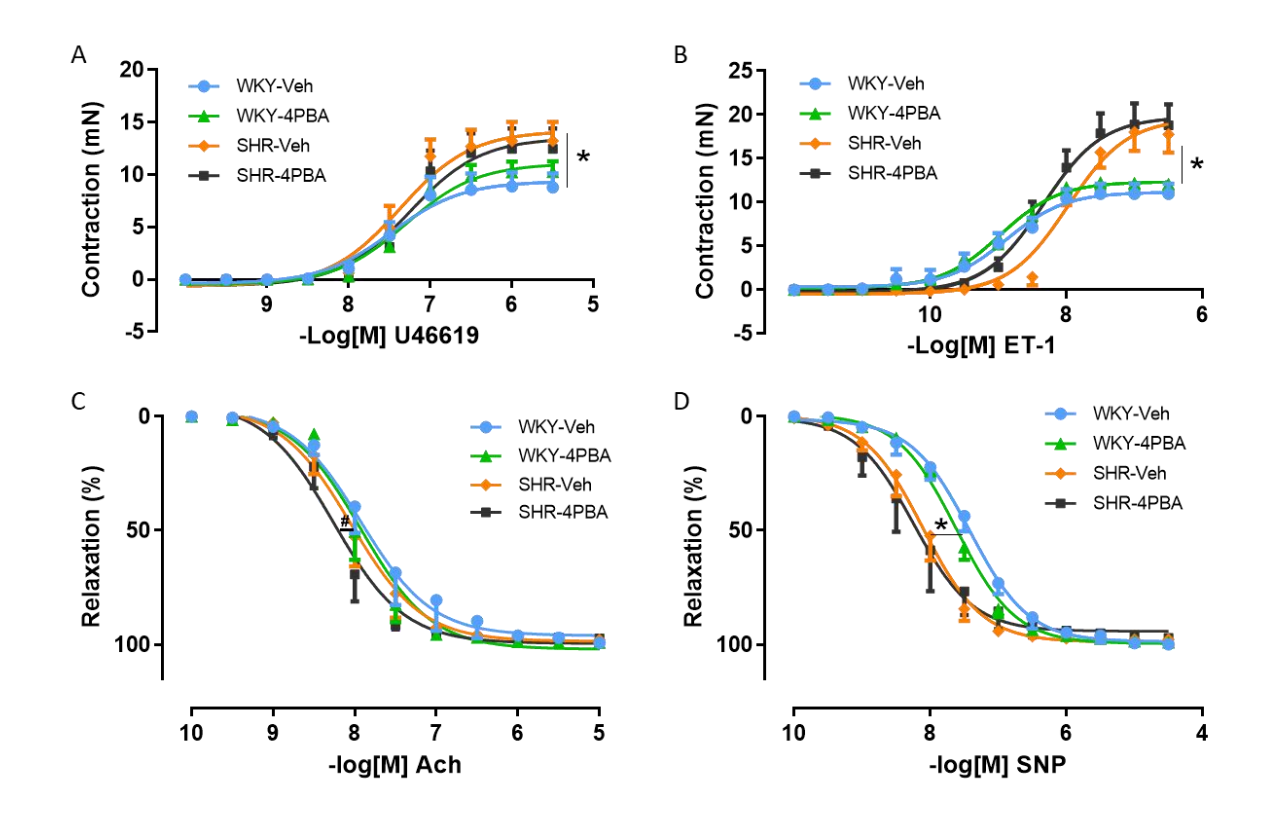
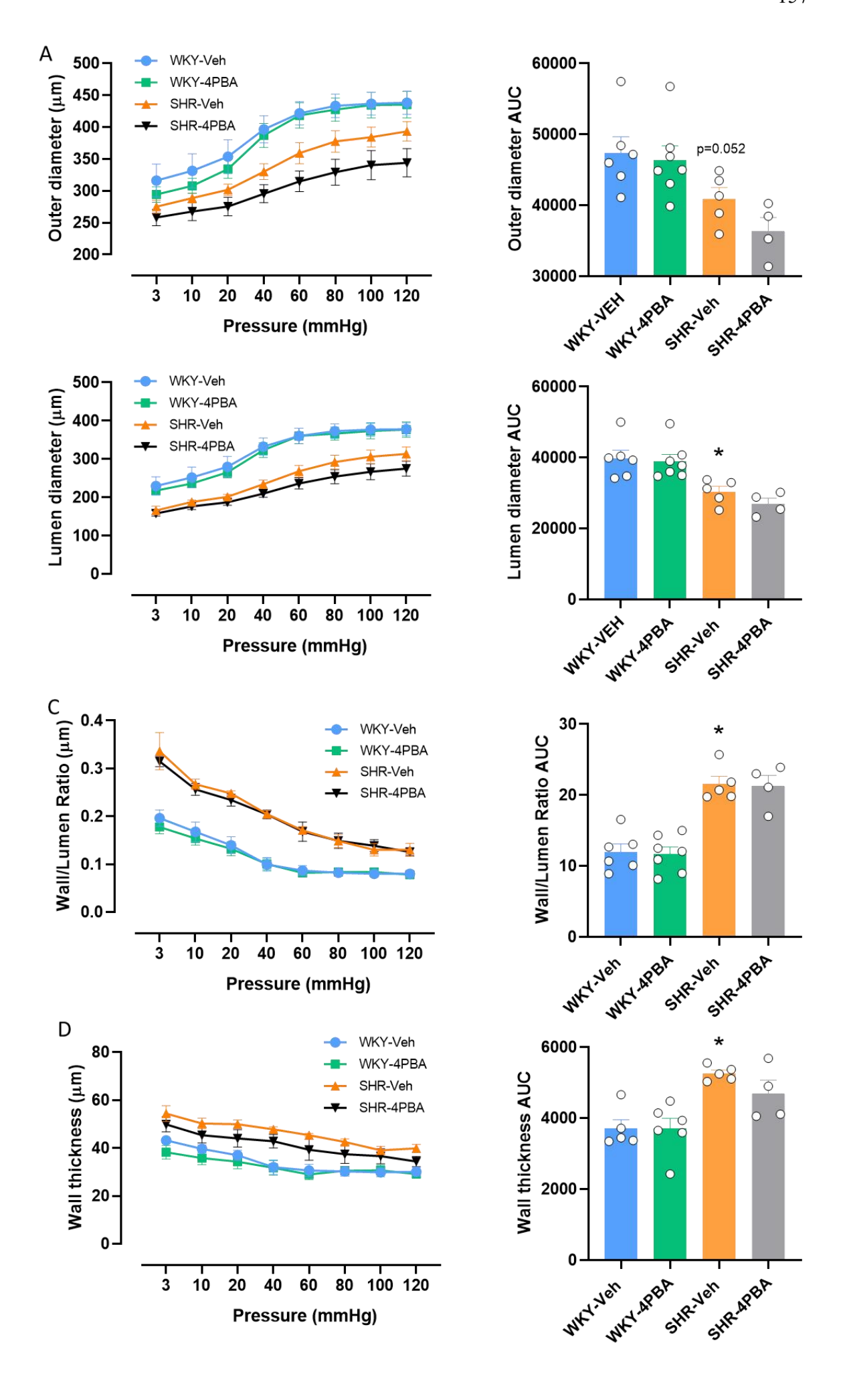


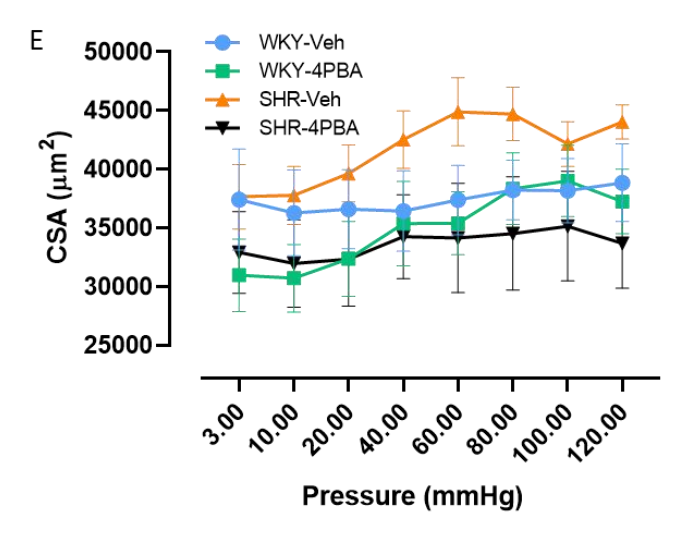
Figure 6.2 Effect of ER stress inhibition on vascular function of WKY and SHRSP rats.

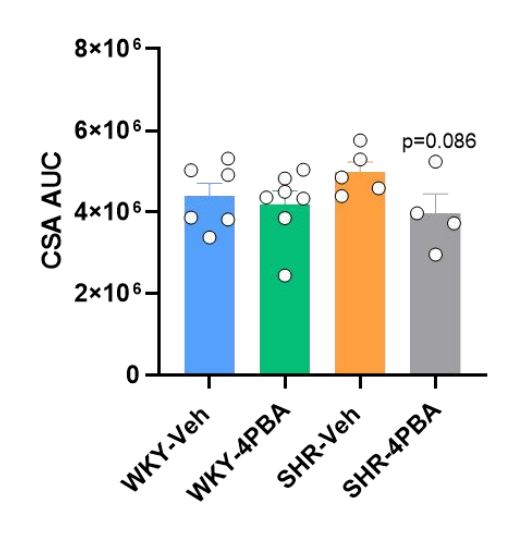
The mesenteric arteries were obtained from rats of four groups: WKY-Veh (blue, n=6), WKY-4PBA (green, n=7), SHR-Veh (orange, n=5), and SHR-4PBA (grey, n=4). Vascular reactivity was assessed by wire myography. Cumulative concentration-response curve (CCRC) was performed in response to the vasoconstrictor U46619 (U4) (A) and ET-1(B) results were expressed as mN. The relaxation of CCRC in response to the vasodilators acetylcholine (ACh) (C) and sodium nitroprusside (SNP) (D) in the vessels as a percentage of constriction to pre-treated 10-7M U4. Differences in half maximal effective concentrations (EC50) and maximal contraction (Emax) across groups are shown by \*p<0.05 compared to WKY-Veh, #p<0.05 compared to SHR-Veh. Data are resented as mean ± S.E.M.

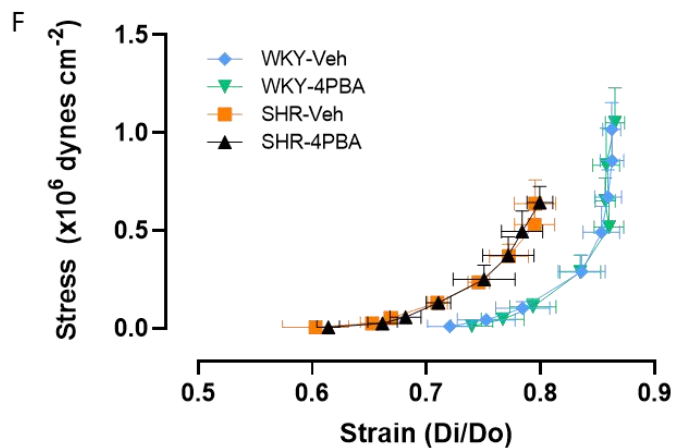
### 6.3.3 Effect of 4PBA treatment on blood vessel structure

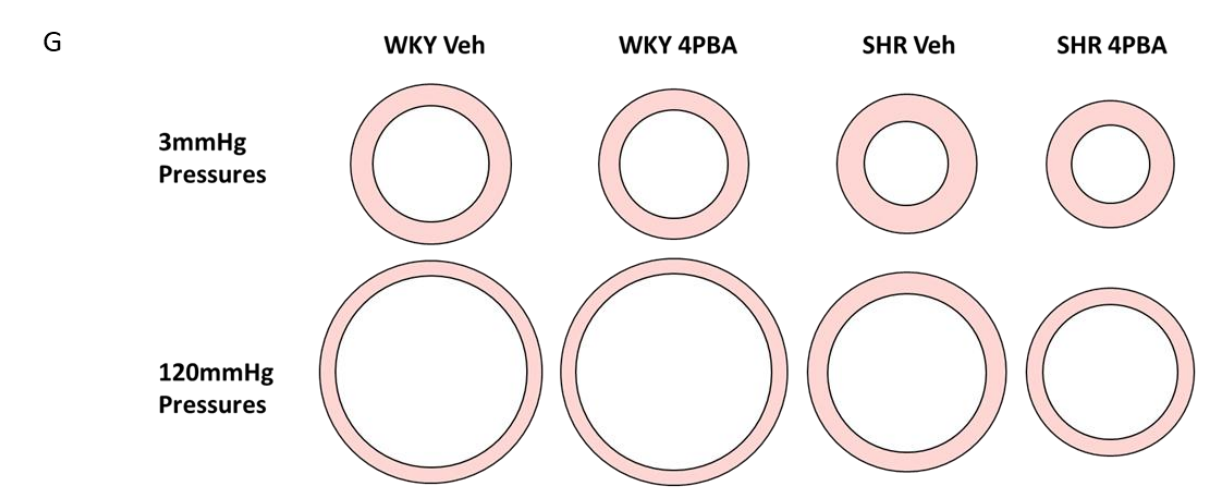
To investigate whether ER stress inhibition influences vascular structure, small mesenteric resistance arteries were isolated from WKY and SHR rats for pressure myography. Vessels from SHR rats have a lower outer diameter (not significant with p=0.052, Figure 6.3A) and lumen diameter (Figure 6.3B) compared with WKY rats. 4PBA treatment did not significantly change either outer or lumen diameter in WKY and SHR (Figure 6.3A and B). The outer diameter shown a slight decreased trend in SHR-4PBA compared with SHR-Veh (Figure 6.3B). In terms of wall-to-lumen ratio and wall thickness, vessels from SHR exhibited higher values compared to WKY, while 4PBA had no significant effect on vessels from either WKY or SHR (Figure 6.3C and D). However, there was a tendency towards decreased wall thickness with 4PBA treatment in SHR, although this reduction was not statistically significant (Figure 6.3D). There was a trend of higher cross-sectional area (CSA) in SHR-Veh compared to WKY-Veh, but no significant differences were observed. 4PBA treatment had no effect on WKY rats. However, CSA appeared lower in SHR-4PBA compared to SHR-Veh with p=0.086 (Figure 6.3E). Vascular stiffness and distensibility were assessed by stress/strain relationships. SHR showed increased stiffness (decreased distensibility) compared to WKY, but 4PBA has no effect on either WKY or SHR vessels (Figure 6.3F).











	WKY 4PBA vs. WKY Veh	SHR Veh vs. WKY Veh	SHR 4PBA vs. SHR Veh
Outer diameter		1	1
Lumen diameter		1	
Wall to lumen Ratio	<del></del> -	1	-
Wall thickness		1	1
Cross-sectional area	<u>—</u>	Û	1

# Figure 6.3 Effect of ER stress inhibition on vascular structure of WKY and SHRSP rats.

Mesenteric arteries were obtained from rats of four groups: WKY-Veh (blue, n=6), WKY-4PBA (green, n=7), SHR-Veh (orange, n=5), and SHR-4PBA (grey, n=4). Vascular outer diameter (A), lumen diameter (B), wall to lumen ratio (C), wall thickness (D), cross - sectional area (CSA) (E) and stress/strain relationship (F) assessed by pressure myography in mesenteric arteries. A summary of pressure myography results (light blue and light red arrows means there is a trend but not significant) and possible structural shape of the blood vessels under 3mmHg and 120mmHg pressure (drawing according to proportional mean values of outer and lumen diameter) were shown on figure G. AUC stands for 'Area Under Curve'. Data are presented as mean ± S.E.M. Statistical significances were determined by one-way ANOVA followed by a Tukey test, \*p<0.05 compared to WKY-Veh.

### 6.4 Discussion

In the previous chapters we have demonstrated that ER stress contributes to hypercontractility and related intracellular signalling pathways in the vasculature during hypertension. To further confirm whether ER stress contributes to vascular function and structure, thereby influencing blood pressure, an in vivo study was conducted using the ER stress inhibitor 4PBA on SHR rats. Our results showed that i) 4PBA lowers BP in established hypertension of SHR from 4 weeks of treatment; ii) 4PBA improved endothelium-dependent relaxation of resistance arteries in SHR; iii) 4PBA exhibited a tendency to improve the resistance artery structure of SHR. These findings suggest that ER stress contributes to functional and structural changes in resistance arteries that underlies the development and progression of hypertension in vivo.

The SHR is a typical animal model of human essential hypertension that involves elevated total peripheral resistance (Dornas and Silva, 2011) with structural and functional alternations in blood vessels of both kidney and mesentery (Dickhout and Lee, 1997, BennettHillier and Thurston, 1996). Changes of vasculature in SHR occurred at 3 and 4 weeks of age, a time when their systolic blood pressure was similar to that of WKY rats (Dickhout and Lee, 2000, Dickhout and Lee, 1997). These early vascular modifications are posited to play a pivotal role in the development of high blood pressure. Interestingly, research has shown that at the age of 5 weeks old SHR, before an increase in blood pressure, the expression of ER stress markers such as GRP78, CHOP, and phospho-IRE1 began to rise in mesenteric arteries compared to WKY (Naiel et al., 2019). It is possible that ER stress contributes to vascular alterations in SHR at the development of hypertension. It is notable that blood vessels in SHR shown hypertrophy of the medial layer (Intengan et al., 1999a, LeeDickhout and Sandow, 2017, Dickhout and Lee, 1997),

which involves an increased rate of protein synthesis (Dickhout and Lee, 2000). The increased load of protein synthesis due to vascular hypertrophy may cause protein translation requirements to exceed the protein folding capacity, thus leading to an accumulation of unfolded proteins in the ER and ER stress.

Several studies have demonstrated that ER stress is related to changes in blood pressure. ER stress inducers, such as tunicamycin, can trigger high blood pressure. Injection of tunicamycin increases blood pressure in mice (Choy et al., 2017, Liang et al., 2013) and in Sprague-Dawley rats (Spitler and Webb, 2014), effects that were improved by treatment with ER stress inhibitor 4-PBA or TUDCA. Besides, ER stress inhibitors have been shown to protect against high blood pressure in various hypertensive models. For instance, 4-PBA reduced blood pressure in Ang II-induced hypertensive mice (Kassan et al., 2012), SHR (Carlisle et al., 2016, Naiel et al., 2019, SpitlerMatsumoto and Webb, 2013), and Dahl saltsensitive hypertensive rats (Yum et al., 2017), while TUDCA had similar effects in Ang II-induced hypertensive mice (Kassan et al., 2012), and SHR (SpitlerMatsumoto and Webb, 2013). Our study showed similar results that 4PBA significantly reduced systolic blood pressure after four weeks of treatment. Unlike other studies, we used rats that were 21 weeks old, indicating that inhibiting ER stress may improve hypertension not just in its early stages but also in more developed stages.

The potential reason for the reduced blood pressure with 4-PBA could be its effect on blood vessel function. Research has shown that long-term treatment with 4-PBA in SHRs leads to an increase in endothelial-dependent vascular dilation and a decrease in adrenergic-mediated vascular constriction in mesenteric arteries on both 5-week old (Naiel et al., 2019) and 12-week-old (Carlisle et al., 2016) rats (treatment started age). In our study with 21-week-old rats, we found similar results that 4-PBA improved endothelialdependent vasodilation in SHR. As for vasoconstriction, we induced contraction using U4 and ET-1, and no significant effect was observed in the SHRs treated with 4-PBA. Our findings indicate that 4-PBA could reverse vascular dysfunction in a hypertensive model by improving the vasodilatory response. Together with other studies, it is likely that ER stress is involved in nitric oxide-mediated vasodilation in hypertensive vessels. Disulfide bond formation is an important step in protein folding and is highly sensitive to changes in redox balance. In a stressed ER, ER stress-associated degradation disposes of misfolded proteins via disulfide bond formation. This process may result in increased ROS generation, such as superoxide (Cao and Kaufman, 2014, Bhattarai et al., 2021). Superoxide anions could rapidly react with nitric oxide to form peroxynitrite and reduce nitric oxide

bioavilability (Guzik et al., 2002). In addition, research has found that mice treated with tunicamycin exhibit impaired endothelium-dependent relaxations with increased ROS levels and reduced nitric oxide bioavailability, which could be reversed by ER stress inhibitor TUDCA (Choy et al., 2017). These studies suggest that ER stress may deplete nitric oxide bioavailability in blood vessels, resulting in impaired nitric oxide-mediated vasodilation, thereby contributing to elevated total peripheral resistance and high blood pressure (Carlisle et al., 2016).

This research observed a trend towards reduced vascular structural changes in SHRs treated with 4-PBA, although these changes were not statistically significant. This could be attributed to the limited sample size or the possibility that such structural changes in the blood vessels may not be directly linked to ER stress in our animal model. Previous studies have observed smooth muscle hypertrophy in young SHRs, potentially associated with ER stress. For instance, 4-PBA treatment has been reported to decrease the media-to-lumen ratio in SHR mesenteric arteries (Naiel et al., 2019). However, our findings did not show a significant difference in this aspect, suggesting the need for further investigation into the underlying mechanisms. Additionally, it's essential to consider that the observed blood pressure reduction with 4-PBA might be attributed to other underlying mechanisms of hypertension or potential off-target effects of the 4-PBA treatment. For example, a study found that 4-PBA reversed the imbalance of renal RAS components in SHRs by reducing ACE and AT1R protein expression and increasing AT2R, ACE2, and MasR expression (Zhu et al., 2023). This suggests that 4-PBA may lower blood pressure by restoring impaired diuresis and natriuresis.

In this study, no change was observed in 4-PBA-treated WKY rats compared to non-treated WKY rats. However, the baseline blood pressure in our WKY rats was higher than that observed in typical WKY rats. Moreover, our WKY rats did not show significant changes in vessel structure or endothelin-dependent vasodilation compared with SHRs, diverging from the results of most other studies. One potential explanation for these differences is the origin of our WKY rats. The WKY colony we have been using, bred in Glasgow since 1990, initially exhibited normal characteristics. However, over time, these rats seem to have developed gradually increasing blood pressure and higher stress levels. This trend is likely due to financial restrictions during the breeding process, resulting in a limited stock of animals from which to choose when identifying new breeders. The choice of WKY rats represents a notable limitation of this study.

Targeting ER stress could be a promising approach to treating hypertension. Rats treated with 4-PBA seem to have no effect on body and tissue weight. Additionally, Naiel et al. have shown that after 1 week of withdrawing 4-PBA treatment in SHR, blood pressure returned to levels similar to those in untreated SHR (Naiel et al., 2019). This suggests that the benefits of ER stress inhibition may not be long-lasting, but the absence of a rebound hypertension crisis after withdrawal indicates the treatment's safety. Clinical hypertension medications, including telmisartan, olmesartan, candesartan, and irbesartan, which are selective AT1 receptor blockers, have been linked to reductions in ER stress. Telmisartan reduced ER stress, thus blunting cardiac hypertrophy (Guan et al., 2011), and decreasing Chop and BiP expression in myocardial of heart failure rats (Sukumaran et al., 2011a). Olmesartan decreased ER stress in rats with heart failure and decreased the expression of BiP in the myocardium (Sukumaran et al., 2011b), and reducing ER stress in kidney of diabetic mice (Lakshmanan et al., 2011). Candesartan (Chiang et al., 2011) and irbesartan (Hartner et al., 2014) inhibited ER stress in rat kidney. In addition, ACE inhibitor perindopril attenuated the ER stress markers expression in renal of diabetic rat (Sun et al., 2009). These studies suggest that clinical hypertension therapies may partially lower blood pressure by inhibiting ER stress, further supporting the potential of ER stress inhibitors in hypertension treatment.

In conclusion, these results provide additional evidence that inhibiting ER stress may reverse high blood pressure and may also contribute to improving functional changes in resistance arteries. This indicates that targeting ER stress could be a potential strategy for the treatment of hypertension.

# **Chapter 7** Final discussion

# 7.1 ER stress in different tissues and different hypertension models

Protein synthesis is essential for cell survival, with the accurate folding of these proteins being a critical aspect of the process. In eukaryotic cells, the ER functions to facilitate the folding and maturation of most secreted and transmembrane proteins, as well as protein quality control (Oakes and Papa, 2015). Cellular stress caused by physiological or pathological factors such as hypertension can result in improperly folded proteins, which triggers UPR (MarciniakChambers and Ron, 2022). UPR is a sophisticated surveillance mechanism that regulates the balance between the protein folding capacity and the load of unfolded proteins that enter the ER (Ron and Walter, 2007a). When protein accumulation is detected, activated UPR increases protein degradation, decreases protein synthesis, and enhances protein folding capacity (Spencer and Finnie, 2020). If the stress cannot be resolved, prolonged ER stress may trigger pro-inflammatory and pro-apoptotic signals (Spencer and Finnie, 2020).

### 7.1.1 ER stress in hypertensive tissues

ER stress is implicated in hypertension across several organs, including the brain, kidneys, heart, aorta, and mesenteric arteries. The central nervous system plays a vital role in regulating short-term and long-term blood pressure. ER stress activation has been found in the subfornical organ of Ang II-induced hypertension, and inhibition of brain ER stress reduces blood pressure (Young, 2017, Young et al., 2012). The kidney is responsible for the reabsorption and excretion of salt and water, which in turn affects blood pressure. In all types of chronic hypertension, there is a presence of abnormal renal-pressure natriuresis (Hall et al., 2012). In the kidney, we did not detect ER stress activation in SHRSP; however, increased levels of PDI were observed in LinA3 mice. Other studies have indicated 4PBA treatment improved renal function by preventing the elevations in urinary albumin excretion and renal fibrosis in hypertensive chronic kidney disease mice (Mohammed-Ali et al., 2017), and improved impaired diuresis and natriuresis in SHR (Zhu et al., 2023).

The heart, a major organ affected by high blood pressure, has various interconnected pathophysiological processes associated with hypertension (Nadar and Lip, 2021). Our results suggested the activation of ER stress in SHRSP heart. Similarly, it has been

indicated that BiP and p-PERK expression increased in heart of DOCA-salt rats, and ER stress inhibitor TUDCA attuned the cardiac inflammation and fibrosis in hypertension (Bal et al., 2019b).

The aorta is a crucial regulator of the entire cardiovascular system and undergoes functional and structural changes during hypertension (Laurent and Boutouyrie, 2015, Lindesay et al., 2018, Stefanadis et al., 1997). Although we did not find increased ER stress markers in the aorta from SHRSP, they were elevated in other hypertension models. For example, ER stress markers BiP, chop, and PDI expression increased in the aorta from SHR (SpitlerMatsumoto and Webb, 2013), and expression of BiP and p-PERK increased in the aorta from DOCA-salt rats (Han et al., 2019a).

In the present study, we investigated resistance mesenteric arteries, as resistance arteries are important to maintain vascular tone. We did not find changes in ER stress markers expression in the entire mesenteric arteries from SHRSP, but we found ER stress to be activated in VSMCs of mesenteric arteries from SHRSP and LinA3 mice. Additionally, ER stress inhibitor 4PBA improved vasodilation of mesenteric arteries in SHR, with similar findings reported in other studies (Naiel et al., 2019, Carlisle et al., 2016). Our results, along with other studies, suggest that ER stress involved in the development of hypertension in various tissues.

# 7.1.2 ER stress in VSMCs of hypertension

In this research, we mainly focused on the VSMCs of resistance arteries. Blood pressure is affected by a balance of the cardiac output and systemic vascular resistance, where most patients with hypertension have normal cardiac output and increased peripheral resistance. According to Poiseuille's Law, the diameter of a blood vessel is the main factor that affects vascular resistance. VSMCs, as the largest component of wall of the resistance arteries, contribute to changes in vessel diameter by vasomotor control mechanisms (Touyz et al., 2018, Brown et al., 2018, Intengan and Schiffrin, 2000). In hypertension, increased vessel contractility, and arterial remodelling are typically observed (Oparil et al., 2018a, Russo et al., 1999). VSMCs critically influence these processes due to their highly plastic and dynamic feature, as well as their ability to undergo phenotypic switch (Touyz et al., 2018). Different changes of cellular signalling transduction could affect VSMCs function during hypertension, where ER stress may be involved. Evidence suggested ER stress could contribute to human VSMC-mediated calcification (Furmanik et al., 2021), and VSMC

phenotypic modulation (Chattopadhyay et al., 2021, Uchida et al., 2022b). A previous study from our group has suggested increasing ER stress activation in VSMCs from SHR (Camargo et al., 2018).

In the present study, increased activity of the PERK pathway was found in VSMCs of hypertensive subjects, SHRSP rats and chronic Ang II mice model compared to their normotensive counterparts. Additionally, increased activation of IRE1 pathway was observed in SHRSP compared to WKY. In the initial phase of ER stress activation, three parallel branches of the UPR work together to enhance the degradation of misfolded proteins and reduce the synthesis of new proteins, thereby playing a role in cell protection (Lin et al., 2007, Shanahan and Furmanik, 2017). Under prolonged ER stress, distinct UPR signalling pathways exhibited different downstream modules and varied activation duration. A study investigating UPR activation duration found that the IRE1 pathway response was attenuated within 8 hours, the ATF6 pathway response diminished more gradually, whereas the PERK pathway response remained active, evident for at least 30 hours post-stress initiation (Lin et al., 2007). This evidence of prolonged PERK pathway activation potentially explaining why the PERK pathway was more readily detectable compared to the IRE1 and ATF6 pathways in our hypertension models. The prolonged activation of ER stress could be caused by pathological stretch during hypertension, leading to VSMC phenotypic changes (Wan et al., 2015).

The alterations in ER stress observed in these hypertension models highlight its potential significance in the pathophysiology of hypertension. Our study further investigated the cellular mechanisms either effecting or regulated by ER stress that contribute to the development and progression of hypertension.

# 7.2 Regulators of ER Stress in Hypertension

# 7.2.1 Oxidative stress regulating ER stress

One of the important regulators of ER stress suggested in hypertension is oxidative stress. Oxidative stress, characterized by increasing ROS bioavailability and altered redox states, is a key factor in hypertension(Harrison, 2013). Excessive ROS production induces protein oxidation and disrupts cell signalling, contributing to proliferation, inflammation, and apoptosis (Touyz et al., 2020). Protein oxidation, which includes sulfenylation, glutathionylation, and disulphide bond formation, among other processes, may impair

protein function and trigger ER stress (ref). These alterations lead to cell and organ damage in hypertension, including vascular dysfunction (Touyz et al., 2020).

The main source of ROS in the vasculature is NADPH oxidase (Nox) (Harrison, 2013, Griendling et al., 2000). Ang II, a vasoactive factor typically elevated in hypertension, increases ROS bioavailability by enhancing the activation of Nox (specifically Nox1, Nox2, and Nox4 in rodents; Nox1, Nox2, Nox4, and Nox5 in humans) through vascular G protein-coupled receptors (Landmesser et al., 2002, RodrigoGonzalez and Paoletto, 2011, TouyzTabet and Schiffrin, 2003, Touyz et al., 2020). In a chronic Ang II dependent hypertension mice model (LinA3), we observed increased ROS and protein oxidation in VSMCs. Similarly, hypertensive human VSMCs showed increased ROS generation, possibly due to elevated Nox1 and Nox2 expression. Other studies also support the rise in Nox levels in both hypertensive model and individuals (Landmesser et al., 2002, RodrigoGonzalez and Paoletto, 2011, TouyzTabet and Schiffrin, 2003, Nosalski et al., 2020, Camargo et al., 2018, Camargo et al., 2022). While Nox levels remained unchanged in LinA3 mice, a decrease in antioxidant expression (Nrf2, DJ-1, and Gpx1) was noted, potentially contributing to oxidative stress. These alterations in the redox environment could be crucial in regulating ER stress.

ER stress has been implicated in association with oxidative stress across multiple contexts (Camargo et al., 2023b, Eletto et al., 2014, Ong and Logue, 2023). The formation of disulfide bridges during protein folding in the ER requires a healthy redox environment, which is crucial for maintaining ER homeostasis (Eletto et al., 2014, Ong and Logue, 2023). Besides, ER molecular chaperones contain conserved cysteine and thiol residues that are susceptible to redox regulation. This can lead to disruptions in protein folding and imbalances in ER calcium levels (Eletto et al., 2014). For example, evidence suggested irreversible oxidation of Cys674 in SERCA2 promotes the development of hypertension by inducing ER stress in the kidneys of mice (Liu et al., 2020). In contrast, protein oxidation may regulate ER stress. Sulfenylation of IRE1 inhibit UPR by blocked XBP1s expression and induce p38/Nrf2 antioxidant response (Hourihan et al., 2016). Besides, sulfenylation and glutathionylation of ER chaperone Bip enhance the Bip activity thus prevents protein aggregation and supports cell survival (Camargo et al., 2023a, Wang et al., 2014).

Our study revealed that Nox4 may play a crucial role in the regulation of the redox environment in the ER during hypertension. We found an increase in the expression of ER stress markers Bip and Chop in the kidneys of Nox4 deficient mice in basal conditions.

However, in the LinA3 hypertensive model, Nox4 deficiency reduced the expression of the ER stress marker PDI, suggesting the presence of different mechanisms under pathological conditions. It has been shown that Nox4 colocalizes with PDI in the ER where they engage in crosstalk under Ang II-stimulated conditions, as evidenced by PDI overexpression increasing Nox4 levels and its deletion reducing Nox4 levels (Fernandes et al., 2009, Janiszewski et al., 2005). However, the role of Nox4 in cardiovascular disease remains controversial. Previous study has suggested that activation of IRE1 pathway by Nox4 derived ROS contributes to vascular hyperproliferation in VSMCs of SHRSP (Camargo et al., 2018). Whereas some studies have supported a protective role of Nox4 in the kidneys and in the vasculature where alterations in ER stress may play a role (Babelova et al., 2012, Lacchini et al., 2017, Nlandu Khodo et al., 2012, Alves-Lopes et al., 2023). These findings collectively suggest that oxidative stress regulates ER stress in a unique manner in hypertension, potentially contributing to development of hypertension, however the exact mechanisms involved warrant further investigation.

### 7.2.2 Induction of ER stress by vasoactive peptides

The vasoactive factors ET-1 and Ang II are important in the pathophysiology of hypertension due to their vasoconstrictor, mitogenic, and proinflammatory functions (Touyz et al., 2020, Touyz et al., 2018, Rautureau and Schiffrin, 2012). Activation of ET-1 and Ang II result in ROS production and calcium channels activation, which if uncontrolled leads to vascular damage <sup>19,32</sup>. Ang II and ET-1 have both been shown to trigger the activation of ER stress. Research indicates that Ang II induces ER stress in the brain (Young et al., 2012), and kidney (Zhu et al., 2023) in models of hypertension. Studies have also shown that Ang II enhances protein aggregation and the UPR in VSMCs, contributing to their pro-inflammatory phenotype, which could be mitigated by overexpressing Bip (Cicalese et al., 2020). Similarly, we found higher activation of PERK in VSMCs and increased expression of PDI in the kidneys in Ang II-dependent hypertension model (LinA3 mice), suggesting the role of Ang II in ER stress activation.

ET-1 was observed to induce ER stress in pulmonary artery smooth muscle (Yeager et al., 2012), renal tissues (De Miguel et al., 2017), and placental tissues during pre-eclampsia (Jain et al., 2012). In this study, we found that ET-1 activated ER stress in cells from both normotensive and hypertensive rats, but via different mechanisms. After 24 hours of ET-1 treatment, cells from hypertensive rats showed an increase in the protein expression of the PERK pathway and ERO1, with the ER stress activation dependent on both ETAR and

ETBR receptors. Cells from normotensive rats exhibited a rise in ATF4 (part of the PERK pathway), XBP1s (part of the IRE1 pathway), and Bip, with the ER stress activation dependent on ETBR. These findings suggest that ET-1 may act upstream of ER stress in hypertension. Additionally, other mechanisms in pathological conditions may contribute to the dysfunction of ET-1 receptors and the activation of ER stress. These findings highlight the potential role of vasoactive peptides in regulating ER stress during hypertension.

#### 7.2.3 MiRNAs and ER stress

Another regulator of ER stress in the development of hypertension is non-coding RNAs (ncRNAs). The ncRNAs are pivotal in the regulation of gene transcription and protein translation, including the aberrant expression of genes and proteins related to ER stress (McMahonSamali and Chevet, 2017, Lin et al., 2023) and development of hypertension (Jusic and Devaux, 2019). It has been found miR-1283 regulates ATF4 thus affect endothelial function in hypertension model (Chen et al., 2021). In this study, we have suggested there are differential expressed (DE) miRNAs in VSMCs of hypertensive human. Some of these DE miRNAs have been highlighted with potential regulating ER stress or related process such as oxidative stress and calcium channel dysfunction during hypertension.

# 7.3 Effects of ER Stress in Hypertension

# 7.3.1 ER stress in blood pressure regulation

ER stress has been implicated in regulation of blood pressure in different animal models. In our study, inhibition of ER stress by 4PBA reduced systolic blood pressures and improved vascular function and structure in later age of SHR. Similarly, in earlier age, 4PBA improved blood pressure and reduced vascular damage were observed in Ang II induced hypertensive mice (Kassan et al., 2012), SHR (Carlisle et al., 2016, Naiel et al., 2019, SpitlerMatsumoto and Webb, 2013), and Dahl salt-sensitive hypertensive rats (Yum et al., 2017). Besides, another ER stress inhibitor TUDCA also reduced the blood pressure in Ang II induced hypertensive mice (Kassan et al., 2012), and SHR (SpitlerMatsumoto and Webb, 2013). Conversely, the activation of ER stress by tunicamycin led to an increase in blood pressure in mice (Choy et al., 2017, Liang et al., 2013) and in Sprague-Dawley rats (Spitler and Webb, 2014). These findings indicate the potential of targeting ER stress in hypertension treatment and underscore the significance of investigating the mechanisms altered by ER stress in hypertension.

### 7.3.2 ER stress regulating oxidative stress

Our research highlighted the link between oxidative stress and ER stress in hypertension. In hypertension models, oxidative stress was found to be upstream, downstream, or both in relation to ER stress (Camargo et al., 2023b, Eletto et al., 2014, Ong and Logue, 2023). Studies have shown that ER stress can lead to oxidative stress, as evidenced by thapsigargin and tunicamycin, which are widely used as ER stress inducers and have been demonstrated to increase ROS levels (Wang et al., 2016, Yen et al., 2017b). We induced ER stress in human VSMCs using tunicamycin and observed an increase in Nox5 expression. However, in tunicamycin only increased significantly ROS levels in hypertensive subjects. Our findings suggest that ER stress could induce Nox expression in cells but only enhances oxidative stress in hypertensive conditions.

Some studies have proposed mechanisms by which ER stress may regulate oxidative stress. The PERK pathway has been found to both promote and mitigate oxidative stress. Study found CHOP, as downstream of PERK/ATF4 pathway, promotes oxidizing conditions in ER by activating ERO1 (Marciniak et al., 2004). The enzyme ERO1 contributes to oxidative stress by reduction the O<sub>2</sub><sup>-</sup> to H<sub>2</sub>O<sub>2</sub> during the re-oxidation of PDI in the process of disulfide bond formation (Sevier and Kaiser, 2008). Additionally, the ER interacts with mitochondria to form specific zones termed mitochondria-associated ER membranes (MAMs). MAMs play pivotal roles in various cellular functions, including facilitating the uptake of Ca<sup>2+</sup> from the ER to the mitochondria, contributing to mitochondrial ROS generation, and induce cell apoptosis (GaoYan and Zhu, 2020). The ER stress sensor PERK has been found to be enriched at the MAMs and plays a structural function (Verfaillie et al., 2012). This can promote ROS-mediated mitochondrial apoptosis following ROS-based ER stress (Verfaillie et al., 2012).

On the other hand, study suggests that ER stress inducers promote the interaction of ERO1 and PERK at the MAMs to support Ca<sup>2+</sup> influx and limiting oxidative stress (Bassot et al., 2023). Additionally, the well-documented PERK/Nrf2 signalling pathway also contributes to the reduction of oxidative stress in cells (Cullinan et al., 2003). Nrf2 activation occurs through its binding to the antioxidant response element (ARE) in the nucleus, leading to the expression of antioxidant genes and thus enabling cellular adaption to oxidative stress (TonelliChio and Tuveson, 2018). Activation of PERK could mediate Nrf2 phosphorylation on Thr-80, which reduces the formation of the Nrf2-Keap1 complex, thereby enhancing the expression of antioxidant genes such as HO-1, SOD, and GPx1

(Cullinan et al., 2003). It has also been found that during ER stress, ATF4 could bind to the promoter of the Nrf2 gene, thereby supporting the expression of Nrf2 and enhancing the antioxidant protective response (Sarcinelli et al., 2020). In hypertension, this protective role of Nrf2 could mitigate oxidative stress and associated vascular dysfunction (Lopes et al., 2015).

The IRE1 signalling pathway has been observed to enhance the expression of TXNIP thus promotes inflammation and cell death (Lerner et al., 2012). TXNIP is known to inhibit the antioxidant enzyme thioredoxin (TRX), thereby facilitating the production of ROS (Choi and Park, 2023). It's been found TXNIP deficiency is associated with decreased ROS generation, whereas its overexpression results in elevated ROS levels (Nishiyama et al., 1999, Ong and Logue, 2023). These observations suggest that IRE1 activation may play a role in mediating oxidative stress through the modulation of TXNIP expression.

Our results together with these findings suggest the complex role of ER stress in maintaining healthy redox environment, which is essential for the normal functioning of cells. Importantly, this evidence indicates that in hypertension, dysregulated ER stress could exacerbate oxidative stress. Consequently, it can be inferred that in hypertension, dysregulated ER stress may amplify oxidative stress, thereby contributing to the pathogenesis of the condition through mechanisms including endothelial dysfunction, inflammation, and dysregulation of Ca<sup>2+</sup> signalling pathways (Camargo et al., 2023a).

# 7.3.3 ER stress inducing vascular hypercontractility

Hypertension involves a fundamental aspect of elevated vascular tone, primarily mediated by an influx of Ca<sup>2+</sup>. Intracellular calcium overload in VSMCs leads to vascular hypercontractility, which could be influenced by dysfunction in calcium channels (Fleckenstein-Grün et al., 1992, Hermsmeyer, 1993). Calcium channel blockers are well-established in hypertension treatment by improving endothelial function (Taddei et al., 1997, Taddei et al., 2002). For example, calcium channel blockers nifedipine and lacidipine reduce blood pressure with decreased oxidative stress marker and increased NO bioavailability in patients with hypertension (CameronLang and Touyz, 2016, Taddei et al., 2002). As a major intracellular calcium storage, the ER is crucial in calcium handling and contributes to calcium dysfunction in hypertension. Calcium dysfunction has been suggested associated with ER stress (Bal et al., 2019a) as ER-resident chaperones like calreticulin and Bip require high Ca<sup>2+</sup> concentrations for their activity (Luciani et al., 2009,

Kiviluoto et al., 2013). Additionally, Ca<sup>2+</sup> store depletion in ER could leads to ER stress, such as the activation of IP3R or the inhibition of SERCA triggers ER stress (Coe and Michalak, 2009, Corbett and Michalak, 2000). We did not conduct an experiment to investigate whether calcium channel dysfunction leads to ER stress in hypertension. However, it has been found that blocking SERCA triggers ER stress and increases blood pressure (Bal et al., 2019a).

In this study, we suggested ER stress could induce calcium channel dysfunction in hypertension. Our study observed an increase in SERCA expression and a decrease in IP3R expression in hypertensive human VSMCs, which may contribute to ER calcium overload in hypertension. This is in line with another study which found that inhibition of ER stress by TUDCA attenuated the increase in SERCA expression in the cardiac tissue of hypertensive models and restored cardiac contractility, reversing high blood pressure (Bal et al., 2019a). These findings suggest that ER stress may contribute to ER Ca2+ overload and thus play a role in hypertension. Furthermore, our research indicates that ER stress inducers enhance IP3R expression and reduce the expression of L-type calcium channels in hypertensive human VSMCs. This is consistent with findings that Chop-induced ERO1 expression triggers Ca<sup>2+</sup> release from IP3R, leading to increased intracellular Ca<sup>2+</sup> and calcium-dependent apoptosis (Li et al., 2009). Additionally, the activation of IRE1, as shown in other studies, downregulates L-type calcium channels in human stem cell-derived cardiomyocytes, indicating that the IRE1 pathway may be essential for maintaining calcium influx under physiological conditions (Bal et al., 2019a). Moreover, we found that specific inhibitors of the IRE1 and PERK pathways improved ET-1-induced Ca<sup>2+</sup> influx in VSMCs from hypertensive rats, but not in VSMCs from normotensive rats, suggesting a specific ER stress pathway regulation of calcium channels in hypertension. These observations collectively contribute to our understanding of how ER stress modulates calcium dysfunction in VSMCs, suggesting a complex interplay between ER stress pathways and calcium channel activation in hypertension.

In hypertension, intracellular calcium homeostasis is perturbed, leading to increased calcium influx, vascular hyperreactivity, and amplified contractile responses to vasoactive peptides, as demonstrated in various hypertension models (Bal et al., 2019a, TouyzDeng and Schiffrin, 1995, Goulopoulou and Webb, 2014, MatsudaLozinskaya and Cox, 1997). Vascular smooth muscle contraction requires the phosphorylation of myosin light chain 20 (p-MLC20) to promote actin—myosin cross-bridge formation (Takeya et al., 2014). A study has found that treatment with ER stress inducers can enhance p-MLC20 expression,

leading to increased vessel contraction and blood pressure (Liang et al., 2013). Moreover, it has been found inhibition ER stress with TUDCA reduced p-MLC20 in coronary arteries of hypertension rats (Choi et al., 2016b). Our study further reveals that the vasoactive peptide ET-1 enhances p-MLC20 expression in hypertensive rats, an effect that can be diminished by ER stress inhibitors. This indicates a potential role of ER stress in the upregulation of p-MLC20, particularly in response to ET-1 in hypertensive conditions. Besides, these findings suggest underlying molecular mechanisms involving the interplay between ER stress, p-MLC20, and vascular reactivity in hypertension.

The key mechanism in the excitation-contraction coupling of VSM involves a rise in intracellular Ca<sup>2+</sup> concentration, which is triggered by mechanical, humoral, or neural stimuli (Touyz et al., 2018). In hypertension, dysregulated calcium signalling results in elevated Ca<sup>2+</sup> levels, contributing to a state of hypercontractility and subsequent vascular remodelling (Touyz et al., 2018). Resistance blood vessels in human and experimental hypertension exhibit impaired functional and structural changes, including decreased vessel relaxation (BennettHillier and Thurston, 1996), increased contractile responses (Naiel et al., 2019, SpitlerMatsumoto and Webb, 2013), and hypertrophy of the medial layer (Touyz et al., 2018, Intengan et al., 1999a, LeeDickhout and Sandow, 2017, Dickhout and Lee, 1997, Mulvany, 1993). In our study, we observed enhanced constriction of mesenteric arteries in response to ET-1 and U46619 in both SHRSP and SHR compared to WKY. Additionally, SHR rats displayed a reduction in endothelium-independent relaxation compared to WKY rats. Structurally, there was an increase in the wall-lumen ratio and wall thickness in the mesenteric arteries of SHR compared to WKY. We found that inhibiting ER stress in hypertensive rats attenuated the hypercontractility of their resistant arteries. This was evidenced by decreased contraction in response to ET-1 and U46619 in SHRSP, and an increase in endothelium-dependent relaxation in SHR. Additionally, there was a trend towards a decreased cross-sectional area in SHR. Other research has demonstrated similar improvements in hypertensive vascular function and structure. Functionally, the inhibition of ER stress by 4PBA and TUDCA improved the vessel constriction and endothelium-dependent relaxation in resistant arteries of SHR(Naiel et al., 2019, Carlisle et al., 2016, Choi et al., 2016a). Structurally, 4-PBA treatment decreased the media-to-lumen ratio in resistance arteries of SHR (Naiel et al., 2019, Carlisle et al., 2016). These findings suggest the regulation of ER stress could modulate both structural and functional damage in resistant arteries during hypertension. Furthermore, these results highlight the potential of targeting ER stress inhibition as a therapeutic approach for improving vascular hypercontractility in hypertension.

# 7.4 Limitations of the study

Our study confirmed the presence of ER stress in various models of hypertension and highlighted the potential of targeting ER stress as a therapeutic approach. The underlying mechanisms involve a complex interplay between ER stress, oxidative stress, and calcium dysfunction, particularly in VSMCs of resistance arteries. However, there are several limitations to this study.

We primarily focus on the changes in intracellular signalling pathways by measuring the expression of proteins and genes. However, we did not measure the direct activation of some pathways, such as Noxs, Nrf2, and calcium channels. Therefore, we can only infer the potential results led by their activation, while the actual impact requires further experimental validation. Most of the mechanistic study was conducted in VSMCs, but the environment differs from isolated cells in tissues or the whole body. Molecular factors from plasma and neighbouring cells, such as endothelial cells, could also contribute to changes in VSMC function, and the effects of hypertension or ER stress inhibitors might be mediated through them. Moreover, the observed protein and gene changes represent a snapshot in time. While we have controlled variables and estimated appropriate dosing times, the actual dynamic changes and duration of action within a living organism cannot be precisely predicted.

Regarding the miRNA study, we used pooled samples, and the results lacked p-values. Consequently, the number of differentially expressed miRNAs was high, but we cannot make definitive selections based only on fold changes. Therefore, the results serve as a reference, but further experiments are needed to validate the functions of significant miRNAs. Moreover, the potential targets of the miRNAs we identified are currently just predictions and require further experimental confirmation.

Our experiments initially suggested that ET-1 induces ER stress in hypertensive VSMCs and verified the roles of ETAR and ETBR. However, whether VSMCs in hypertensive animals or humans are exposed to increased ET-1 stimulation and the long-term effects of heightened ET-1 on ER stress in hypertensive models require further investigation.

For the in vivo study, the sample size was a bit small to produce more reliable results. The observed changes in vascular structure are only trends, and further studies with larger sample sizes are needed to confirm their significance. Additionally, abnormal blood

pressure in the WKY rats might have influenced some vascular function and structural results.

We utilised specific inhibitors of the IRE1 and PERK pathways, indicating that suppressing individual branches of ER stress may have unique function. However, the toxicity of these inhibitors has not yet been fully established, and some effects might not solely be due to ER stress inhibition. While further validation is required for the safety of 4PBA. Additionally, whether 4PBA affects hypertension only through its impact on ER stress needs more experimental evidence before considering it for targeted therapy.

### References:

- 2016. Global, regional, and national comparative risk assessment of 79 behavioural, environmental and occupational, and metabolic risks or clusters of risks, 1990-2015: a systematic analysis for the Global Burden of Disease Study 2015. *Lancet*, 388, 1659-1724.
- 2017. Worldwide trends in blood pressure from 1975 to 2015: a pooled analysis of 1479 population-based measurement studies with 19·1 million participants. *Lancet*, 389, 37-55.
- ABRAHAM, N. G. & KAPPAS, A. 2008. Pharmacological and clinical aspects of heme oxygenase. *Pharmacol Rev*, 60, 79-127.
- ABRAHAM, N. G. & KAPPAS, A. 2011. Mechanism of heme-heme oxygenase system impairment of endothelium contraction in the spontaneously hypertensive rat. *Hypertension*, 58, 772-3.
- ADACHI, T., WEISBROD, R. M., PIMENTEL, D. R., YING, J., SHAROV, V. S., SCHÖNEICH, C. & COHEN, R. A. 2004. S-Glutathiolation by peroxynitrite activates SERCA during arterial relaxation by nitric oxide. *Nat Med*, 10, 1200-7.
- AHSAN, H. 2013. 3-Nitrotyrosine: A biomarker of nitrogen free radical species modified proteins in systemic autoimmunogenic conditions. *Hum Immunol*, 74, 1392-9.
- ALTENHÖFER, S., RADERMACHER, K. A., KLEIKERS, P. W., WINGLER, K. & SCHMIDT, H. H. 2015. Evolution of NADPH Oxidase Inhibitors: Selectivity and Mechanisms for Target Engagement. *Antioxid Redox Signal*, 23, 406-27.
- ALVES-LOPES, R., LACCHINI, S., NEVES, K. B., HARVEY, A., MONTEZANO, A. C. & TOUYZ, R. M. 2023. Vasoprotective effects of NOX4 are mediated via polymerase and transient receptor potential melastatin 2 cation channels in endothelial cells. *J Hypertens*, 41, 1389-1400.
- ALVES-LOPES, R., MONTEZANO, A. C., NEVES, K. B., HARVEY, A., RIOS, F. J., SKIBA, D. S., ARENDSE, L. B., GUZIK, T. J., GRAHAM, D., POGLITSCH, M., STURROCK, E. & TOUYZ, R. M. 2021. Selective Inhibition of the C-Domain of ACE (Angiotensin-Converting Enzyme) Combined With Inhibition of NEP (Neprilysin): A Potential New Therapy for Hypertension. *Hypertension*, 78, 604-616.
- ANGELI, F., VERDECCHIA, P. & REBOLDI, G. 2021. Aprocitentan, A Dual Endothelin Receptor Antagonist Under Development for the Treatment of Resistant Hypertension. *Cardiol Ther*, 10, 397-406.
- ANTO, E. M., SRUTHI, C. R., KRISHNAN, L., RAGHU, K. G. & PURUSHOTHAMAN, J. 2023. Tangeretin alleviates Tunicamycin-induced endoplasmic reticulum stress and associated complications in skeletal muscle cells. *Cell Stress Chaperones*, 28, 151-165.
- ARAKI, S., KAWAHARA, Y., KARIYA, K., SUNAKO, M., FUKUZAKI, H. & TAKAI, Y. 1989. Stimulation of phospholipase C-mediated hydrolysis of phosphoinositides by endothelin in cultured rabbit aortic smooth muscle cells. *Biochem Biophys Res Commun*, 159, 1072-9.
- ARDANAZ, N., YANG, X. P., CIFUENTES, M. E., HAURANI, M. J., JACKSON, K. W., LIAO, T. D., CARRETERO, O. A. & PAGANO, P. J. 2010. Lack of glutathione peroxidase 1 accelerates cardiac-specific hypertrophy and dysfunction in angiotensin II hypertension. *Hypertension*, 55, 116-23.
- ASHRAF, J. V. & AL HAJ ZEN, A. 2021. Role of Vascular Smooth Muscle Cell Phenotype Switching in Arteriogenesis. *Int J Mol Sci*, 22.
- BABELOVA, A., AVANIADI, D., JUNG, O., FORK, C., BECKMANN, J., KOSOWSKI, J., WEISSMANN, N., ANILKUMAR, N., SHAH, A. M., SCHAEFER, L.,

- SCHRODER, K. & BRANDES, R. P. 2012. Role of Nox4 in murine models of kidney disease. *Free Radic Biol Med*, 53, 842-53.
- BACAKOVA, L., TRAVNICKOVA, M., FILOVA, E., MATĚJKA, R., STEPANOVSKA, J., MUSILKOVA, J., ZARUBOVA, J., & MARTINMOLITOR, M. 2018. The Role of Vascular Smooth Muscle Cells in the Physiology and Pathophysiology of Blood Vessels. *In:* SAKUMA, K. (ed.) *Muscle Cell and Tissue*.
- BAL, N. B., HAN, S., KIREMITCI, S., SADI, G., ULUDAG, O. & DEMIREL-YILMAZ, E. 2019a. Hypertension-induced cardiac impairment is reversed by the inhibition of endoplasmic reticulum stress. *J Pharm Pharmacol*, 71, 1809-1821.
- BAL, N. B., HAN, S., KIREMITCI, S., SADI, G., ULUDAG, O. & DEMIREL-YILMAZ, E. 2019b. Hypertension-induced cardiac impairment is reversed by the inhibition of endoplasmic reticulum stress. *Journal of Pharmacy and Pharmacology*, 71, 1809-1821.
- BASSOT, A., CHEN, J., TAKAHASHI-YAMASHIRO, K., YAP, M. C., GIBHARDT, C. S., LE, G. N. T., HARIO, S., NASU, Y., MOORE, J., GUTIÉRREZ, T., MINA, L., MAST, H., MOSES, A., BHAT, R., BALLANYI, K., LEMIEUX, H., SITIA, R., ZITO, E., BOGESKI, I., CAMPBELL, R. E. & SIMMEN, T. 2023. The endoplasmic reticulum kinase PERK interacts with the oxidoreductase ERO1 to metabolically adapt mitochondria. *Cell Rep*, 42, 111899.
- BÁTKAI, S. & THUM, T. 2012. MicroRNAs in Hypertension: Mechanisms and Therapeutic Targets. *Current Hypertension Reports*, 14, 79-87.
- BAZAN, E., CAMPBELL, A. K. & RAPOPORT, R. M. 1992. Protein kinase C activity in blood vessels from normotensive and spontaneously hypertensive rats. *Eur J Pharmacol*, 227, 343-8.
- BEEVERS, G., LIP, G. Y. & O'BRIEN, E. 2001. ABC of hypertension: The pathophysiology of hypertension. *BMJ*, 322, 912-6.
- BENJAMIN, N. & VANE, J. 1996. Nitric oxide and hypertension. Circulation, 94, 1197-8.
- BENNETT, M. A., HILLIER, C. & THURSTON, H. 1996. Endothelium-dependent relaxation in resistance arteries from spontaneously hypertensive rats: effect of long-term treatment with perindopril, quinapril, hydralazine or amlodipine. *J Hypertens*, 14, 389-97.
- BERRIDGE, M. J. 2002. The endoplasmic reticulum: a multifunctional signaling organelle. *Cell Calcium*, 32, 235-49.
- BHASKARAN, M. & MOHAN, M. 2014. MicroRNAs: history, biogenesis, and their evolving role in animal development and disease. *Vet Pathol*, 51, 759-74.
- BHATTARAI, K. R., RIAZ, T. A., KIM, H. R. & CHAE, H. J. 2021. The aftermath of the interplay between the endoplasmic reticulum stress response and redox signaling. *Exp Mol Med*, 53, 151-167.
- BLOCK, K., EID, A., GRIENDLING, K. K., LEE, D. Y., WITTRANT, Y. & GORIN, Y. 2008. Nox4 NAD(P)H oxidase mediates Src-dependent tyrosine phosphorylation of PDK-1 in response to angiotensin II: role in mesangial cell hypertrophy and fibronectin expression. *J Biol Chem*, 283, 24061-76.
- BLOCK, K., GORIN, Y. & ABBOUD, H. E. 2009. Subcellular localization of Nox4 and regulation in diabetes. *Proc Natl Acad Sci U S A*, 106, 14385-90.
- BOESEN, E. I. & POLLOCK, D. M. 2010. Cooperative role of ETA and ETB receptors in mediating the diuretic response to intramedullary hyperosmotic NaCl infusion. *Am J Physiol Renal Physiol*, 299, F1424-32.
- BOLIVAR, J. J. 2013. Essential hypertension: an approach to its etiology and neurogenic pathophysiology. *Int J Hypertens*, 2013, 547809.
- BOUABOUT, G., AYME-DIETRICH, E., JACOB, H., CHAMPY, M. F., BIRLING, M. C., PAVLOVIC, G., MADEIRA, L., FERTAK, L. E., PETIT-DEMOULIERE, B., SORG, T., HERAULT, Y., MUDGETT, J. & MONASSIER, L. 2018. Nox4

- genetic inhibition in experimental hypertension and metabolic syndrome. *Arch Cardiovasc Dis*, 111, 41-52.
- BOUNDS, K. R., CHIASSON, V. L., PAN, L. J., GUPTA, S. & CHATTERJEE, P. 2017. MicroRNAs: New Players in the Pathobiology of Preeclampsia. *Front Cardiovasc Med*, 4, 60.
- BRANDES, R. P., MILLER, F. J., BEER, S., HAENDELER, J., HOFFMANN, J., HA, T., HOLLAND, S. M., GORLACH, A. & BUSSE, R. 2002. The vascular NADPH oxidase subunit p47phox is involved in redox-mediated gene expression. *Free Radic Biol Med*, 32, 1116-22.
- BRITO, R., CASTILLO, G., GONZALEZ, J., VALLS, N. & RODRIGO, R. 2015. Oxidative stress in hypertension: mechanisms and therapeutic opportunities. *Exp Clin Endocrinol Diabetes*, 123, 325-35.
- BROWN, I. A. M., DIEDERICH, L., GOOD, M. E., DELALIO, L. J., MURPHY, S. A., CORTESE-KROTT, M. M., HALL, J. L., LE, T. H. & ISAKSON, B. E. 2018. Vascular Smooth Muscle Remodeling in Conductive and Resistance Arteries in Hypertension. *Arterioscler Thromb Vasc Biol*, 38, 1969-1985.
- BROZOVICH, F. V., NICHOLSON, C. J., DEGEN, C. V., GAO, Y. Z., AGGARWAL, M. & MORGAN, K. G. 2016. Mechanisms of Vascular Smooth Muscle Contraction and the Basis for Pharmacologic Treatment of Smooth Muscle Disorders. *Pharmacol Rev*, 68, 476-532.
- BUELT, A., RICHARDS, A. & JONES, A. L. 2021. Hypertension: New Guidelines from the International Society of Hypertension. *Am Fam Physician*, 103, 763-765.
- BURGER, D., REUDELHUBER, T. L., MAHAJAN, A., CHIBALE, K., STURROCK, E. D. & TOUYZ, R. M. 2014. Effects of a domain-selective ACE inhibitor in a mouse model of chronic angiotensin II-dependent hypertension. *Clin Sci (Lond)*, 127, 57-63.
- CAHILL, P. A. & REDMOND, E. M. 2016. Vascular endothelium Gatekeeper of vessel health. *Atherosclerosis*, 248, 97-109.
- CAI, Y., YU, X., HU, S. & YU, J. 2009. A Brief Review on the Mechanisms of miRNA Regulation. *Genomics, Proteomics & Bioinformatics*, 7, 147-154.
- CAMARGO, L. L., HARVEY, A. P., RIOS, F. J., TSIROPOULOU, S., DA SILVA, R. N. O., CAO, Z., GRAHAM, D., MCMASTER, C., BURCHMORE, R. J., HARTLEY, R. C., BULLEID, N., MONTEZANO, A. C. & TOUYZ, R. M. 2018. Vascular Nox (NADPH Oxidase) Compartmentalization, Protein Hyperoxidation, and Endoplasmic Reticulum Stress Response in Hypertension. *Hypertension*, 72, 235-246.
- CAMARGO, L. L., MONTEZANO, A. C., HUSSAIN, M., WANG, Y., ZOU, Z., RIOS, F. J., NEVES, K. B., ALVES-LOPES, R., AWAN, F. R., GUZIK, T. J., JENSEN, T., HARTLEY, R. C. & TOUYZ, R. M. 2022. Central role of c-Src in NOX5-mediated redox signalling in vascular smooth muscle cells in human hypertension. *Cardiovasc Res*, 118, 1359-1373.
- CAMARGO, L. L., WANG, Y., RIOS, F. J., MCBRIDE, M., MONTEZANO, A. C. & TOUYZ, R. M. 2023a. Oxidative Stress and Endoplasmic Reticular Stress Interplay in the Vasculopathy of Hypertension. *Can J Cardiol*, 39, 1874-1887.
- CAMARGO, L. L., WANG, Y., RIOS, F. J., MCBRIDE, M., MONTEZANO, A. C. & TOUYZ, R. M. 2023b. Oxidative Stress and Endoplasmic Reticular Stress Interplay in the Vasculopathy of Hypertension. *Can J Cardiol*.
- CAMERON, A. C., LANG, N. N. & TOUYZ, R. M. 2016. Drug Treatment of Hypertension: Focus on Vascular Health. *Drugs*, 76, 1529-1550.
- CAO, G., XUAN, X., HU, J., ZHANG, R., JIN, H. & DONG, H. 2022. How vascular smooth muscle cell phenotype switching contributes to vascular disease. *Cell Commun Signal*, 20, 180.

- CAO, S. S. & KAUFMAN, R. J. 2014. Endoplasmic reticulum stress and oxidative stress in cell fate decision and human disease. *Antioxid Redox Signal*, 21, 396-413.
- CARLISLE, R. E., WERNER, K. E., YUM, V., LU, C., TAT, V., MEMON, M., NO, Y., ASK, K. & DICKHOUT, J. G. 2016. Endoplasmic reticulum stress inhibition reduces hypertension through the preservation of resistance blood vessel structure and function. *J Hypertens*, 34, 1556-69.
- CELLI, J. & TSOLIS, R. M. 2015. Bacteria, the endoplasmic reticulum and the unfolded protein response: friends or foes? *Nat Rev Microbiol*, 13, 71-82.
- CHAMLEY-CAMPBELL, J., CAMPBELL, G. R. & ROSS, R. 1979. The smooth muscle cell in culture. *Physiol Rev*, 59, 1-61.
- CHANG, C. Y., PAN, P. H., WU, C. C., LIAO, S. L., CHEN, W. Y., KUAN, Y. H., WANG, W. Y. & CHEN, C. J. 2021. Endoplasmic Reticulum Stress Contributes to Gefitinib-Induced Apoptosis in Glioma. *Int J Mol Sci*, 22.
- CHATTOPADHYAY, A., KWARTLER, C. S., KAW, K., LI, Y., KAW, A., CHEN, J., LEMAIRE, S. A., SHEN, Y. H. & MILEWICZ, D. M. 2021. Cholesterol-Induced Phenotypic Modulation of Smooth Muscle Cells to Macrophage/Fibroblast-like Cells Is Driven by an Unfolded Protein Response. *Arterioscler Thromb Vasc Biol*, 41, 302-316.
- CHEN, B., LU, Y., CHEN, Y. & CHENG, J. 2015. The role of Nrf2 in oxidative stress-induced endothelial injuries. *J Endocrinol*, 225, R83-99.
- CHEN, J., GONG, F., CHEN, M. F., LI, C., HONG, P., SUN, S., ZHOU, C. & QIAN, Z. J. 2019. In Vitro Vascular-Protective Effects of a Tilapia By-Product Oligopeptide on Angiotensin II-Induced Hypertensive Endothelial Injury in HUVEC by Nrf2/NF-kappaB Pathways. *Mar Drugs*, 17.
- CHEN, S., SU, J., WU, K., HU, W., GARDNER, D. G. & CHEN, D. 1998. Early captopril treatment prevents hypertrophydependent gene expression in hearts of SHR. *Am J Physiol*, 274, R1511-7.
- CHEN, S., ZHANG, L., FENG, B., WANG, W., LIU, D., ZHAO, X., YU, C., WANG, X. & GAO, Y. 2022. MiR-550a-3p restores damaged vascular smooth muscle cells by inhibiting thrombomodulin in an <em>in vitro</em> atherosclerosis model. *Eur J Histochem*, 66.
- CHEN, W., LIU, T., LIANG, Q., CHEN, X., TAO, W., FANG, M., XIAO, Y. & CHEN, L. 2021. miR-1283 Contributes to Endoplasmic Reticulum Stress in the Development of Hypertension Through the Activating Transcription Factor-4 (ATF4)/C/EBP-Homologous Protein (CHOP) Signaling Pathway. *Med Sci Monit*, 27, e930552.
- CHEN, Y., LI, S., GUO, Y., YU, H., BAO, Y., XIN, X., YANG, H., NI, X., WU, N. & JIA, D. 2020. Astaxanthin Attenuates Hypertensive Vascular Remodeling by Protecting Vascular Smooth Muscle Cells from Oxidative Stress-Induced Mitochondrial Dysfunction. *Oxid Med Cell Longev*, 2020, 4629189.
- CHERNORUDSKIY, A. L. & ZITO, E. 2017. Regulation of Calcium Homeostasis by ER Redox: A Close-Up of the ER/Mitochondria Connection. *J Mol Biol*, 429, 620-632.
- CHIANG, C. K., HSU, S. P., WU, C. T., HUANG, J. W., CHENG, H. T., CHANG, Y. W., HUNG, K. Y., WU, K. D. & LIU, S. H. 2011. Endoplasmic reticulum stress implicated in the development of renal fibrosis. *Mol Med*, 17, 1295-305.
- CHOI, E. H. & PARK, S. J. 2023. TXNIP: A key protein in the cellular stress response pathway and a potential therapeutic target. *Exp Mol Med*, 55, 1348-1356.
- CHOI, S.-K., LIM, M., BYEON, S.-H. & LEE, Y.-H. 2016a. Inhibition of endoplasmic reticulum stress improves coronary artery function in the spontaneously hypertensive rats. *Scientific Reports*, 6, 31925.
- CHOI, S. K., LIM, M., BYEON, S. H. & LEE, Y. H. 2016b. Inhibition of endoplasmic reticulum stress improves coronary artery function in the spontaneously hypertensive rats. *Sci Rep*, 6, 31925.

- CHOMCZYNSKI, P. & SACCHI, N. 1987. Single-step method of RNA isolation by acid guanidinium thiocyanate-phenol-chloroform extraction. *Anal Biochem*, 162, 156-9.
- CHOUVARINE, P., GELDNER, J., GIAGNORIO, R., LEGCHENKO, E., BERTRAM, H. & HANSMANN, G. 2020. Trans-Right-Ventricle and Transpulmonary MicroRNA Gradients in Human Pulmonary Arterial Hypertension. *Pediatr Crit Care Med*, 21, 340-349.
- CHOY, K. W., LAU, Y. S., MURUGAN, D. & MUSTAFA, M. R. 2017. Chronic treatment with paeonol improves endothelial function in mice through inhibition of endoplasmic reticulum stress-mediated oxidative stress. *PLoS One*, 12, e0178365.
- CICALESE, S., OKUNO, K., ELLIOTT, K. J., KAWAI, T., SCALIA, R., RIZZO, V. & EGUCHI, S. 2020. 78 kDa Glucose-Regulated Protein Attenuates Protein Aggregation and Monocyte Adhesion Induced by Angiotensin II in Vascular Cells. *Int J Mol Sci.* 21.
- CICALESE, S. M., DA SILVA, J. F., PRIVIERO, F., WEBB, R. C., EGUCHI, S. & TOSTES, R. C. 2021. Vascular Stress Signaling in Hypertension. *Circ Res*, 128, 969-992.
- COATS, A. & JAIN, S. 2017. Protective effects of nebivolol from oxidative stress to prevent hypertension-related target organ damage. *J Hum Hypertens*, 31, 376-381.
- COE, H. & MICHALAK, M. 2009. Calcium binding chaperones of the endoplasmic reticulum. *Gen Physiol Biophys*, 28 Spec No Focus, F96-F103.
- COFFMAN, T. M. 2011. Under pressure: the search for the essential mechanisms of hypertension. *Nat Med*, 17, 1402-9.
- CORBETT, E. F. & MICHALAK, M. 2000. Calcium, a signaling molecule in the endoplasmic reticulum? *Trends Biochem Sci*, 25, 307-11.
- CULLINAN, S. B., ZHANG, D., HANNINK, M., ARVISAIS, E., KAUFMAN, R. J. & DIEHL, J. A. 2003. Nrf2 is a direct PERK substrate and effector of PERK-dependent cell survival. *Mol Cell Biol*, 23, 7198-209.
- DAVIS-DUSENBERY, B. N., WU, C. & HATA, A. 2011. Micromanaging vascular smooth muscle cell differentiation and phenotypic modulation. *Arterioscler Thromb Vasc Biol*, 31, 2370-7.
- DE CHAMPLAIN, J., WU, R., GIROUARD, H., KARAS, M., A, E. L. M., LAPLANTE, M. A. & WU, L. 2004. Oxidative stress in hypertension. *Clin Exp Hypertens*, 26, 593-601.
- DE MIGUEL, C., HAMRICK, W. C., HOBBS, J. L., POLLOCK, D. M., CARMINES, P. K. & POLLOCK, J. S. 2017. Endothelin receptor-specific control of endoplasmic reticulum stress and apoptosis in the kidney. *Sci Rep.* 7, 43152.
- DENG, L., BLANCO, F. J., STEVENS, H., LU, R., CAUDRILLIER, A., MCBRIDE, M., MCCLURE, J. D., GRANT, J., THOMAS, M., FRID, M., STENMARK, K., WHITE, K., SETO, A. G., MORRELL, N. W., BRADSHAW, A. C., MACLEAN, M. R. & BAKER, A. H. 2015. MicroRNA-143 Activation Regulates Smooth Muscle and Endothelial Cell Crosstalk in Pulmonary Arterial Hypertension. *Circ Res*, 117, 870-883.
- DICKHOUT, J. G. & LEE, R. M. 1997. Structural and functional analysis of small arteries from young spontaneously hypertensive rats. *Hypertension*, 29, 781-9.
- DICKHOUT, J. G. & LEE, R. M. 2000. Increased medial smooth muscle cell length is responsible for vascular hypertrophy in young hypertensive rats. *Am J Physiol Heart Circ Physiol*, 279, H2085-94.
- DIKALOVA, A. E., ITANI, H. A., NAZAREWICZ, R. R., MCMASTER, W. G., FLYNN, C. R., UZHACHENKO, R., FESSEL, J. P., GAMBOA, J. L., HARRISON, D. G. & DIKALOV, S. I. 2017. Sirt3 Impairment and SOD2 Hyperacetylation in Vascular Oxidative Stress and Hypertension. *Circ Res*, 121, 564-574.

- DONG, X., ZHAO, J., HAN, J., HAN, X. J., ZHAO, C. M., ZOU, A. X. & QI, H. G. 2020. MiR-222-5p promotes the growth and migration of trophoblasts by targeting AHNAK. *Eur Rev Med Pharmacol Sci*, 24, 10954-10959.
- DORNAS, W. C. & SILVA, M. E. 2011. Animal models for the study of arterial hypertension. *J Biosci*, 36, 731-7.
- DUCKERS, H. J., BOEHM, M., TRUE, A. L., YET, S. F., SAN, H., PARK, J. L., CLINTON WEBB, R., LEE, M. E., NABEL, G. J. & NABEL, E. G. 2001. Heme oxygenase-1 protects against vascular constriction and proliferation. *Nat Med*, 7, 693-8.
- DUTTA, S. & RITTINGER, K. 2010. Regulation of NOXO1 activity through reversible interactions with p22 and NOXA1. *PLoS One*, 5, e10478.
- DUVNJAK, L. 2007. Hypertension and the Metabolic Syndrome. *EJIFCC*, 18, 55-60.
- ELETTO, D., CHEVET, E., ARGON, Y. & APPENZELLER-HERZOG, C. 2014. Redox controls UPR to control redox. *J Cell Sci*, 127, 3649-58.
- ELLGAARD, L., MCCAUL, N., CHATSISVILI, A. & BRAAKMAN, I. 2016. Co- and Post-Translational Protein Folding in the ER. *Traffic*, 17, 615-38.
- ELMARASI, M., ELMAKATY, I., ELSAYED, B., ELSAYED, A., ZEIN, J. A., BOUDAKA, A. & EID, A. H. 2024. Phenotypic switching of vascular smooth muscle cells in atherosclerosis, hypertension, and aortic dissection. *J Cell Physiol*, 239, e31200.
- ETTEHAD, D., EMDIN, C. A., KIRAN, A., ANDERSON, S. G., CALLENDER, T., EMBERSON, J., CHALMERS, J., RODGERS, A. & RAHIMI, K. 2016. Blood pressure lowering for prevention of cardiovascular disease and death: a systematic review and meta-analysis. *Lancet*, 387, 957-967.
- EVANS, A. L., BROWN, W., KENYON, C. J., MAXTED, K. J. & SMITH, D. C. 1994. Improved system for measuring systolic blood pressure in the conscious rat. *Med Biol Eng Comput*, 32, 101-2.
- FAZELI, G., STOPPER, H., SCHINZEL, R., NI, C. W., JO, H. & SCHUPP, N. 2012. Angiotensin II induces DNA damage via AT1 receptor and NADPH oxidase isoform Nox4. *Mutagenesis*, 27, 673-81.
- FEAIRHELLER, D. L., BROWN, M. D., PARK, J. Y., BRINKLEY, T. E., BASU, S., HAGBERG, J. M., FERRELL, R. E. & FENTY-STEWART, N. M. 2009. Exercise training, NADPH oxidase p22phox gene polymorphisms, and hypertension. *Med Sci Sports Exerc*, 41, 1421-8.
- FERNANDES, D. C., MANOEL, A. H., WOSNIAK, J., JR. & LAURINDO, F. R. 2009. Protein disulfide isomerase overexpression in vascular smooth muscle cells induces spontaneous preemptive NADPH oxidase activation and Nox1 mRNA expression: effects of nitrosothiol exposure. *Arch Biochem Biophys*, 484, 197-204.
- FIERRO-FERNANDEZ, M., BUSNADIEGO, O., SANDOVAL, P., ESPINOSA-DIEZ, C., BLANCO-RUIZ, E., RODRIGUEZ, M., PIAN, H., RAMOS, R., LOPEZ-CABRERA, M., GARCIA-BERMEJO, M. L. & LAMAS, S. 2015. miR-9-5p suppresses pro-fibrogenic transformation of fibroblasts and prevents organ fibrosis by targeting NOX4 and TGFBR2. *EMBO Rep.* 16, 1358-77.
- FLECKENSTEIN-GRÜN, G., FREY, M., THIMM, F., HOFGÄRTNER, W. & FLECKENSTEIN, A. 1992. Calcium overload--an important cellular mechanism in hypertension and arteriosclerosis. *Drugs*, 44 Suppl 1, 23-30.
- FORRESTER, S. J., BOOZ, G. W., SIGMUND, C. D., COFFMAN, T. M., KAWAI, T., RIZZO, V., SCALIA, R. & EGUCHI, S. 2018. Angiotensin II Signal Transduction: An Update on Mechanisms of Physiology and Pathophysiology. *Physiol Rev*, 98, 1627-1738.
- FÖRSTERMANN, U. & SESSA, W. C. 2012. Nitric oxide synthases: regulation and function. *Eur Heart J*, 33, 829-37, 837a-837d.

- FRIDOVICH, I. 1997. Superoxide anion radical (O2-.), superoxide dismutases, and related matters. *J Biol Chem*, 272, 18515-7.
- FRISHMAN, W. H. 2016. Beta-Adrenergic Receptor Blockers in Hypertension: Alive and Well. *Prog Cardiovasc Dis*, 59, 247-252.
- FUKAI, T., SIEGFRIED, M. R., USHIO-FUKAI, M., GRIENDLING, K. K. & HARRISON, D. G. 1999. Modulation of extracellular superoxide dismutase expression by angiotensin II and hypertension. *Circ Res*, 85, 23-8.
- FULTON, D. J. 2009. Nox5 and the regulation of cellular function. *Antioxid Redox Signal*, 11, 2443-52.
- FURMANIK, M., VAN GORP, R., WHITEHEAD, M., AHMAD, S., BORDOLOI, J., KAPUSTIN, A., SCHURGERS, L. J. & SHANAHAN, C. M. 2021. Endoplasmic Reticulum Stress Mediates Vascular Smooth Muscle Cell Calcification via Increased Release of Grp78 (Glucose-Regulated Protein, 78 kDa)-Loaded Extracellular Vesicles. *Arterioscler Thromb Vasc Biol*, 41, 898-914.
- GALÁN, M., KASSAN, M., KADOWITZ, P. J., TREBAK, M., BELMADANI, S. & MATROUGUI, K. 2014. Mechanism of endoplasmic reticulum stress-induced vascular endothelial dysfunction. *Biochim Biophys Acta*, 1843, 1063-75.
- GALEHDAR, Z., SWAN, P., FUERTH, B., CALLAGHAN, S. M., PARK, D. S. & CREGAN, S. P. 2010. Neuronal apoptosis induced by endoplasmic reticulum stress is regulated by ATF4-CHOP-mediated induction of the Bcl-2 homology 3-only member PUMA. *J Neurosci*, 30, 16938-48.
- GALLO, G., VOLPE, M. & SAVOIA, C. 2021. Endothelial Dysfunction in Hypertension: Current Concepts and Clinical Implications. *Front Med (Lausanne)*, 8, 798958.
- GAO, P., YAN, Z. & ZHU, Z. 2020. Mitochondria-Associated Endoplasmic Reticulum Membranes in Cardiovascular Diseases. *Front Cell Dev Biol*, 8, 604240.
- GARIEPY, C. E., OHUCHI, T., WILLIAMS, S. C., RICHARDSON, J. A. & YANAGISAWA, M. 2000. Salt-sensitive hypertension in endothelin-B receptor-deficient rats. *J Clin Invest*, 105, 925-33.
- GIBBONS, G. H. & DZAU, V. J. 1994. The emerging concept of vascular remodeling. *N Engl J Med*, 330, 1431-8.
- GILL, P. S. & WILCOX, C. S. 2006. NADPH oxidases in the kidney. *Antioxid Redox Signal*, 8, 1597-607.
- GIUSTARINI, D., DALLE-DONNE, I., TSIKAS, D. & ROSSI, R. 2009. Oxidative stress and human diseases: Origin, link, measurement, mechanisms, and biomarkers. *Crit Rev Clin Lab Sci*, 46, 241-81.
- GLEMBOTSKI, C. C. 2007. Endoplasmic reticulum stress in the heart. *Circ Res*, 101, 975-84.
- GOMOLAK, J. R. & DIDION, S. P. 2014. Angiotensin II-induced endothelial dysfunction is temporally linked with increases in interleukin-6 and vascular macrophage accumulation. *Front Physiol*, 5, 396.
- GONGORA, M. C., QIN, Z., LAUDE, K., KIM, H. W., MCCANN, L., FOLZ, J. R., DIKALOV, S., FUKAI, T. & HARRISON, D. G. 2006. Role of extracellular superoxide dismutase in hypertension. *Hypertension*, 48, 473-81.
- GÖRLACH, A., BERTRAM, K., HUDECOVA, S. & KRIZANOVA, O. 2015. Calcium and ROS: A mutual interplay. *Redox Biol*, 6, 260-271.
- GOULOPOULOU, S. & WEBB, R. C. 2014. Symphony of vascular contraction: how smooth muscle cells lose harmony to signal increased vascular resistance in hypertension. *Hypertension*, 63, e33-9.
- GRAY, S. P., DI MARCO, E., KENNEDY, K., CHEW, P., OKABE, J., EL-OSTA, A., CALKIN, A. C., BIESSEN, E. A., TOUYZ, R. M., COOPER, M. E., SCHMIDT, H. H. & JANDELEIT-DAHM, K. A. 2016. Reactive Oxygen Species Can Provide Atheroprotection via NOX4-Dependent Inhibition of Inflammation and Vascular Remodeling. *Arterioscler Thromb Vasc Biol*, 36, 295-307.

- GRIENDLING, K. K., CAMARGO, L. L., RIOS, F. J., ALVES-LOPES, R., MONTEZANO, A. C. & TOUYZ, R. M. 2021. Oxidative Stress and Hypertension. *Circ Res*, 128, 993-1020.
- GRIENDLING, K. K., SORESCU, D., LASSÈGUE, B. & USHIO-FUKAI, M. 2000. Modulation of protein kinase activity and gene expression by reactive oxygen species and their role in vascular physiology and pathophysiology. *Arterioscler Thromb Vasc Biol*, 20, 2175-83.
- GROENENDYK, J., AGELLON, L. B. & MICHALAK, M. 2013. Coping with endoplasmic reticulum stress in the cardiovascular system. *Annu Rev Physiol*, 75, 49-67.
- GROENENDYK, J., AGELLON, L. B. & MICHALAK, M. 2021. Calcium signaling and endoplasmic reticulum stress. *Int Rev Cell Mol Biol*, 363, 1-20.
- GROENENDYK, J., SREENIVASAIAH, P. K., KIM, D. H., AGELLON, L. B. & MICHALAK, M. 2010. Biology of endoplasmic reticulum stress in the heart. *Circ Res*, 107, 1185-97.
- GU, H., YU, J., DONG, D., ZHOU, Q., WANG, J. Y., FANG, S. & YANG, P. 2016. High Glucose-Repressed CITED2 Expression Through miR-200b Triggers the Unfolded Protein Response and Endoplasmic Reticulum Stress. *Diabetes*, 65, 149-63.
- GU, W., HONG, X., LE BRAS, A., NOWAK, W. N., ISSA BHALOO, S., DENG, J., XIE, Y., HU, Y., RUAN, X. Z. & XU, Q. 2018. Smooth muscle cells differentiated from mesenchymal stem cells are regulated by microRNAs and suitable for vascular tissue grafts. *J Biol Chem*, 293, 8089-8102.
- GUAN, H. S., SHANGGUAN, H. J., SHANG, Z., YANG, L., MENG, X. M. & QIAO, S. B. 2011. Endoplasmic reticulum stress caused by left ventricular hypertrophy in rats: effects of telmisartan. *Am J Med Sci*, 342, 318-23.
- GUO, D. F., SUN, Y. L., HAMET, P. & INAGAMI, T. 2001. The angiotensin II type 1 receptor and receptor-associated proteins. *Cell Res*, 11, 165-80.
- GUTIERREZ, T. & SIMMEN, T. 2018. Endoplasmic reticulum chaperones tweak the mitochondrial calcium rheostat to control metabolism and cell death. *Cell Calcium*, 70, 64-75.
- GUZIK, T. J. & TOUYZ, R. M. 2017. Oxidative Stress, Inflammation, and Vascular Aging in Hypertension. *Hypertension*, 70, 660-667.
- GUZIK, T. J., WEST, N. E., PILLAI, R., TAGGART, D. P. & CHANNON, K. M. 2002. Nitric oxide modulates superoxide release and peroxynitrite formation in human blood vessels. *Hypertension*, 39, 1088-94.
- HALL, J. E., GRANGER, J. P., DO CARMO, J. M., DA SILVA, A. A., DUBINION, J., GEORGE, E., HAMZA, S., SPEED, J. & HALL, M. E. 2012. Hypertension: physiology and pathophysiology. *Compr Physiol*, 2, 2393-442.
- HAN, S., BAL, N. B., SADI, G., USANMAZ, S. E., TUGLU, M. M., ULUDAG, M. O. & DEMIREL-YILMAZ, E. 2019a. Inhibition of endoplasmic reticulum stress protected DOCA-salt hypertension-induced vascular dysfunction. *Vascular Pharmacology*, 113, 38-46.
- HAN, S., BAL, N. B., SADI, G., USANMAZ, S. E., TUGLU, M. M., ULUDAG, M. O. & DEMIREL-YILMAZ, E. 2019b. Inhibition of endoplasmic reticulum stress protected DOCA-salt hypertension-induced vascular dysfunction. *Vascul Pharmacol*, 113, 38-46.
- HARDING, H. P., NOVOA, I., ZHANG, Y., ZENG, H., WEK, R., SCHAPIRA, M. & RON, D. 2000. Regulated translation initiation controls stress-induced gene expression in mammalian cells. *Mol Cell*, 6, 1099-108.
- HARDING, H. P., ZHANG, Y., ZENG, H., NOVOA, I., LU, P. D., CALFON, M., SADRI, N., YUN, C., POPKO, B., PAULES, R., STOJDL, D. F., BELL, J. C., HETTMANN, T., LEIDEN, J. M. & RON, D. 2003. An integrated stress response

- regulates amino acid metabolism and resistance to oxidative stress. *Mol Cell*, 11, 619-33.
- HARRISON, D. G. 2013. The mosaic theory revisited: common molecular mechanisms coordinating diverse organ and cellular events in hypertension. *J Am Soc Hypertens*, 7, 68-74.
- HARRISON, D. G. 2014. The immune system in hypertension. *Trans Am Clin Climatol Assoc*, 125, 130-38; discussion 138-40.
- HARTNER, A., CORDASIC, N., KLANKE, B., MENENDEZ-CASTRO, C., VEELKEN, R., SCHMIEDER, R. E. & HILGERS, K. F. 2014. Renal protection by low dose irbesartan in diabetic nephropathy is paralleled by a reduction of inflammation, not of endoplasmic reticulum stress. *Biochim Biophys Acta*, 1842, 558-65.
- HE, X., DENG, J., YU, X. J., YANG, S., YANG, Y. & ZANG, W. J. 2020. Activation of M3AChR (Type 3 Muscarinic Acetylcholine Receptor) and Nrf2 (Nuclear Factor Erythroid 2-Related Factor 2) Signaling by Choline Alleviates Vascular Smooth Muscle Cell Phenotypic Switching and Vascular Remodeling. *Arterioscler Thromb Vasc Biol*, 40, 2649-2664.
- HEAGERTY, A. M., AALKJAER, C., BUND, S. J., KORSGAARD, N. & MULVANY, M. J. 1993. Small artery structure in hypertension. Dual processes of remodeling and growth. *Hypertension*, 21, 391-7.
- HEAGERTY, A. M., HEERKENS, E. H. & IZZARD, A. S. 2010. Small artery structure and function in hypertension. *J Cell Mol Med*, 14, 1037-43.
- HECKER, L., VITTAL, R., JONES, T., JAGIRDAR, R., LUCKHARDT, T. R., HOROWITZ, J. C., PENNATHUR, S., MARTINEZ, F. J. & THANNICKAL, V. J. 2009. NADPH oxidase-4 mediates myofibroblast activation and fibrogenic responses to lung injury. *Nat Med*, 15, 1077-81.
- HERMSMEYER, K. 1993. Calcium channel function in hypertension. *J Hum Hypertens*, 7, 173-6.
- HETZ, C. 2012. The unfolded protein response: controlling cell fate decisions under ER stress and beyond. *Nat Rev Mol Cell Biol*, 13, 89-102.
- HIGA, A. & CHEVET, E. 2012. Redox signaling loops in the unfolded protein response. *Cell Signal*, 24, 1548-55.
- HIGASHI, Y., SASAKI, S., KURISU, S., YOSHIMIZU, A., SASAKI, N., MATSUURA, H., KAJIYAMA, G. & OSHIMA, T. 1999. Regular aerobic exercise augments endothelium-dependent vascular relaxation in normotensive as well as hypertensive subjects: role of endothelium-derived nitric oxide. *Circulation*, 100, 1194-202.
- HIGASHI, Y., SASAKI, S., NAKAGAWA, K., KIMURA, M., NOMA, K., SASAKI, S., HARA, K., MATSUURA, H., GOTO, C., OSHIMA, T., CHAYAMA, K. & YOSHIZUMI, M. 2003. Low body mass index is a risk factor for impaired endothelium-dependent vasodilation in humans: role of nitric oxide and oxidative stress. *J Am Coll Cardiol*, 42, 256-63.
- HIGO, T., HAMADA, K., HISATSUNE, C., NUKINA, N., HASHIKAWA, T., HATTORI, M., NAKAMURA, T. & MIKOSHIBA, K. 2010. Mechanism of ER stress-induced brain damage by IP(3) receptor. *Neuron*, 68, 865-78.
- HOLLIEN, J. & WEISSMAN, J. S. 2006. Decay of endoplasmic reticulum-localized mRNAs during the unfolded protein response. *Science*, 313, 104-7.
- HOSICK, P. A. & STEC, D. E. 2012. Heme oxygenase, a novel target for the treatment of hypertension and obesity? *Am J Physiol Regul Integr Comp Physiol*, 302, R207-14.
- HOURIHAN, J. M., MORONETTI MAZZEO, L. E., FERNÁNDEZ-CÁRDENAS, L. P. & BLACKWELL, T. K. 2016. Cysteine Sulfenylation Directs IRE-1 to Activate the SKN-1/Nrf2 Antioxidant Response. *Mol Cell*, 63, 553-566.
- HSU, Y. H., ZHENG, C. M., CHOU, C. L., CHEN, Y. J., LEE, Y. H., LIN, Y. F. & CHIU, H. W. 2021. Therapeutic Effect of Endothelin-Converting Enzyme Inhibitor on

- Chronic Kidney Disease through the Inhibition of Endoplasmic Reticulum Stress and the NLRP3 Inflammasome. *Biomedicines*, 9.
- HUANG, P. L., HUANG, Z., MASHIMO, H., BLOCH, K. D., MOSKOWITZ, M. A., BEVAN, J. A. & FISHMAN, M. C. 1995. Hypertension in mice lacking the gene for endothelial nitric oxide synthase. *Nature*, 377, 239-42.
- HUO, K. G., RICHER, C., BERILLO, O., MAHJOUB, N., FRAULOB-AQUINO, J. C., BARHOUMI, T., OUERD, S., COELHO, S. C., SINNETT, D., PARADIS, P. & SCHIFFRIN, E. L. 2019. miR-431-5p Knockdown Protects Against Angiotensin II-Induced Hypertension and Vascular Injury. *Hypertension*, 73, 1007-1017.
- HYNYNEN, M. M. & KHALIL, R. A. 2006. The vascular endothelin system in hypertension--recent patents and discoveries. *Recent Pat Cardiovasc Drug Discov*, 1, 95-108.
- ICHIKAWA, T., LI, J., MEYER, C. J., JANICKI, J. S., HANNINK, M. & CUI, T. 2009. Dihydro-CDDO-trifluoroethyl amide (dh404), a novel Nrf2 activator, suppresses oxidative stress in cardiomyocytes. *PLoS One*, 4, e8391.
- IGLARZ, M. & SCHIFFRIN, E. L. 2003. Role of endothelin-1 in hypertension. *Curr Hypertens Rep*, 5, 144-8.
- INSCHO, E. W., IMIG, J. D., COOK, A. K. & POLLOCK, D. M. 2005. ETA and ETB receptors differentially modulate afferent and efferent arteriolar responses to endothelin. *Br J Pharmacol*, 146, 1019-26.
- INTENGAN, H. D., DENG, L. Y., LI, J. S. & SCHIFFRIN, E. L. 1999a. Mechanics and composition of human subcutaneous resistance arteries in essential hypertension. *Hypertension*, 33, 569-74.
- INTENGAN, H. D. & SCHIFFRIN, E. L. 2000. Structure and mechanical properties of resistance arteries in hypertension: role of adhesion molecules and extracellular matrix determinants. *Hypertension*, 36, 312-8.
- INTENGAN, H. D., THIBAULT, G., LI, J. S. & SCHIFFRIN, E. L. 1999b. Resistance artery mechanics, structure, and extracellular components in spontaneously hypertensive rats: effects of angiotensin receptor antagonism and converting enzyme inhibition. *Circulation*, 100, 2267-75.
- ISHIZAKA, N., DE LEON, H., LAURSEN, J. B., FUKUI, T., WILCOX, J. N., DE KEULENAER, G., GRIENDLING, K. K. & ALEXANDER, R. W. 1997. Angiotensin II-induced hypertension increases heme oxygenase-1 expression in rat aorta. *Circulation*, 96, 1923-9.
- ISMAIL, S., STURROCK, A., WU, P., CAHILL, B., NORMAN, K., HUECKSTEADT, T., SANDERS, K., KENNEDY, T. & HOIDAL, J. 2009. NOX4 mediates hypoxia-induced proliferation of human pulmonary artery smooth muscle cells: the role of autocrine production of transforming growth factor-{beta}1 and insulin-like growth factor binding protein-3. *Am J Physiol Lung Cell Mol Physiol*, 296, L489-99.
- ITO, M. & HARTSHORNE, D. J. 1990. Phosphorylation of myosin as a regulatory mechanism in smooth muscle. *Prog Clin Biol Res*, 327, 57-72.
- JAIN, A., OLOVSSON, M., BURTON, G. J. & YUNG, H. W. 2012. Endothelin-1 induces endoplasmic reticulum stress by activating the PLC-IP(3) pathway: implications for placental pathophysiology in preeclampsia. *Am J Pathol*, 180, 2309-20.
- JANISZEWSKI, M., LOPES, L. R., CARMO, A. O., PEDRO, M. A., BRANDES, R. P., SANTOS, C. X. & LAURINDO, F. R. 2005. Regulation of NAD(P)H oxidase by associated protein disulfide isomerase in vascular smooth muscle cells. *J Biol Chem*, 280, 40813-9.
- JHA, J. C., BANAL, C., CHOW, B. S., COOPER, M. E. & JANDELEIT-DAHM, K. 2016. Diabetes and Kidney Disease: Role of Oxidative Stress. *Antioxid Redox Signal*, 25, 657-684.

- JIN, L., LI, M., WANG, H., YIN, Z., CHEN, L., ZHOU, Y., HAN, Y., CUI, Q., ZHOU, Y. & XUE, L. 2021. Transcriptome analysis of arterial and venous circulating miRNAs during hypertension. *Sci Rep*, 11, 3469.
- JUSIC, A. & DEVAUX, Y. 2019. Noncoding RNAs in Hypertension. *Hypertension*, 74, 477-492.
- KANG, K. T., SULLIVAN, J. C. & POLLOCK, J. S. 2018. Superoxide Dismutase Activity in Small Mesenteric Arteries Is Downregulated by Angiotensin II but Not by Hypertension. *Toxicol Res*, 34, 363-370.
- KAPSOKALYVAS, D., SCHIFFERS, P. M., MAIJ, N., SUYLEN, D. P., HACKENG, T. M., VAN ZANDVOORT, M. A. & DE MEY, J. G. 2014. Imaging evidence for endothelin ETA/ETB receptor heterodimers in isolated rat mesenteric resistance arteries. *Life Sci*, 111, 36-41.
- KARNIK, S. S., UNAL, H., KEMP, J. R., TIRUPULA, K. C., EGUCHI, S., VANDERHEYDEN, P. M. & THOMAS, W. G. 2015. International Union of Basic and Clinical Pharmacology. XCIX. Angiotensin Receptors: Interpreters of Pathophysiological Angiotensinergic Stimuli [corrected]. *Pharmacol Rev*, 67, 754-819
- KASSAN, M., GALAN, M., PARTYKA, M., SAIFUDEEN, Z., HENRION, D., TREBAK, M. & MATROUGUI, K. 2012. Endoplasmic reticulum stress is involved in cardiac damage and vascular endothelial dysfunction in hypertensive mice. *Arterioscler Thromb Vasc Biol*, 32, 1652-61.
- KASSAN, M., VIKRAM, A., LI, Q., KIM, Y.-R., KUMAR, S., GABANI, M., LIU, J., JACOBS, J. S. & IRANI, K. 2017a. MicroRNA-204 promotes vascular endoplasmic reticulum stress and endothelial dysfunction by targeting Sirtuin1. *Scientific Reports*, 7, 9308.
- KASSAN, M., VIKRAM, A., LI, Q., KIM, Y. R., KUMAR, S., GABANI, M., LIU, J., JACOBS, J. S. & IRANI, K. 2017b. MicroRNA-204 promotes vascular endoplasmic reticulum stress and endothelial dysfunction by targeting Sirtuin1. *Sci Rep*, 7, 9308.
- KEARNEY, P. M., WHELTON, M., REYNOLDS, K., MUNTNER, P., WHELTON, P. K. & HE, J. 2005. Global burden of hypertension: analysis of worldwide data. *Lancet*, 365, 217-23.
- KIM, D. Y., HWANG, D. I., PARK, S. M., JUNG, S. H., KIM, B., WON, K. J. & LEE, H. M. 2018. Glucose-regulated protein 78 in lipid rafts elevates vascular smooth muscle cell proliferation of spontaneously hypertensive rats by controlling platelet-derived growth factor receptor signaling. *Pflugers Arch*, 470, 1831-1843.
- KIM, H. K., LEE, H. Y., RIAZ, T. A., BHATTARAI, K. R., CHAUDHARY, M., AHN, J. H., JEONG, J., KIM, H. R. & CHAE, H. J. 2021. Chalcone suppresses tumor growth through NOX4-IRE1alpha sulfonation-RIDD-miR-23b axis. *Redox Biol*, 40, 101853.
- KIM, S. & IWAO, H. 2000. Molecular and cellular mechanisms of angiotensin II-mediated cardiovascular and renal diseases. *Pharmacol Rev*, 52, 11-34.
- KIM, S. M. & KANG, J. H. 1997. Peroxidative activity of human Cu,Zn-superoxide dismutase. *Mol Cells*, 7, 120-4.
- KIM, Y. S., GUPTA VALLUR, P., PHAETON, R., MYTHREYE, K. & HEMPEL, N. 2017. Insights into the Dichotomous Regulation of SOD2 in Cancer. *Antioxidants* (*Basel*), 6.
- KIVILUOTO, S., VERVLIET, T., IVANOVA, H., DECUYPERE, J. P., DE SMEDT, H., MISSIAEN, L., BULTYNCK, G. & PARYS, J. B. 2013. Regulation of inositol 1,4,5-trisphosphate receptors during endoplasmic reticulum stress. *Biochim Biophys Acta*, 1833, 1612-24.
- KOHAGURA, K., TANA, T., HIGA, A., YAMAZATO, M., ISHIDA, A., NAGAHAMA, K., SAKIMA, A., ISEKI, K. & OHYA, Y. 2016. Effects of xanthine oxidase

- inhibitors on renal function and blood pressure in hypertensive patients with hyperuricemia. *Hypertens Res*, 39, 593-7.
- KOHAN, D. E. & BARTON, M. 2014. Endothelin and endothelin antagonists in chronic kidney disease. *Kidney Int*, 86, 896-904.
- KONIOR, A., SCHRAMM, A., CZESNIKIEWICZ-GUZIK, M. & GUZIK, T. J. 2014. NADPH oxidases in vascular pathology. *Antioxid Redox Signal*, 20, 2794-814.
- KONUKOGLU, D. & UZUN, H. 2017. Endothelial Dysfunction and Hypertension. *Adv Exp Med Biol*, 956, 511-540.
- KOSTOV, K. 2021. The Causal Relationship between Endothelin-1 and Hypertension: Focusing on Endothelial Dysfunction, Arterial Stiffness, Vascular Remodeling, and Blood Pressure Regulation. *Life (Basel)*, 11.
- KOZOMARA, A., BIRGAOANU, M. & GRIFFITHS-JONES, S. 2019. miRBase: from microRNA sequences to function. *Nucleic Acids Research*, 47, D155-D162.
- KREBS, J., AGELLON, L. B. & MICHALAK, M. 2015. Ca(2+) homeostasis and endoplasmic reticulum (ER) stress: An integrated view of calcium signaling. *Biochem Biophys Res Commun*, 460, 114-21.
- KREBS, J., GROENENDYK, J. & MICHALAK, M. 2011. Ca2+-signaling, alternative splicing and endoplasmic reticulum stress responses. *Neurochem Res*, 36, 1198-211.
- KUBISTA, M., ANDRADE, J. M., BENGTSSON, M., FOROOTAN, A., JONAK, J., LIND, K., SINDELKA, R., SJOBACK, R., SJOGREEN, B., STROMBOM, L., STAHLBERG, A. & ZORIC, N. 2006. The real-time polymerase chain reaction. *Mol Aspects Med*, 27, 95-125.
- KUMAGAE, S., ADACHI, H., JACOBS, D. R., JR., HIRAI, Y., ENOMOTO, M., FUKAMI, A., OTSUKA, M., NANJO, Y., ESAKI, E., KUMAGAI, E., YOSHIKAWA, K., YOKOI, K., OGATA, K., TSUKAGAWA, E., KASAHARA, A., MURAYAMA, K. & IMAIZUMI, T. 2010. High level of plasma endothelin-1 predicts development of hypertension in normotensive subjects. *Am J Hypertens*, 23, 1103-7.
- KUZNETSOV, G., BROSTROM, M. A. & BROSTROM, C. O. 1992. Demonstration of a calcium requirement for secretory protein processing and export. Differential effects of calcium and dithiothreitol. *J Biol Chem*, 267, 3932-9.
- LACCHINI, S., HARVEY, A., LOPES, R., MONTEZANO, A. C., RIOS, F., SCHRODER, K., BRANDES, R. P. & TOUYZ, R. M. 2017. [BP.10.02] NOX4 DEFICIENCY LEADS TO HYPERTENSION AND VASCULAR-RENAL FIBROSIS WITH ENHANCED EFFECTS IN ANG II-DEPENDENT HYPERTENSION. *Journal of Hypertension*, 35, e345.
- LAKSHMANAN, A. P., THANDAVARAYAN, R. A., PALANIYANDI, S. S., SARI, F. R., MEILEI, H., GIRIDHARAN, V. V., SOETIKNO, V., SUZUKI, K., KODAMA, M. & WATANABE, K. 2011. Modulation of AT-1R/CHOP-JNK-Caspase12 pathway by olmesartan treatment attenuates ER stress-induced renal apoptosis in streptozotocin-induced diabetic mice. *Eur J Pharm Sci*, 44, 627-34.
- LAMBETH, J. D. 2004. NOX enzymes and the biology of reactive oxygen. *Nat Rev Immunol*, 4, 181-9.
- LANDMESSER, U., CAI, H., DIKALOV, S., MCCANN, L., HWANG, J., JO, H., HOLLAND, S. M. & HARRISON, D. G. 2002. Role of p47(phox) in vascular oxidative stress and hypertension caused by angiotensin II. *Hypertension*, 40, 511-5.
- LASSEGUE, B. & GRIENDLING, K. K. 2010. NADPH oxidases: functions and pathologies in the vasculature. *Arterioscler Thromb Vasc Biol*, 30, 653-61.
- LAURENT, S. & BOUTOUYRIE, P. 2015. The structural factor of hypertension: large and small artery alterations. *Circ Res*, 116, 1007-21.
- LAURINDO, F. R., ARAUJO, T. L. & ABRAHAO, T. B. 2014. Nox NADPH oxidases and the endoplasmic reticulum. *Antioxid Redox Signal*, 20, 2755-75.

- LAZAR, L., NAGY, B., MOLVAREC, A., SZARKA, A. & RIGO, J., JR. 2012. Role of hsa-miR-325 in the etiopathology of preeclampsia. *Mol Med Rep,* 6, 597-600.
- LAZICH, I. & BAKRIS, G. L. 2011. Endothelin antagonism in patients with resistant hypertension and hypertension nephropathy. *Contrib Nephrol*, 172, 223-234.
- LEBEAU, P. F., PLATKO, K., BYUN, J. H. & AUSTIN, R. C. 2021. Calcium as a reliable marker for the quantitative assessment of endoplasmic reticulum stress in live cells. *J Biol Chem*, 296, 100779.
- LEE, A. H., IWAKOSHI, N. N. & GLIMCHER, L. H. 2003. XBP-1 regulates a subset of endoplasmic reticulum resident chaperone genes in the unfolded protein response. *Mol Cell Biol*, 23, 7448-59.
- LEE, H. Y., KIM, H. K., HOANG, T. H., YANG, S., KIM, H. R. & CHAE, H. J. 2020. The correlation of IRE1alpha oxidation with Nox4 activation in aging-associated vascular dysfunction. *Redox Biol*, 37, 101727.
- LEE, M. Y. & GRIENDLING, K. K. 2008. Redox signaling, vascular function, and hypertension. *Antioxid Redox Signal*, 10, 1045-59.
- LEE, R. M., DICKHOUT, J. G. & SANDOW, S. L. 2017. Vascular structural and functional changes: their association with causality in hypertension: models, remodeling and relevance. *Hypertens Res*, 40, 311-323.
- LERNER, A. G., UPTON, J. P., PRAVEEN, P. V., GHOSH, R., NAKAGAWA, Y., IGBARIA, A., SHEN, S., NGUYEN, V., BACKES, B. J., HEIMAN, M., HEINTZ, N., GREENGARD, P., HUI, S., TANG, Q., TRUSINA, A., OAKES, S. A. & PAPA, F. R. 2012. IRE1α induces thioredoxin-interacting protein to activate the NLRP3 inflammasome and promote programmed cell death under irremediable ER stress. *Cell Metab*, 16, 250-64.
- LI, G., MONGILLO, M., CHIN, K. T., HARDING, H., RON, D., MARKS, A. R. & TABAS, I. 2009. Role of ERO1-alpha-mediated stimulation of inositol 1,4,5-triphosphate receptor activity in endoplasmic reticulum stress-induced apoptosis. *J Cell Biol*, 186, 783-92.
- LI, G., SCULL, C., OZCAN, L. & TABAS, I. 2010. NADPH oxidase links endoplasmic reticulum stress, oxidative stress, and PKR activation to induce apoptosis. *J Cell Biol*, 191, 1113-25.
- LI, J. M. & SHAH, A. M. 2003. Mechanism of endothelial cell NADPH oxidase activation by angiotensin II. Role of the p47phox subunit. *J Biol Chem*, 278, 12094-100.
- LI, J. S. & SCHIFFRIN, E. L. 1995. Effect of chronic treatment of adult spontaneously hypertensive rats with an endothelin receptor antagonist. *Hypertension*, 25, 495-500.
- LI, S., ZHU, J., ZHANG, W., CHEN, Y., ZHANG, K., POPESCU, L. M., MA, X., LAU, W. B., RONG, R., YU, X., WANG, B., LI, Y., XIAO, C., ZHANG, M., WANG, S., YU, L., CHEN, A. F., YANG, X. & CAI, J. 2011. Signature microRNA expression profile of essential hypertension and its novel link to human cytomegalovirus infection. *Circulation*, 124, 175-84.
- LI, X., WEI, Y. & WANG, Z. 2018. microRNA-21 and hypertension. *Hypertension Research*, 41, 649-661.
- LIANG, B., WANG, S., WANG, Q., ZHANG, W., VIOLLET, B., ZHU, Y. & ZOU, M. H. 2013. Aberrant endoplasmic reticulum stress in vascular smooth muscle increases vascular contractility and blood pressure in mice deficient of AMP-activated protein kinase-alpha2 in vivo. *Arterioscler Thromb Vasc Biol*, 33, 595-604.
- LIN, J. H., LI, H., YASUMURA, D., COHEN, H. R., ZHANG, C., PANNING, B., SHOKAT, K. M., LAVAIL, M. M. & WALTER, P. 2007. IRE1 signaling affects cell fate during the unfolded protein response. *Science*, 318, 944-9.
- LIN, S., LONG, H., HOU, L., ZHANG, M., TING, J., LIN, H., ZHENG, P., LEI, W., YIN, K. & ZHAO, G. 2023. Crosstalk between endoplasmic reticulum stress and non-coding RNAs in cardiovascular diseases. *Wiley Interdiscip Rev RNA*, 14, e1767.

- LINDESAY, G., BEZIE, Y., RAGONNET, C., DUCHATELLE, V., DHARMASENA, C., VILLENEUVE, N. & VAYSSETTES-COURCHAY, C. 2018. Differential Stiffening between the Abdominal and Thoracic Aorta: Effect of Salt Loading in Stroke-Prone Hypertensive Rats. *J Vasc Res*, 55, 144-158.
- LITTLE, P. J., NEYLON, C. B., TKACHUK, V. A. & BOBIK, A. 1992. Endothelin-1 and endothelin-3 stimulate calcium mobilization by different mechanisms in vascular smooth muscle. *Biochem Biophys Res Commun*, 183, 694-700.
- LIU, C., CHEN, Y., KOCHEVAR, I. E. & JURKUNAS, U. V. 2014. Decreased DJ-1 leads to impaired Nrf2-regulated antioxidant defense and increased UV-A-induced apoptosis in corneal endothelial cells. *Invest Ophthalmol Vis Sci*, 55, 5551-60.
- LIU, C., YANG, J., WU, H. & LI, J. 2019a. Downregulated miR-585-3p promotes cell growth and proliferation in colon cancer by upregulating PSME3. *Onco Targets Ther*, 12, 6525-6534.
- LIU, G., WU, F., JIANG, X., QUE, Y., QIN, Z., HU, P., LEE, K. S. S., YANG, J., ZENG, C., HAMMOCK, B. D. & TONG, X. 2020. Inactivation of Cys(674) in SERCA2 increases BP by inducing endoplasmic reticulum stress and soluble epoxide hydrolase. *Br J Pharmacol*, 177, 1793-1805.
- LIU, M., SHI, G., ZHOU, A., RUPERT, C. E., COULOMBE, K. L. K. & DUDLEY, S. C., JR. 2018. Activation of the unfolded protein response downregulates cardiac ion channels in human induced pluripotent stem cell-derived cardiomyocytes. *J Mol Cell Cardiol*, 117, 62-71.
- LIU, M., XUE, G., LIU, R., WANG, Y., SHENG, X. & SUN, W. 2023. Saponin from Platycodi radix inactivates PI3K/AKT signaling pathway to hinder colorectal cancer cell proliferation, invasion, and migration through miR-181c/d-5p/RBM47. *Mol Carcinog*, 62, 174-184.
- LIU, X., YUAN, W., YANG, L., LI, J. & CAI, J. 2019b. miRNA Profiling of Exosomes from Spontaneous Hypertensive Rats Using Next-Generation Sequencing. *J Cardiovasc Transl Res*, 12, 75-83.
- LIU, Y., JIANG, G., LV, C. & YANG, C. 2022. miR-222-5p promotes dysfunction of human vascular smooth muscle cells by targeting RB1. *Environ Toxicol*, 37, 683-694.
- LIU, Z., LV, Y., ZHAO, N., GUAN, G. & WANG, J. 2015. Protein kinase R-like ER kinase and its role in endoplasmic reticulum stress-decided cell fate. *Cell Death Dis*, 6, e1822.
- LIVAK, K. J. & SCHMITTGEN, T. D. 2001. Analysis of relative gene expression data using real-time quantitative PCR and the 2(-Delta Delta C(T)) Method. *Methods*, 25, 402-8.
- LOB, H. E., SCHULTZ, D., MARVAR, P. J., DAVISSON, R. L. & HARRISON, D. G. 2013. Role of the NADPH oxidases in the subfornical organ in angiotensin II-induced hypertension. *Hypertension*, 61, 382-7.
- LOPERENA, R. & HARRISON, D. G. 2017. Oxidative Stress and Hypertensive Diseases. *Med Clin North Am*, 101, 169-193.
- LOPES, R. A., NEVES, K. B., TOSTES, R. C., MONTEZANO, A. C. & TOUYZ, R. M. 2015. Downregulation of Nuclear Factor Erythroid 2-Related Factor and Associated Antioxidant Genes Contributes to Redox-Sensitive Vascular Dysfunction in Hypertension. *Hypertension*, 66, 1240-50.
- LUCIANI, D. S., GWIAZDA, K. S., YANG, T. L., KALYNYAK, T. B., BYCHKIVSKA, Y., FREY, M. H., JEFFREY, K. D., SAMPAIO, A. V., UNDERHILL, T. M. & JOHNSON, J. D. 2009. Roles of IP3R and RyR Ca2+ channels in endoplasmic reticulum stress and beta-cell death. *Diabetes*, 58, 422-32.
- MAJZUNOVA, M., DOVINOVA, I., BARANCIK, M. & CHAN, J. Y. 2013. Redox signaling in pathophysiology of hypertension. *J Biomed Sci*, 20, 69.

- MANRIQUE, C., LASTRA, G., GARDNER, M. & SOWERS, J. R. 2009. The renin angiotensin aldosterone system in hypertension: roles of insulin resistance and oxidative stress. *Med Clin North Am*, 93, 569-82.
- MARCINIAK, S. J., CHAMBERS, J. E. & RON, D. 2022. Pharmacological targeting of endoplasmic reticulum stress in disease. *Nature Reviews Drug Discovery*, 21, 115-140.
- MARCINIAK, S. J., YUN, C. Y., OYADOMARI, S., NOVOA, I., ZHANG, Y., JUNGREIS, R., NAGATA, K., HARDING, H. P. & RON, D. 2004. CHOP induces death by promoting protein synthesis and oxidation in the stressed endoplasmic reticulum. *Genes Dev*, 18, 3066-77.
- MARTINEZ-QUINONES, P., MCCARTHY, C. G., WATTS, S. W., KLEE, N. S., KOMIC, A., CALMASINI, F. B., PRIVIERO, F., WARNER, A., CHENGHAO, Y. & WENCESLAU, C. F. 2018. Hypertension Induced Morphological and Physiological Changes in Cells of the Arterial Wall. *Am J Hypertens*, 31, 1067-1078.
- MATSHAZI, D. M., WEALE, C. J., ERASMUS, R. T., KENGNE, A. P., DAVIDS, S. F. G., RAGHUBEER, S., HECTOR, S., DAVISON, G. M. & MATSHA, T. E. 2021. MicroRNA Profiles in Normotensive and Hypertensive South African Individuals. *Front Cardiovasc Med*, 8, 645541.
- MATSUDA, K., LOZINSKAYA, I. & COX, R. H. 1997. Augmented contributions of voltage-gated Ca2+ channels to contractile responses in spontaneously hypertensive rat mesenteric arteries. *Am J Hypertens*, 10, 1231-9.
- MATSUMURA, Y., FUJITA, K., MIYAZAKI, Y., TAKAOKA, M. & MORIMOTO, S. 1995. Involvement of endothelin-1 in deoxycorticosterone acetate-salt-induced hypertension and cardiovascular hypertrophy. *J Cardiovasc Pharmacol*, 26 Suppl 3, S456-8.
- MAYET, J. & HUGHES, A. 2003. Cardiac and vascular pathophysiology in hypertension. *Heart*, 89, 1104-9.
- MCCOY, E. K. & LISENBY, K. M. 2021. Aprocitentan (a Dual Endothelin-Receptor Antagonist) for Treatment-Resistant Hypertension. *J Cardiovasc Pharmacol*, 77, 699-706.
- MCMAHON, M., SAMALI, A. & CHEVET, E. 2017. Regulation of the unfolded protein response by noncoding RNA. *Am J Physiol Cell Physiol*, 313, C243-c254.
- MCMASTER, W. G., KIRABO, A., MADHUR, M. S. & HARRISON, D. G. 2015. Inflammation, immunity, and hypertensive end-organ damage. *Circ Res*, 116, 1022-33.
- MEDINA, M. V., SAPOCHNIK, D., GARCIA SOLA, M. & COSO, O. 2020. Regulation of the Expression of Heme Oxygenase-1: Signal Transduction, Gene Promoter Activation, and Beyond. *Antioxid Redox Signal*, 32, 1033-1044.
- MENIKDIWELA, K. R., RAMALINGAM, L., ALLEN, L., SCOGGIN, S., KALUPAHANA, N. S. & MOUSTAID-MOUSSA, N. 2019. Angiotensin II Increases Endoplasmic Reticulum Stress in Adipose Tissue and Adipocytes. *Sci Rep.* 9, 8481.
- MIAO, C., CHANG, J. & ZHANG, G. 2018. Recent research progress of microRNAs in hypertension pathogenesis, with a focus on the roles of miRNAs in pulmonary arterial hypertension. *Mol Biol Rep*, 45, 2883-2896.
- MILLS, K. T., STEFANESCU, A. & HE, J. 2020. The global epidemiology of hypertension. *Nat Rev Nephrol*, 16, 223-237.
- MINKENBERG, I. & FERBER, E. 1984. Lucigenin-dependent chemiluminescence as a new assay for NAD(P)H-oxidase activity in particulate fractions of human polymorphonuclear leukocytes. *J Immunol Methods*, 71, 61-7.

- MISÁRKOVÁ, E., BEHULIAK, M., BENCZE, M. & ZICHA, J. 2016. Excitation-contraction coupling and excitation-transcription coupling in blood vessels: their possible interactions in hypertensive vascular remodeling. *Physiol Res*, 65, 173-91.
- MIYANO, K., OKAMOTO, S., YAMAUCHI, A., KAWAI, C., KAJIKAWA, M., KIYOHARA, T., TAMURA, M., TAURA, M. & KURIBAYASHI, F. 2020. The NADPH oxidase NOX4 promotes the directed migration of endothelial cells by stabilizing vascular endothelial growth factor receptor 2 protein. *J Biol Chem*, 295, 11877-11890.
- MIYAUCHI, T. & SAKAI, S. 2019. Endothelin and the heart in health and diseases. *Peptides*, 111, 77-88.
- MOHAMMED-ALI, Z., LU, C., MARWAY, M. K., CARLISLE, R. E., ASK, K., LUKIC, D., KREPINSKY, J. C. & DICKHOUT, J. G. 2017. Endoplasmic reticulum stress inhibition attenuates hypertensive chronic kidney disease through reduction in proteinuria. *Sci Rep*, 7, 41572.
- MOHANTY, J. G., JAFFE, J. S., SCHULMAN, E. S. & RAIBLE, D. G. 1997. A highly sensitive fluorescent micro-assay of H2O2 release from activated human leukocytes using a dihydroxyphenoxazine derivative. *J Immunol Methods*, 202, 133-41.
- MONTEZANO, A. C., DULAK-LIS, M., TSIROPOULOU, S., HARVEY, A., BRIONES, A. M. & TOUYZ, R. M. 2015. Oxidative stress and human hypertension: vascular mechanisms, biomarkers, and novel therapies. *Can J Cardiol*, 31, 631-41.
- MONTEZANO, A. C. & TOUYZ, R. M. 2012. Oxidative stress, Noxs, and hypertension: experimental evidence and clinical controversies. *Ann Med*, 44 Suppl 1, S2-16.
- MONTEZANO, A. C. & TOUYZ, R. M. 2014. Reactive oxygen species, vascular Noxs, and hypertension: focus on translational and clinical research. *Antioxid Redox Signal*, 20, 164-82.
- MORAWIETZ, H. 2018. Cardiovascular protection by Nox4. *Cardiovasc Res*, 114, 353-355.
- MOZZINI, C., COMINACINI, L., GARBIN, U. & FRATTA PASINI, A. M. 2017. Endoplasmic Reticulum Stress, NRF2 Signalling and Cardiovascular Diseases in a Nutshell. *Curr Atheroscler Rep*, 19, 33.
- MULVANY, M. J. 1993. Resistance vessel structure and the pathogenesis of hypertension. *J Hypertens Suppl*, 11, S7-12.
- MULVANY, M. J. & AALKJAER, C. 1990. Structure and function of small arteries. *Physiol Rev*, 70, 921-61.
- MULVANY, M. J. & HALPERN, W. 1977. Contractile properties of small arterial resistance vessels in spontaneously hypertensive and normotensive rats. *Circ Res*, 41, 19-26.
- MÜNZEL, T., SINNING, C., POST, F., WARNHOLTZ, A. & SCHULZ, E. 2008. Pathophysiology, diagnosis and prognostic implications of endothelial dysfunction. *Ann Med*, 40, 180-96.
- NADAR, S. K. & LIP, G. Y. H. 2021. The heart in hypertension. *Journal of Human Hypertension*, 35, 383-386.
- NAIEL, S., CARLISLE, R. E., LU, C., TAT, V. & DICKHOUT, J. G. 2019. Endoplasmic reticulum stress inhibition blunts the development of essential hypertension in the spontaneously hypertensive rat. *Am J Physiol Heart Circ Physiol*, 316, H1214-H1223.
- NEMENOFF, R. A., HORITA, H., OSTRIKER, A. C., FURGESON, S. B., SIMPSON, P. A., VANPUTTEN, V., CROSSNO, J., OFFERMANNS, S. & WEISER-EVANS, M. C. 2011. SDF-1α induction in mature smooth muscle cells by inactivation of PTEN is a critical mediator of exacerbated injury-induced neointima formation. *Arterioscler Thromb Vasc Biol*, 31, 1300-8.

- NIFOROU, K., CHEIMONIDOU, C. & TROUGAKOS, I. P. 2014. Molecular chaperones and proteostasis regulation during redox imbalance. *Redox Biol*, 2, 323-32.
- NISHIKIBE, M., TSUCHIDA, S., OKADA, M., FUKURODA, T., SHIMAMOTO, K., YANO, M., ISHIKAWA, K. & IKEMOTO, F. 1993. Antihypertensive effect of a newly synthesized endothelin antagonist, BQ-123, in a genetic hypertensive model. *Life Sci*, 52, 717-24.
- NISHIYAMA, A., MATSUI, M., IWATA, S., HIROTA, K., MASUTANI, H., NAKAMURA, H., TAKAGI, Y., SONO, H., GON, Y. & YODOI, J. 1999. Identification of thioredoxin-binding protein-2/vitamin D(3) up-regulated protein 1 as a negative regulator of thioredoxin function and expression. *J Biol Chem*, 274, 21645-50.
- NIU, Y. & TANG, G. 2019. miR-185-5p targets ROCK2 and inhibits cell migration and invasion of hepatocellular carcinoma. *Oncol Lett*, 17, 5087-5093.
- NLANDU KHODO, S., DIZIN, E., SOSSAUER, G., SZANTO, I., MARTIN, P. Y., FERAILLE, E., KRAUSE, K. H. & DE SEIGNEUX, S. 2012. NADPH-oxidase 4 protects against kidney fibrosis during chronic renal injury. *J Am Soc Nephrol*, 23, 1967-76.
- NOSALSKI, R., MIKOLAJCZYK, T., SIEDLINSKI, M., SAJU, B., KOZIOL, J., MAFFIA, P. & GUZIK, T. J. 2020. Nox1/4 inhibition exacerbates age dependent perivascular inflammation and fibrosis in a model of spontaneous hypertension. *Pharmacol Res*, 161, 105235.
- NOVOA, I., ZHANG, Y., ZENG, H., JUNGREIS, R., HARDING, H. P. & RON, D. 2003. Stress-induced gene expression requires programmed recovery from translational repression. *EMBO J*, 22, 1180-7.
- OAKES, S. A. & PAPA, F. R. 2015. The role of endoplasmic reticulum stress in human pathology. *Annu Rev Pathol*, 10, 173-94.
- OCHOA, C. D., WU, R. F. & TERADA, L. S. 2018. ROS signaling and ER stress in cardiovascular disease. *Mol Aspects Med*, 63, 18-29.
- OLTRA, M., VIDAL-GIL, L., MAISTO, R., SANCHO-PELLUZ, J. & BARCIA, J. M. 2020. Oxidative stress-induced angiogenesis is mediated by miR-205-5p. *J Cell Mol Med*, 24, 1428-1436.
- ONG, G. & LOGUE, S. E. 2023. Unfolding the Interactions between Endoplasmic Reticulum Stress and Oxidative Stress. *Antioxidants (Basel)*, 12.
- OPARIL, S., ACELAJADO, M. C., BAKRIS, G. L., BERLOWITZ, D. R., CIFKOVA, R., DOMINICZAK, A. F., GRASSI, G., JORDAN, J., POULTER, N. R., RODGERS, A. & WHELTON, P. K. 2018a. Hypertension. *Nat Rev Dis Primers*, 4, 18014.
- OPARIL, S., ACELAJADO, M. C., BAKRIS, G. L., BERLOWITZ, D. R., CÍFKOVÁ, R., DOMINICZAK, A. F., GRASSI, G., JORDAN, J., POULTER, N. R., RODGERS, A. & WHELTON, P. K. 2018b. Hypertension. *Nat Rev Dis Primers*, 4, 18014.
- OWENS, G. K., KUMAR, M. S. & WAMHOFF, B. R. 2004. Molecular regulation of vascular smooth muscle cell differentiation in development and disease. *Physiol Rev*, 84, 767-801.
- PADILLA, J. & JENKINS, N. T. 2013. Induction of endoplasmic reticulum stress impairs insulin-stimulated vasomotor relaxation in rat aortic rings: role of endothelin-1. *J Physiol Pharmacol*, 64, 557-64.
- PAKOS-ZEBRUCKA, K., KORYGA, I., MNICH, K., LJUJIC, M., SAMALI, A. & GORMAN, A. M. 2016. The integrated stress response. *EMBO Rep*, 17, 1374-1395.
- PALAO, T., SWARD, K., JONGEJAN, A., MOERLAND, P. D., DE VOS, J., VAN WEERT, A., ARRIBAS, S. M., GROMA, G., VANBAVEL, E. & BAKKER, E. N. 2015a. Gene Expression and MicroRNA Expression Analysis in Small Arteries of Spontaneously Hypertensive Rats. Evidence for ER Stress. *PLoS One*, 10, e0137027.

- PALAO, T., SWÄRD, K., JONGEJAN, A., MOERLAND, P. D., DE VOS, J., VAN WEERT, A., ARRIBAS, S. M., GROMA, G., VANBAVEL, E. & BAKKER, E. N. 2015b. Gene Expression and MicroRNA Expression Analysis in Small Arteries of Spontaneously Hypertensive Rats. Evidence for ER Stress. *PLoS One*, 10, e0137027.
- PALMA, F. R., HE, C., DANES, J. M., PAVIANI, V., COELHO, D. R., GANTNER, B. N. & BONINI, M. G. 2020. Mitochondrial Superoxide Dismutase: What the Established, the Intriguing, and the Novel Reveal About a Key Cellular Redox Switch. *Antioxid Redox Signal*, 32, 701-714.
- PANZA, J. A., CASINO, P. R., BADAR, D. M. & QUYYUMI, A. A. 1993. Effect of increased availability of endothelium-derived nitric oxide precursor on endothelium-dependent vascular relaxation in normal subjects and in patients with essential hypertension. *Circulation*, 87, 1475-81.
- PARAVICINI, T. M. & TOUYZ, R. M. 2008. NADPH oxidases, reactive oxygen species, and hypertension: clinical implications and therapeutic possibilities. *Diabetes Care*, 31 Suppl 2, S170-80.
- PEDRUZZI, E., GUICHARD, C., OLLIVIER, V., DRISS, F., FAY, M., PRUNET, C., MARIE, J. C., POUZET, C., SAMADI, M., ELBIM, C., O'DOWD, Y., BENS, M., VANDEWALLE, A., GOUGEROT-POCIDALO, M. A., LIZARD, G. & OGIER-DENIS, E. 2004. NAD(P)H oxidase Nox-4 mediates 7-ketocholesterol-induced endoplasmic reticulum stress and apoptosis in human aortic smooth muscle cells. *Mol Cell Biol*, 24, 10703-17.
- PINTO-SIETSMA, S. J. & PAUL, M. 1998. A role for endothelin in the pathogenesis of hypertension: fact or fiction? *Kidney Int Suppl*, 67, S115-21.
- POLLOCK, D. M. & POLLOCK, J. S. 2001. Evidence for endothelin involvement in the response to high salt. *Am J Physiol Renal Physiol*, 281, F144-50.
- POVLSEN, A. L., GRIMM, D., WEHLAND, M., INFANGER, M. & KRÜGER, M. 2020. The Vasoactive Mas Receptor in Essential Hypertension. *J Clin Med*, 9.
- POYNTON, R. A. & HAMPTON, M. B. 2014. Peroxiredoxins as biomarkers of oxidative stress. *Biochim Biophys Acta*, 1840, 906-12.
- PRESCOTT, G., SILVERSIDES, D. W., CHIU, S. M. & REUDELHUBER, T. L. 2000. Contribution of circulating renin to local synthesis of angiotensin peptides in the heart. *Physiol Genomics*, 4, 67-73.
- QIAN, Z., ZHU, L., LI, Y., LI, Y., WU, Y., FU, S. & YANG, D. 2021. Icarrin prevents cardiomyocyte apoptosis in spontaneously hypertensive rats by inhibiting endoplasmic reticulum stress pathways. *J Pharm Pharmacol*, 73, 1023-1032.
- RADI, R., CASSINA, A., HODARA, R., QUIJANO, C. & CASTRO, L. 2002. Peroxynitrite reactions and formation in mitochondria. *Free Radic Biol Med*, 33, 1451-64.
- RAJARAM, R. D., DISSARD, R., FAIVRE, A., INO, F., DELITSIKOU, V., JAQUET, V., CAGARELLI, T., LINDENMEYER, M., JANSEN-DUERR, P., COHEN, C., MOLL, S. & DE SEIGNEUX, S. 2019. Tubular NOX4 expression decreases in chronic kidney disease but does not modify fibrosis evolution. *Redox Biol*, 26, 101234.
- RASTOGI, R., GENG, X., LI, F. & DING, Y. 2016. NOX Activation by Subunit Interaction and Underlying Mechanisms in Disease. *Front Cell Neurosci*, 10, 301.
- RAUTUREAU, Y. & SCHIFFRIN, E. L. 2012. Endothelin in hypertension: an update. *Curr Opin Nephrol Hypertens*, 21, 128-36.
- RAY, R., MURDOCH, C. E., WANG, M., SANTOS, C. X., ZHANG, M., ALOM-RUIZ, S., ANILKUMAR, N., OUATTARA, A., CAVE, A. C., WALKER, S. J., GRIEVE, D. J., CHARLES, R. L., EATON, P., BREWER, A. C. & SHAH, A. M. 2011. Endothelial Nox4 NADPH oxidase enhances vasodilatation and reduces blood pressure in vivo. *Arterioscler Thromb Vasc Biol*, 31, 1368-76.

- REICHARD, J. F., MOTZ, G. T. & PUGA, A. 2007. Heme oxygenase-1 induction by NRF2 requires inactivation of the transcriptional repressor BACH1. *Nucleic Acids Res.* 35, 7074-86.
- RENNA, N. F., DE LAS HERAS, N. & MIATELLO, R. M. 2013. Pathophysiology of vascular remodeling in hypertension. *Int J Hypertens*, 2013, 808353.
- REPETTO, M., SEMPRINE, J. & BOVERIS, A. 2012. Lipid peroxidation: chemical mechanism, biological implications and analytical determination. *Lipid peroxidation*, 1, 3-30.
- RIZZONI, D., AGABITI-ROSEI, C. & DE CIUCEIS, C. 2023. State of the Art Review: Vascular Remodeling in Hypertension. *Am J Hypertens*, 36, 1-13.
- RODRIGO, R., GONZALEZ, J. & PAOLETTO, F. 2011. The role of oxidative stress in the pathophysiology of hypertension. *Hypertens Res*, 34, 431-40.
- RODRIGUEZ-ITURBE, B., FERREBUZ, A., VANEGAS, V., QUIROZ, Y., MEZZANO, S. & VAZIRI, N. D. 2005. Early and sustained inhibition of nuclear factor-kappaB prevents hypertension in spontaneously hypertensive rats. *J Pharmacol Exp Ther*, 315, 51-7.
- ROE, N. D. & REN, J. 2012. Nitric oxide synthase uncoupling: a therapeutic target in cardiovascular diseases. *Vascul Pharmacol*, 57, 168-72.
- RON, D. & HUBBARD, S. R. 2008. How IRE1 reacts to ER stress. Cell, 132, 24-6.
- RON, D. & WALTER, P. 2007a. Signal integration in the endoplasmic reticulum unfolded protein response. *Nature Reviews Molecular Cell Biology*, 8, 519-529.
- RON, D. & WALTER, P. 2007b. Signal integration in the endoplasmic reticulum unfolded protein response. *Nat Rev Mol Cell Biol*, 8, 519-29.
- ROSSI, C., ZINI, R., RONTAUROLI, S., RUBERTI, S., PRUDENTE, Z., BARBIERI, G., BIANCHI, E., SALATI, S., GENOVESE, E., BARTALUCCI, N., GUGLIELMELLI, P., TAGLIAFICO, E., ROSTI, V., BAROSI, G., VANNUCCHI, A. M., MANFREDINI, R. & INVESTIGATORS, A. 2018. Role of TGF-beta1/miR-382-5p/SOD2 axis in the induction of oxidative stress in CD34+ cells from primary myelofibrosis. *Mol Oncol*, 12, 2102-2123.
- ROUSSET, F., CARNESECCHI, S., SENN, P. & KRAUSE, K. H. 2015. NOX3-TARGETED THERAPIES FOR INNER EAR PATHOLOGIES. *Curr Pharm Des*, 21, 5977-87.
- RUSSO, D., MINUTOLO, R., CLIENTI, C., DE NICOLA, L., IODICE, C., SAVINO, F. A. & ANDREUCCI, V. E. 1999. Endothelin-1 released by vascular smooth muscle cells enhances vascular responsiveness of rat mesenteric arterial bed exposed to high perfusion flow. *Am J Hypertens*, 12, 1119-23.
- SAITO, T. & SAETROM, P. 2010. MicroRNAs targeting and target prediction. *New Biotechnology*, 27, 243-249.
- SANDOVAL, Y. H., ATEF, M. E., LEVESQUE, L. O., LI, Y. & ANAND-SRIVASTAVA, M. B. 2014. Endothelin-1 signaling in vascular physiology and pathophysiology. *Curr Vasc Pharmacol*, 12, 202-14.
- SANTILLO, M., COLANTUONI, A., MONDOLA, P., GUIDA, B. & DAMIANO, S. 2015. NOX signaling in molecular cardiovascular mechanisms involved in the blood pressure homeostasis. *Front Physiol*, **6**, 194.
- SANTOS, C. X., HAFSTAD, A. D., BERETTA, M., ZHANG, M., MOLENAAR, C., KOPEC, J., FOTINOU, D., MURRAY, T. V., COBB, A. M., MARTIN, D., ZEH SILVA, M., ANILKUMAR, N., SCHRODER, K., SHANAHAN, C. M., BREWER, A. C., BRANDES, R. P., BLANC, E., PARSONS, M., BELOUSOV, V., CAMMACK, R., HIDER, R. C., STEINER, R. A. & SHAH, A. M. 2016. Targeted redox inhibition of protein phosphatase 1 by Nox4 regulates eIF2alpha-mediated stress signaling. *EMBO J*, 35, 319-34.
- SARCINELLI, C., DRAGIC, H., PIECYK, M., BARBET, V., DURET, C., BARTHELAIX, A., FERRARO-PEYRET, C., FAUVRE, J., RENNO, T.,

- CHAVEROUX, C. & MANIÉ, S. N. 2020. ATF4-Dependent NRF2 Transcriptional Regulation Promotes Antioxidant Protection during Endoplasmic Reticulum Stress. *Cancers (Basel)*, 12.
- SCHERER, N. M. & DEAMER, D. W. 1986. Oxidative stress impairs the function of sarcoplasmic reticulum by oxidation of sulfhydryl groups in the Ca2+-ATPase. *Arch Biochem Biophys*, 246, 589-601.
- SCHIEBER, M. & CHANDEL, N. S. 2014. ROS function in redox signaling and oxidative stress. *Curr Biol*, 24, R453-62.
- SCHIFFRIN, E. L. 1998. Endothelin and endothelin antagonists in hypertension. *J Hypertens*, 16, 1891-5.
- SCHIFFRIN, E. L. 2004. Remodeling of resistance arteries in essential hypertension and effects of antihypertensive treatment. *Am J Hypertens*, 17, 1192-200.
- SCHIFFRIN, E. L. 2012. Vascular remodeling in hypertension: mechanisms and treatment. *Hypertension*, 59, 367-74.
- SCHIFFRIN, E. L., DENG, L. Y. & LAROCHELLE, P. 1993. Morphology of resistance arteries and comparison of effects of vasoconstrictors in mild essential hypertensive patients. *Clin Invest Med*, 16, 177-86.
- SCHIFFRIN, E. L., PARK, J. B., INTENGAN, H. D. & TOUYZ, R. M. 2000. Correction of arterial structure and endothelial dysfunction in human essential hypertension by the angiotensin receptor antagonist losartan. *Circulation*, 101, 1653-9.
- SCHIFFRIN, E. L. & TOUYZ, R. M. 1998. Vascular biology of endothelin. *J Cardiovasc Pharmacol*, 32 Suppl 3, S2-13.
- SCHRODER, K., ZHANG, M., BENKHOFF, S., MIETH, A., PLIQUETT, R., KOSOWSKI, J., KRUSE, C., LUEDIKE, P., MICHAELIS, U. R., WEISSMANN, N., DIMMELER, S., SHAH, A. M. & BRANDES, R. P. 2012. Nox4 is a protective reactive oxygen species generating vascular NADPH oxidase. *Circ Res*, 110, 1217-25.
- SCHURMANN, C., REZENDE, F., KRUSE, C., YASAR, Y., LOWE, O., FORK, C., VAN DE SLUIS, B., BREMER, R., WEISSMANN, N., SHAH, A. M., JO, H., BRANDES, R. P. & SCHRODER, K. 2015. The NADPH oxidase Nox4 has antiatherosclerotic functions. *Eur Heart J*, 36, 3447-56.
- SCIARRETTA, S., ZHAI, P., SHAO, D., ZABLOCKI, D., NAGARAJAN, N., TERADA, L. S., VOLPE, M. & SADOSHIMA, J. 2013. Activation of NADPH oxidase 4 in the endoplasmic reticulum promotes cardiomyocyte autophagy and survival during energy stress through the protein kinase RNA-activated-like endoplasmic reticulum kinase/eukaryotic initiation factor 2alpha/activating transcription factor 4 pathway. *Circ Res*, 113, 1253-64.
- SEPULVEDA-FRAGOSO, V., ALEXANDRE-SANTOS, B., SALLES, A. C. P., PROENCA, A. B., DE PAULA ALVES, A. P., VAZQUEZ-CARRERA, M., NOBREGA, A. C. L., FRANTZ, E. D. C. & MAGLIANO, D. C. 2021. Crosstalk between the renin-angiotensin system and the endoplasmic reticulum stress in the cardiovascular system: Lessons learned so far. *Life Sci*, 284, 119919.
- SEVIER, C. S. & KAISER, C. A. 2008. Ero1 and redox homeostasis in the endoplasmic reticulum. *Biochimica et Biophysica Acta (BBA) Molecular Cell Research*, 1783, 549-556.
- SHAHID, M. & BUYS, E. S. 2013. Assessing murine resistance artery function using pressure myography. *J Vis Exp*.
- SHANAHAN, C. M. & FURMANIK, M. 2017. Endoplasmic Reticulum Stress in Arterial Smooth Muscle Cells: A Novel Regulator of Vascular Disease. *Curr Cardiol Rev*, 13, 94-105.
- SHARIFI, A. M., HE, G., TOUYZ, R. M. & SCHIFFRIN, E. L. 1998. Vascular endothelin-1 expression and effect of an endothelin ETA antagonist on structure

- and function of small arteries from stroke-prone spontaneously hypertensive rats. *J Cardiovasc Pharmacol*, 31 Suppl 1, S309-12.
- SHIMIZU, T., HIGASHIJIMA, Y., KANKI, Y., NAKAKI, R., KAWAMURA, T., URADE, Y. & WADA, Y. 2021. PERK inhibition attenuates vascular remodeling in pulmonary arterial hypertension caused by BMPR2 mutation. *Sci Signal*, 14.
- SHIRAKURA, T., NOMURA, J., MATSUI, C., KOBAYASHI, T., TAMURA, M. & MASUZAKI, H. 2016. Febuxostat, a novel xanthine oxidoreductase inhibitor, improves hypertension and endothelial dysfunction in spontaneously hypertensive rats. *Naunyn Schmiedebergs Arch Pharmacol*, 389, 831-8.
- SIES, H. & JONES, D. P. 2020. Reactive oxygen species (ROS) as pleiotropic physiological signalling agents. *Nat Rev Mol Cell Biol*, 21, 363-383.
- SILVA, I. V. G., DE FIGUEIREDO, R. C. & RIOS, D. R. A. 2019. Effect of Different Classes of Antihypertensive Drugs on Endothelial Function and Inflammation. *Int J Mol Sci*, 20.
- SIMIC, D. V., MIMIC-OKA, J., PLJESA-ERCEGOVAC, M., SAVIC-RADOJEVIC, A., OPACIC, M., MATIC, D., IVANOVIC, B. & SIMIC, T. 2006. Byproducts of oxidative protein damage and antioxidant enzyme activities in plasma of patients with different degrees of essential hypertension. *J Hum Hypertens*, 20, 149-55.
- SIWECKA, N., ROZPEDEK-KAMINSKA, W., WAWRZYNKIEWICZ, A., PYTEL, D., DIEHL, J. A. & MAJSTEREK, I. 2021. The Structure, Activation and Signaling of IRE1 and Its Role in Determining Cell Fate. *Biomedicines*, 9.
- SMITH, R. E., TRAN, K., SMITH, C. C., MCDONALD, M., SHEJWALKAR, P. & HARA, K. 2016. The Role of the Nrf2/ARE Antioxidant System in Preventing Cardiovascular Diseases. *Diseases*, 4.
- SONG, M. K., PARK, Y. K. & RYU, J. C. 2013. Polycyclic aromatic hydrocarbon (PAH)-mediated upregulation of hepatic microRNA-181 family promotes cancer cell migration by targeting MAPK phosphatase-5, regulating the activation of p38 MAPK. *Toxicol Appl Pharmacol*, 273, 130-9.
- SORESCU, D., WEISS, D., LASSEGUE, B., CLEMPUS, R. E., SZOCS, K., SORESCU, G. P., VALPPU, L., QUINN, M. T., LAMBETH, J. D., VEGA, J. D., TAYLOR, W. R. & GRIENDLING, K. K. 2002. Superoxide production and expression of nox family proteins in human atherosclerosis. *Circulation*, 105, 1429-35.
- SOUFI-ZOMORROD, M., HAJIFATHALI, A., KOUHKAN, F., MEHDIZADEH, M., RAD, S. M. & SOLEIMANI, M. 2016. MicroRNAs modulating angiogenesis: miR-129-1 and miR-133 act as angio-miR in HUVECs. *Tumour Biol*, 37, 9527-34.
- SPENCER, B. G. & FINNIE, J. W. 2020. The Role of Endoplasmic Reticulum Stress in Cell Survival and Death. *Journal of Comparative Pathology*, 181, 86-91.
- SPITLER, K. M., MATSUMOTO, T. & WEBB, R. C. 2013. Suppression of endoplasmic reticulum stress improves endothelium-dependent contractile responses in aorta of the spontaneously hypertensive rat. *Am J Physiol Heart Circ Physiol*, 305, H344-53.
- SPITLER, K. M. & WEBB, R. C. 2014. Endoplasmic reticulum stress contributes to aortic stiffening via proapoptotic and fibrotic signaling mechanisms. *Hypertension*, 63, e40-5.
- STEFANADIS, C., DERNELLIS, J., VLACHOPOULOS, C., TSIOUFIS, C., TSIAMIS, E., TOUTOUZAS, K., PITSAVOS, C. & TOUTOUZAS, P. 1997. Aortic function in arterial hypertension determined by pressure-diameter relation: effects of diltiazem. *Circulation*, 96, 1853-8.
- STEVENS, F. J. & ARGON, Y. 1999. Protein folding in the ER. Semin Cell Dev Biol, 10, 443-54.
- STOKER, A. W. 2005. Protein tyrosine phosphatases and signalling. *J Endocrinol*, 185, 19-33.

- SUI, H., WANG, W., WANG, P. H. & LIU, L. S. 2005. Effect of glutathione peroxidase mimic ebselen (PZ51) on endothelium and vascular structure of stroke-prone spontaneously hypertensive rats. *Blood Press*, 14, 366-72.
- SUI, H., XIAO, S., JIANG, S., WU, S., LIN, H., CHENG, L., YE, L., ZHAO, Q., YU, Y., TAO, L., KONG, F. M., HUANG, X. & CUI, R. 2023. Regorafenib induces NOX5-mediated endoplasmic reticulum stress and potentiates the anti-tumor activity of cisplatin in non-small cell lung cancer cells. *Neoplasia*, 39, 100897.
- SUKUMARAN, V., VEERAVEEDU, P. T., GURUSAMY, N., YAMAGUCHI, K., LAKSHMANAN, A. P., MA, M., SUZUKI, K., KODAMA, M. & WATANABE, K. 2011a. Cardioprotective effects of telmisartan against heart failure in rats induced by experimental autoimmune myocarditis through the modulation of angiotensin-converting enzyme-2/angiotensin 1-7/mas receptor axis. *Int J Biol Sci*, 7, 1077-92.
- SUKUMARAN, V., WATANABE, K., VEERAVEEDU, P. T., GURUSAMY, N., MA, M., THANDAVARAYAN, R. A., LAKSHMANAN, A. P., YAMAGUCHI, K., SUZUKI, K. & KODAMA, M. 2011b. Olmesartan, an AT1 antagonist, attenuates oxidative stress, endoplasmic reticulum stress and cardiac inflammatory mediators in rats with heart failure induced by experimental autoimmune myocarditis. *Int J Biol Sci*, 7, 154-67.
- SUN, H. L., SUN, L., LI, Y. Y., SHAO, M. M., CHENG, X. Y., GE, N., LU, J. D. & LI, S. M. 2009. ACE-inhibitor suppresses the apoptosis induced by endoplasmic reticulum stress in renal tubular in experimental diabetic rats. *Exp Clin Endocrinol Diabetes*, 117, 336-44.
- SUN, L., LIN, P., CHEN, Y., YU, H., REN, S., WANG, J., ZHAO, L. & DU, G. 2020. miR-182-3p/Myadm contribute to pulmonary artery hypertension vascular remodeling via a KLF4/p21-dependent mechanism. *Theranostics*, 10, 5581-5599.
- SUNDARAM, A., SIEW KEAH, L., SIRAJUDEEN, K. N. & SINGH, H. J. 2013. Upregulation of catalase and downregulation of glutathione peroxidase activity in the kidney precede the development of hypertension in pre-hypertensive SHR. *Hypertens Res*, 36, 213-8.
- SUZUKI, N., MIYAUCHI, T., TOMOBE, Y., MATSUMOTO, H., GOTO, K., MASAKI, T. & FUJINO, M. 1990. Plasma concentrations of endothelin-1 in spontaneously hypertensive rats and DOCA-salt hypertensive rats. *Biochem Biophys Res Commun*, 167, 941-7.
- TACKLING, G. & BORHADE, M. B. 2020. Hypertensive Heart Disease. *StatPearls*. Treasure Island (FL).
- TADDEI, S., VIRDIS, A., GHIADONI, L., SUDANO, I. & SALVETTI, A. 2002. Effects of antihypertensive drugs on endothelial dysfunction: clinical implications. *Drugs*, 62, 265-84.
- TADDEI, S., VIRDIS, A., GHIADONI, L., ULERI, S., MAGAGNA, A. & SALVETTI, A. 1997. Lacidipine restores endothelium-dependent vasodilation in essential hypertensive patients. *Hypertension*, 30, 1606-12.
- TAILLE, C., EL-BENNA, J., LANONE, S., DANG, M. C., OGIER-DENIS, E., AUBIER, M. & BOCZKOWSKI, J. 2004. Induction of heme oxygenase-1 inhibits NAD(P)H oxidase activity by down-regulating cytochrome b558 expression via the reduction of heme availability. *J Biol Chem*, 279, 28681-8.
- TAKEUCHI, F., LIANG, Y. Q., ISONO, M., TAJIMA, M., CUI, Z. H., IIZUKA, Y., GOTODA, T., NABIKA, T. & KATO, N. 2021. Integrative genomic analysis of blood pressure and related phenotypes in rats. *Dis Model Mech*, 14.
- TAKEYA, K., WANG, X., SUTHERLAND, C., KATHOL, I., LOUTZENHISER, K., LOUTZENHISER, R. D. & WALSH, M. P. 2014. Involvement of myosin regulatory light chain diphosphorylation in sustained vasoconstriction under pathophysiological conditions. *J Smooth Muscle Res*, 50, 18-28.

- TANG, P., DANG, H., HUANG, J., XU, T., YUAN, P., HU, J. & SHENG, J. F. 2018. NADPH oxidase NOX4 is a glycolytic regulator through mROS-HIF1α axis in thyroid carcinomas. *Sci Rep*, 8, 15897.
- TESKE, B. F., BAIRD, T. D. & WEK, R. C. 2011. Methods for analyzing eIF2 kinases and translational control in the unfolded protein response. *Methods Enzymol*, 490, 333-56.
- THOMPSON, M. D., MEI, Y., WEISBROD, R. M., SILVER, M., SHUKLA, P. C., BOLOTINA, V. M., COHEN, R. A. & TONG, X. 2014. Glutathione adducts on sarcoplasmic/endoplasmic reticulum Ca2+ ATPase Cys-674 regulate endothelial cell calcium stores and angiogenic function as well as promote ischemic blood flow recovery. *J Biol Chem*, 289, 19907-16.
- TONELLI, C., CHIO, I. I. C. & TUVESON, D. A. 2018. Transcriptional Regulation by Nrf2. *Antioxid Redox Signal*, 29, 1727-1745.
- TOTH, A., NICKSON, P., MANDL, A., BANNISTER, M. L., TOTH, K. & ERHARDT, P. 2007. Endoplasmic reticulum stress as a novel therapeutic target in heart diseases. *Cardiovasc Hematol Disord Drug Targets*, 7, 205-18.
- TOUYZ, R. M. 2000. Oxidative stress and vascular damage in hypertension. *Curr Hypertens Rep*, 2, 98-105.
- TOUYZ, R. M. 2002. Impaired vasorelaxation in hypertension: beyond the endothelium. *J Hypertens*, 20, 371-3.
- TOUYZ, R. M. 2004. Reactive oxygen species, vascular oxidative stress, and redox signaling in hypertension: what is the clinical significance? *Hypertension*, 44, 248-52.
- TOUYZ, R. M. 2005. Reactive oxygen species as mediators of calcium signaling by angiotensin II: implications in vascular physiology and pathophysiology. *Antioxid Redox Signal*, 7, 1302-14.
- TOUYZ, R. M., ALVES-LOPES, R., RIOS, F. J., CAMARGO, L. L., ANAGNOSTOPOULOU, A., ARNER, A. & MONTEZANO, A. C. 2018. Vascular smooth muscle contraction in hypertension. *Cardiovasc Res*, 114, 529-539
- TOUYZ, R. M., ANAGNOSTOPOULOU, A., RIOS, F., MONTEZANO, A. C. & CAMARGO, L. L. 2019. NOX5: Molecular biology and pathophysiology. *Exp Physiol*, 104, 605-616.
- TOUYZ, R. M., CHEN, X., TABET, F., YAO, G., HE, G., QUINN, M. T., PAGANO, P. J. & SCHIFFRIN, E. L. 2002. Expression of a functionally active gp91phox-containing neutrophil-type NAD(P)H oxidase in smooth muscle cells from human resistance arteries: regulation by angiotensin II. *Circ Res*, 90, 1205-13.
- TOUYZ, R. M., DENG, L. Y., HE, G., WU, X. H. & SCHIFFRIN, E. L. 1999. Angiotensin II stimulates DNA and protein synthesis in vascular smooth muscle cells from human arteries: role of extracellular signal-regulated kinases. *J Hypertens*, 17, 907-16.
- TOUYZ, R. M., DENG, L. Y. & SCHIFFRIN, E. L. 1995. Ca2+ and contractile responses of resistance vessels of WKY rats and SHR to endothelin-1. *J Cardiovasc Pharmacol*, 26 Suppl 3, S193-6.
- TOUYZ, R. M., MERCURE, C., HE, Y., JAVESHGHANI, D., YAO, G., CALLERA, G. E., YOGI, A., LOCHARD, N. & REUDELHUBER, T. L. 2005. Angiotensin II-dependent chronic hypertension and cardiac hypertrophy are unaffected by gp91phox-containing NADPH oxidase. *Hypertension*, 45, 530-7.
- TOUYZ, R. M., RIOS, F. J., ALVES-LOPES, R., NEVES, K. B., CAMARGO, L. L. & MONTEZANO, A. C. 2020. Oxidative Stress: A Unifying Paradigm in Hypertension. *Can J Cardiol*, 36, 659-670.

- TOUYZ, R. M., TABET, F. & SCHIFFRIN, E. L. 2003. Redox-dependent signalling by angiotensin II and vascular remodelling in hypertension. *Clin Exp Pharmacol Physiol*, 30, 860-6.
- TRAN, Q.-K., OHASHI, K. & WATANABE, H. 2000. Calcium signalling in endothelial cells. *Cardiovascular Research*, 48, 13-22.
- TRENSZ, F., BORTOLAMIOL, C., KRAMBERG, M., WANNER, D., HADANA, H., REY, M., STRASSER, D. S., DELAHAYE, S., HESS, P., VEZZALI, E., MENTZEL, U., MENARD, J., CLOZEL, M. & IGLARZ, M. 2019. Pharmacological Characterization of Aprocitentan, a Dual Endothelin Receptor Antagonist, Alone and in Combination with Blockers of the Renin Angiotensin System, in Two Models of Experimental Hypertension. *J Pharmacol Exp Ther*, 368, 462-473.
- TROTT, D. W., THABET, S. R., KIRABO, A., SALEH, M. A., ITANI, H., NORLANDER, A. E., WU, J., GOLDSTEIN, A., ARENDSHORST, W. J., MADHUR, M. S., CHEN, W., LI, C. I., SHYR, Y. & HARRISON, D. G. 2014. Oligoclonal CD8+ T cells play a critical role in the development of hypertension. *Hypertension*, 64, 1108-15.
- TYKOCKI, N. R. & WATTS, S. W. 2010. The interdependence of endothelin-1 and calcium: a review. *Clin Sci (Lond)*, 119, 361-72.
- UCHIDA, T., ODA, T., YAMAMOTO, T., INAMITSU, M., SAKAI, C., UCHINOUMI, H., SUETOMI, T., NAKAMURA, Y., OKAMOTO, Y., TATEDA, S., FUJII, S., TANAKA, S., NAWATA, J., OKAMURA, T., KOBAYASHI, S. & YANO, M. 2022a. Endoplasmic reticulum stress promotes nuclear translocation of calmodulin, which activates phenotypic switching of vascular smooth muscle cells. *Biochem Biophys Res Commun*, 628, 155-162.
- UCHIDA, T., ODA, T., YAMAMOTO, T., INAMITSU, M., SAKAI, C., UCHINOUMI, H., SUETOMI, T., NAKAMURA, Y., OKAMOTO, Y., TATEDA, S., FUJII, S., TANAKA, S., NAWATA, J., OKAMURA, T., KOBAYASHI, S. & YANO, M. 2022b. Endoplasmic reticulum stress promotes nuclear translocation of calmodulin, which activates phenotypic switching of vascular smooth muscle cells. *Biochemical and Biophysical Research Communications*, 628, 155-162.
- UNGER, T., BORGHI, C., CHARCHAR, F., KHAN, N. A., POULTER, N. R., PRABHAKARAN, D., RAMIREZ, A., SCHLAICH, M., STERGIOU, G. S., TOMASZEWSKI, M., WAINFORD, R. D., WILLIAMS, B. & SCHUTTE, A. E. 2020. 2020 International Society of Hypertension global hypertension practice guidelines. *J Hypertens*, 38, 982-1004.
- UPTON, J. P., WANG, L., HAN, D., WANG, E. S., HUSKEY, N. E., LIM, L., TRUITT, M., MCMANUS, M. T., RUGGERO, D., GOGA, A., PAPA, F. R. & OAKES, S. A. 2012. IRE1alpha cleaves select microRNAs during ER stress to derepress translation of proapoptotic Caspase-2. *Science*, 338, 818-22.
- VAN DER VLIET, A., DANYAL, K. & HEPPNER, D. E. 2018. Dual oxidase: a novel therapeutic target in allergic disease. *Br J Pharmacol*, 175, 1401-1418.
- VAN THIEL, B. S., VAN DER PLUIJM, I., TE RIET, L., ESSERS, J. & DANSER, A. H. 2015. The renin-angiotensin system and its involvement in vascular disease. *Eur J Pharmacol*, 763, 3-14.
- VANE, J. R., ANGGÅRD, E. E. & BOTTING, R. M. 1990. Regulatory functions of the vascular endothelium. *N Engl J Med.* 323, 27-36.
- VANHOUTTE, P. M. 1989. Endothelium and control of vascular function. State of the Art lecture. *Hypertension*, 13, 658-67.
- VERFAILLIE, T., RUBIO, N., GARG, A. D., BULTYNCK, G., RIZZUTO, R., DECUYPERE, J. P., PIETTE, J., LINEHAN, C., GUPTA, S., SAMALI, A. & AGOSTINIS, P. 2012. PERK is required at the ER-mitochondrial contact sites to convey apoptosis after ROS-based ER stress. *Cell Death Differ*, 19, 1880-91.

- VIGNE, P., BREITTMAYER, J. P. & FRELIN, C. 1992. Thapsigargin, a new inotropic agent, antagonizes action of endothelin-1 in rat atrial cells. *Am J Physiol*, 263, H1689-94.
- VIRDIS, A., GHIADONI, L. & TADDEI, S. 2011. Effects of antihypertensive treatment on endothelial function. *Curr Hypertens Rep*, 13, 276-81.
- VISHNOI, A. & RANI, S. 2017. MiRNA Biogenesis and Regulation of Diseases: An Overview. *Methods Mol Biol*, 1509, 1-10.
- WAN, X. J., ZHAO, H. C., ZHANG, P., HUO, B., SHEN, B. R., YAN, Z. Q., QI, Y. X. & JIANG, Z. L. 2015. Involvement of BK channel in differentiation of vascular smooth muscle cells induced by mechanical stretch. *Int J Biochem Cell Biol*, 59, 21-9.
- WANG, C., LI, T., TANG, S., ZHAO, D., ZHANG, C., ZHANG, S., DENG, S., ZHOU, Y. & XIAO, X. 2016. Thapsigargin induces apoptosis when autophagy is inhibited in HepG2 cells and both processes are regulated by ROS-dependent pathway. *Environ Toxicol Pharmacol*, 41, 167-79.
- WANG, D. & ATANASOV, A. G. 2019. The microRNAs Regulating Vascular Smooth Muscle Cell Proliferation: A Minireview. *Int J Mol Sci*, 20.
- WANG, J., PAREJA, K. A., KAISER, C. A. & SEVIER, C. S. 2014. Redox signaling via the molecular chaperone BiP protects cells against endoplasmic reticulum-derived oxidative stress. *Elife*, 3, e03496.
- WARNER, T. D., ALLCOCK, G. H. & VANE, J. R. 1994. Reversal of established responses to endothelin-1 in vivo and in vitro by the endothelin receptor antagonists, BQ-123 and PD 145065. *Br J Pharmacol*, 112, 207-13.
- WEBB, R. C. 2003. Smooth muscle contraction and relaxation. *Adv Physiol Educ*, 27, 201-6.
- WEBER, M. A., BLACK, H., BAKRIS, G., KRUM, H., LINAS, S., WEISS, R., LINSEMAN, J. V., WIENS, B. L., WARREN, M. S. & LINDHOLM, L. H. 2009. A selective endothelin-receptor antagonist to reduce blood pressure in patients with treatment-resistant hypertension: a randomised, double-blind, placebo-controlled trial. *Lancet*, 374, 1423-31.
- WELSH, D. G., TRAN, C. H. T., HALD, B. O. & SANCHO, M. 2018. The Conducted Vasomotor Response: Function, Biophysical Basis, and Pharmacological Control. *Annu Rev Pharmacol Toxicol*, 58, 391-410.
- WENCESLAU, C. F., MCCARTHY, C. G., EARLEY, S., ENGLAND, S. K., FILOSA, J. A., GOULOPOULOU, S., GUTTERMAN, D. D., ISAKSON, B. E., KANAGY, N. L., MARTINEZ-LEMUS, L. A., SONKUSARE, S. K., THAKORE, P., TRASK, A. J., WATTS, S. W. & WEBB, R. C. 2021. Guidelines for the measurement of vascular function and structure in isolated arteries and veins. *Am J Physiol Heart Circ Physiol*, 321, H77-H111.
- WHELTON, P. K., CAREY, R. M., ARONOW, W. S., CASEY, D. E., JR., COLLINS, K. J., DENNISON HIMMELFARB, C., DEPALMA, S. M., GIDDING, S., JAMERSON, K. A., JONES, D. W., MACLAUGHLIN, E. J., MUNTNER, P., OVBIAGELE, B., SMITH, S. C., JR., SPENCER, C. C., STAFFORD, R. S., TALER, S. J., THOMAS, R. J., WILLIAMS, K. A., SR., WILLIAMSON, J. D. & WRIGHT, J. T., JR. 2018. 2017

  ACC/AHA/AAPA/ABC/ACPM/AGS/APhA/ASH/ASPC/NMA/PCNA Guideline for the Prevention, Detection, Evaluation, and Management of High Blood Pressure in Adults: A Report of the American College of Cardiology/American Heart Association Task Force on Clinical Practice Guidelines. *J Am Coll Cardiol*, 71, e127-e248.
- WILLIAMS, G. H. 2005. Aldosterone biosynthesis, regulation, and classical mechanism of action. *Heart Fail Rev*, 10, 7-13.

- WILSON, M. A. 2011. The role of cysteine oxidation in DJ-1 function and dysfunction. *Antioxid Redox Signal*, 15, 111-22.
- WU, R. F., MA, Z., LIU, Z. & TERADA, L. S. 2010. Nox4-derived H2O2 mediates endoplasmic reticulum signaling through local Ras activation. *Mol Cell Biol*, 30, 3553-68.
- WU, Y., YUE, Y., FU, S., LI, Y., WU, D., LV, J. & YANG, D. 2019. Icariside II prevents hypertensive heart disease by alleviating endoplasmic reticulum stress via the PERK/ATF-4/CHOP signalling pathway in spontaneously hypertensive rats. *J Pharm Pharmacol.* 71, 400-407.
- WYNNE, B. M., CHIAO, C. W. & WEBB, R. C. 2009. Vascular Smooth Muscle Cell Signaling Mechanisms for Contraction to Angiotensin II and Endothelin-1. *J Am Soc Hypertens*, 3, 84-95.
- XIE, F., WU, D., HUANG, S. F., CAO, J. G., LI, H. N., HE, L., LIU, M. Q., LI, L. F. & CHEN, L. X. 2017. The endoplasmic reticulum stress-autophagy pathway is involved in apelin-13-induced cardiomyocyte hypertrophy in vitro. *Acta Pharmacol Sin*, 38, 1589-1600.
- XIE, X., LU, J., KULBOKAS, E. J., GOLUB, T. R., MOOTHA, V., LINDBLAD-TOH, K., LANDER, E. S. & KELLIS, M. 2005. Systematic discovery of regulatory motifs in human promoters and 3' UTRs by comparison of several mammals. *Nature*, 434, 338-45.
- XU, J., WANG, G., WANG, Y., LIU, Q., XU, W., TAN, Y. & CAI, L. 2009. Diabetesand angiotensin II-induced cardiac endoplasmic reticulum stress and cell death: metallothionein protection. *J Cell Mol Med*, 13, 1499-512.
- XUAN, Y. T., WANG, O. L. & WHORTON, A. R. 1994. Regulation of endothelin-induced Ca2+ mobilization in smooth muscle cells by protein kinase C. *Am J Physiol*, 266, C1560-7.
- YAN, Y. F., CHEN, H. P., HUANG, X. S., QIU, L. Y., LIAO, Z. P. & HUANG, Q. R. 2015. DJ-1 Mediates the Delayed Cardioprotection of Hypoxic Preconditioning Through Activation of Nrf2 and Subsequent Upregulation of Antioxidative Enzymes. *J Cardiovasc Pharmacol*, 66, 148-58.
- YANAGISAWA, M., KURIHARA, H., KIMURA, S., TOMOBE, Y., KOBAYASHI, M., MITSUI, Y., YAZAKI, Y., GOTO, K. & MASAKI, T. 1988. A novel potent vasoconstrictor peptide produced by vascular endothelial cells. *Nature*, 332, 411-5.
- YANG, Q. & HORI, M. 2021. Characterization of Contractile Machinery of Vascular Smooth Muscles in Hypertension. *Life (Basel)*, 11.
- YANG, Y., TIAN, T., WANG, Y., LI, Z., XING, K. & TIAN, G. 2019. SIRT6 protects vascular endothelial cells from angiotensin II-induced apoptosis and oxidative stress by promoting the activation of Nrf2/ARE signaling. *Eur J Pharmacol*, 859, 172516.
- YEAGER, M. E., BELCHENKO, D. D., NGUYEN, C. M., COLVIN, K. L., IVY, D. D. & STENMARK, K. R. 2012. Endothelin-1, the unfolded protein response, and persistent inflammation: role of pulmonary artery smooth muscle cells. *Am J Respir Cell Mol Biol*, 46, 14-22.
- YEN, J.-H., WU, P.-S., CHEN, S.-F. & WU, M.-J. 2017a. Fisetin Protects PC12 Cells from Tunicamycin-Mediated Cell Death via Reactive Oxygen Species Scavenging and Modulation of Nrf2-Driven Gene Expression, SIRT1 and MAPK Signaling in PC12 Cells. *International Journal of Molecular Sciences*, 18, 852.
- YEN, J. H., WU, P. S., CHEN, S. F. & WU, M. J. 2017b. Fisetin Protects PC12 Cells from Tunicamycin-Mediated Cell Death via Reactive Oxygen Species Scavenging and Modulation of Nrf2-Driven Gene Expression, SIRT1 and MAPK Signaling in PC12 Cells. *Int J Mol Sci*, 18.
- YILDIRIM, Z., BABOO, S., HAMID, S. M., DOGAN, A. E., TUFANLI, O., ROBICHAUD, S., EMERTON, C., DIEDRICH, J. K., VATANDASLAR, H.,

- NIKOLOS, F., GU, Y., IWAWAKI, T., TARLING, E., OUIMET, M., NELSON, D. L., YATES, J. R., 3RD, WALTER, P. & ERBAY, E. 2022. Intercepting IRE1 kinase-FMRP signaling prevents atherosclerosis progression. *EMBO Mol Med*, 14, e15344.
- YOUNG, C. N. 2017. Endoplasmic reticulum stress in the pathogenesis of hypertension. *Exp Physiol*, 102, 869-884.
- YOUNG, C. N., CAO, X., GURUJU, M. R., PIERCE, J. P., MORGAN, D. A., WANG, G., IADECOLA, C., MARK, A. L. & DAVISSON, R. L. 2012. ER stress in the brain subfornical organ mediates angiotensin-dependent hypertension. *J Clin Invest*, 122, 3960-4.
- YUAN, J., CHEN, M., XU, Q., LIANG, J., CHEN, R., XIAO, Y., FANG, M. & CHEN, L. 2017. Effect of the Diabetic Environment On the Expression of MiRNAs in Endothelial Cells: Mir-149-5p Restoration Ameliorates the High Glucose-Induced Expression of TNF-alpha and ER Stress Markers. *Cell Physiol Biochem*, 43, 120-135.
- YUM, V., CARLISLE, R. E., LU, C., BRIMBLE, E., CHAHAL, J., UPAGUPTA, C., ASK, K. & DICKHOUT, J. G. 2017. Endoplasmic reticulum stress inhibition limits the progression of chronic kidney disease in the Dahl salt-sensitive rat. *Am J Physiol Renal Physiol*, 312, F230-F244.
- ZEESHAN, H. M., LEE, G. H., KIM, H. R. & CHAE, H. J. 2016. Endoplasmic Reticulum Stress and Associated ROS. *Int J Mol Sci*, 17, 327.
- ZELKO, I. N., MARIANI, T. J. & FOLZ, R. J. 2002. Superoxide dismutase multigene family: a comparison of the CuZn-SOD (SOD1), Mn-SOD (SOD2), and EC-SOD (SOD3) gene structures, evolution, and expression. *Free Radic Biol Med*, 33, 337-49.
- ZENG, L., LI, Y., YANG, J., WANG, G., MARGARITI, A., XIAO, Q., ZAMPETAKI, A., YIN, X., MAYR, M., MORI, K., WANG, W., HU, Y. & XU, Q. 2015. XBP 1-Deficiency Abrogates Neointimal Lesion of Injured Vessels Via Cross Talk With the PDGF Signaling. *Arterioscler Thromb Vasc Biol*, 35, 2134-44.
- ZENG, X. & YANG, Y. 2024. Molecular Mechanisms Underlying Vascular Remodeling in Hypertension. *RCM*, 25.
- ZHANG, F., GUO, X., XIA, Y. & MAO, L. 2021. An update on the phenotypic switching of vascular smooth muscle cells in the pathogenesis of atherosclerosis. *Cell Mol Life Sci*, 79, 6.
- ZHANG, H., ZHANG, X. & ZHANG, J. 2018. MiR-129-5p inhibits autophagy and apoptosis of H9c2 cells induced by hydrogen peroxide via the PI3K/AKT/mTOR signaling pathway by targeting ATG14. *Biochem Biophys Res Commun*, 506, 272-277.
- ZHANG, I. X., HERRMANN, A., LEON, J., JEYARAJAN, S., ARUNAGIRI, A., ARVAN, P., GILON, P. & SATIN, L. S. 2023. ER stress increases expression of intracellular calcium channel RyR1 to modify Ca(2+) homeostasis in pancreatic beta cells. *J Biol Chem*, 299, 105065.
- ZHANG, J., FAN, P.-H., LIN, G.-M., CHANG, W.-C. & LIU, H.-W. 2020. 2.14 Recent Progress in Unusual Carbohydrate-Containing Natural Products Biosynthesis. *In:* LIU, H.-W. & BEGLEY, T. P. (eds.) *Comprehensive Natural Products III.* Oxford: Elsevier.
- ZHANG, J., JIA, J., ZHAO, L., LI, X., XIE, Q., CHEN, X., WANG, J. & LU, F. 2016. Down-regulation of microRNA-9 leads to activation of IL-6/Jak/STAT3 pathway through directly targeting IL-6 in HeLa cell. *Mol Carcinog*, 55, 732-42.
- ZHANG, J., ZHAO, W. S., WANG, X., XU, L. & YANG, X. C. 2018. Palmitic Acid Increases Endothelin-1 Expression in Vascular Endothelial Cells through the Induction of Endoplasmic Reticulum Stress and Protein Kinase C Signaling. *Cardiology*, 140, 133-140.

- ZHANG, J. R. & SUN, H. J. 2021. MiRNAs, lncRNAs, and circular RNAs as mediators in hypertension-related vascular smooth muscle cell dysfunction. *Hypertens Res*, 44, 129-146.
- ZHANG, M., BREWER, A. C., SCHRODER, K., SANTOS, C. X., GRIEVE, D. J., WANG, M., ANILKUMAR, N., YU, B., DONG, X., WALKER, S. J., BRANDES, R. P. & SHAH, A. M. 2010. NADPH oxidase-4 mediates protection against chronic load-induced stress in mouse hearts by enhancing angiogenesis. *Proc Natl Acad Sci USA*, 107, 18121-6.
- ZHAO, Y., ZHANG, L., QIAO, Y., ZHOU, X., WU, G., WANG, L., PENG, Y., DONG, X., HUANG, H., SI, L., ZHANG, X., ZHANG, L., LI, J., WANG, W., ZHOU, L. & GAO, X. 2013. Heme oxygenase-1 prevents cardiac dysfunction in streptozotocin-diabetic mice by reducing inflammation, oxidative stress, apoptosis and enhancing autophagy. *PLoS One*, 8, e75927.
- ZHOU, J., LI, Y. S. & CHIEN, S. 2014. Shear stress-initiated signaling and its regulation of endothelial function. *Arterioscler Thromb Vasc Biol*, 34, 2191-8.
- ZHOU, X., LU, B., FU, D., GUI, M., YAO, L. & LI, J. 2020. Huoxue Qianyang decoction ameliorates cardiac remodeling in obese spontaneously hypertensive rats in association with ATF6-CHOP endoplasmic reticulum stress signaling pathway regulation. *Biomed Pharmacother*, 121, 109518.
- ZHU, J., SHAO, A., WANG, C., ZENG, C. & WANG, H. 2023. Inhibition of endoplasmic reticulum stress restores the balance of renal RAS components and lowers blood pressure in the spontaneously hypertensive rats. *Clin Exp Hypertens*, 45, 2202367.
- ZIMMERMAN, M. C., LAZARTIGUES, E., LANG, J. A., SINNAYAH, P., AHMAD, I. M., SPITZ, D. R. & DAVISSON, R. L. 2002. Superoxide mediates the actions of angiotensin II in the central nervous system. *Circ Res*, 91, 1038-45.
- ZITO, E. 2015. ERO1: A protein disulfide oxidase and H2O2 producer. *Free Radic Biol Med*, 83, 299-304.
- ZOU, W., YUE, P., KHURI, F. R. & SUN, S. Y. 2008. Coupling of endoplasmic reticulum stress to CDDO-Me-induced up-regulation of death receptor 5 via a CHOP-dependent mechanism involving JNK activation. *Cancer Res*, 68, 7484-92.

i